Heterogeneous carbapenem resistance among carbapenemase-producing Klebsiella pneumoniae

Adriana Chiarelli

Sorbonne Université Site de Jussieu

École Doctorale: Complexité du Vivant

Thèse présentée par

Adriana Chiarelli

pour obtenir le grade de Docteur

Heterogeneous carbapenem resistance among carbapenemase-producing *Klebsiella pneumoniae*

Soutenance prévue le 28 Juin 2021

Jury composé de :

Pr Jean-Emmanuel Hugonnet	Sorbonne Université	Président
Pr Katy Jeannot	Université de Bourgogne-Franche-Comté	Rapporteur
Pr Jan Michiels	KU Leuwen	Rapporteur
Dr Christophe Beloin	Institut Pasteur	Examinateur
Dr Rémy Bonnin	Université Paris Saclay	Co-Directeur
Dr Philippe Glaser	Institut Pasteur	Directeur

Acknowledgements

The PhD journey is not a solo experience.

During the past almost four years I had the opportunity to work together with remarkable people and friends. I would like to take this opportunity and express my gratitude towards them.

First and foremost, I would like to express my gratitude to my supervisor and research director Philippe Glaser and co-supervisor Rémy Bonnin, for giving me the opportunity to conduct this thesis under their guidance, for their many ideas and suggestions and their scientific support. I am particularly thankful to Philippe for his constant availability in the most urgent situations (even on weekends and during holidays!) and to providing me with some extra time to finish my experimental work and write this manuscript in the best conditions (although I do not recommend writing a thesis with an ongoing pandemic...).

My special thanks go to my current labmates Nicolas Cabanel, Isabelle Rosinski Chupin, Dieudonne Pengdbamba Zongo, and previous ones (Alexandre Santos Almeida, Rafael Patiño Navarrete, Emanuela Ursino, Lisa Barel, Noah Rabenandrasana, Virginie Guerin) for their support, valuable discussions, and the good moments we shared. I am particularly indebted to Isabelle for the several constructive discussions and her kind encouragement, as well as Nicolas, the "good giant" and rock of the EERA lab: many things would have not been possible without you. Thank you for your invaluable support and for having kept a sense of humour when I had lost mine. Lisa and Emanuela, I have great memories of those months together, we had a lot of fun and supported each other.

Thanks to the "Bicêtre side" of the unit EERA, in particular I am grateful to Thierry Naas, Agnes Jousset and Laurent Dortet for the interesting discussions and proficient collaboration.

I would like to thank Marie-Therese Vicente for kindly assisting me in administrative procedures before the arrival of Reine Bouyssie, who also kindly and efficiently helped me in the last administrative steps of my PhD.

I wish to thank Gregory Batt and Virgile Andreani, for their insightful comments, and suggestions on how to address the issue of heteroresistance. I am particularly grateful to Virgile, who kindly helped me in setting up the ScanLag system and understanding the obscure world of MatLab.

Additionally, I would like to express my deepest appreciation to Thomas Obadia, who supported me in the statistical analysis of the work on heteroresistance. Thank you for kindly putting your time and energy into that.

I am grateful to the members of my TAC committee: Ivo Gomperts Boneca, Francois-Xavier Weill, Marie-Cécile Ploy and Jean-Emmanuel Hugonnet for their assistance throughout this journey.

I also want to thank Christophe Beloin, Pierre-Alexandre Kaminski, and Giulia Manina for the interesting discussion we had during my mid-thesis meeting of the Microbiology Department. Your comments and suggestions have also contributed to the advancement of this thesis.

I wish to thank Jan Michiels and Katy Jeannot for using their time and their expertise to critically examine my work, even in very busy times.

I am grateful to the Pasteur-Paris University International doctoral program (PPU), which gave me the opportunity to undertake this PhD, in agreement with Sorbonne University. I wish to thank Susanna Celli, previous dean of the PPU program, for being caring to us and taking the time to listen to our PhD frustrations. Thanks to Mariana Mesel-Lemoine from the MAASC program in Pasteur for your precious career advice and Monica Sala, for guiding me towards my next steps.

I am sincerely thankful to all the members of Carmen Buchresier's Lab: Pedro, Tobias, Monica, Daniel, Viviane, Silke, Ana, Sonia, Christophe, Laura for laughing together and supporting me emotionally. Carmen, thank you for all the champagne you poured to us every Friday, for the Christmas parties, for your advice and scientific support. I am pleased to have had the possibility of meeting you during my journey.

More than just research and writing went into this achievement. I owe where I am today to a lot of amazing people.

Marta, Emilia, Lukas, Matthias, and Berenice, not only my PPU peeps, but especially friends and family. You have been there in the most difficult moments throughout this PhD and in the nicest ones. I am just deeply grateful to have met you.

Viola, I don't even know where to start with. Thank you for your unconditional support and friendship, you are amazing. Giorgia, Piergiuseppe, Paolo, Francesca, Umberto, thanks for the great moments we have shared, for the jokes, the laughs, the lightness, and the sense of family you have given to me.

Thanks to Benoit and Solène, the "rue bailleul crew", for being extremely kind to me and welcoming. I consider myself lucky to have met my neighbor Solenn: thank you for supporting me during the lockdown and the PhD writing and for sharing cherished moments together.

To all these people: you have been part of my Parisian family and my PhD journey would have not been the same without all of you.

I was not expecting the PhD to be such a roller-coaster. I experienced moments of joy and despair, feelings that would affect me as much as it did to people surrounding me. Yet, Tobias, you gave me the courage to appreciate and accept my weaknesses. You took care of them, without judgement, but love. You always had my back, encouraging me when I felt defeated, and supported me unwaveringly. Thank you for being the way you are.

I am very grateful to my family, for their support over these years, and for reminding me to breathe when I have been stressed out. Thanks to old and new friends, for your support, the multiple zoom video-calls, phone calls, funny and sweet text messages, that helped me to go through these crazy pandemic times.

Table of contents

Symbols and Abbreviations

ALE	Adaptive Laboratory Evolution
AMR	Antimicrobial Resistance
AR	Adaptive Resistance
ARGs	Antibiotic Resistance Genes
AST	Antibiotic Susceptibility Testing
AUC	Area Under the Curve
bla	ß-lactamase
BMD	Broth Microdilution
BSI	Bloodstream Infections
CA	Community Associated
cAMP	cyclic AMP
CFU	Colony Forming Unit
CG	Clonal group
CLSI	Clinical and Laboratory Standards Institute
C_{max}	Highest drug concentration reached in serum
CPKp	Carbapenemase-producing *Klebsiella pneumoniae*
CPS	Capsule
cps	Capsule operon
CRE	Carbapenem resistant *Enterobacterales*
CRKp	Carbapenem-resistant *Klebsiella pneumoniae*
D-Ala-D-Ala	D-alanyl-D-alanine
DDD	Defined Daily Doses
ECDC	European Centers for Disease and Control
EDTA	Ethylenediaminetetraacetic acid
EF-G	Translation elongation factor G
EPEC	Enteropathogenic *E. coli*
ESBL	Extended-spectrum ß-lactamases
Etest	Epsilon Test
ETP	Ertapenem
ETC	Electron Transport Chain
EUCAST	European Committee on Antimicrobial Susceptibility Testing
FACS	Fluorescent Analysis Cell Sorting
Fe-S	Iron Sulfur cluster
G20	Group of Twenty
GlcNAc	N-acetylglucosamine
HAIs	Hospital acquired infections
HGT	Horizontal gene transfer
HR	Heteroresistance
HV	Hypervirulent
ICEs	Integrative and conjugative elements
ICU	Intensive care unit
IE	Inoculum Effect

IMF	International Monetary Fund
IMP	Imipenem
IS	Insertion Sequence
Kp	*Klebsiella pneumoniae*
KPC	*Klebsiella pneumoniae* carbapenemase
KPC-Kp	Kp producing KPC
LMICs	Low- and middle-income countries
LPS	Lipopolysaccharide
MBC	Minimum bactericidal concentration
MBLs	Metallo-β-lactamases
MDK	Minimum duration for killing
MDK99	Minimum duration for killing 99% of the bacterial population
MDR	Multi-drug resistant
MEM	Meropenem
MGEs	Mobile genetic elements
MIC	Minimum inhibitory concentration
MLST	Multilocus sequence typing
MRSA	Methicillin-Resistant *Staphylococcus aureus*
MurNAc	N-acetylmuramic acid
NRC	National Reference Center
OM	Outer Membrane
OMP	Outer membrane porin
O_2^-	Superoxide radicals
PAE	Post-antibiotic effect
PAP	Population Analysis Profiling
PBPs	Penicillin-binding proteins
PDR	Pan-drug resistant
PG	Peptidoglycan
(p)ppGpp	Guanosine (penta)tetraphosphate
PK-PD	Pharmacokinetic/Pharmacodynamic
RND	Resistance-Nodulation-cell Division
ROS	Hydroxyl Radicals
SBLs	Serine β-lactamases
SCV	Small Colony Variant
SIR	Susceptible/Intermediate/Resistant
SNP	Single-nucleotide polymorphism
ST	Sequence Type
TA	Toxin-antitoxin system
ToA	Time of Appearance
TCA	Tricarboxylic Acid Cycle
TDtest	Tolerance Disk Test
U.S. FDA	United States Food and Drug Administration
WGS	Whole genome sequencing
WHO	World Health Organization

XDR	Extensively-drug resistant

You cannot stop the waves,
but you can learn how to surf

I. Abstract

Klebsiella pneumoniae is a major cause of nosocomial infections. The emergence and global dissemination of carbapenem-resistant *K. pneumoniae* (CRKp) have dramatically hampered antimicrobial treatment options. Infections due to CRKp correlate with increased hospital stay, poor outcomes and high mortality rates. Resistance is mainly driven by the acquisition of carbapenemases but *K. pneumoniae* isolates producing carbapenemases (CPKp) show variable resistance to carbapenems and heteroresistance (HR), particularly to imipenem (IMP).

HR refers to the occurrence of various susceptibility levels within monoclonal populations, likely resulted from the co-existence of subpopulations with distinct behaviours. HR is preliminary visualized by the appearance of colonies within the drug inhibition halo in agar-based Antimicrobial Susceptibility Testing. Despite its clinical importance, mechanisms mediating HR among CPKp remain largely unknown. Microbial heterogeneity within isogenic populations can be driven by multiple mechanisms, allowing bacteria to thrive in stressful conditions such as scarcity of nutrients or exposure to antibiotics.

In this regard, the main purpose of my PhD project was to characterize and elucidate mechanisms behind the heterogeneity of resistance among CPKp clinical isolates.

Following the serendipitous observation of colony morphology variations among the collected clinical isolates of CPKp, I combined phenotypic characterization of the colony variants from eight CPKp clinical isolates with whole genome sequencing (WGS) to uncover the genetic bases of such heterogeneity. I showed that the loss of the colony mucoid aspect in monoclonal populations is relatively frequent and results from diverse alterations occurring in genes involved in capsule (CPS) synthesis. Moreover, colony variants exhibited divergences not only in terms of CPS content, but also in other bacterial traits such as biofilm production, autoaggregation, and carbapenem susceptibility. Yet, I could not establish a convincing link with HR. Given those findings, discrimination of different colony variants in the clinical microbiology laboratory becomes essential to avoid misinterpretations on the phenotype of clinical isolates. Presumably, colony phenotypic switch might be beneficial *in vivo* to successfully colonize the patients and ultimately establishing an infection.

Next, I showed that IMP HR is prevalent across *K. pneumoniae* producing the KPC carbapenemase (KPC-Kp) and associated with heterogeneous survival to high doses of carbapenem at single colony level, as assessed by using the ScanLag setup. Complementation of these data with WGS of surviving colonies allowed me to uncover the complexity of HR in KPC-Kp, which arises from at least three different phenomena: resistance due to mutations, tolerance corresponding to the colonies emerging early and persistence, corresponding to the late appearing colonies. The detection of these subpopulations is likely favoured by the instability of IMP. Notably, I observed a broad landscape of mutations in different cellular components and essential physiological processes, which pave the way for future research on their contribution to evolution of resistance and survival within the host, in addition to considerably increase our knowledge of *K. pneumoniae* intrinsic resistome.

II. Introduction

2.2. Antibiotic resistance – an increasing threat to human health

2.2.1. Antibiotics: discovery, classification, and targets

Antibiotics account arguably for one of the greatest breakthroughs of the 20th century in modern medicine, as their discovery marked the beginning of a new era for the human history. Such "magic bullets" have greatly reduced illness and death from infectious diseases and improved life expectancy in much of the world's population. Interestingly, there is historical evidence of humankind's efforts in fighting infectious diseases already in the premodern era by using substances with antimicrobial activity. For example, it was recently found out that a Anglo-Saxon recipe from 1000 years ago – the "Bald's eyesalve", could effectively kill MRSA (methicillin-resistant *Staphylococcus aureus*) (Harrison et al., 2015). In addition, traces of tetracycline were found in human skeletons remains from Nubia and from late Roman period skeletons of Egypt (Cook et al., 1989).

The concept of antibiosis - literally "against life", from the Greek roots ἀντι anti, "against" and βίος bios, "life", was already introduced in 1877, when Louis Pasteur and Robert Koch observed that an airborne bacillus could inhibit the growth of *Bacillus anthracis* (Hudson et al., 2008). Yet, it was only in 1928, with the serendipitous discovery of penicillin from the *Penicillium notatum* mold by Alexander Fleming (Fleming, 1980) that the term antibiotic was coined, referring to compounds that could cure infectious diseases. Besides the difficulties encountered in the purification of penicillin by Sir Fleming, sufficient quantities for clinical purposes were finally purified by an Oxford team in 1940 (Chain et al., 2005), leading to a large scale production in USA and subsequent introduction of this "wonder drug" in clinical practice in 1943. The extraordinary success of penicillin triggered an intensive research into antibacterial products from natural compounds. In mid-1950s, Albert Schatz in Waksman's laboratory identified the genus *Streptomyces* as great producer of natural compounds exerting antibacterial, antiviral and antifungal activities (Waksman et al., 1946), kicking off the "Golden Age" for antibiotics discovery. The findings of that period were revolutionary and determining for the development and production of more than half of the molecules of our current antibiotic arsenal (Figure 1).

Unfortunately, the excitement of those years led to an extensive use of antimicrobial agents that, combined with a decline in the discovery pipeline from the 1970s onwards, have favoured the emergence and dissemination of resistant bacterial pathogens (Figure 1).

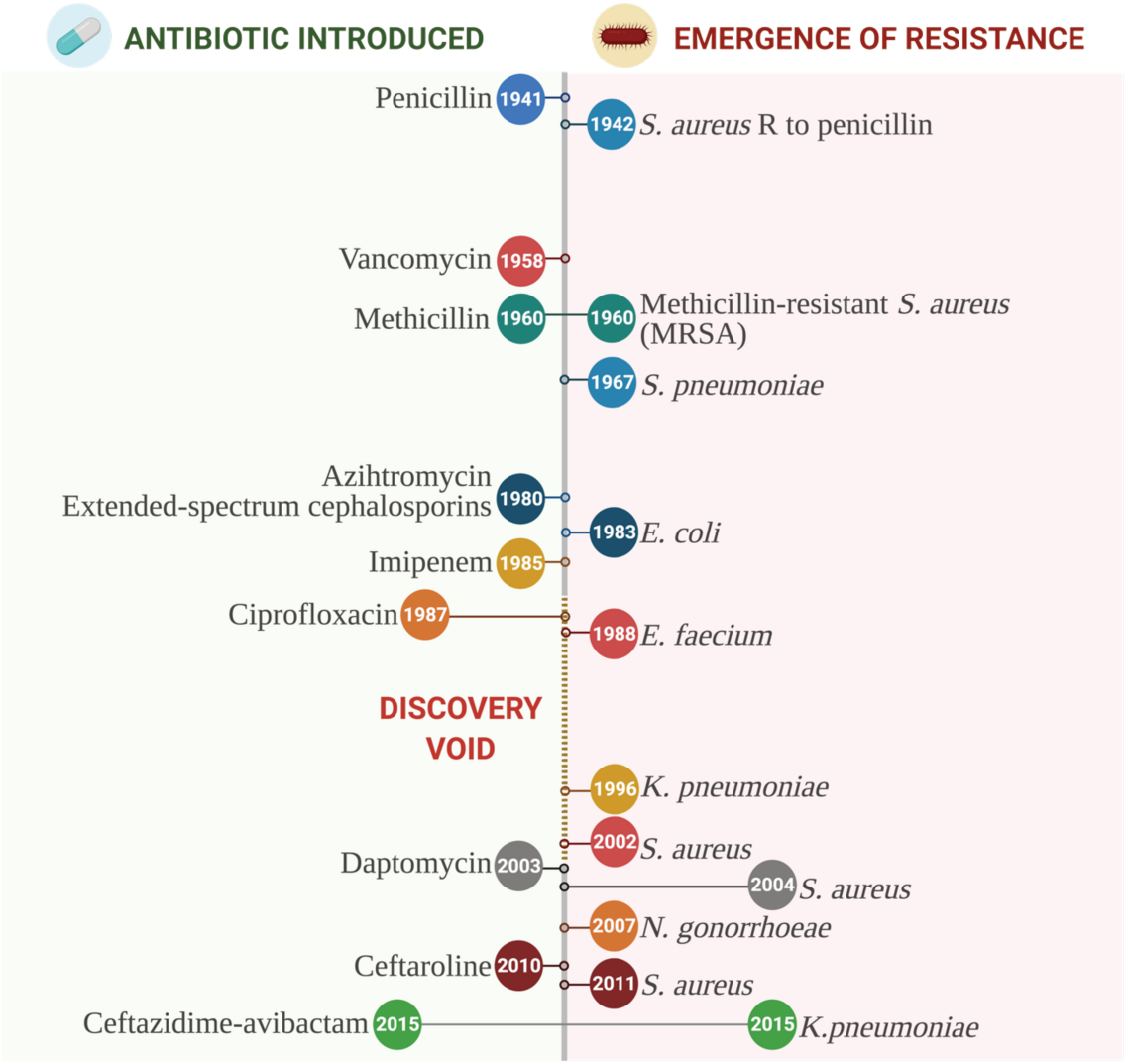

Figure 1. Timeline of antibiotic discovery and concomitant emergence of resistance. Created with BioRender.com

Antibiotics can be distinguished according to four main features: spectrum of activity, type of action, function, and molecular target (Table 1).

Based on the type of action, it is possible to discriminate between bactericidal and bacteriostatic agents (Table 1). A bactericidal antibiotic is assumed to kill bacteria, whereas a bacteriostatic drug is only able to inhibit the growth of bacterial populations. This categorization is based on *in vitro* observation, and, as such, it is somehow arbitrary when it comes to clinical practice. Parameters including the size of bacterial inoculum, growth characteristics of the culture, dose and degradation rate of the antibiotic can challenge the definition of the antibiotic activity. In addition, *in vitro* assessment does not reflect the *in vivo* situation, in which the antibacterial concentration may vary upon the body site (Craig, 2003). There are evidences of similar efficacy of bactericidal and bacteriostatic agents when treating clinical infections, including skin and soft tissue infections, pneumonia, bloodstream infection (Wald-Dickler et al., 2018).

Class	Spectrum of activity	Type of action	Function	Target
β-lactams		Bactericidal	Inhibition of peptidoglycan synthesis	Penicillin-binding proteins (PBPs)
Penicillins	Narrow: 1st and 2nd generations			
	Broad: 3rd and 4th generations			
Cephalosporins	Narrow: 1st generation			
	Broad: 2nd, 3rd and 4th generations			
Carbapenems e.g., imipenem, meropenem	Broad			
Aminoglycosides e.g., streptomycin,kanamycin, gentamicin	Broad	Bactericidal	Protein synthesis inhibition	30S ribosomal subunit
Tetracyclines e.g., tetracycline,doxycycline	Broad	Bacteriostatic		
Phenicols e.g., chloramphenicol, florfenicol	Broad	Bacteriostatic		50S ribosomal subunit
Macrolides e.g., azythromicin	Narrow	Bacteriostatic		
Fluoroquinolones e.g., ciprofloxacin, norfloxacin	Broad	Bactericidal	DNA synthesis inhibition	Gyrase and Topoisomerase IV
Polymixins e.g., colistin	Broad	Bactericidal	Cell membrane integrity	Lipopolysaccharide
Fosfomycin	Broad	Bactericidal	Inhibition of peptidoglycan synthesis	MurA enzyme
Sulfonamides e.g., sulfamethoxazole	Broad	Bacteriostatic	Folate synthesis inhibition	Dihydropteroate synthetase

Table 1: List of classes of antibiotics and their relevant properties. This table groups the most important antibiotics used in Enterobacterales. Each class include drugs with similar chemical structures. Each drug acts on essential cellular processes, e.g., DNA and protein biosynthesis, translation, and cell membrane integrity. Broad or narrow spectrum of activity depends on which microorganisms are targeted. Their activity can lead (bactericidal) or not (bacteriostatic) to loss of cell viability.

Factors other than microbial killing are rather influencing the treatment outcome, including optimal dosing, pharmacokinetic/pharmacodynamic modelling (PK-PD), tissue penetration and, ultimately, emergence of resistance. According to PK-PD principles, bactericidal

antibiotics can be distinguished into three types of compounds (Craig, 2003): (a) time-dependent killing (according to time spent over MIC); (b) concentration-dependent killing (according to the highest concentration reached) and (c) time and concentration-dependent killing (Figure 2).

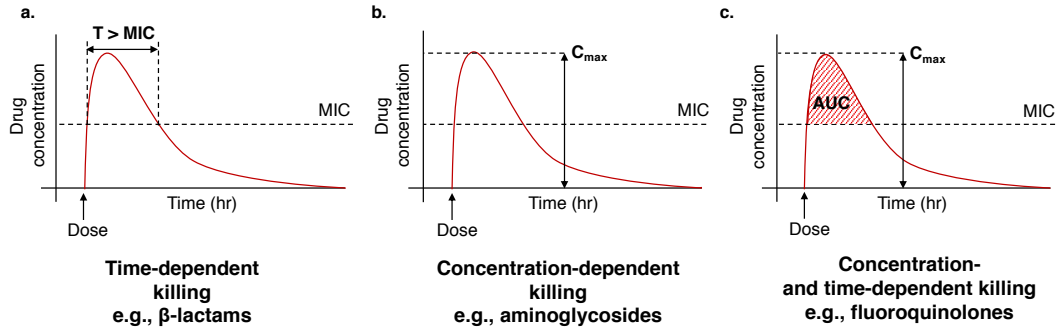

Figure 2: PK/PD parameters associated with the efficacy of the antibiotics. According to PK/PD principles, bactericidal drugs are distinguished into three categories. a) Time-dependent killing, b) concentration-dependent and c) concentration- and time-dependent compounds. T = time; MIC = Minimal Inhibitory Concentration; C_{max} = highest concentration reached in serum; AUC = area under the curve.

Based on spectrum of activity, antimicrobial agents may be simplistically classified into narrow- and broad-spectrum compounds (Table 1). Narrow antibiotics usually target a restricted number of causative microorganisms, whereas the broad-spectrum agents are effective against multiple species, therefore conferring the benefit of covering several clinical situations. However, the drawback is that drugs with broad-spectrum activity target also commensal bacteria, thereby facilitating selection of resistance. Hence, the narrow spectrum are usually preferred in the clinical practice, upon correct pathogen identification and antibiotic susceptibility testing (AST), owing to their specificity, along with the reduced likelihood to select for cross-resistance in untargeted pathogens and to modify the host microbiota (Melander et al., 2018).

Based on their function and molecular targets, antibiotics may be subdivided into several classes. Overall, they target biological processes that are essential for bacterial growth and cellular functions. The main targets include (a) cell wall synthesis and peptidoglycan (PG) cross-linking, (b) DNA and RNA synthesis machineries and (c) protein synthesis. In addition, certain agents can affect (d) folate synthesis and (e) cell membrane integrity. Antibacterial agents can also be classified **according to their chemical structures**. The major chemical classes of antibiotics used against Enterobacterales are β-lactams, followed by aminoglycosides (often combined with a β-lactams), tetracyclines, phenicols, macrolides, fluoroquinolones, antimicrobial peptides, fosfomycin, sulfonamides/trimethoprim (Table 1).

2.2.1.2. β-lactams and their importance

Dorothy Hodgkin uncovered the β-lactam structure of penicillin in 1945 (Hodgkin, 1949) (Figure 3). Since then, β-lactams have represented a cornerstone in the treatment of a range of bacterial infections, including life-threatening infections in intensive care units (ICUs). Importantly, given the absence of the β-lactam targets in eukaryotic cells, such drugs have been considered safe for treatment of infections in both animals and humans. However, adverse events including neurological, renal and hepatic complication, may arise depending on dosing regimens (Imani et al., 2017).

Broad-spectrum penicillins are among the most prescribed antibiotics to treat serious infections at global scale. In 2015, 39% of total antibiotic consumption, expressed in defined daily doses (DDD), was ascribed to these molecules, with the highest rates observed in USA, France and Italy (Klein et al., 2018). In Europe, consumption rates vary widely across countries[1].

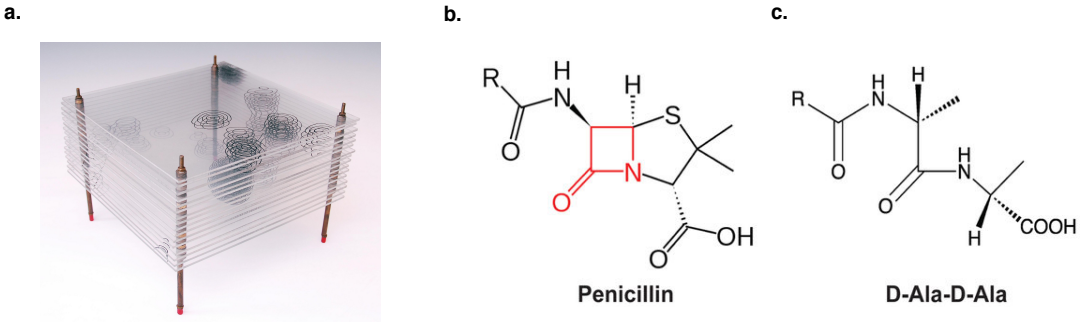

Source: Wikipedia, Museum of History of Science, University of Oxford under Wikimedia Commons for Ada Lovelace Day 2013

Figure 3: Discovery of β-lactam structure of penicillin in 1945. Based on X-ray crystallography, Dorothy Hodgkin, and Barbara Low (Oxford), in collaboration with C.W. Bunn and A. Turner-Jones (I.C.I. Alkali Division, Northwich) uncovered the β-lactam ring in the penicillin structure. In figure 3a, the 3D map of a fraction of one crystal salt of penicillin. Individual atoms and their position are represented by the contours, which are lines of electron density. In the middle (Figure 3b), the penicillin core structure, where "R" is the variable group and four-member β-lactam ring is highlighted in red. In figure 3c, the mimicry of β-lactam antibiotics to D-alanyl-D-alanine (D-Ala-D-Ala).

The mechanism of action of β-lactams was clarified in 1965, when Blumberg and Strominger observed a structural similarity between penicillins and D-Ala-D-Ala of the peptidoglycan (Figure 3c) in both Gram positive and Gram Negative bacteria (Blumberg and Strominger, 1974). The β-lactam moiety interferes with the PG synthesis through inactivation of Penicillin-Binding Proteins (PBPs) (Blumberg and Strominger, 1974). The PG confers mechanical rigidity to the bacterial cell wall by alternating units of N-acetylglucosamine (GlcNAc) and N-acetylmuramic acid (MurNAc). There are at least four PBPs in most of bacterial species; the

[1]ECDC. Antimicrobial consumption in the EU/EEA, annual epidemiological report for 2018. Stockholm: ECDC; 2019

different β-lactams exhibit various affinity towards PBPs, leading to diverse effects on cell growth and division (Sauvage et al., 2008). PBPs catalyse the transpeptidation step of the PG biosynthesis, leading to the formation of a cross-bridge between two D-Ala-D-Ala MurNAc peptides and ensure the elongation of uncross-linked glycan strands, indicated as transglycosylation (Sauvage et al., 2008). During transpeptidation, PBPs form a transient covalent acyl-enzyme complex with the D-Ala-D-Ala MurNAc pentapeptide through the serine residue in their active site (Sauvage et al., 2008). Due to the structural similarity of the β-lactam ring to the MurNAc pentapeptide, the PBPs form a stable acyl-enzyme with β-lactams that results in an irreversible β-lactam ring opening and inhibition of the PG biosynthesis (Tipper and Strominger, 1965). The bactericidal effect of β-lactams is time-dependent, meaning that the drug is effective if its plasma concentration is greater than the minimum bactericidal concentration (MBC).

β-lactam antibiotics are classified into four major chemical groups: penicillins, cephalosporins, carbapenems, and monobactams (Figure 4). These classes are distinguished based on the type of ring fused to the shared β-lactam moiety, a four membered ring. Penicillins, cephalosporins, and carbapenems, have a byciclic core (β-lactam ring fused to another 5- or 6-membered sulfur containing ring), whereas a monocyclic β-lactam ring is observed for monobactams (Figure 4).

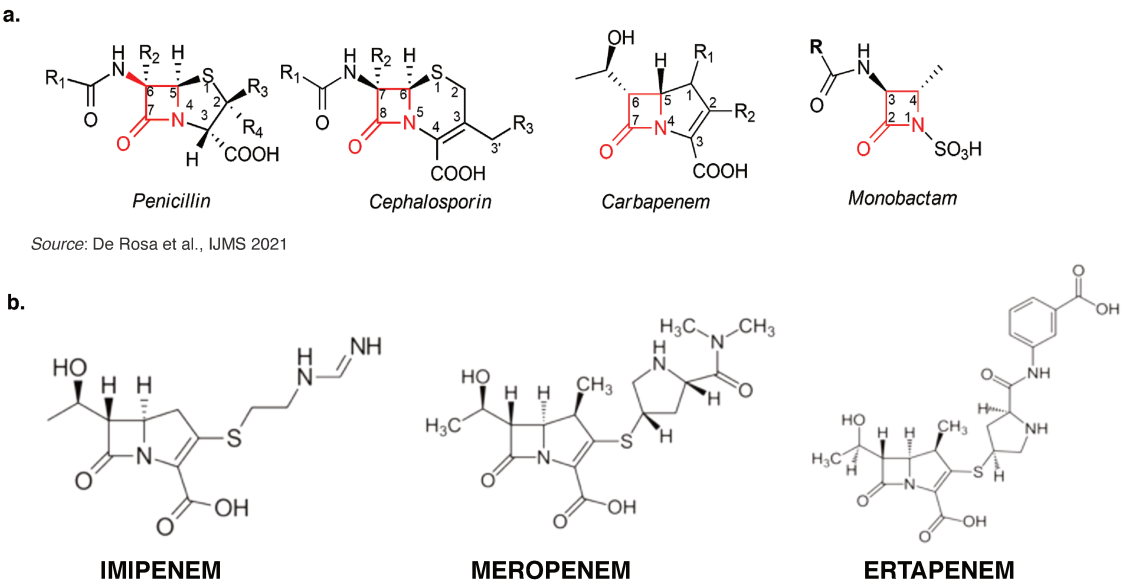

Figure 4: Main classes of β-lactam drugs. The four-member β-lactam ring is highlighted in red. Monobactams exhibit a monocyclic β-lactam ring, highlighted in red. In Figure 4b, the structure of three clinically important carbapenems: imipenem (IMP), meropenem (MEM) and ertapenem (ETP)

2.2.1.2.1. Carbapenems: the last resort β-lactam drugs

Carbapenems are commonly administered as "last-line" drugs for treatment of severe infections caused by MDR Gram-negative bacteria (Paterson and Bonomo, 2005). Importantly, carbapenems are effective against ESBL-producing organisms, due to their stability against ESBLs-driven drug hydrolysis (Papp-Wallace et al., 2011). However, between 2000 and 2015, following the increased incidence of ESBL-producing Gram negative bacilli, highest consumption rates of carbapenems have been observed at global scale, concomitantly with the emergence and dissemination of carbapenem resistant bacteria (Klein et al., 2018).

Carbapenems exhibit a 4:5 β-lactam ring fused to a double bond between C-2 and C-3 and the substitution of a sulphur moiety by a methylene group (Papp-Wallace et al., 2011) (Figure 4). Stability against β-lactamases is given by the *trans* configuration of the β-lactam ring at C-5 and C-6 and the *R* configuration at C-8 (Papp-Wallace et al., 2011). Carbapenems derive from thienamycin, a β-lactamase inhibitor naturally produced by *Streptomyces cattleya* (McGowan, 1998). Later, a more chemically stable compound was synthesized: the MK0787 molecule[2], subsequently renamed as imipenem (IMP) and first approved for medical use in 1985. Unlike the other carbapenems, IMP has a bicyclic core with a modified pyrroline ring (1β-hydrogen (R=H)) fused to the β-lactam moiety (figure 4b) (Papp-Wallace et al., 2011). IMP inhibits cell wall synthesis in multiple Gram negative and Gram-positive bacteria (mainly staphylococci), including MDR isolates. In *Escherichia coli*, IMP preferentially targets PBP-2, followed by PBP-1a, and PBP-1b (Zhanel et al., 2007). IMP is co-administered in a 1:1 ratio with cilastatin, an inhibitor of the renal dehydropeptidase-1 (DHP-I) that avoids drug deactivation in the human body (Graham et al., 1987). *In vitro* stability of imipenem has been reported to be strongly dependent on storage conditions (Nickolai et al., 1985). Moreover, drug degradation occurring during incubation can impact on determination of susceptibility levels, yielding to variations in the estimated MICs, thereby biasing their Susceptible/Intermediate/Resistant (SIR) classification (Lallemand et al., 2016).

Another important carbapenem is meropenem (MEM), approved in 1996 (Blumer, 1997). MEM structurally differs from IMP (Figure 4b) by the additional methyl group in the C-1 position, providing stability against DHP-I and to the dimethyl-carbonylpyrrolidinethio side-chain at C-2, which enhances the activity against several Enterobacterales and *Pseudomonas aeruginosa* (Drusano, 1997). As for IMP, MEM binds with the highest affinity to PBP2 but also to PBP1a and 1b and PBP3 in *E. coli* (Drusano, 1997). Unlike the other β-lactams, monotherapy with MEM or IMP in Gram-negative organisms may lead to a long post-antibiotic effect (PAE), ranging from 2 to 9 h (Zhanel and Craig, 1994). PAE refers to the delayed regrowth of bacteria following short exposure (typically 1 or 2 hours) to an antibiotic (Bowker et al., 1996). Hence, PAE effect allows to administer higher dosages less frequently, resulting in amelioration of bacterial killing. MEM is indeed administered in high-dose intravenous prolonged-infusion to

[2] https://patents.google.com/patent/US4194047

increase the likelihood of target attainment, or, in other words, the bacterial killing (Bulik et al., 2010).

A third carbapenem, ertapenem (ETP) (figure 4b), is licensed in the EU for the treatment of intra-abdominal and gynaecological infections, in addition to community-acquired pneumonia. In USA, ETP is also prescribed in case of skin infections and for severe urinary tract infections (Livermore, 2003). ETP has a broad spectrum of activity as IMP and MEM, but it is less active against non-fermenters (Pseudomonas *spp*. and Acinetobacter *spp*. notably). Similar to MEM and IMP, ETP exhibits the highest affinity for PBP2 in *E. coli*, followed by PBP3, as opposed to IMP, which only shows low affinity for PBP3 (Sumita et al., 1990). In addition, ETP and MEM saturate their primary PBP targets in *E. coli* at lower concentrations than IMP (Livermore, 2003). Since ETP is a larger and negatively charged compound, its permeation of Gram-negative bacteria OM is slower than what seen for MEM and IMP (Nikaido et al., 1983). The half-life of ETP is four times longer than the two other molecules and it could be administrated once a day (Keating and Perry, 2005).

2.2.1.3. β-lactamase Inhibitors

β-lactamase inhibitors are agents blocking the activity of β-lactamases, therefore preventing the hydrolysis of β-lactams. β-lactamase inhibitors are co-administered with β-lactam drugs to restore their efficacy against β-lactamase-producing bacteria (Drawz and Bonomo, 2010). A widely used combination is amoxicillin/clavulanate, first launched as Augmentin[3] in UK in 1981. Clavulanic acid, together with sulbactam and tazobactam, possesses a β-lactam core that undergo chemical modifications to permanently inactivate the β-lactamase (figure) (Abeles and Maycock, 1976), reasons why they are also referred to as "suicide inhibitors".

Alternatively, β-lactamase inhibitors such as avibactam and relebactam do not possess a β-lactam ring and they rather bind reversibly or irreversibly to the active site of β-lactamase with high affinity, resulting in the formation of a covalent acyl-enzyme complex. Avibactam (Novexel, Paris) acts as a reversible inhibitor of all class A and class C β-lactamases, including ESBLs and *Klebsiella pneumoniae* carbapenemases (KPCs) (Bush, 2015). Ceftazidime–avibactam (Avycaz®)[4] was approved by the United States Food and Drug Administration (U.S. FDA) for treatment of serious intra-abdominal and urinary-tract infections, but also hospital-acquired and ventilator-associated pneumonia. Ceftazidime–avibactam combination is also approved for the treatment of nosocomial pneumonia in Europe, and under investigation for infections in pediatric patients (Bradley et al., 2016).

[3] https://patents.google.com/patent/US6756057B2/en
[4] Avycaz® (ceftazidime-avibactam) package insert. 2018. https://www.allergan.com/assets/pdf/avycaz_pi

2.2.2. When are bacteria defined susceptible to antimicrobials?

From a biological perspective, resistance reflects the ability of a microorganism to withstand exposure to a set concentration of an antimicrobial agent. Antimicrobial susceptibility is generally defined based on *in vitro* parameters. According to the ISO 20776-1 standard[5] and EUCAST guidelines[6], bacteria can be classified as *susceptible* or *resistant* to a certain drug based on the probability to successfully treat the infection, they are responsible for. In some cases, bacterial isolates are anciently defined as *intermediate* to a certain drug when the probability to achieve therapeutic success is uncertain. Clinical microbiologists can better evaluate this trait by estimating the minimum inhibitory concentration (MIC)[7] which is the lowest concentration of antibiotic that inhibits bacterial growth over a 20-h period in cultures starting from a standard initial cell density[8]. In addition, a clinician should consider pharmacodynamics and pharmacokinetics (PK/PD) of antibiotics when establishing the necessary doses to eradicate the infection. Resistance is usually attributed when clinical isolates exhibit an MIC above the clinical breakpoints[9,9] and it is often associated with poor treatment outcomes. A bacterial species is defined as *intrinsically resistant* to a given drug if the range of the average MICs across isolates falls in the resistant category[10]. However, resistance can be also acquired, and the reduced susceptibility may vary depending on the isolate under investigation and the acquired resistance genes. Mechanisms behind intrinsic and acquired resistance will be discussed further in this chapter. In some cases, the reduced susceptibility does not result in clinical failure, but it contributes to survival of bacterial populations and future emergence of extremely resistant variants. The word "resistance" indeed does not provide a full picture on the variety of altered susceptibility profiles that might arise upon exposure to antibiotics, not necessarily causing modifications of the MIC.

2.2.3. Why does antibiotic resistance matter?

Antimicrobial resistance (AMR) is a rising global health issue[10]. In EU/EEA countries, drug-resistant pathogens are responsible for approximately 670,000 infections every year, and about 33,000 deaths directly result from these infections (Cassini et al., 2019), with a significant burden on healthcare systems. AMR is also a development and economic challenge, as acknowledged by institutions such as International Monetary Fund (IMF), the World Bank[11],

[5] https://www.iso.org/ref
[6] https://www.eucast.org/fileadmin/src/media/PDFs/EUCAST_files/EUCAST_SOPs/EUCAST_definitions_of_clinical_breakpoints_and ECOFFs.pdf/
[7] "Methods for the determination of susceptibility of bacteria to antimicrobial agents. Terminology," 1998
[8] Clinical and Laboratory Standards Institute (CLSI). Performance Standards for Antimicrobial Susceptibility Testing. 27th ed. CLSI supplement M100 (ISBN 1-56238-804-5 [Print]; ISBN 1-56238-805-3
[9] https://www.eucast.org/clinical_breakpoints/
[10] World Health Organization. (2015). Global action plan on antimicrobial resistance. World Health Organization. https://apps.who.int/iris/handle/10665/193736
[11] World Bank. 2017. "Drug-Resistant Infections: A Threat to Our Economic Future." Washington, DC: World Bank. License: Creative Commons Attribution CC BY 3.0 IGO

World Health Organization (WHO) and the Group of Twenty (G20), calling for urgent need to pledge to united approaches to contain AMR evolution in a One Health perspective. Decades of inadequate use of antibiotics, not only in human medicine but also in the agriculture and livestock production to sustain and indulge humankind's needs[12] have indeed favoured the emergence of drug-resistant isolates by imposing a strong selective pressure on bacterial populations (Shallcross and Davies, 2014).

AMR represent a great challenge in low- and middle-income countries (LMICs), where gathering biological and epidemiological data is challenging, a scarce public awareness and understanding of antibiotics and antibiotic resistance and lack of local guidelines to halt the spread of AMR. Multiple factors have fuelled the dissemination of resistance, resulting in an enormous burden in LMICs. Drivers of resistance may vary from country to country (Iskandar et al., 2020), and even across regions. Although food and water are acknowledged to be a major vehicle of resistance in LMICs, there are multiple socio-economic drivers crucial for selection of bacterial resistance. Among them, one can cite inadequate farmers practices due to poor safety measures and controls (Om and McLaws, 2016), the overuse of antibiotics in farms due to their over-the-counter availability (Borg and Scicluna, 2002) and to their irrelevant price, poor sanitation and scarce hygiene conditions (Iskandar et al., 2020). Other factors contributing to AMR globally include climate change (MacFadden et al., 2018), international travelling and globalization (Schwartz and Morris, 2018), pandemics (Murray, 2020) and residuals of heavy metals and biocides in the environment (You and Silbergeld, 2014). On top of that, the disengagement of pharmaceutical companies in developing new antibacterial agents has worsened the antibiotic resistance crisis.

A plethora of bacterial pathogens has evolved and gained multiple resistance features, which may confer a multi-drug resistant (MDR), extensively-resistant (XDR) or even pan-drug resistant (PDR) phenotype (Magiorakos et al., 2012). Health-care facilities are considered major hotspots for the emergence of new highly resistant bacteria, due to the high incidence of severe infections, the heavy use of broad-spectrum molecules in restricted environments and insufficient hygiene practices (Cassini et al., 2019; David et al., 2019). Hospital acquired infections (HAIs) have a tremendous burden on public health worldwide and substantial repercussions on the global economy. According to WHO[13] and ECDC[14], the number of HAIs per year is estimated at 4.5 million and account for 37,000 attributable deaths in Europe per year. Of great concern is the dissemination of the ESKAPE isolates (Rice, 2008), including the six nosocomial pathogens *Enterococcus faecium*, *S. aureus*, *K. pneumoniae*, *A. baumannii*, *P. aeruginosa* and *Enterobacter spp*. ESKAPE refers also to their ability to effectively *escape*

[12](for the World Healthcare-Associated Infections Resistance Forum participants et al., 2015, 2015)
[13] https://www.who.int/gpsc/country_work/gpsc_ccisc_fact_sheet_en.pdf
[14]European Centre for Disease Prevention and Control. Point prevalence survey of healthcare-associated infections and antimicrobial use in European acute care hospitals – ECDC PPS validation protocol version 3.1.2. Stockholm: ECDC; 2019

antibiotics, a feature that makes them *superbugs*, often associated with enhanced morbidity and mortality, thereby resulting in increased health care costs (Founou et al., 2017). In addition, WHO established in 2017 a list of antibiotic-resistant bacteria with a considerable community- and health-care burden, urgently calling for research and development of new antibiotics (Tacconelli et al., 2018). Carbapenem resistant Enterobacterales (CRE) are among the most critical. Resistance to carbapenem is a relevant public health issue in Europe, with an occurrence above 10% for *K. pneumoniae* in many EU/EEA countries, notably in the southern and eastern part of Europe[15]. Carbapenem resistance often co-occurs with resistance to several other key antimicrobials, dramatically reducing treatment options for invasive infections caused by such MDR bacteria.

2.2.4. Overview on "classical" antibiotic resistance mechanisms

The molecular mechanisms of antibiotic resistance have been widely investigated, further providing us with a better knowledge of structural components and functions of bacterial cells. Overall, bacteria can be naturally resistant or acquire the resistance phenotype to a given drug.

Natural resistance can be constitutive or induced (also known as adaptive resistance). Constitutive resistance is a common trait across microorganisms from the same species, independently of the drug exposure and gain of resistance determinants. Bacteria are commonly intrinsically resistant to a certain drug because naturally devoid of the drug target sites or due to low permeability of the OM and efflux of the antibiotic (Blair et al., 2015). For instance, Gram negative bacteria's OM is an efficient barrier for the entry of many large compounds like vancomycin, instead effective against Gram-positive bacteria (Blair et al., 2015). With the advent of high-throughput technologies, several studies have demonstrated that additional genetic loci also contribute to intrinsic resistance (Blake and O'Neill, 2013; Fajardo et al., 2008). More recently, the whole repertoire of chromosomally encoded, non-acquired elements directly or indirectly affecting resistance has been indicated as "intrinsic resistome" (Olivares et al., 2013). However, it is important to distinguish the concept of "intrinsic resistance" from "intrinsic resistome". The latter encompasses not only the classical resistance determinants but also genes involved in metabolic processes and bacterial physiology, for which mutations are selected in the presence of sub-inhibitory doses of antibiotics (Prim et al., 2017). About 3% of a bacterial genome was estimated to belong to the intrinsic resistome (Olivares et al., 2013). Conversely, intrinsic resistance refers to a trait that exist independently of the antibiotic selective pressure and usually not transferable by HGT (Prim et al., 2017).

A relatively unexplored mechanism of resistance is adaptive resistance (AR). Environmental cues, e.g., stress, starvation, growth state, and subinhibitory levels of the antibiotics, can cause a transient resistance to a given antibiotic by the mean of alterations in

[15] European Centre for Disease Prevention and Control. Antimicrobial resistance in the EU/EEA (EARS-Net) - Annual Epidemiological Report 2019. Stockholm: ECDC; 2020

gene and/or protein expression in response to the environmental trigger. In contrast to intrinsic resistance, which is a stable trait that can be passed to the offspring, adaptive resistance confers a temporary resistant phenotype, which is rapidly loss in the absence of the inducing condition. Main mechanisms regulating the emergence of adaptive resistance are dysregulation of porins and efflux pumps (Fernández and Hancock, 2012). For instance, *E. coli* exposed to tetracycline may display a downregulation of a number of porins (Lin et al., 2010) or, subinhibitory concentrations of the non-antibiotic drug diazepam deplete porin expression and induce efflux systems in *E. coli* and *K. pneumoniae*, thereby promoting emergence of adaptive resistance and cross-resistance to other drugs, e.g., nalidixic acid, and β-lactams (Tavío et al., 2004). An additional example is the indole-induced expression of multidrug efflux pump genes (e.g. *acrD*, *mdtA*) in *E. coli* (Hirakawa et al., 2005).

Bacterial populations can also acquire resistance through mutations in the chromosome or due to the gain of antibiotic resistance genes (ARGs) by HGT. The resistance phenotype might emerge from a large bacterial population exposed to antibiotics, for instance during the treatment of an infectious episode, following Darwin's theory of natural selection (Amábile-Cuevas, 2013). The mutations can indeed be beneficial in a particular environment, allowing bacteria to grow better and multiply. Acquired resistance represents a major concern, especially when mediated by HGT, which promotes rapid and successful dissemination of ARGs intra- and inter-species. Lateral transfer of resistance determinants is mediated by mobile genetic elements (MGEs) including plasmids, transposons, integrons, insertion sequences (ISs) and integrative and conjugative elements (ICEs), altogether constituting the "mobilome" (Gillings, 2013). Common platforms are large, conjugative plasmids, which often co-carry multiple resistance genes. The mobilome implements the diversity within prokaryote genomes by recombination of mobile elements and contributes to enrich the resistome (Garriss et al., 2009; Toussaint and Chandler, 2012). In addition, albeit not transferable *per se*, some of the genes conferring intrinsic resistance have been captured into such mobile genetic elements, and subsequently transmitted to a broad range of bacterial species. Examples include the ESBL $bla_{\text{CTX-M-8}}$ gene, likely originating from *Kluyvera georgiana* (Poirel et al., 2002), or the colistin resistance gene mcr-2 from *Moraxella pluranimalium* (Poirel et al., 2017). Additionally, genes encoding plasmid-mediated AmpC β-lactamases, originally located in the chromosome of several Enterobacterales (Jacoby, 2009), have also moved onto MGEs and disseminate among different species (e.g., bla_{DHA}-like from *Morganella morganii* or bla_{CMY}-like from Citrobacter *spp.*).

Overall, major molecular mechanisms providing natural or acquired resistance include prevention of drug access to targets due to altered membrane permeability or hyperactivation of efflux-pumps, modification of the drug target site, drug modification and drug cleavage mediated by enzymes (Figure 6).

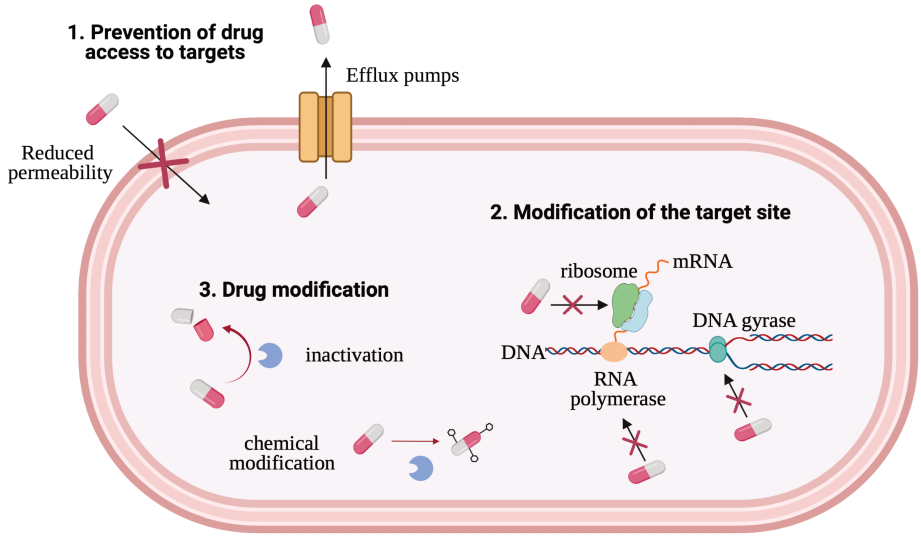

Figure 6: Major underlying mechanisms of antibiotic resistance. 1. Antibiotic resistance can arise upon alteration of the membrane permeability or overexpression of efflux pump systems that prevent the entry of the drug within the cell or the periplasm; 2. Modification of the drug target sites, e.g., ribosome, RNA polymerase or DNA gyrase as in the case of fluoroquinolone resistance, lead to drug insensitivity. 3. Drug modification. For example, β-lactams resistance can involve their enzymatic hydrolysis; enzymatic transfer of chemical groups to the drug molecule can mediate resistance to aminoglycosides, impairing the binding of the drug to its bacterial target. Created with BioRender.com

2.2.4.1. β-lactam resistance and β-lactamases

In Gram Negative bacteria, β-lactam antibiotics enter the cell through the porins in the OM, and bind to their target, the PBPs, to inhibit the cell wall biosynthesis (figure 7). Resistance may arise through three main events: (i) enzymatic degradation by β-lactamases (ii) alteration of membrane permeability and efflux of β-lactams and, (iii) target alterations or the synthesis of targets with reduced affinity to β-lactams.

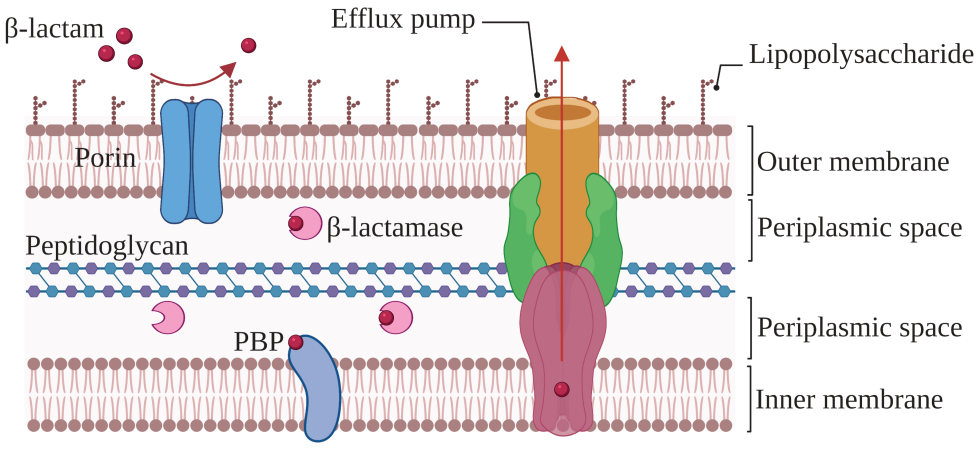

Figure 7: Common mechanisms causing β-lactam resistance. β-lactamases are in the periplasmic space, where they can compete with PBP to bind to β-lactam molecules. Other mechanisms involve efflux pump or altered OM permeability, which impedes or reduce the entry of the β-lactam drugs. Created with BioRender.com

2.2.4.1.1. Enzymatic degradation by β-lactamases

Production of β-lactamases is a major mechanism of β-lactam resistance in Gram negative bacteria. These enzymes are usually located in the periplasmic space, where the cleavage of the β-lactam ring occurs (Pradel et al., 2009). The first β-lactamase identified in Gram negatives was the cephalosporinase AmpC of *E. coli* (Abraham and Chain, 1988), although originally not designated as such. β-lactamases may be chromosomally or plasmid-encoded (Nikaido et al., 1983). According to the Ambler scheme (Ambler, 1980), β-lactamases are classified into four groups (A, B, C and D) based on their amino acid (AA) motifs (Ambler, 1980). In addition, classes A (penicillinases), C (cephalosporinases), and D (oxacillinase) can be grouped into serine β-lactamases, whereas the B group includes the metallo-β-lactamases (MBL).

Serine β-lactamases (SBLs) share an Ser-Xaa-Xaa-Lys motif with PBP (Tooke et al., 2019) and the serine moiety in their active site is employed for the two-step antibiotic inactivation (Figure 8). The formation of the acyl-enzyme complex is followed by the opening of the β-lactam ring and antibiotic hydrolysis (Figure 8).

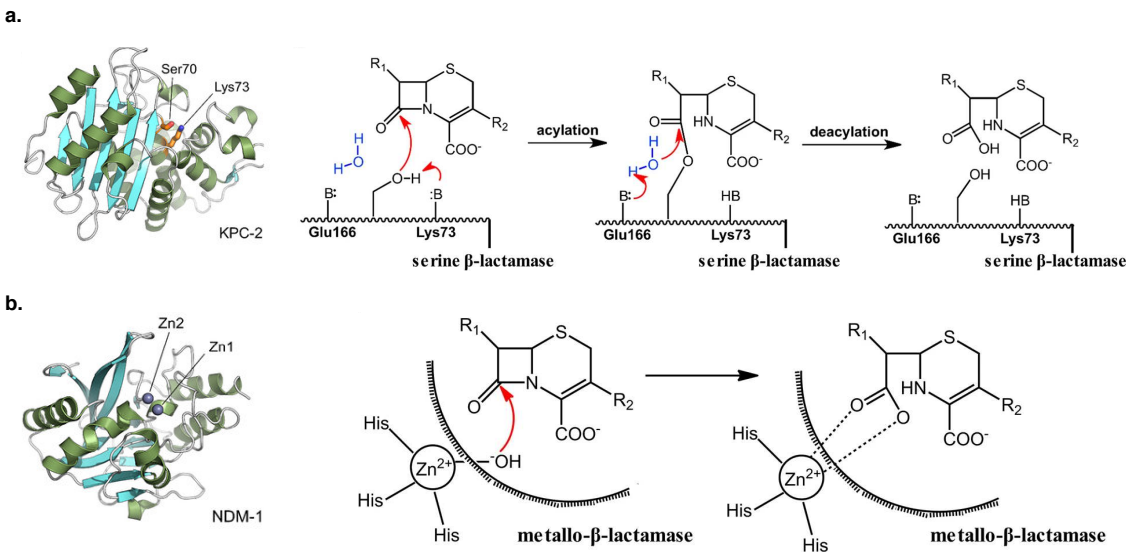

Figure 8: The distinct catalytic mechanisms of β-lactamases from Class A to B. (a) Example of structure of serine-β-lactamase (KPC-2). Serine-based β-lactamases inactivate the drug in a two-step process. Key components of the catalytic process and AA residues from Class A are highlighted, (b) Example of structure of metallo-β-lactamase (NDM-1). Class B metallo-β-lactamases employs Zn^{2+}ions for the catalytic process. Here only one Zn^{2+}ion is shown, but some Class B metallo-β-lactamases possess two Zn^{2+} ions in the active site. Adapted from He Y *et al.*, Sci Rep 2020.

In **class A β-lactamases**, the serine residue is important for the catalytic activity, whereas Lys73 and Glu166 (KPC-2 numbering) are employed for acylation and deacylation steps, respectively (Figure 8a). Clinically relevant serine-β-lactamases include notably ESBLs (e.g., CTX-M-like enzymes), and *K. pneumoniae* carbapenemases (KPC). KPC enzymes act also on carbapenems, including imipenem, ertapenem, meropenem, or doripenem. First detected in *K. pneumoniae*, KPC disseminated to other Gram-Negative bacilli, likely facilitated by the

location of KPC onto a broad diversity of plasmids (Yigit et al., 2001) and association with successful clonal lineages (as ST258). CTX-M enzymes, like other ESBLs, show an extended hydrolytic spectrum, including third and fourth generation cephalosporins, monobactams except cefoxitin and carbapenems. CTX-M dissemination has been referred to as "CTX-M pandemic" due to the increasing number of descriptions worldwide (Cantón and Coque, 2006). As for KPC, the successful dissemination might be justified by the genetic surroundings of $bla_{\text{CTX-M}}$ genes, often highly mobilizable plasmids and transposons, but also because of their association with successful clones like *E. coli* ST131 (Cantón and Coque, 2006).

Class C β-lactamases, alternatively indicated as cephalosporinases, were originally detected in the chromosome of several Gram-Negative bacteria, conferring resistance to cephalothin, cefazolin, cefoxitin and most penicillins. A clinically relevant example is the inducible chromosomal AmpC β-lactamase, found in Enterobacter and Klebsiella *spp.* (Fisher and Mobashery, 2014), and constitutively expressed at a very low level in *E. coli* (Jaurin et al., 1981). *Cis* and *trans* mutations in the regulatory cascade lead to high and constitutive expression of *ampC* (Caroff et al., 2000). In *E. coli*, due to the absence of the cascade, only *cis* mutations in the *ampC* promoter/attenuator region (Jaurin et al., 1981) and gene amplifications (Edlund and Normark, 1981) have been observed, all leading to constitutive overexpression of *ampC*. In addition, Enterobacterales may acquire plasmid-borne *ampC* genes by HGT (Mata et al., 2012).

Class D β-lactamases, or oxacillinases, are a very heterogeneous group of enzymes. Currently, there are 1046 unique OXA sequences identified[16]. Located on both chromosomes and mobile elements, OXA-type encoding genes have been identified in diverse bacterial species such as *Acinetobacter*, *Shewanella*, *Pseudomonas*, and *Burkholderia* (Poirel et al., 2010; Sanschagrin et al., 1995). OXA enzymes usually exhibit narrow substrate profile, acting only on penicillins and first generation cephalosporins. Extended spectrum of activity allows hydrolysis of later generation cephalosporins and, in some cases, of carbapenems. OXA-23-like β-lactamases, OXA-40-like, OXA-48-like, OXA-58-like are among the most diffused variants that also show activity against carbapenems (Evans and Amyes, 2014). The OXA-48-like enzymes hydrolyze carbapenems less efficiently than KPC carbapenemases and Metallo-β-lactamase (MBLs) but can yield to higher levels of carbapenem resistance when associated with impaired OM permeability and ESBLs carriage (Poirel et al., 2012).

Class B or Metallo-β-lactamases (MBLs) differ from serine-β-lactamases because they require a zinc ion for β-lactam hydrolysis (Figure 8b). The active site of MBLs can have up to two zinc-ion binding sites, which are not conserved between the different MBLs and exhibit different metal-ion affinities (Page and Badarau, 2008). MBL enzymes are further divided into three subgroups - B1, B2, and B3, based on structural differences and substrate profiles. B1 subclass include the clinically relevant IMP, NDM, and VIM types (Makena et al., 2015b; Nordmann et al., 2011; Zhao and Hu, 2011). These β-lactamases display hydrolytic activity towards several narrow-spectrum β-lactams except for monobactams (Boyd et al., 2020;

[16] http://bldb.eu/

Marshall et al., 2017). In addition, B1-types hydrolyze carbapenems, like imipenem and meropenem. For instance, NDM-1 displays similar catalytic activity for imipenem (0.09 $\mu M^{-1} s^{-1}$) and meropenem (0.06 $\mu M^{-1} s^{-1}$) (Shen et al., 2013). Typically, genes encoding IMP and VIM enzymes are embedded in class I integrons (Walsh et al., 2005). Conversely, *bla*$_{NDM}$ genes are dispersed across a broad diversity of plasmid types as IncF, IncA/C, IncL/M, IncH, and IncN associated to IS*Aba125*-based transposon (Bonnin et al., 2012; Villa et al., 2010) within diverse host genetic backgrounds (Mathers et al., 2015).

On the other hand, B2 and B3 MBLs are ubiquitously distributed across species and they are usually not transmissible because of their chromosomal location. Exceptions include the subclass B3 enzymes AIM-1, whose encoding gene was originally found in the chromosome of a *P. aeruginosa* isolate but later detected in *K. pneumoniae* (Zhou et al., 2019), and *bla*$_{LMB-1}$ gene, which was found to be flanked by ISCR mobilization sequences on a plasmid in *Rheinheimera pacifica*, suggesting previous acquisition from another organism (Dabos et al., 2020).

MBLs from subclass 2 (example CphA from Aeromonas *spp.*) are active exclusively against carbapenems (Naas et al., 2017), whereas B3 enzymes can hydrolyze several β-lactams, including monobactam. Irrespective of subclass, metal chelators such as ethylenediaminetetraacetic acid (EDTA) (Drawz and Bonomo, 2010) inhibit MBLs activity but not clavulanic acid, sulbactam, tazobactam, or avibactam (Boyd et al., 2020).

2.2.4.1.2. Alteration of membrane permeability and efflux of β-lactams

In Gram-negative bacteria, the OM is the outermost layer of bacterial cell wall. It allows the uptake of nutrients, passive diffusion of small hydrophilic substances through transmembrane channels named as outer membrane porins (OMPs) (Delcour, 2009). Porins are homotrimers of β-barrel giving rise to a central pore, which allows the passage of molecules, including toxic compounds like antibiotics. In addition, porins act as osmolytes, preventing osmotic shock due to accumulation of detergents within the cell.

Structural changes within porins, loss of their function or complete inactivation by mutations can lead to reduced permeability to antibiotics and acquisition of resistance. In *K. pneumoniae*, the major porins are OmpK35 (homolog of OmpF in *E. coli*) and OmpK36 (homolog of OmpC in *E. coli*) (Sugawara et al., 2016). Similar to what observed for *ompC* and *ompF* genes in *E. coli*, osmoregulation of *K. pneumoniae* porins depends on the two-component system (TCS) EnvZ-OmpR (Tsai et al., 2011). Under high-osmolarity conditions, phosphorylation of the transcriptional regulator OmpR by the sensor kinase EnvZ activates *ompK36* transcription and represses *ompK35*. Conversely, in low-osmolarity conditions, OmpK35 is the expressed porin (Tsai et al., 2011). OmpK35 pore is wider than *E. coli* OmpF and it allows a rapid transport of substances such as β-lactams, especially hydrophobic and large compounds, e.g., cefepime. Hence, *ompK35* deletion leads to drastic decrease of susceptibility levels to cephalosporins. On the other hand, deletion of *ompK36* alone does not have a large impact on most of the antibiotic MICs, except for cephalotin and ceftriaxone (Sugawara et al., 2016). Interestingly, most of carbapenem-resistant *K. pneumoniae* clinical isolates lack the major porins (Clancy et al., 2013;

Poulou et al., 2013). Double porin mutants (Δ*ompK35*Δ*ompK36*) show increased resistance levels in bacterial strains harbouring β-lactamases, although associated with a reduction of relative growth in nutrient media, suggesting a high fitness cost (Fajardo-Lubián et al., 2019; Sugawara et al., 2016). However, another study reported that double deletion mutants Δ*ompK35*Δ*ompK36* retain susceptibility to ceftaroline (Khalid et al., 2020), likely due to the use of alternative channels for diffusion of the β-lactam drug when the main porins are absent, as previously showed (Beceiro et al., 2011).

Another common mechanism yielding to β-lactam resistance involves efflux systems. Efflux pumps are membrane bound proteins that play a role in the regulation of cellular homeostasis by expelling toxic substrates, fatty acids, heavy metals, and, most importantly, antibiotics from the cell towards the environment (Du et al., 2018). Efflux pumps are ubiquitously distributed across different bacterial species and they are distinguished into six families, including the ATP-binding cassette (ABC) family, the major facilitator superfamily (MFS), the multidrug and toxin extrusion (MATE) family, the small multidrug resistance (SMR) family, the resistance-nodulation-cell division (RND) superfamily and the proteobacterial antimicrobial compound efflux (PACE) family (Du et al., 2018). In Gram negative bacilli, the RND efflux pumps are usually trimeric channels with various sizes and high degree of permeability that contribute to resistance to multiple drugs in clinical isolates of *K. pneumoniae* (Padilla et al., 2010; Zhong et al., 2014), *E. coli* (Oethinger et al., 2000; Okusu et al., 1996) and *P. aeruginosa* (Kriengkauykiat et al., 2005). The most investigated RND in *E. coli* and *K. pneumoniae* is the efflux pump AcrAB-TolC, which is a tripartite complex including the periplasmic protein AcrA, the constituvely expressed pump AcrB and the outer membrane porin TolC (Pos, 2009). TolC takes part to other tripartite efflux systems including MFS, e.g., the EmrAB-TolC pump (Lewis, 2000), and ABC-superfamily transporters, e.g., the MacAB-TolC pump (Turlin et al., 2014). The AcrAB-TolC is an example of a proton motive force (PMF)-driven efflux pump, where the pulse of cations guides the entry and subsequent exclusion of substrates such as multiple antibiotics, dyes, bile salts and detergents (Pos, 2009). Despite the broad substrate specificity, the efflux pump AcrAB-TolC in *E. coli* does not contribute to resistance to small hydrophilic β-lactams. Indeed, owing to their size and charge, such molecules can still cross very efficiently the OM of WT cells through the porins. For instance, the speed of penicillin influx through AcrB is ~0.3 nmol/s/mg cells (Lim and Nikaido, 2010), being slower compared to the expected influx rate through the OM, which accounts for ~10 nmol/s/mg (Li et al., 2015). This means that efflux of small hydrophylic β-lactams has only a minor effect on the MIC in *E. coli*, as confirmed by Mazzariol A and co-workers (Mazzariol et al., 2000). However, hydrophobic, e.g., oxacillin or cloxacillin, or large (third- or fourth-generation cephalosporins) β-lactams have a much slower turnover rate through the OM, and the exclusion of the drug mediated by AcrB can be determining for the MIC values (Mazzariol et al., 2000).

Since the pioneering study of Pages *et al*., increasing evidences highlighted the complex interplay between efflux mechanism, β-lactamase production and impaired membrane permeability and its contribution to β-lactam susceptibility of *K. pneumoniae* isolates (Pages et al., 2009). In some clinical isolates, overproduction of RamA - a global transcription activator (George et al., 1995), leads to upregulation of *acrAB-tolC*-mediated efflux and down-regulation of *ompK35*, resulting in an overall increase of MICs of β-lactams (Källman et al., 2009, 2008; Saw et al., 2016). Other examples of drug efflux systems and their implication in antimicrobial resistance include the efflux pump MexAB-OprM of *P. aeruginosa*, responsible for reduced susceptibility to a variety of drugs including β-lactams (Horna et al., 2018); the OqxAB (Li et al., 2019) and MacAB (Fitzpatrick et al., 2017) systems, whose overexpression has been associated with eravacycline resistance and heteroresistance in clinical isolates of *K. pneumoniae* (J. Zheng et al., 2018).

2.2.4.1.3. Target alterations

Several bacterial species may acquire resistance to β-lactams through mutations in the PBPs sequences or, alternatively, by gaining modified PBPs with low β-lactam affinity. This mechanism has been extensively observed in clinically relevant Gram-positive bacteria, e.g., *S. aureus* showing reduced susceptibility to β-lactams upon acquisition of a *mecA* gene encoding PBP(2A), responsible for the Methicillin-Resistant Staphylococci (MRSA) (Pinho et al., 2001). The *mecA* gene is located on a chromosomal cassette (SCCmec), predicted to be acquired by HGT from a coagulase-negative staphylococcus species (Shore and Coleman, 2013). In Gram-negative bacteria, this mechanism is rare but some examples include alterations of genes encoding PBP2 (Spratt, 1988) and PBP1 (Ropp et al., 2002) in *Neisseria gonorrhoeae*, the PBP3 in *Haemophilus influenzae* (Matic et al., 2003) and the PBP4 in *P. aeruginosa* (Moya et al., 2009). Likewise, clinical isolates of *Helicobacter pylori* display increased resistance to amoxicillin due to alterations in *ftsI*, the gene encoding PBP3 (Rimbara et al., 2018). Recently, it was also reported that mutations in *ftsI* gene encoding PBP3 from *E. coli* ST38 lead to reduced susceptibility to diverse β-lactams (Patiño-Navarrete et al., 2020).

2.2.5. The role of bacterial metabolism in antibiotic resistance

There is a growing body of evidence proving the existence of a crosstalk between metabolism and resistance to an antibiotic agent. On the one hand, the antibiotic susceptibility might depend on the physiological state of the bacteria. For instance, stationary phase (non-growing) bacteria are less susceptible to diverse antibiotics than exponentially growing bacteria and starvation, by inducing the stringent response, leads to a dormant state, thereby contributing to treatment failure (Lewis, 2007). Likewise, pre-treatment with chloramphenicol inhibits bacterial growth, and, in parallel, induces resistance to ß-lactams, as observed already in 1950 in *Enterococci* (Jawetz et al., 1950). On the other hand, antibiotics have an impact on bacterial metabolism and physiology (Stokes et al., 2019). Although alterations have been shown as drug-specific (Hoerr et al., 2016; Vincent et al., 2016), common metabolic changes across

antibiotics with similar modes of action can be tracked to uncover molecular targets of novel antibiotics (Vincent et al., 2016; Zampieri et al., 2017b). In line with these observations, numerous mutations in metabolic functions contributing to a decrease of susceptibility to diverse antibiotics have been characterized in several bacterial species like *E. coli* and *S. aureus*. Hence, metabolic functions have been included in the intrinsic resistome (Baquero and Martínez, 2017). *E. coli* mutants deficient for the metabolic enzyme isocitrate dehydrogenase have been shown to be resistant to nalidixic acid (Helling and Kukora, 1971). In addition, deoxythymidine 5′-diphosphate (dTDP)-rhamnose synthesis plays a crucial role in the rapid upregulation of *gyrA* in response to quinolone antibiotics (Zampieri et al., 2017b).

Alterations in metabolic pathways may also lead to other phenotypic changes underlying acquisition of resistance. Small colony variants (SCVs) are atypical colonies with a pinpoint appearance exhibiting slow growth, usually due to mutations in the thymidylate synthase gene (Besier et al., 2007; Chatterjee et al., 2008) or defects in the electron transport chain (ETC), due to altered menadione or hemin biosynthesis (Dean et al., 2014; von Eiff et al., 1997). Originally recovered from clinical samples of *S. aureus* (Johns et al., 2015; Proctor, 2019), SCVs have been also detected in several other pathogens as *P. aeruginosa* (Evans, 2015), *E. coli* (Colwell, 1946), *K. pneumoniae* (Ronde-Oustau et al., 2017; Silva et al., 2016). SCVs are associated with chronic infections (Evans, 2015; Johns et al., 2015) and antimicrobial resistance (Singh et al., 2009). Notably, SCVs in *S. aureus* have been associated with reduced susceptibility to aminoglycosides (Proctor, 2019). In *E. coli*, SCVs were found in strains mutated for *ygiP* (also named *ubiJ*), showing impaired ubiquinone biosynthesis and resistance to erythromycin, kanamycin and D-cycloserine (Xia et al., 2017). Likewise, SCVs have been associated with heterogeneous resistance to colistin in *K. pneumoniae* (Silva et al., 2016). From a practical point of view, since their growth can take up to 48-72 hours, classical AST may be not optimal to estimate the drug resistance levels in these variants (Proctor and von Humboldt, 1998).

In vitro screening procedures have been developed to select and enrich for metabolic mutations (Van den Bergh et al., 2016). Recently, Lopatkin *et al*., set up cycling exposure to three representative bactericidal drugs (streptomycin, ciprofloxacin and carbenicillin) with increasing temperature during the selection phase to increase the metabolic activity (Lopatkin et al., 2021). By using this strategy, they selected alterations in metabolic genes, although at lower frequency compared to canonical resistance mutations in conventional experimental evolution screening. Such modifications lead to reduced cellular respiration activity, unsuccessful activation of the TCA cycle mediating the drug toxicity and ultimately, failed drug lethality. For example, mutations in *icd*, *purH* and *fre* were detected upon treatment with ciprofloxacin or streptomycin and, notably, these mutations were also shown to be overrepresented in a collection of 7243 *Escherichia coli* genomes, suggesting a potential clinical relevance (Lopatkin et al., 2021).

How bactericidal antibiotics kill bacteria is likely a multifactorial process. The cell death has been associated with the cell's metabolic state (Kohanski et al., 2007; Wang and Zhao, 2009). The proposed model argues that bacteria exposed to bactericidal antibiotics alter their

cellular metabolic state, in which malfunctioning of the tricarboxylic acid (TCA) cycle and hyper stimulation of the electron transport chain leads to destabilization of iron-sulfur (Fe-S) clusters, formation of hydroxyl radicals by Fenton chemistry and eventually cell death (Figure 9)(Keaton et al., 2013; Kohanski et al., 2010).

However, following these publications, several studies presented divergent findings. For instance, Keren and co-workers showed that killing of bactericidal antibiotics is unrelated to ROS accumulation but rather depends on antibiotic concentrations (Keren et al., 2013). In addition, these authors did not observe any difference in the killing activity of norfloxacin and ofloxacin between aerobic and anaerobic conditions, whereas ampicillin and low doses of kanamycin under anaerobic conditions exhibited slightly higher killing activity. Ezraty *et al*., showed that aminoglycoside-induced lethality was not due to ROS production but rather to the enhanced drug uptake mediated by proton motive force (PMF) generated by Fe-S clusters, which mature the respiratory chains (Ezraty et al., 2013). However, they did not observe the same results with β-lactams (ampicillin), suggesting alternative routes that these drugs employ to achieve bacterial killing. Altogether, these data suggest that assuming that there is a unified mechanism of killing across all bacterial species, all antibiotics and perhaps even all antibiotic concentrations is very likely an underestimation of the complex biology of bacteria. Acquisition of resistance might lead to a fitness cost, which has been shown to be suppressed by mutation leading to functional metabolic rearrangements, as observed by metabolomics of bacterial populations that evolved resistance to a given drug (Zampieri et al., 2017a) or by transcriptomic analysis of an amoxicillin-resistant *E. coli* isolate (Händel et al., 2013).

These intriguing results should be a springboard to further exploring the interplay between the metabolic state of cells and antibiotic resistance. Remarkably, understanding this crosstalk may offer an insight into the optimization of current treatment regimens and lead to the discovery of alternative antimicrobial therapeutic strategies (Baquero and Martínez, 2017; Stokes et al., 2019).

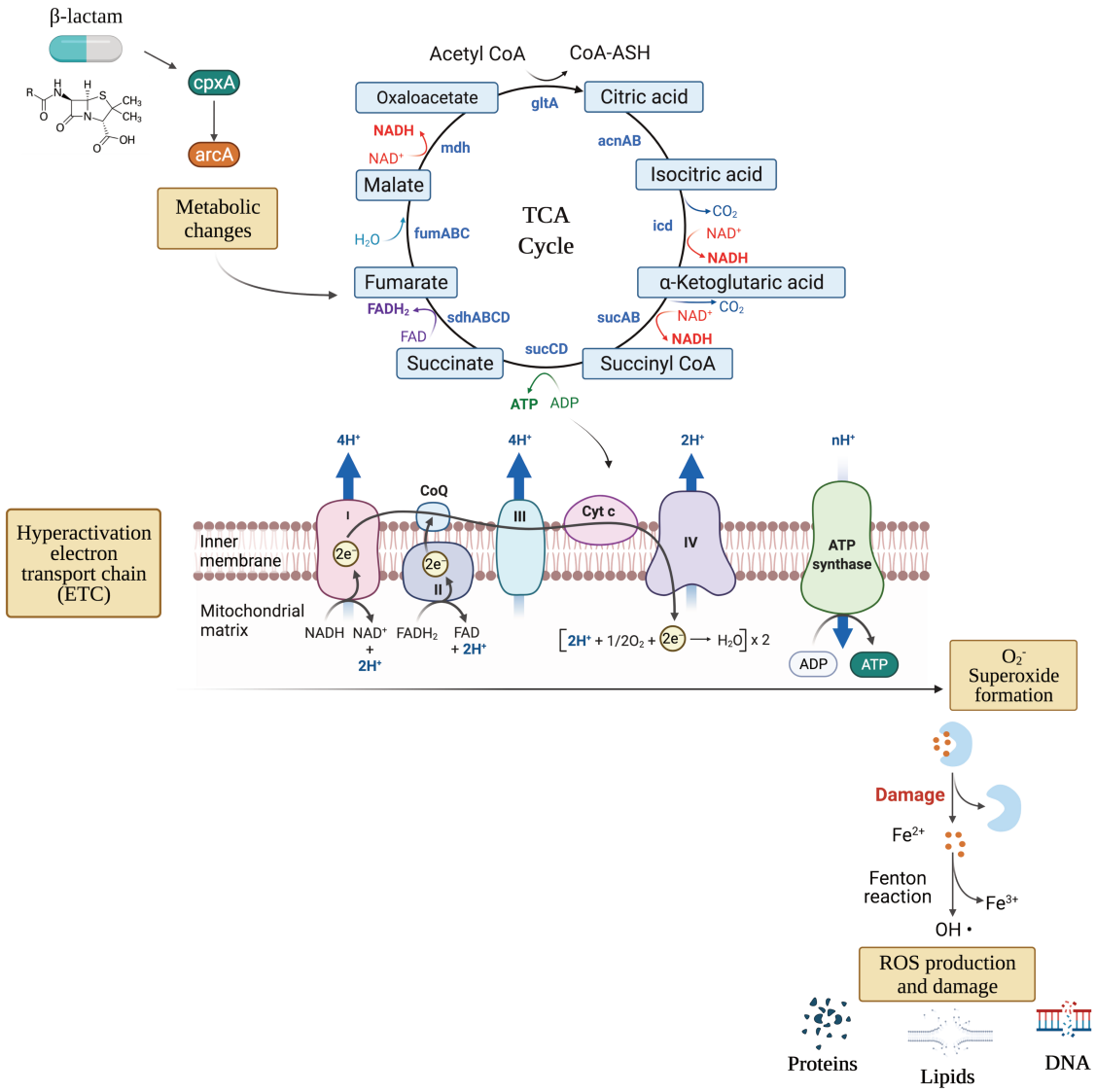

Figure 9: Proposed model of ROS-mediated antibiotic killing. Bactericidal antibiotics, e.g., β-lactams, cause metabolic dysfunctions (likely due to activation of two-component system ArcA through CpxA) that stimulate the TCA cycle, hyperactivation of the electron transport chain (ETC) and formation of superoxide radicals (O_2^-). Destabilized ferrous iron from damaged Fe-S clusters leads to the accumulation of hydroxyl radicals (ROS) which damage proteins, lipid, and DNA. Created with BioRender.com

2.2.6. Enhancing bacterial survival through phenotypic heterogeneity

Microbial populations inhabit multiple and diverse niches, facing oscillations between abundance of nutrients, which allows a prolific bacterial growth, and hostile environments, whereby individuals adopt strategies to cope with limited nutrient. In addition, human activities are drastically shaping the climate and environment, increasingly forcing microbes to confront perturbations (Cavicchioli et al., 2019). Understanding the trajectories driving adaptation to unpredictable fluctuations in microbial populations may provide relevant insights into the dynamics of bacterial life.

Classically, rapid adaptation to environmental changes can be achieved *via* gene expression regulation, but also by the selection of stable *de novo* mutations (Andersson et al., 2015), alterations in gene dosage and copy number (Andersson and Hughes, 2009; Laehnemann et al., 2014) or by gene exchange through HGT (Gogarten and Townsend, 2005). In addition, standing genetic variation, i.e., the fixation of alternative alleles of small effect at a given locus and the spread of more recessive alleles (Barrett and Schluter, 2008), provides a fast adaptation to changing environments (Matuszewski et al., 2015). The foodborne pathogen *Campylobacter jejuni*, for example, contains multiple contingency *loci* (Parkhill et al., 2000), also referred to as hypermutable DNA regions that allow adaptation during serial passage in a mouse model of campylobacteriosis (Jerome et al., 2011). Other examples of contingency *loci* include genes involved in the biosynthesis of LPS and capsule polysaccharide (Lukácová et al., 2008; Salvatore et al., 2002), providing bacterial populations with the capacity to counteract the host immune response and improve colonization of ecological niches.

Although individuality in bacteria was already noticed in 1976 in cells from the same *E. coli* population exhibiting slightly different swimming behaviours in response to a temporal gradient of serine (Spudich and Koshland, 1976), it is only with recent single-cell based technologies that we could appreciate and quantify phenotypic cell-to-cell variability within a bacterial population in a given environment (X. Wang et al., 2014), therefore improving the understanding of the phenomenon.

Phenotypic diversification may arise from random variation in biological processes, hereto referred as "noise" (Davidson and Surette, 2008), or enhanced by environmental stimuli e.g., starvation, nutrient limitation, antibiotic exposure and depending on regulatory networks (Geiger et al., 2014; Zhu et al., 2019). Such phenotypic diversification can reflect a *bet-hedging* strategy, whereby at least one fraction of cells ensures the trade-offs in fecundity and longevity in case of abrupt environmental shift and maximize the fitness of the population (Grimbergen et al., 2015). One typical biological example of bet-hedging is the sporulation process, activated upon starvation for carbon and/or nitrogen, whereby bacteria can switch with different kinetics to dormant, thick-walled structures named as spores (Tam et al., 2006). Although formation of an endospore is a costly, low-fecundity trait, it ensures endurance of bacterial populations to a number of stressors, including antibiotic assault (Gray et al., 2019; Nicholson et al., 2002), until the surrounding conditions become permissive again for growth and reproduction (Paredes-Sabja et al., 2011). Alternatively, the *division of labor* will contribute to microbial survival by promoting the emergence of subpopulations that perform distinct metabolic roles, as classically observed in the matrix biofilm formation (Dragoš et al., 2018).

Phenotypic heterogeneity can also play a role in pathogenesis. For instance, clonal populations of *Salmonella enterica* serovar *Typhi* show bistable expression of Type III Secretion System 1 (T3SS-1), a key factor in Salmonella pathogenesis in the mouse gut and under laboratory conditions that mimic the intestinal environment (Sánchez-Romero and Casadesús, 2018). Such bistability promotes a successful intestinal infection and survival against antibiotics (Arnoldini et al., 2014).

Another example is given by phenomena of phase variation, a reversible on-off switching in the expression of surface factors, e.g., type I fimbriae or the methylation-dependent Ag43 in *E. coli* (Henderson et al., 1999; Wallecha et al., 2002). Moreover, the enteropathogenic *E. coli* (EPEC) has been shown to undergo differentiation into non-virulent and hyper-virulent subpopulations, which also yields to heterogeneous colony variants with slow growing and fast growing bacteria detected by using the ScanLag system (Levin-Reisman et al., 2014). Altogether, these studies highlight the relevant role of *in vitro* single-cell analysis to gain further insights on *in vivo* properties of bacterial populations contributing to their adaptation and survival.

2.2.6.1. Phenotypic heterogeneity and antimicrobial resistance

We have been used to think of bacterial resistance as clear-cut scenario, whereby susceptible cells exposed to bactericidal concentrations of antibiotic are killed, whereas survivors are simplistically indicated as "resistant". Somewhere along the line, we came to an understanding of the complexity of the bacterial response to antibiotics. Just like in the case of harsh environmental conditions like starvation, bacterial populations exposed to antibiotic exposure might diversify into distinct subpopulations to ensure their longevity. Alternative phenotypic strategies include tolerance, persistence and heteroresistance (Aertsen and Michiels, 2005; Smits et al., 2006). Before diving deeper into these strategies, it is indispensable to recall the definition of resistance; resistance is a *stable* and *inheritable* trait that enables bacteria to withstand high concentrations of antibiotic, regardless the length of the treatment (Brauner et al., 2016). As stated above, bacteria can be intrinsically resistant to a certain drug or gain resistance by *de novo* mutation or acquisition of ARGs via HGT. Despite being conceptually and mechanistically different from resistance, these alternative strategies may constitute a stepping-stone for further evolution of resistance and, eventually, contribute to therapeutic failure (Band and Weiss, 2019; Levin-Reisman et al., 2017; Windels et al., 2019).

2.2.6.2. Antibiotic tolerance and persistence (with a focus on β-lactams)

Tolerance is defined as the ability of a bacterial population to survive otherwise lethal doses of bactericidal antibiotics (Brauner et al., 2016). If the tolerance phenotype involves only a fraction of populations, this is referred to as "heterotolerance" or persistence (Balaban et al., 2019). Tolerance and persistence do not affect the susceptibility levels of bacterial population (Balaban et al., 2019), as opposed to resistance that causes increase of the MIC.

The concept of persistence in bacteria was already introduced in 1944, when Joseph Bigger noticed that only few cells survived to penicillin in homogeneous cultures of *Staphylococcus pyogenes* (now *S. aureus*) (Bigger, 1944). Persister cells are indeed rare non-growing variants, transiently refractory to high doses of bactericidal antibiotics that can revert to a susceptible phenotype when the antibiotic is removed. The persistent subpopulation is heterogeneous (Balaban et al., 2004) and can be further distinguished into: type I persisters, which are generated by a trigger event e.g., starvation during stationary phase, thus also referred to as

"triggered persistence" and type II persisters, which are continuously generated during the growth of the population, alternatively indicated as "spontaneous persistence" (Gefen et al., 2008). Both types can restore the susceptible phenotype by resuming normal growth upon drug removal.

2.2.6.2.1. How to quantify tolerance and persistence

Despite the growing interest towards tolerance, experimental techniques to measure this phenotype are not completely established. For clinical purposes, tolerance was originally attributed to clinical isolates exhibiting a MBC significantly greater (usually 32-fold) than the MIC, where the MBC is defined as the lowest concentration of antibacterial agent that reduces the viability of the initial bacterial inoculum (typically 99.9%) (van Asselt et al., 1996). The MBC can be determined by assessing the viability (CFU/mL) of a bacterial culture challenged with antibiotic concentrations above the MIC over a 24 h period or at a single time point after a broth microdilution assay (Figure 10).

However, the MBC method can easily produce artifacts due to technical aspects such as Eagle effect[17], type of tubes used (adherence may give rise to erroneous results), the bacterial phase growth[18], the number of bacteria in the inoculum assayed (aka inoculum effect) and the presence of free β-lactamases in the medium, particularly influent when cell-wall targeting drugs are assayed.

Alternatively, Brauner and collaborators proposed to estimate drug tolerance by determining the MDK (minimum duration of killing), i.e. the time needed to effectively kill at least 99% (MDK99) of bacterial cells at concentrations well above the MIC (Brauner et al., 2016) (Figure 10). Kill-curve assays performed on exponential bacterial cultures allow to measure and compare the MDK of several bacterial strains simultaneously. Typically, MDK values higher than susceptible isolates are indicative of a tolerant pattern (Brauner et al., 2017). In addition, bacterial populations that include a fraction of persisters exhibit a biphasic killing pattern (Figure 10), whereby the rapid killing of the susceptible cells is followed by a slower killing of persister cells. Upon drug removal, persister cells start growing at normal rates, thereby reproducing the exact same biphasic pattern when treatment is applied again (Figure 10)

[17]Retarded killing/increased proportion of survivors at supra-MIC antibiotic concentrations (Eagle, 1948)

[18]Increased survival in stationary phase and exaggeration of the Eagle effect in late-logarithmic phase (Taylor et al., 1983)

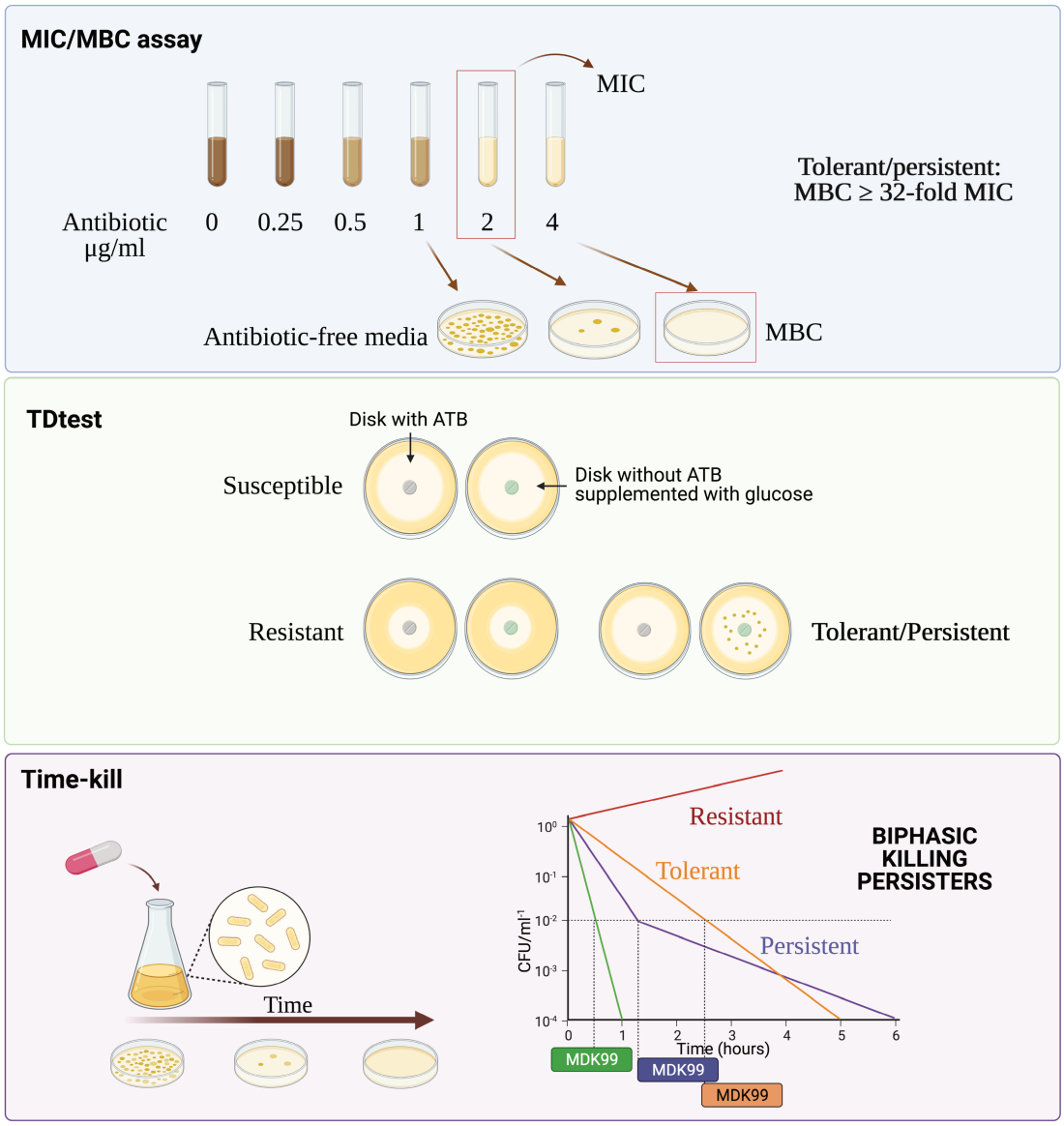

Figure 10: Methods to quantify tolerance. Tolerance can be quantified by measuring the ratio between minimal bactericidal concentration (MBC) and minimum inhibitory concentration (MIC), as calculated by broth microdilution assay. TD test was recently developed for detection of tolerance profile. Time-kill curves are commonly performed to assess minimum duration of killing (MDK) values. Typically, bacteria are treated with a given dose of antibiotic and CFU counting is performed at time points. Tolerant (in orange) and persistent (in violet) isolates exhibit higher MDK than susceptible isolates (in green). Persister cells (in violet) exhibit a biphasic killing. Created with BioRender.com

A newly developed assay to quantify tolerance and persistence is the Tolerance Disk Test (TDtest) (Gefen et al., 2017) (Figure 10). The assay is a modification of the Kirby-Bauer disk diffusion antibiotic susceptibility testing that allows to better discriminate between susceptible and tolerant bacteria. Briefly, in a classic disc diffusion assay, the inhibition zone induced by the antibiotic in the disk provides information on the population ability to withstand the given drug concentration. The concentration of antibiotics is predicted to be higher than the MIC in the inhibitory zone. In the TDtest, the antibiotic disc is replaced with another one containing

nutrient that will diffuse in the agar and feed putative tolerant subpopulations. If the strain is tolerant, it will then display regrowing colonies within the surrounding area of the disk. A recent work showed that TDtest results correlate well with time-kill curves performed on *S. aureus* (Kotková et al., 2019), confirming the reliability of this assay.

The ScanLag assay was also developed by the team of N. Balaban (Levin-Reisman et al., 2014). By monitoring the colony time of appearance (ToA) on solid media and by quantifying colony diameter growth rate (Figure 11a), this automated method allows to discriminate between heterogeneous phenotypes occurring within a population exposed to stressors such as antibiotics. Notably, the material required to perform the experiment is relatively simple and cost-effective, a feature that makes this system an attractive option for many laboratories. An array of standard office scanners (up to six) is connected to a computer, where the in-house developed software ScanningManager[19] periodically acquire images of the plates. For instance, images can be acquired every 20 minutes for a period of 48 hours. Raw data are then processed using in-house developed scripts in MatLab. Colonies are detected based on the intensity threshold. Usually, only objects above 10 pixels are counted but it is possible to adjust this parameter. In addition, detection of a colony starts at approximately 10^5 bacteria. According to the authors, some aspects should be carefully ensured not to compromise the results of the analysis: the scanner resolution, which should be 4,800 x 9,600 to gain high-quality images; temperature gradient on the flatbed surface and volume of the solid medium might influence bacterial growth, which can be averaged by performing replicates; finally, manual filtration of defects due to particles of dust that may have been mistakenly counted as colonies by the software.

Typically, spreading of a bacterial culture on regular nutrient agar without antibiotic leads to colony appearance within a few hours (about 9 h for *E. coli*) and their ToA distribution is narrow (Figure 11b, blue bars). However, heterogeneity of growth rate and lag time can also be detected by the ScanLag setup. Diverse ToA and growth rates were observed for a library of wild-type and mutated *E. coli* isolates growing on nutrient media (Levin-Reisman et al., 2010) (Figure 11b, brown, green and yellow bars in the graphs). Notably, the ScanLag system can also successfully detect very small fractions of bacteria in a population showing an extended lag time, i.e., the time required for the population to restore growth upon a transient stress. Stationary phase (SP) cultures of hipA7 *E. coli* mutants (Gefen et al., 2008), for instance, show a bimodal distribution of lag times due to the slow emergence of persister cells, which constitute the tail of the overall distribution (Levin-Reisman and Balaban, 2016) (Figure 11d). If the bimodal distribution is only observed in SP, the authors suggest the occurrence of Type I persistence; conversely, a bimodal distribution appearing also in exponential phase (EP) might be indicative of Type II persistence (see paragraph 2.2.6.2. Antibiotic tolerance and persistence (with a focus on β-lactams)). Altogether, this evidence supports the powerful ability of ScanLag

[19]Available at http://www.phys.huji.ac.il/bio_physics/nathalie/publications.html

to provide a quantitative measurement of heterogeneous phenotypes in a bacterial population, namely the tolerant and persistent slow-growing population.

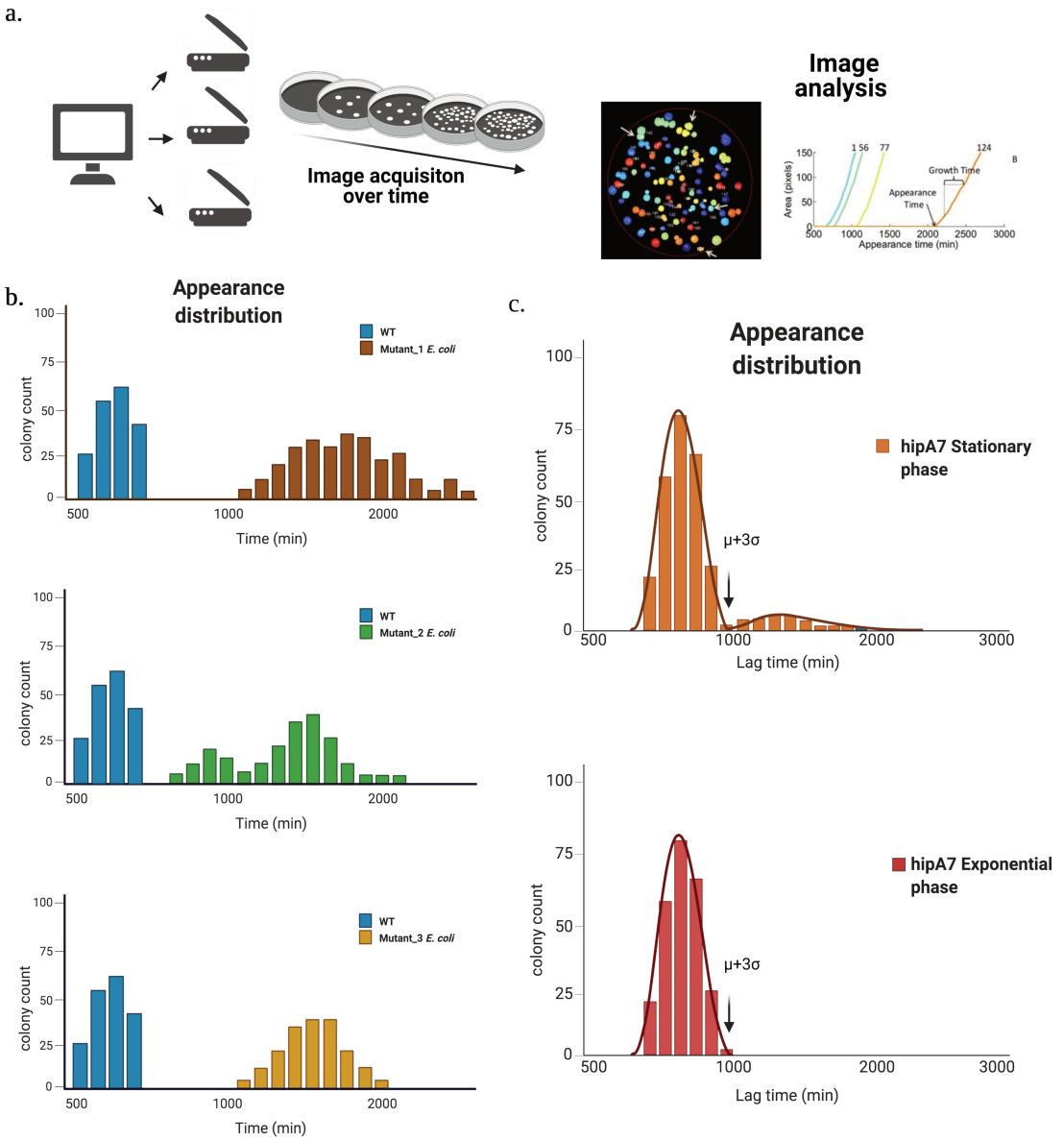

Figure 11: ScanLag workflow and detection of growth heterogeneity among *E. coli* populations. a) Images are acquired over time using scanners branched to a computer. As a result, for each colony the growth rate and time of appearance will be estimated. **b)** In blue, example of WT *E. coli* culture growing on regular nutrient agar; brown, green, and yellow indicate different mutants showing heterogeneous growth. **c)** Bimodal and tailed distribution of an *E. coli* isolate mutated in hipA7 showing persistence. The colonies appearing three standard deviations away from the mean of the main gaussian peak are defined as persisters, also indicated as "tail of the distribution". Created with BioRender.com

2.2.6.2.2. Molecular mechanisms of tolerance

The main mechanism of tolerance involves a decreased rate of killing upon exposure to bactericidal antibiotics, that can result from either slowing down or cessation of growth (tolerance "by slow growth") or by a delay in growth (tolerance "by lag") (Fridman et al., 2014).

Unfavourable growth conditions such as the localization of bacterial cells within the host body site (Abshire and Neidhardt, 1993), may give rise to tolerance by "slow growth". It has long been known that the killing efficacy of β-lactams is only achieved in exponentially growing cells with ongoing cell wall synthesis (Lederberg and Zinder, 1948; Lee et al., 2018). See also paragraph 2.3.5. The role of bacterial metabolism in antibiotic resistance.

A bacterial population may also display "tolerance by lag" (Fridman et al., 2014) (Figure 12). The lag phase is the latency period required by bacterial cells to adapt and switch from stationary phase to an actively growing state when environmental conditions become permissive again for growth. An extended lag phase can protect bacterial populations from disturbances, and it can emerge as *de novo* trait following exposure to stressors, such as antibiotics. The "tolerance by lag" is strictly dependent on the duration of the antibiotic treatment rather than the nature of the source of stress (Fridman et al., 2014; Levin-Reisman et al., 2019).

Tolerance can be also intended as a social trait, where the population structure plays a role in the phenotype. This is the case of heavily structured communities such as biofilm or the production of public goods as isolates secreting enzymes degrading the antibiotic, e.g., β-lactamases (Meredith et al., 2018; Sorg et al., 2016). β-lactam inactivation by resistant bacteria may sustain the survival of sensitive cells to otherwise lethal antibiotic doses, particularly at high cell densities (Domingues et al., 2017; Yurtsev et al., 2013). Moreover, persistence can reduce population growth and provide an indirect benefit for both the individual and its neighbours optimizing the allocation of resources in competitive environments (Gardner et al., 2007).

2.2.6.2.3. Genetic bases of tolerance and persistence

Although tolerance and heterotolerance are generally acknowledged to be survival strategies without inherent resistance mechanisms (Kint et al., 2012), genetic alterations in specific loci can influence the propensity of a bacterial strain to slow growing or form dormant subpopulations (Germain et al., 2013; Moyed and Bertrand, 1983). The genetic bases of tolerance and heterotolerance (persistence) have been first investigated using Transposon (Tn) insertion mutagenesis, recently paired with deep sequencing (Tn-seq). Typically, a library of knockout mutants, e.g., the KEIO collection of *E. coli* (Baba et al., 2006), is challenged with an antibiotic for a variable duration to identify critical genomic loci for tolerance/persistence. Besides the *hipA* locus (Moyed and Bertrand, 1983), other candidate loci identified in *E. coli* include: *metG* encoding methionyl-tRNA synthetase, *tktA* encoding transketolase A and *glpD* encoding glycerol-3-phosphate dehydrogenase (Girgis et al., 2012). Bacterial species other than *E. coli* have also been investigated by Tn-seq; for instance, five top genes of *Burkholderia thailandensis* and *Burkholderia pseudomallei* were putatively involved in tolerance to MEM: BTH_I0069 (a type VI toxin targeting peptidoglycan), *ldcA* (peptidoglycan recycling), *prc* (periplasmic regulation by proteolysis), *degS* and *rpoE* (envelope stress response) (Held et al., 2018).

A major pitfall of transposon mutagenesis is that it only detects mutations truncating non-essential genes that have a major effect on the phenotype (increased persister level), thus overlooking essential genes and the minor contribution of other components. On the other hand, it has been shown that a short exposure to a given antibiotic usually selects for mutations conferring tolerance or a higher tendency to form persister associated with a certain fitness cost (Fridman et al., 2014). Compensatory mutations can mitigate the cost of resistance mutations (Maisnier-Patin and Andersson, 2004), although these are not responsible *per se* for increased antibiotic tolerance. If the antibiotic is periodically applied, such mutations may become advantageous and further selected. The *loci* involved may be considered as the true or 'deep' responsible for enhancing the population level of persistence/tolerance. Under these conditions, it is possible to dissect the population dynamics behind evolution to tolerance. One experimental procedure following these principles that has been largely used across different studies is the adaptive laboratory evolution (ALE), where isolates are subjected to intermittent exposure to high doses of antibiotics (Fridman et al., 2014; Khare and Tavazoie, 2020; Mechler et al., 2015; Sulaiman and Lam, 2020; Van den Bergh et al., 2016), and evolved strains are then sequenced and analysed phenotypically to unveil genetic loci contributing to tolerance/persistence.

Adaptive laboratory evolution (ALE) has been largely used to investigate the role of *de novo* mutations in determining resistance (Jahn et al., 2017). Nevertheless, a pioneering study investigating tolerance rather than resistance dates back as early as 1983 (Moyed and Bertrand, 1983). Moyed and colleagues treated log-phase *E. coli* cultures with high intermittent doses of ampicillin and isolated high-persistence mutants in the *hip* locus, later named as *hipBA* (Black et al., 1991), with 1000-fold higher persistence levels than the wild-type strain. HipBA is a toxin-antitoxin system (Hall et al., 2017). Under stress conditions, the toxin HipA inhibits translation and bacterial growth, forcing bacteria to go into a dormant state (Germain et al., 2013). Overexpression of TA modules, as detected by several microarray studies has often been observed in persisters of *E. coli* (Correia et al., 2006). An imbalance between the expression of the toxin and the corresponding antitoxin has also been shown to increase the persister fraction in *E. coli* (Keren et al., 2004). Mutations in *hipQ* (Wolfson et al., 1990) and *hipA7*, an allelic variant of *hipA* (Korch et al., 2003) were associated with higher rate of persister cells upon exposure to DNA replication and cell wall synthesis inhibitors. Despite their apparent similarity, killing curves and quantitative measurement of their switching rates revealed that these two *loci* generate different types of persistence: type I persisters and type II for the *hipA7* and the *hipQ* strain, respectively (Gefen et al., 2008). Wild-type (wt) *E. coli* seems to contain a fraction of both types of persister cells (Balaban et al., 2004).

In the last decades, these preliminary observations have been corroborated by theoretical models predicting that regular, periodic exposure to high doses of antibiotic - a condition mimicking the clinical practice, is optimal for the emergence of tolerance. Furthermore, a large amount of experimental data has been generated from populations of *E. coli* (Fridman et al., 2014; Sulaiman and Lam, 2020; Van den Bergh et al., 2016), but also for *S. aureus* (Mechler et al.,

2015) and ESKAPE pathogens (Michiels et al., 2016). Whole-genome comparison of evolved clones with the ancestral strain facilitated a high-throughput detection of tolerance/persistence candidate loci. Four recent ALE experiments on *E. coli* cultures identified different loci associated with tolerance (Sulaiman and Lam, 2021). Interestingly, the landscape of mutations detected in different studies was quite diverse, likely due to the variations in experimental conditions, whereby factors such bacterial growth phase, antibiotic used, and the length of exposure are crucial. For instance, Fridman *et al*., obtained mutations in eight genes upon cyclic exposure of diluted stationary phase *E. coli* cultures to high doses of ampicillin (15xMIC). These mutations were associated with an extension of lag-time and higher drug tolerance (example of tolerance "by lag") (Fridman et al., 2014). Among the genes affected, two loci, *vapB*, encoding the antitoxin of the vapBC TA module, where *vapC* encodes a tRNA(fMet)-specific endonuclease and *metG*, coding for methionyl-tRNA synthetase, were previously reported to contribute to increased rate of persistence (Gerdes and Maisonneuve, 2012; Kaspy et al., 2013). The same group reported later that prolongation of cyclic exposure can lead to accumulation of mutations in the promoter of *ampC*, encoding the constitutively and weakly expressed naturally-occurring cephalosporinase (Levin-Reisman et al., 2017), eventually fostering the acquisition of full resistance to ampicillin. Daily treatment of stationary-phase *E. coli* with high doses of aminoglycoside led to a different set of mutations in the evolved strains (Van den Bergh et al., 2016). The genes affected were *oppB*, *nuoN*, and *gadC*, encoding a permease protein part of an oligopeptide ABC transporter, the NADH-quinone oxidoreductase subunit N, and a glutamate antiporter, respectively. No significant differences among the mutated and WT isolates were observed in the lag time. However, competition experiments revealed that these three mutations confer a benefit in the presence of antibiotic, mainly due to the large proportion of persister cells (approximately 1000-fold more than the ancestral strain), which was, on the contrary, associated with a limited fitness cost in absence of antibiotic.

Two recent studies integrated evolution experiments with transcriptomic analysis (Khare and Tavazoie, 2020) and proteomics (Sulaiman and Lam, 2020), simultaneously comparing multiple tolerant mutants to cross-combinations of antibiotics. Khare *et al*., further deleted the *hipBA* locus in the *E. coli* strain deleted for 10 type II TA systems (Δ10TA). In addition, they employed a combination of ampicillin with either ciprofloxacin or kanamycin and carried out the experiment in the exponential phase of growth (in contrast with the stationary phase in Van den Bergh's work and diluted stationary phase in Balaban's group works). Most of the mutations here identified affected genes essential during translation in protein synthesis. In particular, they identified frequent independent mutations in *metG*, previously associated with extended lag time and increased persistence (Fridman et al., 2014; Girgis et al., 2012) and *pth*, coding for the enzyme peptidyl tRNA hydrolase involved in recycling tRNAs in the cell (Das and Varshney, 2006). Transcriptional analyses of *metG* and *pth* mutants in exponential phase revealed common markers, which when highly expressed, are associated with persister formation. This aspect could facilitate enrichment and isolation of the hyperpersistent

populations, for instance by using FACS sorting. Upregulated genes in persister cells were mostly involved in stress regulons such as the SOS and phage shock response, whereas most of metabolic pathways e.g., electron transport chain, ATP production were downregulated. Finally, Sulaiman *et al*., challenged mid-exponential *E. coli* cultures with three different bactericidal antibiotics (ampicillin, ciprofloxacin, and apramycin) (Sulaiman and Lam, 2020). They selected different mutations, including *fusA*, encoding the translation elongation factor G (EF-G), which is essential during translation elongation and modulates the basal level of ppGpp by the RelA pathway (Macvanin et al., 2000); *cyaA*, encoding the adenylate cyclase, required for the formation of cyclic AMP (cAMP) (Botsford and Harman, 1992). *ΔcyaA* mutant precludes the synthesis of the signaling molecule cAMP, exhibits constitutive catabolite repression and slow growth (Perrenoud and Sauer, 2005), in addition to increased tolerance to β-lactam antibiotics (Molina-Quiroz et al., 2018). Historically, *cyaA* mutant were selected as mecillinam resistant (Aono et al., 1979). Another interesting mutation occurs in *icd*, encoding NADP-dependent isocitrate dehydrogenase. As previously reported (Hill et al., 1989), the mutation resulted from the insertion of an e14 prophage inserted in the coding sequence and, although no direct link has been observed with increased persistence, it seems to be an unstable region and hotspot under stressful conditions (Sekowska et al., 2016), likely due to activation of the SOS response. In addition, by performing proteomics analysis, they identified protein candidates potentially contributing to tolerance (GrcA, RaiA and RRF, AhpF, NuoF and CysP), all related to pathways such translation, DNA damage response, electron transport chain and peptide transporter.

Interestingly, despite the diversity of *loci* identified across the different studies, mechanisms of tolerance/heterotolerance appear to involve key cellular processes including SOS response, electron transport chain, protein and amino acid transport, cAMP biosynthesis, accumulation of active toxins and reduced growth rate, in agreement with the knowledge that multidrug tolerance arises following impairment of any major biosynthetic process (Pontes and Groisman, 2020).

2.2.6.2.4. Morphological changes and implications in tolerance towards β-lactams

Inhibition of peptidoglycan biogenesis by β-lactam antibiotics leads to perturbations in cell morphology such as delay or restriction of cell division, formation of filamentous or spherical cells prior to lysis (Zahir et al., 2020). Different classes of β-lactams can elicit varying morphological changes and distinct growth inhibitory mechanisms depending on their specific targets (PBP). In *E. coli*, it is widely accepted that inhibition of the cell wall building enzymes PBP1a and 1b leads to cell shape elongation, rapidly followed by bulging that culminates in cell lysis (figure 12) (Spratt, 1975). Examples of such β-lactam agents include amoxicillin, cephaloridine, and cefsulodin (Curtis et al., 1979). Targeting the essential PBP2, involved in cell elongation or PBP3, involved in septal formation and cell division, results in round and filamentous morphologies, respectively (Spratt, 1975). Examples of β-lactams with great affinity to PBP2 include mecillinam and carbapenems, which have different PBP profiles

depending on the specific compound. For example, molecules such as imipenem and meropenem display high affinity for PBP2 of *E. coli*, but, in addition, meropenem binds simultaneously to PBP3 and PBP1a and 1b with relatively high affinity, in contrast to imipenem. Therefore, a distinct morphological effect is observed in WT *E. coli* treated with MEM, where cells may exhibit a spindle, short filamentous shape with bulge prior to lysis (figure 12b). Likewise, simultaneous inhibition of PBP2 and PBP3 (e.g., aztreonam and mecillinam or meropenem) was shown to yield to aberrant morphologies reminiscent of what seen with meropenem (Godinez et al., 2019).

In addition to PBP specificity, the type of morphological changes in bacterial cells depends upon the β-lactam drug concentration (figure 12). For instance, cell filamentation prior to cell-lysis can be induced upon PBP3 inhibition with low doses of β-lactam e.g., cephalexin (Chung et al., 2009). Filaments are long strands of non-dividing bacteria with high LPS concentration (Buijs et al., 2006). Filamentous cells have been shown to evade immune killing in the host during infection (Allison et al., 1992) and resist phagocytosis (Justice et al., 2014), complicating pathogen eradication. In addition, filamentous cells are transiently refractory to β-lactams killing due to delayed lysis, therefore, the duration of this state may be crucial in conferring antibiotic tolerance. Interestingly, a recent study demonstrated that filamentous growth observed in *E. coli* strains with seven mutated loci (*fkpB, pnp, ubiF, dedD, ftsP, galU, and surA*) during exposure to three PBP3 inhibitors - cephalexin, aztreonam and piperacillin, led to delayed cell lysis and no change in MIC to β-lactams, suggesting a tolerance phenotype (Zahir et al., 2020). Altogether, these data suggest that transient filamentation improves bacterial survival under hostile conditions.

Inhibition of PBP2 with low dosage of drugs such as imipenem or mecillinam leads to formation of ovoid cells, also referred to as spheroplasts (figure 12), eventually culminating in cell lysis due to subsequent binding to PBP1a and PBP1b. Spheroplasts are L-form-like bacterial cells devoid of their peptidoglycan layer that can arise in osmoprotective conditions and upon inhibition of bacterial cell wall synthesis, e.g., with lysozyme or β-lactams (Cross et al., 2019; Westblade et al., 2020). In contrast to L-form of Gram-positive, spheroplasts do not divide in the presence of antibiotic but they retain metabolic activity (Claessen and Errington, 2019). Upon drug removal, spheroplasts can rapidly revert to normal rods, ultimately contributing to antibiotic tolerance, as shown for β-lactams (Cross et al., 2019; Westblade et al., 2020). However, formation of spheroplasts seems to be highly dependent on incubation conditions. Factors such as the type of growth medium, osmolarity, and temperature may affect such morphological changes (Cushnie et al., 2016). Isotonic environments are essential to preserve their integrity and to avoid their lysis. In addition, spheroplasts can be stabilized with mutations in genes involved in these metabolic pathways may be crucial to stabilize cell-wall deficient state. For instance, mutations in *B. subtilis yqiD* gene (homolog of *ispA* of *E. coli*) – encoding a farnesyl pyrophosphate involved in isoprenoid synthetic pathway, support stable L-form proliferation in *B. subtilis* cells with arrested cell wall synthesis in osmostabilized growth medium (Kawai et al., 2019).

Round cell morphology was also observed in *E. coli* mutants (e.g., Δ*ybgF*, Δ*rssa*, Δ*pgpA*) due to stable bulges formation upon treatment with cefsulodin (i.e., binding to PBP1a and b) (figure 12a) (Zahir et al., 2019). Curvy, bulging cells were instead observed in E. coli mutated for Δ*tolA*, Δ*ygfA*, Δ*gmR* (figure 12a) (Zahir et al., 2019). Interestingly, these mutants exhibited late or slow cell lysis, likely due to cell envelope stabilization that postpones the PG degradation, and were shown to revert back to rod-shape when cefsulodin was removed (Zahir et al., 2019). Hence, genetic alterations leading to stable bulging cells eventually contribute to antibiotic tolerance by avoiding cefsulodin-induced lysis eventually contributing to antibiotic tolerance by avoiding cefsulodin-induced lysis.

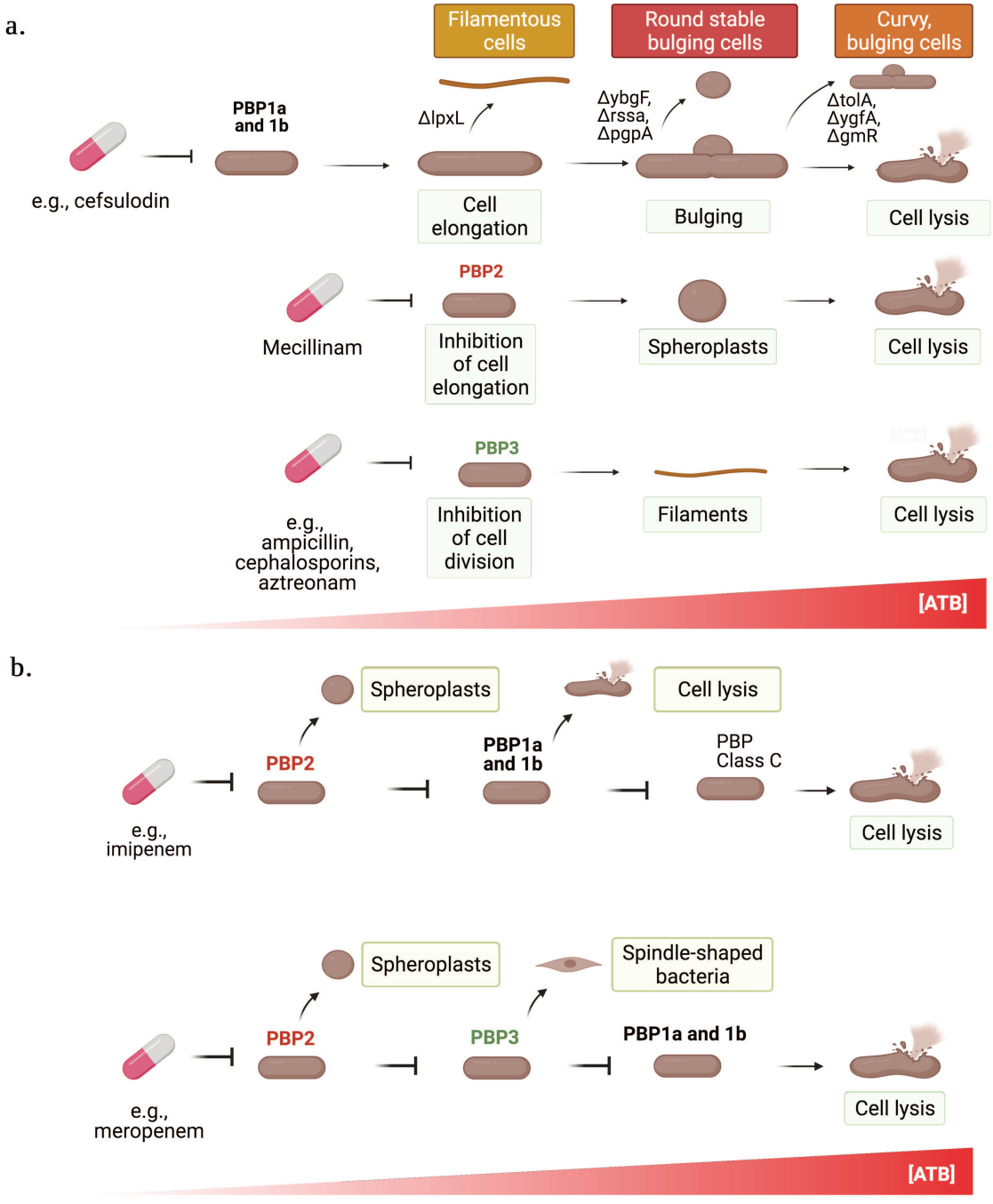

Figure 12: Morphological changes vary upon the class of PBP inhibited and according to drug concentrations.
a) Inhibition of PBP1a and 1b leads to elongation, followed by bulging that culminates in cell lysis. In isolates with Δ*lpxL,* cell elongation may be followed to filamentation, whereas the bulging step may lead to formation of spheroplast or curvy, bulging cells in backgrounds harbouring Δ*ybgF*, Δ*rssa*, Δ*pgpA* and Δ*tolA,* Δ*ygfA,* Δ*gmR*, respectively. Inhibition of PBP2 leads to spheroplasts formation and PBP3 to filaments, prior to cell lysis, b) Carbapenem drug (here imipenem and meropenem) preferentially target PBP2. Meropenem, however, can simultaneously target PBP3, giving rise to spindle-shaped bacteria, and afterwards, binding to PBP1a and 1b, thus inducing cell lysis.

2.2.6.3. Antibiotic heteroresistance

Preliminary evidence of heteroresistance (HR) dates back to late 1940s (Alexander and Leidy, 1947a), when during a screening of large populations of Type B *H. influenzae,* a small fraction of colonies surviving high doses of streptomycin (1,000 units per cc) was noticed. This subpopulation exhibited various degrees of susceptibilities to streptomycin, it occurred randomly at very low frequencies (2.9×10^{-11} to 5.3×10^{-11}), consistent with the hypothesis of mutated resistant variants, and it was stable across several generations (Alexander and Leidy, 1947a). Notably, these isolates were associated with persistent infections in patients treated with streptomycin, therefore the resistant subpopulation might have played a role in the treatment failure (Alexander and Leidy, 1947b). Later on, HR was noticed in *S. aureus* as the occurrence of colony variants within the same population with various levels of resistance to cephalexin and oxacillin (Kayser et al., 1970). HR was also reported among methicillin-resistant *S. aureus* (MRSA), where the resistance phenotype was associated with SCVs emerging on isotonic media (Barber, 1964; Churcher, 1968). In addition, it was later showed that the resistant phenotype was retained even in the absence of the antibiotic (Ryffel et al., 1994). At that time, one hypothesis was that highly resistant subpopulation originated from alterations in the transcriptional or translational regulation of the gene encoding PBP(2a) (Chambers et al., 1985). Thereupon, HR has been also detected among fungi (Ferreira and Santos, 2017), other Gram-positive (Alam et al., 2001; Engel et al., 2014; Khan et al., 2008; Sieradzki et al., 1999) and several Gram-negative bacteria (Meletis et al., 2011; Nicoloff et al., 2019; Nodari et al., 2015; Søgaard, 1985). Over the past decade, HR has become an attractive research topic (Figure 13). Nevertheless, its definition has been controversial for long time and attempts have been made to clarify the general mechanism behind HR (Andersson et al., 2019; El-Halfawy and Valvano, 2015). In addition, the lack of standardized methodologies to characterize HR has precluded the comparison among studies and thus, a general understanding of the phenomenon.

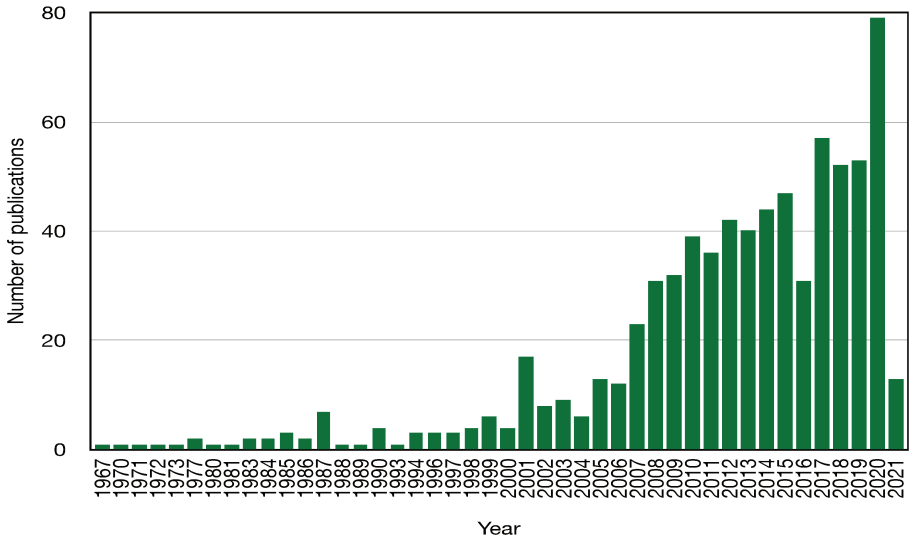

Figure 13: Timeline of publications on heteroresistance from the PubMed website using the key word "heteroresistance" (updated to Mars, 2021)

2.2.6.3.1. How to quantify heteroresistance

Detection of HR in clinical microbiology laboratories might be challenging, due to the unstable nature of the phenomenon in the absence of drug selection and the low proportion of more resistant cells responsible for the HR phenotype. However, there is general agreement on the fact that HR can be preliminary detected by visualization of scattered colonies on agar-based susceptibility testing (Etest and disk diffusion assay) (Figure 14) (El-Halfawy and Valvano, 2015). In addition, the "skip wells" phenomenon in broth microdilution (BMD), alternatively referred to as the "paradoxical effect"[20] and leading to irreproducible MIC results, has been attributed to an HR profile (Guérin et al., 2016; Landman et al., 2013).

[20]Absence of growth in certain wells but growth observed at higher concentrations of the antibiotic.

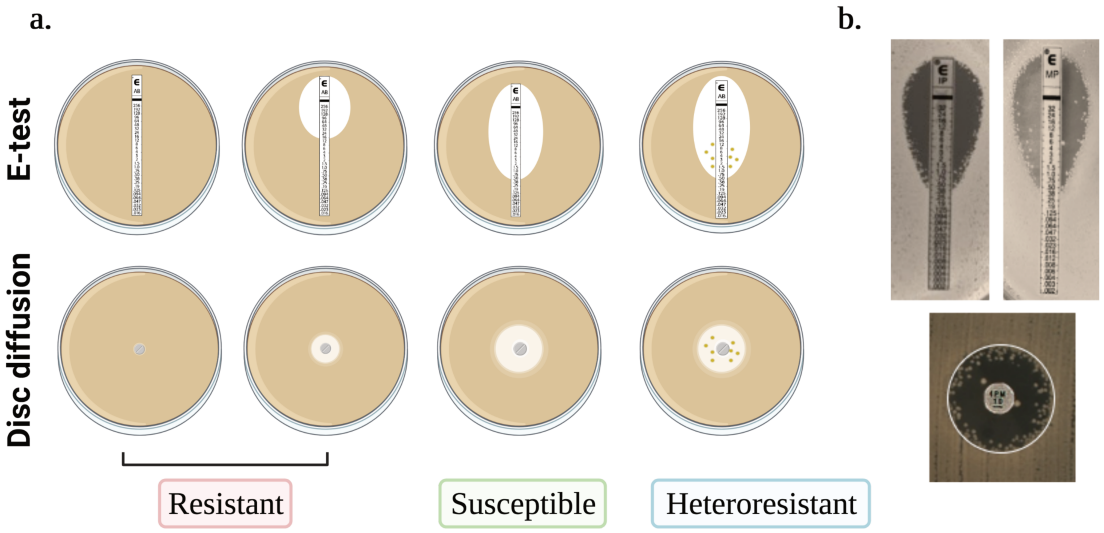

Figure 14: Preliminary detection of HR by agar-based susceptibility testing. In fig 14a, classic antimicrobial susceptibility testing on agar (Etest on top and Kirby-Bauer/disc diffusion assay in the bottom). HR is visualized at first by the emergence of scattered colonies within the drug inhibition halo. In figure 14b, examples of Etest and disc diffusion test performed in our laboratory for screening of resistance and HR. Created with BioRender.com

The HR phenotype is commonly confirmed when a bacterial strain displays subpopulations growing at ≥8 × MIC for the given drug (Andersson et al., 2019; El-Halfawy and Valvano, 2015, p.). The golden standard method to quantify this ability is the Population Analysis Profile (PAP) (El-Halfawy and Valvano, 2015, p.). PAP is typically performed by spreading a stationary phase bacterial culture onto plates supplemented with 2-fold antibiotic increments, followed by counting of CFUs appearing at the highest antibiotic concentration at 24 hours (Figure 16). In a modified PAP assay, the population analysis profile-area under the curve (PAP-AUC) has been widely used for detection of vancomycin HR in *S. aureus* (Wootton, 2001). In this study, a bacterial density of approximately 10^6 cells/ml is spread onto media supplemented with 4 mg/L vancomycin (clinical breakpoint for vancomycin). HR is thus assigned to isolates showing colonies arising upon 48 hours of incubation (Wootton, 2001).

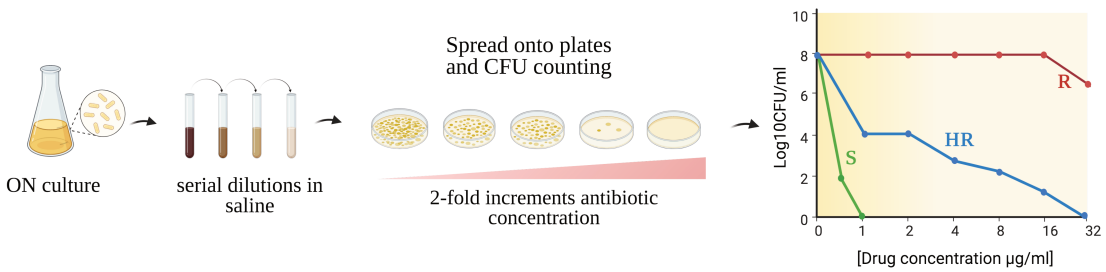

Figure 16: PAP analysis workflow for HR confirmation.

However, PAP is very time-consuming and inappropriate for routine use in clinical laboratories. In addition, the final interpretation of the phenotype is not always straightforward due to the influence of factors including the bacterial species, the inoculum size effect (IE), bacterial physiology, type of antibiotic and presence of drug-hydrolysing enzymes (e.g., β-lactamase). These aspects might challenge the comparison among studies and thus, a general understanding of the phenomenon. The IE can yield artifacts, especially when drugs inhibiting peptidoglycan synthesis and bacteria producing ESBLs and/or carbapenemases are employed (Adler et al., 2015; Smith and Kirby, 2018). Indeed, IE was greatly observed with β-lactams (Lenhard and Bulman, 2019). Another challenge is given by the physiological state of the bacterial population; stationary phase bacteria are more refractory to killing by β-lactams than exponentially growing cells, likely due to a decreased rate of cell division (Tuomanen et al., 1986) and increased production of ROS (Shin et al., 2021). Accordingly, a linear correlation between growth rates and β-lactam-mediated lysis rates has been shown (Lee et al., 2018). Additionally, methods such as agar plates supplemented with a linear gradient of antibiotic concentrations (Liu et al., 2011), flow cytometry using a fluorescent penicillin derivative (Jarzembowski et al., 2009) or GFP constructs to measure the expression of resistance genes in the populations (X. Wang et al., 2014) have been used to characterize HR. Recently, droplet microfluidics has been also employed for detection of HR (Scheler et al., 2020). Finally, the ScanLag method (Levin-Reisman et al., 2014) has been used to investigate HR in fungi (Rosenberg et al., 2018), in addition to persistence (Levin-Reisman et al., 2010).

2.2.6.3.2. Clinical significance

The clinical impact of HR is controversial and poorly understood. The main questions that clinicians ask are: how prevalent is HR among clinical isolates? Which drugs are affected? Does HR reduce therapeutic options? or, more specifically, are these subpopulations potentially able to affect treatment outcomes?

Past evidence in this regard is mixed, likely due to the lack of standardized methods to investigate HR, confusion on its definition and scarcity of *in vivo* studies, thus not allowing to evaluate clinical implications of HR. Recent studies have attempted to shed light on this aspect by systematically screening large collections of known pathogens in combination with a panel of different relevant drugs for clinical practice. In addition, Band and co-workers showed that a clinical isolate of *E. cloacae* having low-frequency subpopulations (1%-10% of the whole population) transiently resistant to the "last-resort drug" colistin, led to treatment failure in a mouse model (Band et al., 2018). Interestingly, transcriptional analyses also revealed substantial differences between the two populations (R and S), where the highly R showed up-regulation of colistin resistance genes. Nicoloff and co-workers showed a vast prevalence of HR (27% among 766 bacteria-antibiotic combinations) among 41 clinical Gram-negative isolates tested against 28 different antibiotics, by using PAP assay (Nicoloff et al., 2019b). By mean of whole genome sequencing (WGS), the authors further showed that the HR profile was

largely associated with spontaneous tandem gene amplification of canonical resistance genes that could not be detected by conventional AST.

HR isolates may be misclassified as susceptible (Band and Weiss, 2019), thus leading to an inappropriate treatment choice. Subsequent exposure to antibiotics may enrich for the resistant subpopulation, ultimately affecting treatment outcome. Misclassification of isolates may also come from the way susceptibility testing is carried out in clinical microbiology laboratories. To define the MIC of a population to a given drug, the bacterial inoculum should be prepared by picking at least 3 to 5 well-isolated colonies of the same morphological type from an agar plate[21]. However, if the population is mixed i.e., due to either monoclonal or polyclonal HR, and only few clones are analysed, heteroresistance will be under-reported (Hughes and Andersson, 2017) and high variability among MICs might be observed, depending on the picked colonies. Furthermore, HR to a certain antibiotic was reported to cause, as a collateral effect, an increased resistance to other antimicrobials (Sakoulas et al., 2006) or to host-antimicrobial lysozyme (Napier et al., 2014). Finally, this heterogeneity may precede the emergence of more stable genetic changes, thereby accelerating the evolution of resistance in the population, as also shown for yeast (Bódi et al., 2017).

2.2.6.3.3. Mechanisms of heteroresistance

Several definitions and mechanisms have been attributed to HR. In order to correctly identify the phenotype and shed light on the genetic bases of the phenomenon, four aspects should be investigated when studying HR (Andersson et al., 2019): (i) clonality of resistant subpopulations (ii) the stability of the observed phenotype (iii) the resistance levels of the subpopulations and (iv) the frequency at which they arise.

Heteroresistance can be **polyclonal**, i.e., resulted from the combination of different clones with diverse susceptibility profiles or from a fraction of pre-existing mutants within the susceptible population enriched under antibiotic treatment. In this case, HR is reminiscent of "classical" resistance, whereby a subpopulation may exhibit various mutations (SNPs, frameshifts, insertions, and deletions) conferring resistance. Usually, only permissive mutations (associated with low fitness cost) can confer a stable resistant phenotype. Classic resistance can be distinguished from HR based on the **frequency** at which subpopulations arise. Usually, classic resistant mutants are considered to emerge at low frequency (typically lower than 10^{-7}), whereas in HR clinical isolates the frequency is generally higher, but it can vary depending on the method used to investigate HR, the given antibiotic, and its concentration during selection.

Common mechanisms of polyclonal HR include overexpression of efflux pumps systems and reduced membrane permeability, all canonical mechanisms of antibiotic resistance. For

[21]Clinical and Laboratory Standards Institute (CLSI). Performance Standards for Antimicrobial Susceptibility Testing. 27th ed. CLSI supplement M100 (ISBN 1-56238-804-5 [Print]; ISBN 1-56238-805-3 [Electronic]). Clinical and Laboratory Standards Institute, 950 West Valley Road, Suite 2500, Wayne, Pennsylvania 19087 USA, 2017

instance, HR to colistin in *A. baumannii* isolates was linked to increased expression of efflux pump genes e.g., *adeABC* and *adeIJK* (Machado et al., 2018) and/or mutations in *lpxC* and *lpxD* genes involved in LPS lipid A biosynthesis (Chen et al., 2020), whereas the interplay between down-regulation of OprD porin and upregulation of efflux genes (*mexE* and *mexY*), plays a major role in HR to imipenem in *P. aeruginosa* (Xu et al., 2020).

Monoclonal HR exclusively relies on pure clones that show resistant subpopulations at various frequencies, on average ranging from 1×10^{-7} to 1×10^{-4}. Monoclonal HR may result from *stable* or *transient* heterogeneity in the bacterial population. Unstable HR is quite common, and it refers to poorly reproducible resistant phenotype upon drug removal, due to reversion of the subpopulation to a susceptible phenotype. Therefore, HR thus defined recalls the well-known concept of adaptive resistance (AR). As detailed previously, AR describes the emergence of a reversible resistance pattern, generally due to alterations in gene expression and rapidly lost when the antibiotic is removed (Hughes and Andersson, 2017). However, AR may also arise due to enrichment of rare highly unstable and reversible genetic variants within a bacterial population (Hughes and Andersson, 2017), such as gene duplications/amplifications (Andersson and Hughes, 2009). The transient nature of this type of resistance is likely due to the fitness cost associated with the expression of certain genes responsible for the resistance phenotype or co-amplified with it. Likewise, the transient nature of unstable monoclonal HR might also be due to the appearance of mutations compensating for the high fitness cost associated with primary mutations or gene duplications/amplifications also restoring antibiotic susceptibility. The emergence of *compensatory mutations* usually generates a mixed bacterial population, with most of cells displaying resistance loss and a small fraction with the primary mutation responsible for resistance. For instance, HR to aminoglycosides in several Gram Negative pathogens has been associated with highly costly mutations in *cpxA* or *ubiJ*, leading to small colony variant (SCV), slow growth and resistance to aminoglycosides (Nicoloff et al., 2019). In the absence of selective pressure, the high fitness cost was counteracted by loss of function in regulatory genes e.g., *cpxR* or amplification of *ubi* genes, respectively (Nicoloff et al., 2019).

Spontaneous gene amplifications are frequent events in bacterial populations, typically generated via homologous recombination between repeated sequences like IS elements, transposase genes and ribosomal RNA operons (Reams and Roth, 2015). The first report defining HR as caused by gene amplification was in *S. Typhimurium* (Hjort et al., 2016), where the HR profile to colistin was due to unstable tandem amplifications of a chromosomal region encompassing the gene *pmrD*, a positive regulator of lipid A modification. It was also found out that unstable tobramycin resistance in *A. baumannii* was due to RecA-dependent amplification of the plasmid-borne *aadB* gene encoding an aminoglycoside adenylyltransferase (Anderson et al., 2018). Notably, amplification of chromosomal or plasmid regions with resistance genes was shown to be the main mechanism conferring HR in four Gram-negative pathogens analysed (*A. baumannii*, *E. coli*, *K. pneumoniae* and *S. Typhimurium*) (Nicoloff et al., 2019).

Other reported mechanisms of HR include alterations in regulatory genes, as observed for polymyxin HR in *K. pneumoniae* (Jayol et al., 2015) or overexpression of efflux-pumps genes (Bergmiller et al., 2017). However, there is a lack of information on the stability of the phenomenon, which is crucial to correctly discriminate among the multiple facets of HR. Finally, to simplify HR detection, it is important to consider the resistance level of subpopulations. Most isolates may display subpopulations of cells by classic AST that can grow at doses proximal to the MIC. To discriminate between different situations, it is recommended to define a specific antibiotic concentration (usually eightfold above the resistance level of the main population) at which subpopulations may be indicative of an HR pattern. Divergent results among several studies are due to different cut-off levels and unclear information on which MIC is considered; since most of the assays used to characterize HR are agar-based, it is intuitive to think that the MIC as calculated by Etest should be considered. Moreover, as the final bacterial inoculum size differ across the various methods used to measure the MIC (BMD uses 5×10^5 CFU/mL, whereas disk diffusion/Etest use $(1\text{-}2)\times10^8$ CFU/mL) (Balouiri et al., 2016), clarifying what MIC is considered for the purpose of HR investigation would possibly reduce the discrepancies among studies.

2.4. *Klebsiella pneumoniae* – a story of success

2.4.1. Taxonomy, metabolic features, and niche adaptation

K. pneumoniae is a Gram-negative, non-motile, facultative anaerobic bacillus, ranging from 0.3 to 1 μm in diameter and 0.6-6 μm in length, often encompassed with a capsule. Member of the Enterobacterales genera, like *E. coli, K. pneumoniae* belongs to the genus Klebsiella, whose definition has been controversial for long time. Originally, the genus *Klebsiella* was split into three subspecies based on the type of disease caused: *K. pneumoniae*, *K. ozaenae*, and *K. rhinoscleromatis* (Cowan et al., 1960). Later on, by 16S rRNA and *rpoB* analysis, three major clusters were defined: cluster 1, including the three aforementioned subspecies of *K. pneumoniae*; cluster 2, including the environmental isolates *Klebsiella ornithinolytica*, *Klebsiella planticola*, and *Klebsiella terrigena*, and cluster 3 containing *Klebsiella oxytoca* (Drancourt et al., 2001). In parallel, another study defined four major phylogroups on the bases of *gyrA* and *parC* sequences: Kp1 to Kp4 (Brisse and Verhoef, 2001). Other two phylogroups were later added on the bases of 1217 core-genes phylogeny, Kp5 and Kp6 (Blin et al., 2017). Over the past years, whole genome-based studies revealed that each phylogroup corresponds to distinct taxa. Altogether, these taxa constitute the *K. pneumoniae* species complex (KpSC), which include *K. pneumoniae sensu stricto* (Kp1), *K. quasipneumoniae* subsp. *quasipneumoniae* (Kp2) and subsp. *Similipneumoniae* (Kp4), *K. Variicola* (Kp3) (subsp. *tropica* and subsp. *Variicola*), *K. quasivariicola* (Kp5) and *K. Africana* (Kp6) (Wyres et al., 2020).

Klebsiella *spp.* members are ubiquitously distributed across a multitude of ecological habitats, ranging from environmental, including sewage, surface, food and drinking waters, soils, effluents to host-associated niches (like mammals) (Wyres and Holt, 2018). This reflects the extreme metabolic versatility of Klebsiella *spp* isolates, much larger than *E. coli* or *S. enterica* (Blin et al., 2017), which is likely contributing to infection at different host body sites and enhancing the survival odds. In addition, different Klebsiella *spp*. strains are able to use different carbon sources (Blin et al., 2017), and certain members (*K. pneumoniae*, *K. oxytoca* or *K. planticola*) are diazotrophs (Chen et al., 2016), namely able to convert atmospheric nitrogen N_2 into ammonium NH_3 as nitrogen source. Overall, such flexibility is also mirrored by the relatively easiness by which most of *Klebsiella* organisms can be cultivated onto standard laboratory media and selective differential media for *Enterobacterales*, including Drigalski and MacConkey agar[22]. *K. pneumoniae* forms round, dome-shaped and usually mucoid colonies at 30 or 37 °C in neutral conditions (pH 7.2). The mucoid aspect of colonies may vary upon the size of the capsular layer, which is also present in other species of *Enterobacterales*, therefore making species identification from colony appearance less intuitive.

[22] ISBN: 978-0-387-30746-6

2.4.2. From commensalism to pathogenicity

K. pneumoniae sensu stricto (hereto defined as *K. pneumoniae*) is a common cause of hospital-acquired infections (HAIs), in the United States (Magill et al., 2014) and in Europe (Cassini et al., 2016). Notably, *K. pneumoniae* is responsible for about 90 000 deaths in EU each year in health care settings due to severe bloodstream infections (BSI) and intravenous or urinary catheter infections in patients admitted at intensive care units (ICU) (Cassini et al., 2016).

K. pneumoniae primarily inhabits the gut flora and, to a minor extent, the oropharyngeal tract and the skin of healthy individuals (Bagley, 1985). According to different studies and depending on the sampling method, *K. pneumoniae* carriage frequencies can range from 6% to 30-37% among individuals recently admitted at the hospital[23] (Gorrie et al., 2017). Major risk factors for *K. pneumoniae* colonization and infections in health-care settings are previous antimicrobial exposure, comorbidities, admission to ICU and length of hospitalization (Pollack et al., 1972). Indeed, the colonization levels are significantly higher in hospitalized patients, with reported carrier rates ranging from 19% to 77% in the stool and 19% in the pharynx (Gorrie et al., 2017; Podschun and Ullmann, 1998). A crucial reservoir of *K. pneumoniae* in health-care settings is the gut microbiome of hospitalized patients (Gorrie et al., 2017)), followed by other sources, including hospital workers' hands (Puig-Asensio et al., 2019), contaminated medical and surgical equipment, air-conditioning units, sinks, drains, and wards (Aranega-Bou et al., 2019; Betteridge et al., 2013; Clarivet et al., 2016).

2.4.3. Clinical manifestations

Clinical features of *K. pneumoniae* infections can vary with the type of virulence factors expressed and the geographical distribution, e.g., severe invasive disease in Taiwan and some Asian areas (Yu et al., 2007). In addition, host features such as underlying diseases e.g., diabetes mellitus, genetic predisposition, and alcoholism, can predispose to disease and aggravate its clinical manifestation (Yu et al., 2007).

Infections are usually distinguished into community-associated (CA), affecting a broad range of individuals and healthcare-associated (HA) infections, when diagnosed 48 hours later than the patients' admission at the hospital. *K. pneumoniae* is the second most important cause (after *E. coli*) of catheter-associated urinary tract infections and frequently responsible for BSIs in health-care settings. Hypervirulent (HV) isolates - exhibiting enhanced virulence, are responsible for CA liver abscesses, meningitis and metastatic spread to distant body sites in 11-80% of cases (Fung et al., 2002; Lederman and Crum, 2005). Infections caused by HV isolates were mostly reported in Taiwan, China and South Africa (Struve et al., 2015). Mortality rates of CA meningitis range from 30% to 83% in adults, with neurological sequelae in surviving patients (Sun et al., 2021). Defining features of HV isolates are the hypermucoviscous phenotype and specific capsular serotypes, primarily serotypes K1 or K2 (Pomakova et al., 2012). In other mammals, *K. pneumoniae* can be causative agent for clinical mastitis in dairy cows,

resulting in loss of milk production and in some cases death of affected cows (Schukken et al., 2012).

Other members of Klebsiella *spp.* can also cause a variety of opportunistic infections in humans. *K. pneumoniae* subsp. *rhinoscleromatis* and *K. pneumoniae* subsp. *ozaenae* have been reported as causative agents of chronic diseases, rhinoscleroma and atrophic rhinitis or ozaena (Botelho-Nevers et al., 2007; Chand and MacArthur, 1997). *K. oxytoca* is a major cause for neonatal infections involving the bloodstream (Egger et al., 2017), the central nervous system (CNS) (Carrie et al., 2019), lung (Gera et al., 2015), skin and soft tissues. *K. plantiicola* has been also implicated as a cause of neonatal sepsis (Podschun et al., 1998), although this species is mainly found in soil and water habitats.

2.4.4. Virulence determinants and contribution to pathogenesis

Although *K. pneumoniae* is considered an extracellular pathogen, there is some evidence of intracellular persistence within a vacuolar compartment (Cano et al., 2015). *K. pneumoniae* is also defined as a "stealth pathogen" because of its ability to "hide" from the host immune system rather than "attacking" (Paczosa and Mecsas, 2016). Evasion of the host immune defences is thus achieved via prevention of the antimicrobial action of soluble innate immune effectors (Kidd et al., 2017) and phagocytosis (Cortés et al., 2002). However, there are also evidences that *K. pneumoniae* can destabilize host defenses; it can manipulate maturation of dendritic cells and phagosome, mucosal immunity by inducing IL10 response, control cell death by triggering cellular apoptosis, and abrogate TLR-mediated inflammatory response (Bengoechea and Sa Pessoa, 2019).

K. pneumoniae employs various surface structures to evade and target host immune defenses, generating different levels of pathogenicity. Four well-characterized virulence factors are: capsule (CPS), lipopolysaccharide (LPS), fimbriae (type 1 and 3) and siderophores (Paczosa and Mecsas, 2016) (Figure 16).

LPS leads to activation of complement pathway and *Klebsiella* engulfment by cells in the respiratory epithelium and phagocytosis by macrophages, thereby promoting the pathogen clearance. Modification of LPS can play a crucial role in the evasion of bactericidal action of complement response (Alvarez et al., 2000) and in counteracting the bactericidal action of cationic antimicrobial peptides (CAMPs) and polymyxins (Kidd et al., 2017). Iron-transport systems are important to sustain the bacterial growth and replication. Four siderophores have been detected in *K. pneumoniae*: enterobactin, yersiniabactin, salmochelin, and aerobactin.

Enterobactin (ent) is a catecholate siderophore that is widely distributed across a number of enterobacterial isolates (Raymond et al., 2003). Ent shows the highest affinity for free Fe^{3+} iron compared to the other systems. Yersiniabactin (ybt) is commonly found among clinical isolates of *K. pneumoniae*, typically embedded within the high pathogenicity island (HPI), which is responsible for the dissemination of severe diseases caused by pathogenic yersiniae (Carniel, 2001). Aerobactin (iuc) is a hydroxamate siderophore and it plays a critical role in hypervirulence (Russo et al., 2015). In addition to iuc, carriage of salmochelin (iro) is also

associated with invasive disease and are common amongst HV *K. pneumoniae* isolates (Lam et al., 2018).

Most clinical *K. pneumoniae* isolates express type 1 and type 3 fimbriae. Type 1 fimbriae are adhesins ubiquitously distributed across several members of Enterobacterales (Klemm and Schembri, 2000). These fimbriae mediate adhesion to structures containing mannose and play an important role in urinary tract colonization by *K. pneumoniae* (Struve et al., 2008). Type 1 fimbriae expression was shown to be impeded by the presence of a polysaccharide capsule in *K. pneumoniae* (Schembri et al., 2005). Type 3 fimbriae are non-channelled fimbriae encoded by the highly conserved chromosomal *mrkA* gene cluster (Allen et al., 1991). Although type 3 fimbriae *K. pneumoniae* strongly promotes biofilm formation (Langstraat et al., 2001), they were shown not to impact on the ability of *K. pneumoniae* to colonize the gut or lung and urinary tract of mice (Struve et al., 2009).

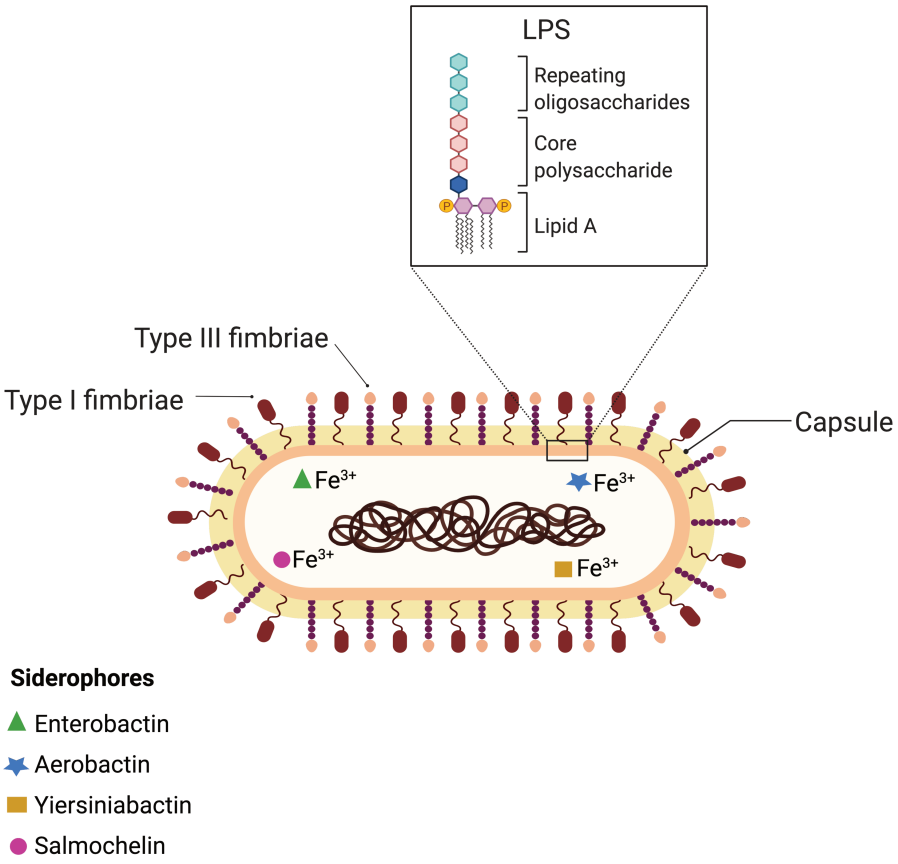

Figure 16: Major virulence factors in *K. pneumoniae*.

Other factors playing a role in *K. pneumoniae* pathogenicity include the OMPs (Brunson et al., 2019), efflux pumps (Bialek-Davenet et al., 2015), colibactin (Lu et al., 2017). For example, the non-specific porin OmpA plays a role in immune evasion by impeding TLR activation, thereby limiting the inflammatory response (March et al., 2011). Likewise, the porin OmpK36 has been

shown to have an antiphagocytic effect that contributes to enhance virulence in the murine model (March et al., 2013). Importantly, other virulence factors e.g., heavy metal resistance genes and genes upregulating cps production, *rmpA and rmpA2* can be carried onto plasmids, thereby facilitating the inter- and intra-species dissemination. In some cases, these plasmids co-harbour resistance genes and they are found within *K. pneumoniae* high risk clones (Turton et al., 2019; Xu et al., 2019), combining HV and MDR phenotypes.

2.4.4.1. The capsule: a major player in *K. pneumoniae* pathogenesis

The capsule is considered a major virulence factor in *K. pneumoniae*, offering protection from immune host response by reducing macrophage-mediated phagocytosis (March et al., 2013). In addition, CPS may contribute to resistance to CAMPs and polymyxins (Llobet et al., 2008). However, *K. pneumoniae* capsule is not required for resistance to bile stress (Tan et al., 2020). Capsule assembly and export occur via a Wzy-dependent pathway, identical to *E. coli* Group 1 capsule synthesis (Rendueles et al., 2017). The first step requires a glycosyltransferase (GT), WcaJ or WbaP, which links glucose (WcaJ) or galactose (WbaP) to a lipid carrier, undecaprenyl phosphate (Und-P). These oligosaccharides are transferred to the periplasmic space by Wzx translocase and polymerized by Wzy. Capsule length is controlled by Wzc and exported to the extracellular space by Wza, an outer membrane exporter (Figure 17). Finally, the capsule is anchored to the cell surface, most likely by Wzi (Rendueles et al., 2017) (Figure 17). Altogether, these genes constitute the *cps* operon (Wyres et al., 2016).

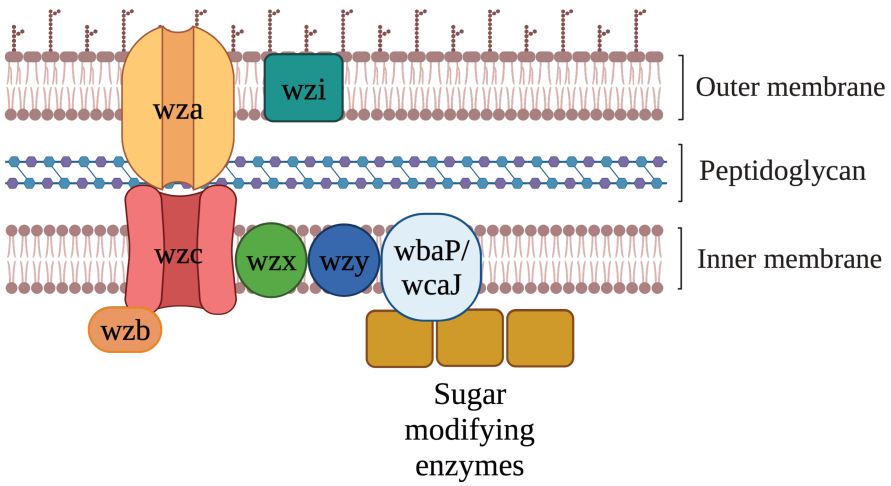

Figure 17. Schematic representation of group 1 CPS biosynthesis. Created with BioRender.com

To date, 79 capsular-types (K-type) have been reported in clinical isolates of *K. pneumoniae* (Pan et al., 2015). Recent studies shed light on the role of the different genes orchestrating capsule production in *K. pneumoniae*. CPS production is tightly regulated by a complex network of genes outside the *cps* cluster (Dorman et al., 2018).

Excessive production of capsule has been associated with HV isolates, controlled by either the chromosomally encoded *magA* gene (Yu et al., 2006), or plasmid-borne *rmpA* elements (Hsu et al., 2011). In addition, amino acid alterations of *wzc* encoding sequence, e.g., *wzc*G565A, have been associated with an hypermucoid and hypercapsulated phenotype with enhanced resistance to phagocytosis (Ernst et al., 2020a). On the other hand, non-capsulated mutants may provide different effects. For instance, *Δwza* mutants are unable to export capsular polysaccharide (Wei et al., 2018), whereas *Δwzy* deletion blocks capsule polymerization (Ho et al., 2011). Knockout mutants Δ*wzi,* Δ*wza,* Δ*wzb* or Δ*wzc* show a reduced amount or absence of capsule, corresponding to a rough, non-mucoid appearance on plate, along with an increased susceptibility to neutrophilic phagocytosis (Lin et al., 2017). A non-capsulated variant generated upon *wcaJ* inactivation was shown to be more refractory to phagocytosis, produce more biofilm on polystyrene surfaces and displayed an altered colistin susceptibility compared to the capsulated parental *K. pneumoniae* (Pal et al., 2019). However, Tan et al demonstrated that a Δ*wcaJ* mutant imposed a fitness cost in the mammalian gut (Tan et al., 2020). Interestingly, loss of mucoid-capsular phenotype may also occur within the host due to various mutations in the *cps* cluster (H. Lee et al., 2019).

Furthermore, diversity in capsule production may take place within a bacterial population, referred as to capsule switch from capsulated to non-capsulated variant. A recent study showed that capsule production within carbapenem resistant *K. pneumoniae* clinical isolates is heterogeneous and can be deduced by the appearance of mixed populations of mucoid and hypomucoid colony variants, indicative of genetic events occurring in the *cps* operon (Ernst et al., 2020). The hypomucoid variants impaired for capsule production are frequently observed in specimens from patients with UTIs. Interestingly, using a intraperitoneal mouse infection model, the authors showed that non-capsulated strains persist more efficiently compared to capsulated strains, due to their enhanced ability to form biofilm and invade epithelial cells in the mouse bladder (Ernst et al., 2020).

Altogether, these results suggest a role of capsule diversification in promoting the evolution and adaptation of *K. pneumoniae* populations. In addition, capsule-deficient mutants may represent a reservoir for antibiotic resistance genes in patients (Ernst et al., 2020).

2.4.5. Modulation of genetic content in *K. pneumoniae*

K. pneumoniae genomes are approximately 5 Mb in size, encoding about 5,000 genes, of which less than 50% belong to the core genome i.e. shared by all isolates (Wyres et al., 2020). Hence, most the genome architecture relies on the accessory genes. *K. pneumoniae* pangenome, i.e., the whole gene repertoire of the species, is defined "open" and extremely plastic, due to the tendency to easily gain novel genetic determinants through HGT and undergo chromosomal recombination (Holt et al., 2015). In *K. pneumoniae*, diversity of the genetic content is largely attributed to acquisition of plasmids harbouring accessory genes with diverse functions, including antibiotic resistance, virulence factors, and conjugation properties (Hendrickx et al., 2020; Mathers et al., 2015). Typically, *K. pneumoniae* isolates harbour one or more plasmids,

ranging from a few to several hundred kb. Larger plasmids are commonly present in single copy and smaller plasmids may amount to ten or more copies (Navon-Venezia et al., 2017; Ramirez et al., 2019).

Comprehensive analysis of several *K. pneumoniae* isolates by WGS allowed to detect multiple large genomic rearrangements (up to 20% of the entire genome), possibly contributing to diversification of the whole phylogroup (Wyres et al., 2019). Large recombination events seem to be confined to related *K. pneumoniae* phylogroups and limited by biological and/or ecological barriers (Holt et al., 2015).

Albeit rare, there is also evidence of a large events of homologous recombination occurring within the same phylogroup. Typically, these are mediated by plasmid conjugation, generating composed plasmids ("mosaic") promoting the co-transmission of virulence-encoding and resistance-encoding elements, or by events occurring at the capsule (*cps*) locus. Mosaic plasmids are highly abundant in *Klebsiella* (73%, n = 598/ 8272 in total) (Pesesky et al., 2019). For instance, the bla_{KPC}, originally acquired by an ancestral strain of the CC258, has spread through different plasmid backbones within the ST258/512 lineage (David et al., 2020). Extensive chromosomal recombination frequently results from horizontal transfer and rearrangements of *cps* locus genes have been widely reported (Wyres et al., 2019, 2015). For instance, the hospital associated clone ST258 is a hybrid lineage, evolved from the replacement of 20% of the *K. pneumoniae* ST11 genome with a 1.1 Mb genomic region from a ST442 strain (L. Chen et al., 2014). The acquired region encompasses the *cps* biosynthesis locus, another allele of the *tonB* MLST locus and it shows multiple genetic landmarks (L. Chen et al., 2014), suggesting the previous occurrence of recombination events. Hence, the *cps* region was proposed to be a hotspot for DNA recombination events that could represent a general strategy for *K. pneumoniae* to rapidly diversify in novel clades.

2.4.6. Clonal diversity and the concept of high-risk clones

Prior to the introduction of whole-genome based technologies, *K. pneumoniae* strains were typically characterized by using molecular methods including repetitive sequence-based PCR (rep-PCR), pulsed-field gel electrophoresis (PFGE), and multilocus sequence typing (MLST). The MLST method has been extensively used to define sequence types (ST) or clones for *K. pneumoniae* based on the genetic variation in 7 housekeeping genes (*rpoB, gapA, mdh, pgi, phoE, infB*, and *tonB*) (Diancourt et al., 2005). Closely related STs are named as clonal groups (CGs). MLST is well adapted for clonal group level analysis of *K. pneumoniae* population. However, it lacks discriminatory power for outbreak characterization and source attribution. Genome sequencing based typing methods like whole genome phylogeny based on SNPs detection and core genome cgMLST filled the gap by providing a higher resolution of discontinuities across *K. pneumoniae* clonal groups (Bialek-Davenet et al., 2014).

K. pneumoniae clones can also be distinguished from one another on the basis of accessory gene content (Holt et al., 2015). Several deep-rooted *K. pneumoniae* lineages originate from a single common ancestor, giving rise to a star-like phylogeny (Figure 18).

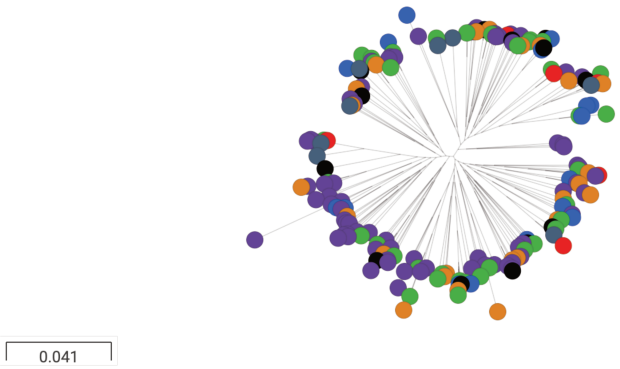

Figure 18: Core gene phylogeny for *K. pneumoniae*. Unrooted maximum likelihood phylogenetic tree for 283 isolates sampled from diverse sources and locations; tips are coloured by country. Tree, country of origin and source information are available for interactive viewing at https://microreact.org/project/BJClQz9H.

Epidemiological studies have allowed the identification of high-risk clones that have disseminated at global scale, therefore also referred to as "global problem clones" (Wyres et al., 2020). Woodford *et al.* originally defined as 'high-risk clone' the isolates coming from the same ST but sampled from different geographic areas and at different times. In addition, these STs are more likely to cause outbreaks worldwide and persist across diverse niches (Woodford et al., 2011). *K. pneumoniae* high-risk clones can be divided into hypervirulent, mainly responsible for community-acquired invasive infections (Struve et al., 2015) and multidrug-resistant (MDR), leading cause of healthcare associated infections (Cerqueira et al., 2017).

Interestingly, HV clones of *K. pneumoniae* rarely display multiple antimicrobial resistance features (Struve et al., 2015). Infections caused by HV are commonly associated with three prevalent clonal groups (CG23, CG65 and CG86), and, to a minor extent, by CG25, CG66 and CG380 (Wyres et al., 2020). MDR lineages can be quite diverse and include mainly eight clones (CG15, CG20, CG29, CG37, CG147, CG101, CG258 and CG307) (Wyres et al., 2020). CG258 is the most successful clonal group due to its enhanced dissemination and extensively drug resistant profiles (Chmelnitsky et al., 2013). CG258 is largely responsible for international outbreaks caused by CRKp (Navon-Venezia et al., 2017) and encompasses mainly three STs: ST258, ST11 and ST512. CG258 has been widely found in association with bla_{KPC} (Navon-Venezia et al., 2017), whose dissemination likely occurred upon the acquisition of the plasmid harbouring KPC in an ancestral strain (David et al., 2020). However, non-CG258 KPC-Kp isolates are emerging in Europe. For instance, ST307 and ST273 KPC-Kp isolates have been reported in Sicilia (Italy) (Bonura et al., 2015), and in Colombia (Ocampo et al., 2016), where CG-258 KPC-Kp was previously known to be endemic. Furthermore, over 1,010 CPKp isolates collected in France, only 66 were KPC-Kp (6.5%) and only 8 out of 63 sequenced isolates (12.7%) belong to CG258 (Bonnin et al., 2020). Altogether, these studies suggest an ongoing shift in the KPC-Kp

epidemiology in Europe. Certainly, the emergence of novel high-risk clones is of great concern as it poses a further threat for the public health.

2.4.7. β-lactam resistance in *K. pneumoniae*

SHV-1, a chromosomally encoded narrow-spectrum β-lactamase active against penicillins, was first reported in *K. pneumoniae* in 1972[24]. At that time, it was commonly believed that SHV β-lactamases were exclusively found in the chromosome, but later evidence demonstrated the extrachromosomal location of the bla_{SHV-1} gene in some *K. pneumoniae* isolates (Nugent and Hedges, 1979). Subsequently, substitution in the AA sequence of SHV β-lactamases e.g., a substitution of glycine at position 238 in SHV-1 by serine in SHV-2 led to the emergence of ESBL in several Enterobacterales, including *K. pneumoniae.* In the following years, the global explosion of *K. pneumoniae* isolates producing the Cefotaximase-Munich (CTX-M)-type ESBL (Livermore et al., 2007), led to an increased use of carbapenem antibiotics that, unfortunately, fostered the global emergence of carbapenem resistance.

Carbapenem resistant *K. pneumoniae* (CRKp) represent a serious menace with implications for public health and society. In Europe, the percentage of *K. pneumoniae* isolates showing resistance to carbapenems is above 10%, predominantly in the Southern and Eastern areas (Figure 19). In addition, a 6-fold increase of mortality rates has been reported between 2007 and 2015 for CRKp infections in Europe (Cassini et al., 2016), likely due to the scarcity of therapeutic alternatives currently available for those MDR infections.

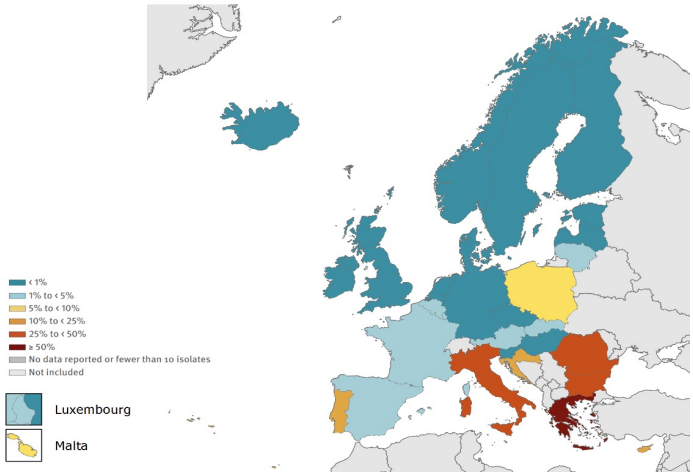

Source: European Centre for Disease Prevention and Control. Antimicrobial resistance in the EU/EEA (EARS-Net) - Annual Epidemiological Report 2019. Stockholm: ECDC; 2020

Figure 19: *Klebsiella pneumoniae*. Percentage of invasive isolates resistant to carbapenems (imipenem and/or meropenem), by country, EU/EEA, 2019[25].

[24]Originally, SHV-1 was designated as PIT-2 after the name of Pitton, who discovered it. Later, it was renamed as SHV-1 by Matthew *et al.* (Matthew et al., 1979). In those years, the confusion on the designation likely led to underreported cases of resistance.

[25]https://www.ecdc.europa.eu/sites/default/files/documents/surveillance-antimicrobial-resistance-Europe-2019.pdf

2.4.7.1. Main routes to β-lactam resistance in *K. pneumoniae*

K. pneumoniae is intrinsically resistant to penicillin due to the chromosomally encoded β-lactamase SHV-1. Furthermore, clinical isolates frequently show ESBL production due to mutations that expand the hydrolysis spectrum of SHV-type penicillinases or insertion of transposable elements upstream their promoter, in concomitance with several other acquired ESBLs genes, altogether conferring the resistance phenotype (Martínez-Martínez, 2008). The acquisition of β-lactamases with hydrolytic activity towards carbapenems is a frequent event in *K. pneumoniae* clinical isolates. Higher resistance levels to carbapenems are achieved with the co-occurrence of OM permeability defects and ESBL overproduction (Girlich et al., 2009).

Yet, our current understanding on the role played by different porins of *K. pneumoniae* in the evolution of β-lactam resistance and the regulation of their expression is limited. A recent study combined the proteomic and WGS approaches to shed light on the impact of OM remodelling in reduced sensitivity to β-lactams of *K. pneumoniae*. Isolates deficient for both OmpK35 and OmpK36 (Δ*ompK35*Δ*ompK36*) but not possessing β-lactamases already displayed MICs above the EUCAST and CLSI breakpoints to all β-lactams, with a stronger effect on ceftazidime (CAZ) and ERT (Rocker et al., 2020). MIC increase might result from decreased drug permeation rates, which simultaneously allow other β-lactamases to reduce periplasmic drug levels. However, Rocker *et al*. showed that the β-lactamase SHV-1 contributes very little to carbapenem resistance in *K. pneumoniae*. Interestingly, truncated *ompK35* genes are enriched in the predominant CC258 *K. pneumoniae* lineage whereas mutations in *ompK36* and other porins (e.g., OmpK37, OmpK38, OmpK26, PhoE, or LamB) are rare and randomly distributed across the whole *Klebsiella* phylogeny (Rocker et al., 2020). Mutations in *ompK35* have been prevalently detected globally in concomitance with the emergence of β-lactamase-mediated resistance. OmpK35 contributes to the entry into the periplasm of other antibiotics like aminoglycosides, quinolones, and macrolides (Rocker et al., 2020). Therefore, *ompK35* alterations may lead to cross-resistance and dramatically impair therapeutic options. Alternative porins OmpK37 and OmpK38 are like OmpK36, possess a similar pore but they show low permeability rates to ertapenem, ceftriaxone, and cefotaxime. OmpK26 does not allow carbapenem permeation and its overexpression might play a role in isolates deficient for the major porins selected by carbapenem treatment. The porin LamB is specific for the passage of sugars but not β-lactam antibiotics, in contrast with PhoE (Rocker et al., 2020).

Altogether, these data suggest a complex regulation of antibiotic permeability in *K. pneumoniae*, varying upon the size and the charge of the drug and microbial features, in addition to be likely influenced by the surrounding environments, e.g., host factors and phage predation.

2.4.7.2. Carbapenemase-producing *K. pneumoniae* (CPKp): a global menace

The most prevalent carbapenemases in *K. pneumoniae* are KPC-, NDM-, VIM- and OXA-48-like, with their distribution of CPKp varying according to the country and region (Queenan et al., 2010). Since carbapenem resistance genes are easily transferable through plasmids among

bacteria and mobility of populations enhances the risk of transmission of multidrug-resistant organisms (van der Bij and Pitout, 2012), travelling of individuals in endemic areas or countries may impact on the geographical distribution of CPKp.

KPC-Kp isolates represent a global threat (Munoz-Price et al., 2013; Nordmann et al., 2009), with an XDR phenotype and associated with high mortality rates (Munoz-Price et al., 2013). In Europe, large inter-country variations are observed for KPC-Kp isolates, with endemic spread in countries such as Greece, Italy and Romania and sporadic cases in countries like Spain, France, Germany[26]. In France, the first KPC positive *K. pneumoniae* clinical isolates was detected in 2005 (Naas et al., 2005) and monitored since 2012 by the National Reference Center (NRC) for tracking carbapenem-resistant Enterobacterales that is established at the Kremlin-Bicêtre Hospital[27]. In addition to North-America, KPC-Kp are endemic in South-American countries like Colombia, Brazil and Argentina, whereas in Asia, endemic spread was reported in China (Li et al., 2014) and Taiwan (Tseng et al., 2015). The successful spread of *bla*$_{KPC}$ worldwide across *Klebsiella* isolates has been linked to the CG258 clade, prevalent in Europe (the EuSCAPE Working Group et al., 2019). At least 79 KPC variants have been identified (www.bldb.eu), with the KPC-2 and the KPC-3 being the most frequently detected. Classically, a *bla*$_{KPC}$ gene is embedded in a Tn*4401* transposon, which seems to be the main driver of KPC dissemination onto numerous plasmids of different sizes (Naas et al., 2008). Tn*4401* is approximately 10 kb in length and contains a Tn*3* transposase gene, a Tn*3* resolvase gene, the *bla*$_{KPC}$ and two insertion sequences, IS*Kpn6* and IS*Kpn7* (Naas et al., 2008). To date, at least 6 different isoforms of Tn*4401* exist, which differ by deletions just upstream *bla*$_{KPC}$ providing different promoter regions, and consequently different expression levels of the *bla*$_{KPC}$ gene (Chmelnitsky et al., 2014; Naas et al., 2012). For instance, the promoter activity of Tn*4401a* and Tn*4401h* isoforms result in a 23- and 4-fold increase in KPC expression, respectively, compared to the Tn*4401b* isoform (Cheruvanky et al., 2017). Rarely, *bla*$_{KPC}$ is also found in non-Tn*4401* elements, generally exhibiting partial IS*Kpn6* and sometimes having an IS*26* transposon (Y.-T. Chen et al., 2014, p. 2-). Typically, *bla*$_{KPC}$ travels across *K. pneumoniae* isolates onto large, self-conjugating plasmids, co-harbouring multiple resistance genes. FIIK is a common plasmid replicon in Klebsiella *spp.*(Villa et al., 2010).

The most frequent class B carbapenemases detected among *K. pneumoniae* isolates are NDM, VIM and the IMP-types (Jeon et al., 2015). Since 2008, when NDM-1 was first detected in *K. pneumoniae* and *E. coli* in a patient travelling from India back to Sweden, NDM-producing *K. pneumoniae* rapidly disseminated (Jeon et al., 2015), becoming endemic in the Indian subcontinent (Dortet et al., 2014). Interestingly, the *bla*$_{NDM}$ genes does not seem to be associated with specific *K. pneumoniae* clones, as seen for KPC, and its diffusion in western countries is

[26] European Centre for Disease Prevention and Control. Antimicrobial resistance in the EU/EEA (EARS-Net) - Annual Epidemiological Report 2019. Stockholm: ECDC; 2020

[27] https://www.cnr-resistance-antibiotiques.fr/presentation-de-lequipe-1.html

mostly associated with travelling of patients in endemic areas. VIM-like enzymes are the second prevalent carbapenemases in *K. pneumoniae* in Italy (9.2%) (Giani et al., 2013).

Of the several Class D carbapenemases, mainly OXA-48 and derivatives have been reported in *K. pneumoniae* (Evans and Amyes, 2014). A *K. pneumoniae* strain producing OXA-48 was first identified in 2001 in Turkey (Poirel et al., 2004), with endemic foci established in the Mediterranean basin and France (Castanheira et al., 2019; Dortet et al., 2017). In France, large outbreaks of OXA-48-producing *K. pneumoniae* were mainly associated with environmental sources for these isolates, such as hospital sink drains, mattress and all disposable supplies (Pantel et al., 2016) and interchange of health-care personnel between two different hospital wards (Semin-Pelletier et al., 2015). OXA-48 is the most frequent carbapenemase detected in France, accounting for 69.4% of the 1,010 CPKp analyzed from the NRC collection (Bonnin et al. 2020).

2.4.7.3. Challenges in definition of susceptibility levels in CPKp isolates

A prompt and rapid detection of CPKp isolates is essential to improve management of severe infections, infection control and reduce mortality rates associated with these infections. In the clinical microbiology laboratory, current approaches are molecular tests, such as PCR-based (Lee et al., 2015), DNA microarray (Braun et al., 2014), MALDI-TOF MS (Carvalhaes et al., 2014) and phenotypic assays, e.g., the carbapenem inactivation method (CIM) (van der Zwaluw et al., 2015), the Modified Hodge test in combination with EDTA or boronic acid (Song et al., 2015) and the SuperCarba (Girlich et al., 2013).

Classically, MIC is determined by broth microdilution (BMD), Etest and disc diffusion assay, or, more frequently, using automated methods such as Vitek 2 (Biomerieux) and Phoenix system (Becton Dickinson - BD). CPKp may exhibit a wide range of carbapenem MICs and frequently below the clinical breakpoint (Munoz-Price et al., 2013; Nordmann et al., 2009; Steward et al., 2003). As a matter of fact, the clinical breakpoints have been frequently modified and recently lowered to 1 μg/ml to improve detection of CPKp[28,29]. Major discrepancies derive from the MIC measurements of the automated systems, which yield to major errors that can affect treatment choice and its outcome (Tenover et al., 2006; Woodford et al., 2010). Carbapenem monotherapy failure has been observed among KPC-producing *K. pneumoniae*, whose resistance levels to imipenem or meropenem were underappreciated (Weisenberg et al., 2009). Underlying factors of this variability may be the complex expression of the bla_{KPC} (Cheruvanky et al., 2017; Naas et al., 2012), the bacterial cell density (Lenhard and Bulman, 2019), the bacterial lifestyle (Amanatidou et al., 2019; Kim and Anthony, 1981; Li et al., 2018) and the presence of inner colonies in the inhibition halo (Gaibani et al., 2018; Nordmann et al., 2009),

[28]Clinical and Laboratory Standards Institute (CLSI). Performance Standards for Antimicrobial Susceptibility Testing. 27th ed. CLSI supplement M100 (ISBN 1-56238-804-5 [Print]; ISBN 1-56238-805-3 [Electronic]). Clinical and Laboratory Standards Institute, 950 West Valley Road, Suite 2500, Wayne, Pennsylvania 19087 USA, 2017.

[29] https://www.eucast.org/clinical_breakpoints/

suggesting the presence of subpopulations with different degrees of resistance, i.e. heteroresistance.

2.4.8. Alternative strategies to escape antibiotic treatment in *K. pneumoniae*

2.4.8.1. Tolerance and persistence in *K. pneumoniae*

Treatment failure of *K. pneumoniae* infections has been largely attributed to acquisition of *de novo* mutations and novel resistance determinants via HGT. In addition to genetic resistance mechanisms, the production of biofilm helps *K. pneumoniae* to evade host immune responses during infection, and its architecture allows to hide fractions of slow-growing bacteria from antibiotics, eventually causing therapy failure (Mah and O'Toole, 2001).

Alternative survival strategies such as tolerance, persistence and HR are poorly characterized in *K. pneumoniae*. In Enterobacterales, most of the studies on tolerance and HR (persistence) have been conducted in *E. coli,* where intermittent high-dose antibiotic exposure led to enhanced persistence levels and cross-tolerance to other antibiotics. However, the degree of tolerance may vary depending on the species and/or the background of the strain under investigation (Abokhalil et al., 2020; Kaldalu et al., 2016). Given the clinical relevance of *K. pneumoniae*, the high degree of inter-strain variability and the evidence of tolerance and persistence being antecedent stages to evolution of stable resistance (Levin-Reisman et al., 2017), specific studies are required to gain further insights on alternative strategies adopted by *K. pneumoniae* to survive antibiotic exposure.

In the recent years, there has been increasing interest towards such aspects and some reports have characterized tolerance to different compounds and nutritional stress in *K. pneumoniae*. Yaikhan T. and coworkers have shown that exposure to indole and derivatives may impact on the *K. pneumoniae* tolerance to β-lactam antibiotics (Yaikhan et al., 2019). Interestingly, the effect of indole varied according to the susceptibility pattern towards carbapenems: the susceptible *K. pneumoniae* strain tolerated better ampicillin, displayed higher resistance levels to meropenem and ceftriaxone and restored susceptibility to imipenem, amoxicillin, and cefoxitin upon exposure towards synthetic indole. Conversely, the carbapenem resistant isolate displayed increased resistance levels to imipenem but became more susceptible to meropenem.

Recently, the adaptation to the biocide chlorhexidine in two clinical strains of CPKp (KPC-3 and OXA-48) was investigated (Bleriot et al., 2020). Interestingly, the OXA-48 producing *K. pneumoniae* strain exhibited a biphasic killing curve in the presence of a chlorhexidine-imipenem combination, indicative of persisters formation. This pattern was next attributed to a novel toxin-antitoxin (TA) system in *K. pneumoniae*, the PemI/PemK, and to the RelE/RelB TA system, both carried onto the OXA-48 plasmid. Consistently, the biphasic pattern was lost when the OXA-48 plasmid was cured. Since the TA systems are known to contribute to persisters formation in other species (Gerdes and Maisonneuve, 2012; Moyed and

Bertrand, 1983), the authors hypothesized that TA systems PemI/PemK and RelE/RelB contributed to the formation of persisters and biofilm in *K. pneumoniae* isolates.

The stringent response is crucial for adaptation and survival under unfavourable growth conditions[30]. One of the main regulators of the stringent response is *spoT,* which was recently characterized in *K. pneumoniae* (Davis and Brown, 2020). The *spoT* gene was shown to play a pivotal role in *K. pneumoniae* in response to carbon and phosphate starvation, as well as providing protection against heat, osmotic and ethanol stress (Davis and Brown, 2020). In addition, since *spoT* mutants exhibited less mucoid colonies and were deficient for the capsule, the authors speculated that the stringent response may contribute to capsule production.

Few reports have also investigated persisters formation rates in *K. pneumoniae*. Ren *et al*. (Ren et al., 2015) reported increased persisters levels in a laboratory strain and a clinical strain of *K. pneumoniae* following step by step antibiotic feeding with three different molecules (ciprofloxacin, kanamycin and ceftriaxone) to reach serum peak concentration, as would be the case *in vivo*. Persistence levels vary with the type of drug and strain under investigation; for instance, upon 24 hours of treatment, the clinical isolate displayed a higher number of survivors with ciprofloxacin than the control isolates, likely due to enhanced emergence of resistant mutants provoked by sublethal doses of the drug.

Persisters formation in *K. pneumoniae* was also shown to be growth phase-dependent: in stationary phase, bacterial cells are more tolerant against meropenem than those in exponential phase (Li et al., 2018). By analyzing 68 clinical isolates, it was also shown that rates of persistence to meropenem in *K. pneumoniae* isolates from blood are extremely variable and correlated with specific genotypes (CC15 and CC23) (J. S. Lee et al., 2019). However, persister fractions were not associated with underlying diseases of the patient and/or poor clinical outcome.

In the work from Ernst *et al*., the subpopulations of capsule-deficient/hypomucoid variants displayed enhanced ability to form biofilm (Ernst et al., 2020b). Since biofilm communities can provide antibiotic tolerance due to low penetration of the antibiotic (Stewart, 2002) and the increased levels of persisters (Mah and O'Toole, 2001), the authors speculated that heterogeneous capsule production might reflect a phenotypic diversification strategy to establish successful and recalcitrant infections in the host.

Finally, the formation of persister cells has been compared between *K. pneumoniae* and *Proteus mirabilis* isolates upon 24-hours challenge with high doses of ciprofloxacin (Abokhalil et al., 2020). While *K. pneumoniae* exhibited slightly higher fraction of persister cells than *P. mirabilis* (2.3%), persister cells from both isolates were extremely heterogeneous and displayed filamentous length during regrowth, likely caused by inhibition of cell division.

[30]Cashel M, Gentry D R, Hernandez V J, Vinella D. The stringent response. In: Neidhardt F C, Curtiss III R, Ingraham J L, Lin E C C, Low K B, Magasanik B, Reznikoff W S, Riley M, Schaechter M, Umbarger H E, editors. Escherichia coli and Salmonella: cellular and molecular biology. 2nd ed. Washington, D.C.: ASM Press; 1996. pp. 1458–1496.

Interestingly, the persisters level of *K. pneumoniae* was significantly reduced by adding sucrose at 5 mM during exposure to ciprofloxacin; a complete eradication of *K. pneumoniae* persisters was achieved by supplementing ciprofloxacin with salicylate or silver nitrate.

Clinical implications of persister formation in *K. pneumoniae* are still unclear. Certainly, one pitfall of studies on persisters is that pure *in-vitro* culture analysis may not accurately reflect the *in vivo* conditions.

2.4.8.2. Heteroresistance – a blurry concept in *K. pneumoniae*

Heteroresistance has been widely reported among *K. pneumoniae* isolates towards colistin (Band et al., 2018; Bardet et al., 2017; Silva et al., 2016), followed by carbapenems (Adams-Sapper et al., 2018; López-Camacho et al., 2019; Nodari et al., 2015; Pournaras et al., 2010; Tato et al., 2010), and other few molecules (Naparstek et al., 2012; J.-X. Zheng et al., 2018).

Despite the methodological discrepancies among different studies, the underlying genetic mechanism of HR to colistin in *K. pneumoniae* relies on alterations of the two-component systems PmrAB and PhoPQ, or MgrB, a negative regulator of the PhoPQ signaling (Bardet et al., 2017). In one study, heterogeneity of colistin resistance resulted from 25 bp deletion in the *phoP* gene occurring in a fraction of cells of a resistant population (Jayol et al., 2015). However, HR is usually investigated in susceptible populations showing heterogeneity by Etest/disk diffusion assay or through the skip-well phenomenon, i.e., "Eagle effect". In the light of the recently proposed parameters for evalutation of HR (Andersson et al., 2019), colistin HR in *K. pneumoniae* rather recalls the concept of polyclonal HR, where the exposure to high doses of colistin selects for resistant mutants, thus relies on genetic modifications occurring at various frequencies.

Heteroresistance to carbapenems has been mostly reported among KPC-Kp (Adams-Sapper et al., 2015; Nodari et al., 2015; Pournaras et al., 2010). To date, only one report describes the occurrence of imipenem HR among VIM-1 *K. pneumoniae* isolates (Tato et al., 2010). By using PAP assay, HR was attributed to three VIM-1 isolates due to the presence of subpopulations arising at a frequency ranging from 3×10^{-7} to 5×10^{-6} at the highest imipenem concentration (32 μg/ml). The authors speculated that heterogeneity of imipenem resistance could be due to the variable expression of the bla_{VIM} or to the presence of other resistance mechanisms, such as porin deficiency; by variations in copy number of the bla_{VIM} plasmid. However, no further assays were performed to confirm their mechanistic hypotheses. Interestingly, one recent study characterized the HR profile visualized by disc diffusion of two OXA-48–producing *K. pneumoniae* (OXA-48-Kp) isolates (López-Camacho et al., 2019). Since the frequency of subpopulations growing at high doses of meropenem was similar to mutation frequency assays (ca. 5×10^{-6}), and colonies analysed showed stable high resistance levels, the authors concluded that it was incorrect to define such isolates as HR. Instead, they propose that in OXA-48-Kp, the appearance of colonies within the inhibition halo of diffusion assays indicates regrowth of persisters.

Despite the high incidence of HR among KPC-Kp and the clinical importance of carbapenems, we know very little on mechanisms mediating carbapenem HR in *K. pneumoniae* isolates. Heteroresistance can be the consequence of multiple, not totally related processes, including selection of (stable and unstable) resistant mutants and emergence of persisters. A first attempt to clarify the mechanism of carbapenem HR in *K. pneumoniae* dates back to 2010, when Pournaras and co-workers observed a modest increase of bla_{KPC} expression (ranging from 0.475-fold to 1.07-fold) in the meropenem-HR subpopulations of six KPC-Kp isolates (Pournaras et al., 2010). A later study reported that survival of HR KPC-Kp strains to high bactericidal concentrations of imipenem resulted from a combination of three aspects: (i) a high inoculum size (greater than 3.3×10^6 CFU/ml) (ii) carriage of the bla_{KPC} gene, and (iii) the emergence of subpopulations with decreased expression of the major OMP, OmpK36 (Adams-Sapper et al., 2015). Specifically, the authors suggested that survival might be favored in the first place by imipenem degradation driven by KPC and the high inoculum density, followed by gain of high level of resistance among the subpopulations resulted from adaptive changes in response to stress induced by the carbapenem drug (Adams-Sapper et al., 2018). However, in the case of carbapenemase-producing isolates, the experimental conditions to investigate the presence of subpopulations should be carefully chosen to avoid artifacts and misinterpretations of the phenomenon.

Recently, Nicoloff *et al.* showed that HR is prevalent among pathogenic bacteria and largely caused by unstable tandem gene amplifications of chromosomal and/or plasmid regions harbouring resistance genes (Nicoloff et al., 2019). However, out of 10 *K. pneumoniae* tested, only one showed HR to imipenem by Etest, subsequently confirmed by PAP, whereas 7/10 showed HR to ertapenem and none to meropenem. This result is not surprising since none of the selected isolates produced a carbapenemase, indirectly confirming the link between carbapenemase production and the HR phenotype, as previously suggested (Adams-Sapper et al., 2015; Nodari et al., 2015).

Further studies are necessary to understand HR mechanisms towards carbapenems and its clinical implications. Intuitively, the rise of carbapenem heteroresistance might further challenge the clinical management of CPKp and contribute to therapy failure, as observed in the murine model for colistin HR (Band et al., 2018).

III. General Aim & Research objectives

Carbapenems, which belong to the β-lactam family of antibiotics, are considered the last resort drugs to fight multi-drug resistant (MDR) Gram-negative bacteria. Resistance is frequently due to the acquisition of carbapenemase-encoding genes responsible for the degradation of carbapenems. *K. pneumoniae* harbouring carbapenemase genes (CPKp) commonly show varying carbapenem MICs and exhibit heteroresistance[31], possibly affecting treatment outcomes. Although frequently observed, especially among KPC-Kp isolates, underlying mechanisms causing heterogeneity in resistance phenotype and whether additional factors are responsible for heteroresistance are largely unknown. The coexistence of subpopulations with distinct traits is likely one mechanism responsible for the HR phenotype. Given the potential clinical burden of heteroresistance, understanding this phenomenon is crucial.

The overarching purpose of my PhD project was to elucidate the phenomenon of heteroresistance among CPKp by characterizing the surviving bacteria leading with an apparent decreased susceptibility and identifying genetic factors contributing to the carbapenem resistance phenotype and to heteroresistance.

My research project involved three main objectives:

1. Assessment of phenotypic variability and genotypic diversity on collections of clinical CPKp isolates (from the French NRC and other collaborators) through:
- Phenotypic characterization of susceptibility levels and heteroresistance.
- Whole genome sequencing (WGS)
- Bioinformatic analysis to identify *loci* and/or mutations explaining the phenotype.

For this first part of the thesis, I have employed methods routinely used in the EERA unit or classically used to characterize HR, like Etest and PAP assay.

2. Investigating the bases of diversity by:
- Characterizing the heterogeneity at population and single cell-level.
- Phenotypic and genotypic analysis of subpopulations.

In this second part, I tested, with the help from members of the unit and following advice from colleagues, different approaches to characterize the surviving populations, to eventually choose the ScanLag system, which I set up together with Nicolas Cabanel, to track the growth of clinical isolates at single-colony level.

[31] Heterogeneous susceptibility levels of carbapenem resistance within isogenic populations, typically visualized by colonies growing in the inhibition zone of the drug on solid media

3. Validation of the contribution of the different factors to the resistance phenotype and their interplay *via* genetic manipulation of multi-susceptible isolates to functionally test former observations.

Results from objectives 1 and 2 provide a wealth of new information for further functional investigation. However, in the timeframe of the PhD thesis, I was only able to perform some very preliminary analysis to test some hypotheses.

With this project, we expected (a) to gain a better understanding of this bet-hedging strategy adopted by several resistant microbes, (b) to shed light on how heteroresistant microorganisms evolve into a definitive resistant phenotype and (c) to provide rational bases for predicting the carbapenem-resistance of *K. pneumoniae* isolates by inferring relationships between microbial traits and genomic components.

IV. Results

ARTICLE I

Diversity of mucoid to non-mucoid switch among carbapenemase-producing *Klebsiella pneumoniae*

Adriana Chiarelli, Nicolas Cabanel, Isabelle Rosinski-Chupin, Pengdbamba Dieudonné Zongo, Thierry Naas, Rémy A. Bonnin, and Philippe Glaser

Carbapenemase-producing *Klebsiella pneumoniae* (CPKp) is a leading cause of intractable multidrug-resistant (MDR) infections in hospitals. Understanding the reasons behind the successful dissemination and persistence of this pathogen may significantly improve its clinical management.

In the very beginning of my PhD, we collected CPKp isolates selected from the National Reference Center (NRC) collection, Bicêtre, and Nice hospitals, with the major objective of characterizing the diversity of resistance levels to carbapenems and the occurrence of heteroresistance.

The observation of colony variants exhibited by most of the isolates coming from different sources and different hospitals on solid media was suggestive of an intrinsic heterogeneity of the bacterial populations. After having ruled out that this was due to contamination with other Klebsiella *spp.* or other species, I developed some hypotheses on possible events causing the diverse colony appearance, which kicked off this study.

A major hypothesis was that loss and/or reduction of the capsule (CPS) caused the translucent colony aspect. In fact, as I mention in the Introduction, *K. pneumoniae* usually forms dome-shaped, mucoid colonies that are indicative of production of the extracellular capsule layer. Therefore, I selected eight CPKp isolates from various STs and producing different types of carbapenemase to go further in this analysis.

According to my main hypothesis, I first assessed, per each isolate, whether there was any difference between the "normal", mucoid colony and the translucent, "non-mucoid" one in terms of capsule production. The assay used was based on quantification of uronic acid, a major component of the capsule in *K. pneumoniae*, followed by India Ink staining and visualization under the microscope. Despite the numerous technical difficulties encountered, I finally managed to show, with the precious technical and emotional support of Emanuela Ursino (a lab member at the time), differences in the capsule content between the colony variants of the eight isolates. In addition, I estimated that the frequency of this "switch" on Tryptic Soy Agar (TSA) media was overall high, with inter-strain variations likely due to the different genomic background of the isolates and increased along with colony evolution on

plate. At this stage, we are not aware whether the transition occurs also the other way round, from non-mucoid back to mucoid.

Whole genome comparison of the colony variants from the eight CPKp strains was used to infer the genetic bases of the spontaneous capsule loss. As a result, we could observe mutations occurring at the *cps* operon of some non-mucoid variants, but for some others, the analysis of the genome sequence was not straightforward owing to the poor coverage of the *cps* operon obtained. This issue, which will be further addressed in the General Discussion, was rapidly fixed by using another commercial kit for library preparation. Hence, we could successfully collect additional non-mucoid variants and sequence them. This approach allowed to reveal that spontaneous loss/reduction of capsule most frequently resulted of IS elements hopping into essential genes for capsule synthesis.

Next, I showed that the capsule loss had also an impact on phenotypic properties contributing to virulence, such as *in vitro* biofilm formation and autoaggregative property.

Considering that my main research question involved the HR phenomenon, I next measured carbapenem susceptibility levels and observed differences between the mucoid and non-mucoid variant. For most of the isolates analysed, the loss of capsule was associated with either no change or increase in susceptibility to carbapenems except for one isolate, likely due to pre-existing defect in the O-antigen of the LPS. These findings were consistent with the general concept that a population might exhibit various susceptibility levels to a particular drug. However, we could not show a convincing link with heteroresistance.

To our knowledge, this work is among the most extensive studies revealing the genetic bases of the spontaneous emergence of colony variants on solid media among CPKp clinical isolates. As the colony opacity differences in stored isolates may go undetected, researchers may be unconsciously working with mixed populations. This could be problematic for many studies, especially those involving virulence and resistance.

Chiarelli *et al. BMC Microbiology* (2020) 20:325
https://doi.org/10.1186/s12866-020-02007-y

BMC Microbiology

RESEARCH ARTICLE Open Access

Diversity of mucoid to non-mucoid switch among carbapenemase-producing *Klebsiella pneumoniae*

Adriana Chiarelli[1,2,3], Nicolas Cabanel[1,2], Isabelle Rosinski-Chupin[1,2], Pengdbamba Dieudonné Zongo[1,2], Thierry Naas[1,4], Rémy A. Bonnin[1,4†] and Philippe Glaser[1,2*†]

Abstract

Background: *Klebsiella pneumoniae* is a leading cause of intractable hospital-acquired multidrug-resistant infections and carbapenemase-producing *K. pneumoniae* (CP*Kp*) are particularly feared. Most of the clinical isolates produce capsule as a major virulence factor. Recombination events at the capsule locus are frequent and responsible for capsule diversity within *Klebsiella spp*. Capsule diversity may also occur within clonal bacterial populations generating differences in colony aspect. However, little is known about this phenomenon of phenotypic variation in CP*Kp* and its consequences.

Results: Here, we explored the genetic causes of in vitro switching from capsulated, mucoid to non-mucoid, non-capsulated phenotype in eight clinical CP*Kp* isolates. We compared capsulated, mucoid colony variants with one of their non-capsulated, non-mucoid isogenic variant. The two colony variants were distinguished by their appearance on solid medium. Whole genome comparison was used to infer mutations causing phenotypic differences. The frequency of phenotypic switch was strain-dependent and increased along with colony development on plate. We observed, for 72 non-capsulated variants that the loss of the mucoid phenotype correlates with capsule deficiency and diverse genetic events, including transposition of insertion sequences or point mutations, affecting genes belonging to the capsule operon. Reduced or loss of capsular production was associated with various in vitro phenotypic changes, affecting susceptibility to carbapenem but not to colistin, in vitro biofilm formation and autoaggregation.

Conclusions: The different impact of the phenotypic variation among the eight isolates in terms of capsule content, biofilm production and carbapenem susceptibility suggested heterogeneous selective advantage for capsular loss according to the strain and the mutation. Based on our results, we believe that attention should be paid in the phenotypic characterization of CP*Kp* clinical isolates, particularly of traits related to virulence and carbapenem resistance.

Keywords: Capsule, Carbapenem, Insertion sequence, Biofilm, *Klebsiella pneumoniae*

* Correspondence: pglaser@pasteur.fr
†Rémy A. Bonnin and Philippe Glaser contributed equally to this work.
[1]EERA Unit "Ecology and Evolution of Antibiotic Resistance", Institut Pasteur - Assistance Publique/Hôpitaux de Paris - University Paris-Saclay, Paris, France
[2]UMR CNRS 3525, 75015 Paris, France
Full list of author information is available at the end of the article

Background

Klebsiella pneumoniae is a Gram negative, capsulated, non-motile, rod-shaped bacterium commonly found in the gut flora of healthy individuals, but it can be also found in the environment, particularly in soil and water [1]. Of great concern are infections caused by *K. pneumoniae*, mostly targeting the respiratory and urinary tracts and causing life-threatening infections including pneumonia, sepsis, meningitis, and pyogenic liver abscesses, particularly in health-care settings [2]. Colistin and carbapenems are last-line drugs for *K. pneumoniae* infections but *K. pneumoniae* lineages showing resistance to those drugs emerged and disseminated worldwide, challenging the already limited treatment options [3, 4]. World Health Organization (WHO) included carbapenemase-producing *K. pneumoniae* (CP*Kp*) in the list of PRIORITY 1 critical pathogens for new drugs [5]. An understanding of the pathobiology of *K. pneumoniae* infections would help in developing new control strategies and possible vaccines [6]. Several virulence factors, including the lipopolysaccharide (LPS), fimbriae, siderophores and the capsular polysaccharide (CPS), are contributing to *K. pneumoniae's* ability to thrive in the environment and in the host.

The capsule can ensure resistance to antimicrobial peptides, phagocytosis, and complement-mediated killing [7–10]. More than 77 capsular-types (K-type) have been reported in clinical isolates of *K. pneumoniae* [11]. Large-scale recombination events involving the capsule biosynthesis (cps) region drive an extensive variation, even within the same clonal complex (CC), as described for CC258 isolates [12]. The genes responsible for capsule synthesis are organized into an operon, from *galF* through *cpsACP*, *wzi*, *wza*, *wzb*, *wzc* and *ugd*, with conserved functions and organization and additional glycosyltransferase genes [11] (Fig. 1).

Recent studies shed light on the role of the different genes orchestrating capsule production in *K. pneumoniae*. Mutations in *wza*, *wzb*, *wzc* and *wzy* resulted in reduced amount or absence of capsule, corresponding to a rough, non-mucoid appearance on plate, along with decreased serum resistance and high susceptibility to neutrophilic phagocytosis [13]. On the other hand, inactivation of *wcaJ*, a glycosyltransferase involved in colanic acid synthesis, led to a non-capsulated, non-mucoid variant, which was less efficiently phagocytosed compared to the capsulated *K. pneumoniae*, and which showed a better ability to form biofilm on polystyrene surfaces, and an altered colistin susceptibility [14]. However, capsule production is controlled by a complex regulatory network involving several genes outside the *cps* cluster [15]. Interestingly, loss of mucoid-capsular phenotype has also been reported to occur within the host due to various mutations in the *cps* cluster [16]. Capsule loss due to mutations in the *cps* operon has been shown to occur among clinical ST258 isolates, leading to a better ability to form biofilm and persist in the mice bladder [17]. Altogether, these data suggest an evolutionary advantage that capsule loss can confer to *K. pneumoniae* in the human host and environment under certain circumstances. When analyzed in the laboratory, clinical isolates of *K. pneumoniae* may exhibit mixed populations, noticed by the presence of heterogeneous colony appearance on solid media. This phenomenon may reflect changes in the capsule production within a clonal bacterial population. It is referred as to phenotypic variation, usually from capsulated to non-capsulated variant. However, appearance of colony variants due to changes in capsule biosynthesis might also occur in vitro depending on medium, time and temperature of incubation [18]. This could subsequently lead to the storage and transfer of mixed samples across different clinical laboratories, thus hampering the correct phenotypic characterization of clinical isolates.

Here, we explored the genetic causes of in vitro switching from capsulated, mucoid (M) to non-capsulated, non-mucoid (NM) phenotype in eight clinical CP*Kp* isolates. The frequency of phenotypic switch was strain-dependent and increased along with colony development on plate. The loss of the mucoid phenotype resulted from diverse genetic events: Insertion Sequence (IS) transposition, deletion or point mutations occurring in genes of the *cps* locus. In one variant, a second mutation inactivated *rfaH*, a regulatory gene of capsular polysaccharide biosynthesis [19]. Variation of the impact of the phenotypic switch among the eight isolates in terms of capsule content, biofilm production and carbapenem susceptibility suggested heterogeneous selective advantage for capsular loss according to the strain and the mutations.

Results

Non-mucoid variants arise at various frequencies in different *K. pneumoniae* strains

All along a screening of clinical CP*Kp* strains, we noticed that upon isolation from − 80 °C glycerol stocks, CP*Kp* often exhibited a heterogeneous population with mostly mucoid (M) colonies but also a variable proportion of colonies with a translucent, non-mucoid (NM) appearance on plate. This observation led us to analyze more systematically the population heterogeneity. Hence, we selected eight CP*Kp* isolates belonging to seven STs (ST107, ST16, ST11, ST147, ST383, ST39, ST855) and expressing different carbapenemases (KPC, VIM-1, OXA-48 and OXA-181), as shown in Table 1. The population heterogeneity could be better visualized on TSA medium. We also observed that, when streaked on TSA, M colonies could give rise to either a mixed

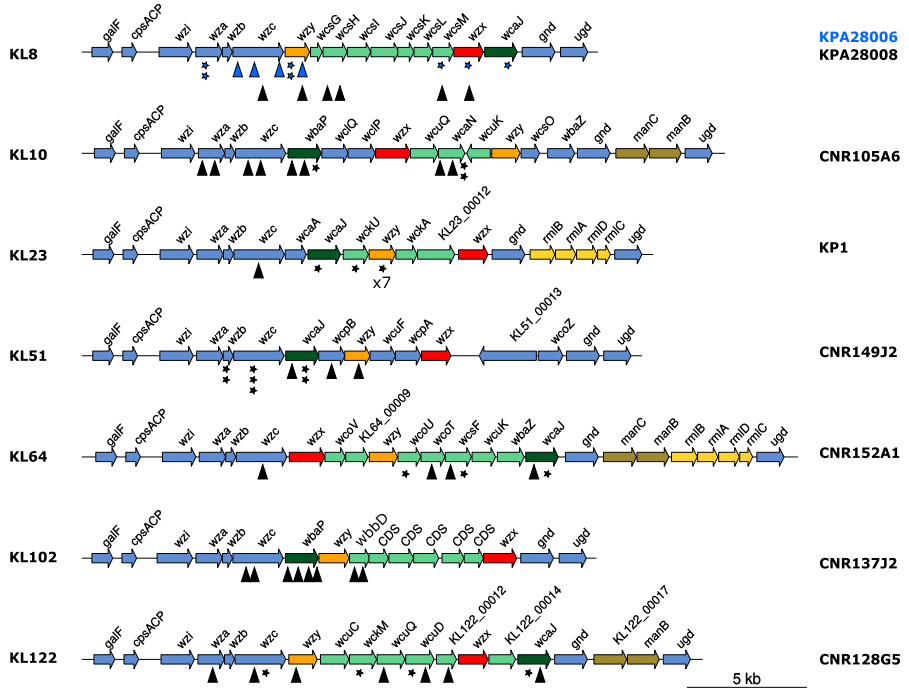

Fig. 1 Capsular *loci* maps. Capsular regions from the seven capsular types investigated in this work are represented from *galF* to *ugd*. Genes are indicated by arrows. Blue arrows correspond to core genes from the different capsule loci. Glycosyltransferases are indicated in green. Orange and red arrows represent genes encoding the polymerase and the flippase, respectively. In yellow/dark yellow the genes involved in sugar/repeat unit synthesis (non-conserved). KL numbers are indicated on the left and the analyzed strain of each K-type on the right. IS insertions are represented by triangles and other mutations events by stars as specified in Table 2. Two strains of capsular type KL8 were investigated, blue signs correspond to KPA28006 and black ones to KPA28008

population (M and NM) or to a pure M population. Furthermore, M colonies might exhibit non-mucoid sectors (Fig. 2a). On the other hand, NM colonies re-isolated on TSA led to homogeneous NM population. The ability of M colonies to produce NM segments was dependent on the incubation time (> 24 h), indicating further selection and growth advantage of NM variants at later growth stages on solid medium.

In order to determine whether the frequency of switching from M to NM was variable among the selected strains, we quantified colony variants by counting the number of colonies exhibiting non-mucoid segments after 24 h incubation at 37 °C and after 24 and 48 additional hours of incubation at 25 °C (Fig. 2b). Re-isolation of bacteria from these segments confirmed that they led to stable NM colonies. We observed, for the eight strains, a high rate of colony switching, ranging from 10% to more than 40% colonies with NM sectors after 72 h of incubation. We observed the highest frequency (from 15% at 24 h to 47% of the population at 72 h) for *K. pneumoniae* CNR137J2 belonging to ST107 and expressing KL102-type capsule.

Different mutational events led to a non-mucoid phenotype

To characterize the diversity of the NM variants selected on TSA plates, we isolated 6 to 11 independent NM isolates for each of the eight strains and performed whole genome sequencing (WGS) to compare them with the original isolates. In total, we analyzed 72 NM variants. Libraries were first constructed by tagmentation (>50x coverage). However, we obtained a low or even partial

Table 1 Strains analyzed in this work

Strain[&]	ST[a]	wzi	K-type[b]	Resistance genes
KP1 [20] SAMN14419408	ST39	wzi83	KL23	**aminoglycoside:** *aac*(6′)-Ib3; *aac*(3)-Iia; aph(6)-Id; **macrolide**: *mph*(E); *msr*(E); **phenicol**: *catA*1; *catB2*; **sulphonamide:** *sul*1;*sul2*; **tetracycline:** *tet*(D); **trimethoprim:** *dfrA*14; *dfrB*1; **β-lactam**: bla_{SHV-40}; bla_{OXA-9}; bla_{SCO-1}; bla_{VIM-1}; **fosfomycin:** *fosA*
CNR128G5 SAMN14419403	ST383	wzi162	KL122	**aminoglycoside:** aadA2b; *aac*(3)-IIa; *aac*(6′)-Ib3; *rmtB*; **quinolone:** *oqxA*; **sulphonamide:** *sul*1; **tetracycline:** *tet*(A); **β-lactam:** bla_{OXA-9}; $bla_{SHV-145}$; $bla_{CTX-M-14}$; $bla_{CTX-M-15}$; bla_{KPC-2}; bla_{OXA-1}; bla_{TEM-1B}; **fosfomycin:** *fosA*
CNR152A1 SAMN14419404	ST147	wzi64	KL64	**aminoglycoside:** *aph*(3″)-Ib; aph(6)-Id; **sulphonamide:** *sul2*; **trimethoprim:** *dfrA*14; **β-lactam:** bla_{SHV-11}; $bla_{CTX-M-15}$; bla_{KPC-3}; bla_{TEM-1B}
CNR105A6 SAMN14419407	ST855	wzi100	KL10	**aminoglycoside:** *aac*(6′)-Ib; *aadA*1; *aph*(3″)-Ib; *aph*(6)-Id; **phenicol:** *catA*1; **sulphonamide:** *sul*1; **tetracycline:** *tet*(B); **β-lactam:** bla_{SHV-81}; bla_{KPC-2}; bla_{OXA-9}; bla_{TEM-1A}
KPA28006 [21] SAMN14419405	ST11	wzi334	KL8	**aminoglycoside:** *aph*(3′)-VIa; *aadA*1; *aac*(6′)-Iq; **phenicol:** *cmlA*1; **sulphonamide:** *sul*1; *sul2*; **tetracycline:** *tet*(B); *tet*(D); **trimethoprim:** *dfrA*15; **β-lactam:** bla_{KPC-2}; $bla_{SHV-182}$; $bla_{CTX-M-2}$
KPA28008 [21] SAMN14419406	ST11	wzi334	KL8	**aminoglycoside:** *aph*(3′)-VIa; **quinolone:** *oqxA*; *oqxB*; **tetracycline:** *tet*(D); **β-lactam:** bla_{KPC-2}; $bla_{SHV-182}$; $bla_{CTX-M-2}$
CNR149J2 SAMN14419409	ST16	wzi50	KL51	**aminoglycoside:** *aac*(6′)-Ib-cr; *aadA2*; aph(3′)-Ia; **quinolone:** *qnrS*1; **macrolide:** *mph*(A); **sulphonamide:** *sul*1; **trimethoprim:** *dfrA*12; **β-lactam:** $bla_{SHV-145}$; $bla_{CTX-M-15}$; bla_{OXA-1}; $bla_{OXA-181}$; bla_{TEM-1B}
CNR137J2 SAMN14419410	ST107	wzi173	KL102	**aminoglycoside:** *aac*(3)-IId; *aph*(3″)-Ib; *aph*(6)-Id; **quinolone:** *qnrS*1; **macrolide:** *mph*(A); **sulphonamide:** *sul2*; **tetracycline**: *tet*(A); **trimethoprim:** *dfrA*17; **β-lactam:** $bla_{SHV-145}$; bla_{LAP-2}; bla_{OXA-48}; bla_{TEM-1B}

&Sequence accession numbers are also indicated, [a]*ST* = Sequence Type; [b]K-type = capsular type

coverage of the AT-rich *cps* locus (Fig. S1), precluding the confident identification of mutations responsible for the NM phenotype. Similarly, Wyres et al. were recently unable to determine the K-type of 129 out of 393 *K. pneumoniae* genomes sequenced by tagmentation [22]. The 72 NM variants were sequenced following enzymatic digestion of the genomic DNA by a mix of nucleases, providing a uniform coverage of the *K. pneumoniae* genome and no discrimination of AT-rich regions (Fig. S1). We identified in all the isolates analyzed, a mutation in the *cps* locus (Fig. 1, Table 2), predicted to be responsible for the NM phenotype. In 26 NM variants, up to five additional mutations were detected elsewhere in the genome. These mutations might have also contributed to the overgrowth of the NM sector (Table S1). In particular, in the NM3 variant of strain CNR149J2 we identified a four-base pair (bp) duplication disrupting the *rfaH* gene, an activator of capsule biosynthesis [19]. Fifty-six percent (40/72) of NM mutants resulted from IS insertion (IS*1*-, IS*L3*-, IS*5*-like) in different essential genes for capsule synthesis (Table 2). In the other variants, we identified point mutations ($n = 14$), including five non-sense mutations or indels ($n = 18$) (Table 2). The genes most frequently affected were *wcaJ* (22.2%), a colanic acid biosynthesis UDP-glucose lipid carrier transferase which mediates the first step of capsule biosynthesis in *Escherichia coli* [23] and plays a role in virulence and phage sensitivity in *K. pneumoniae* [24], followed by *wzc* (20.8%), encoding a putative tyrosine-kinase and *wzy* (15.3%) encoding the polymerase. Other mutated genes encode different glycosyltransferases involved in the complex *cps* synthesis (29.2%) or essential genes like *wza, wzb* and *wzx* (5.6, 2.8 and 2.8%, respectively). In the case of KP1 strain, seven out of the eleven independent NM isolates analyzed shared the same mutation in *wzy*: a deletion of one T in a track of nine T residues, likely resulting from a slippage of the DNA polymerase during chromosome replication.

Phenotypic comparison of mucoid and non-mucoid variants

For each CP*Kp* strain, we selected one NM variant with different mutations in *wcaJ, wzc, wzx, wzy* (indicated by the "&" symbol in Table 2) and investigated their impact on phenotypes contributing to their dissemination and persistence in the host.

To evaluate the impact of mutations on capsule production, we quantified uronic acid, a major constituent of the polysaccharidic capsule. In seven out of eight pairs, the NM variant showed a significantly lower amount of uronic acid compared to M variant, confirming that the loss of the mucoid trait resulted from the loss or the reduction of capsule production (Fig. 3). In the remaining strain, KP1, the NM variant (frameshifted in *wzy*), although it did not reach significance, showed a 2-fold decrease in the uronic acid production. The impact on the capsule synthesis in the NM variants was confirmed by capsule visualization by India ink negative staining (Fig. 3).

We investigated and compared the ability of M and NM variants to form biofilm on polystyrene surfaces. For six out of eight strains (CNR152A1, CNR105A6, KPA28006, KPA28008, CNR137J2, and KP1) the NM

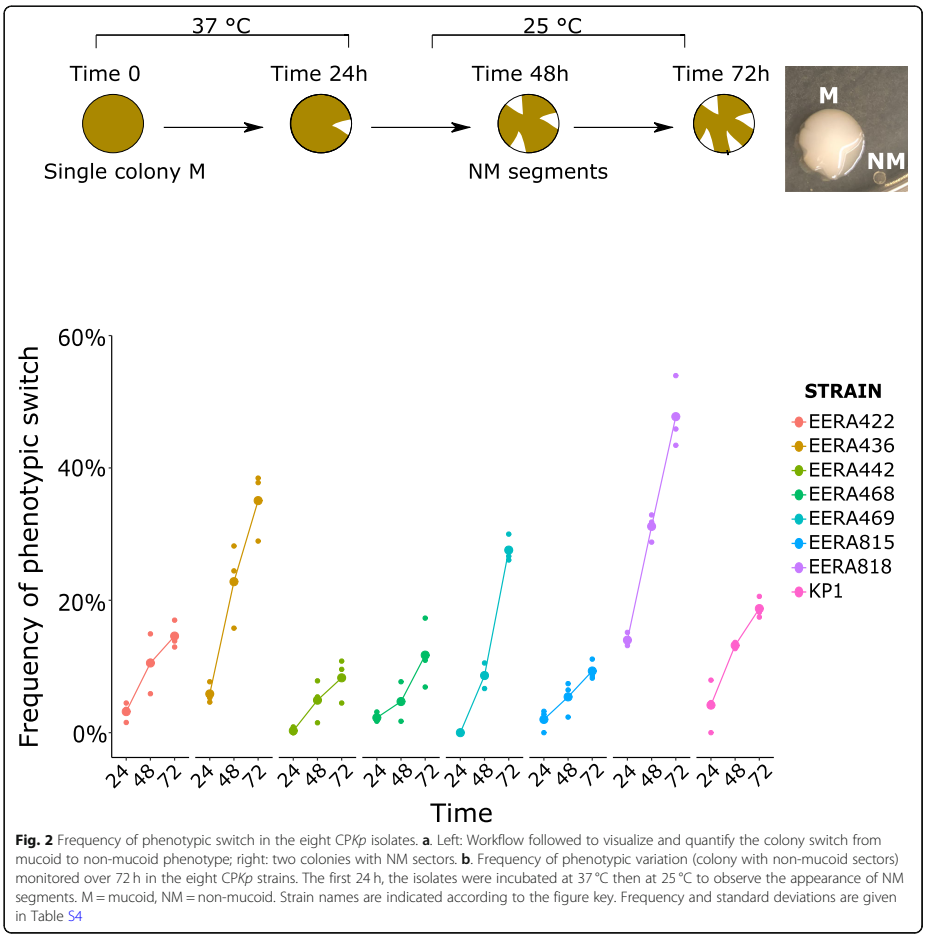

Fig. 2 Frequency of phenotypic switch in the eight CP*Kp* isolates. **a**. Left: Workflow followed to visualize and quantify the colony switch from mucoid to non-mucoid phenotype; right: two colonies with NM sectors. **b**. Frequency of phenotypic variation (colony with non-mucoid sectors) monitored over 72 h in the eight CP*Kp* strains. The first 24 h, the isolates were incubated at 37 °C then at 25 °C to observe the appearance of NM segments. M = mucoid, NM = non-mucoid. Strain names are indicated according to the figure key. Frequency and standard deviations are given in Table S4

variants significantly produced more biofilm after 24 h of incubation (Fig. 4a) compared to the parental M strains. However, in the case of CNR149J2 the NM variant produced less biofilm than the parental strain. This opposite phenotypic effect of capsule loss might be related to the mutation in *rfaH*, which has been shown to have a pleiotropic effect [19]. Therefore, the contribution of the capsule to biofilm formation on polystyrene was variable according to strain- and/or mutations.

Autoaggregation might contribute to biofilm formation [26, 27]. The autoaggregative behavior of M and NM derivatives was quantified in spent M63/Glu minimal medium over 24 h at room temperature. Interestingly, all the NM variants but one (CNR149J2) showed, overall, a better ability to autoaggregate under the tested conditions (Fig. 4b). Particularly, the NM variants of CNR152A1, CNR105A6, KPA28006, KPA28008, KP1, which produce more biofilm, showed an increased autoaggregation compared to the parental isolates.

Curli production contributes to biofilm formation and capsule loss can unmask the fimbriae [28]. We compared M and NM isolates for curli production by the

Table 2 Mutations in the capsule synthesis cluster detected in non-mucoid variants

Strain	NM Variant	Gene	Mutation[a, b]
CNR128G5	NM1	*wza*	IS*Kpn25* (pos 382)
	NM2	*wzc*	IS*903b* (pos 2036)
	NM3	*wzc*	G1699T (D567Y)
	NM4[c]	*wzy*	IS*Kpn25* (pos 319)
	NM5	*wckM*	**Δ**4 bp (AAAC) (pos 729); (*)
	NM6	*wcuQ*	IS*Kpn25* (pos 332)
	NM7	*wcuD*	**Δ**A (pos 38); (*)
	NM8	*wcuD*	IS*Kpn25* (pos 1073)
	NM9	*KL122_00012*	IS*Kpn25* (pos 796)
	NM10	*wcaJ*	insAA[d] (pos 744); (*)
	NM11	*wcaJ*	IS*1*-like [e] (pos 840)
CNR152A1	NM1	*wzc*	IS*Kpn26* (pos 738)
	NM2[c]	*wcaJ*	IS*903b* (pos 602)
	NM3	*wcaJ*	T389A (I130N); G452C (G151A)
	NM4	*wcoT*	IS*903b* (pos 866)
	NM5	*wcsF*	IS*903b* (pos 1126)
	NM6	*wcsF*	G118T; (*)
	NM7	*wcoU*	insA[d] (pos 811); (*)
CNR105A6	NM1	*wza*	IS*1*-like (pos 998)
	NM2	*wza*	IS*1*-like (pos 998)
	NM3	*wzc*	IS*903b* (pos 2073)
	NM4[c]	*wzc*	IS*1*-like (pos 542)
	NM5	*wbaP (wcaJ)*	IS*903b* (pos 699)
	NM6	*wbaP (wcaJ)*	IS1-like (pos 316)
	NM7	*wbaP (wcaJ)*	T997G (S333A)
	NM8	*wcaN*	**Δ**18bp (pos 190–208); (*)
	NM9	*wcaN*	IS*1*-like (pos 358)
	NM10	*wcaN*	IS*1*-like (pos 358)
	NM11	*wcaN*	C79A (V27L)
KPA28006	**NM1**[c]	*wzc*	IS*903b* (pos 715)
	NM2	*wzc*	IS*1*-like (pos 244)
	NM3	*wzc*	IS*1*-like (pos 2146)
	NM4	*wzy*	**Δ**C (pos 274); (*)
	NM5	*wzy*	**Δ**C (pos 274); (*)
	NM6	*wcsM*	**Δ**A (pos 339); (*)
	NM7	*wcaJ*	**Δ**A (pos 1279); (*)
	NM8	*wzx*	**Δ**A (pos 422); (*)
	NM9	*wza*	A278T (L93Q)
KPA28008	NM1	*wzc*	IS*1*-like (pos 950)
	NM2	*wzy*	IS*1*-like (pos 319)
	NM3	*wcsM*	IS*903b* (pos 505)
	NM4[c]	*wzx*	IS*1*-like (pos 342)
	NM5	*wcsH*	IS*1*-like (pos 605)
	NM6	*wcsH*	IS*1*-like (pos 914)

Table 2 Mutations in the capsule synthesis cluster detected in non-mucoid variants *(Continued)*

Strain	NM Variant	Gene	Mutation[a, b]
CNR149J2	NM1	*wzb*	C447A (*)
	NM2	*wzc*	T345A (*)
	NM3[c]	*wzc*	**Δ**11bp (pos 635); (*)
	NM4	*wzc*	G787C (A263P)
	NM5	*wcaJ*	IS*1*-like (pos 905)
	NM6	*wcaJ*	T1145G (L382R)
	NM7	*wcaJ*	A111T (*)
	NM8	*wcpB*	IS*1*-like (pos 347)
	NM9	*wzy*	IS*Kox3* (pos 591)
	NM10	*wzb*	T68G (L23R)
CNR137J2	NM1	*wzc*	IS*903b* (pos 209)
	NM2	*wzc*	IS*1*-like (pos 760)
	NM3	*wbaP (wcaJ)*	IS*1*-like (pos 616)
	NM4	*wbaP (wcaJ)*	IS*1*-like (pos 1312)
	NM5	*wbaP (wcaJ)*	IS*1*-like (pos 247)
	NM6[c]	*wbaP (wcaJ)*	IS*1*-like (pos 888)
	NM7	*wbbD*	IS*1*-like (pos 319)
	NM8	*wbbD*	IS*1*-like (pos 284)
KP1	NM1	*wzc*	IS*1*-like (pos 469)
	NM2	*wzy*	T736C (S246P)
	NM3	*wzy*	**Δ**T (pos 864); (*)
	NM4	*wzy*	**Δ**T (pos 864); (*)
	NM5	*wzy*	**Δ**T (pos 857); (*)
	NM6[c]	*wzy*	**Δ**T (pos 864); (*)
	NM7	*wzy*	**Δ**T (pos 864); (*)
	NM8	*wzy*	**Δ**T (pos 864); (*)
	NM9	*wcaJ*	A31T; (*)
	NM10	*wckU*	**Δ**A (pos 16); (*)

[a]In parentheses are indicated: for point mutations, the amino acid change and for other mutations, the position in the gene, [b] the star indicates either a non-sense mutation or a frameshift [c]; NM variant selected for in depth phenotypic analysis (in bold); [d] Ins for insertion; [e]IS1-like correspond to IS*1R*, IS*15D*, IS*1F*, ISKpn*14* and closely related ISs

Congo red (CR) assay. Among the eight strains analyzed, only one tested positive: CNR128G5, which shows a high level of biofilm formation independently of the M or NM phenotype (Fig. S2). For all the analyzed isolates, we did not observe differences between NM and M variants in the CR assay (Fig. S2), suggesting that capsule loss did not impact significantly on fimbriae production in these isolates.

Since the eight strains analyzed harbored a carbapenemase-encoding gene, we compared the susceptibility of both the parental and the NM variants towards carbapenems, which are targeting bacterial cell wall synthesis. Interestingly, we found that minimum inhibitory concentrations (MICs) for the clinically relevant carbapenems (ertapenem, meropenem, imipenem) determined by E-test were different in five out of the eight strains for the M and NM variants. Four NM variants showed an increased susceptibility to those drugs. On the other hand, for CNR152A1, the NM variant (CNR152A1-NM2) - mutated in *wcaJ*, was surprisingly more resistant than the parental M strain (Fig. 5). In order to determine whether this effect resulted exclusively from the mutation in *wcaJ*, genomes were carefully checked for any additional mutation, IS insertion or recombination but we did not identify any in genes known to contribute to β-lactam resistance such as the major porins (*ompK35* and *ompK36*) and their regulator *ompR*/*envZ* and the PBPs (PBP1F, 1A, 1B, 2, 2D). In order to determine whether this effect was isolate or mutation specific, we determined the susceptibility to

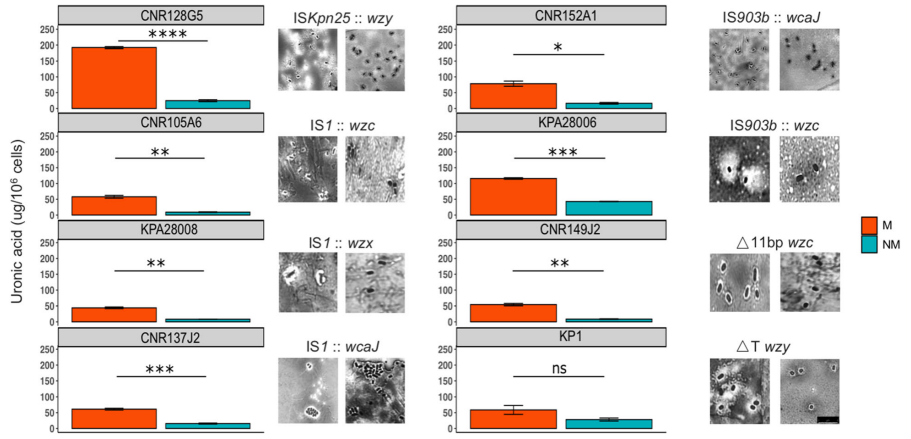

Fig. 3 Capsule quantification and visualization in M and NM variants. Uronic acid assay [25] was carried out to quantify capsular polysaccharides in the eight *CPKp* and their selected NM variants. In all but one couple (KP1), the NM variant exhibited a significant decrease in CPS production compared to the WT isolate. In particular, a stronger difference was noticed in the case of CNR128G5 (*p*-value ****), followed by CNR137J2 and KPA28006. India ink staining was performed to visually detect decrease/absence of capsule in the non-mucoid variant (right image). The scale bar in each image represent 5 μm. Non-mucoid isolates selected for each *K. pneumoniae* strain showed different mutation events (Table 2).
M = mucoid, NM = non-mucoid

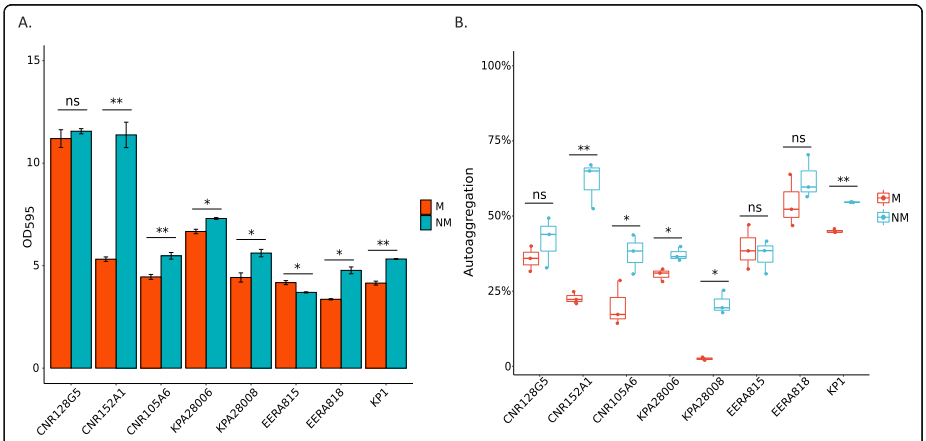

Fig. 4 In vitro biofilm production and autoaggregation. **a.** The WT isolates and the selected NM variants were characterized for their ability to produce biofilm in M63 minimal medium supplemented with glucose. In six out of eight couples (CNR152A1, CNR105A6, KPA28006, KPA28008, CNR137J2 and KP1), the NM variant was more efficient in biofilm formation than the parental M strain. Only CNR149J2 showed an opposite trend: the M variant showed a better ability to form biofilm under tested conditions. *p*-values of < 0.001 ***, < 0.01 ** and < 0.05 * were considered significant. **b**. Autoaggregation assay of M and NM variant in spent M63/Glu medium. M = mucoid, NM = non-mucoid are indicated according to the figure key

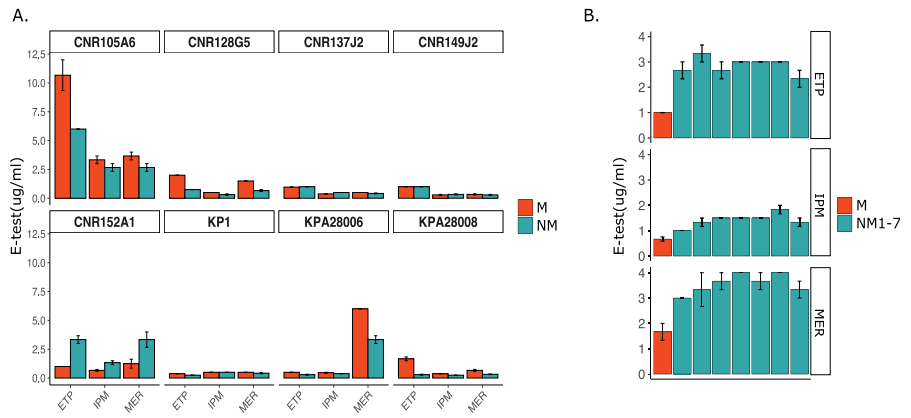

Fig. 5 Carbapenem susceptibility profiles of the eight CP*Kp* strains and their NM variants. **a**. The carbapenem susceptibility of the eight CP*Kp* strains and the NM variants was quantified by E-test. ETP = ertapenem; IPM = imipenem and MER = meropenem. Four out of eight NM variants selected showed an increase in susceptibility towards the carbapenem tested, whereas the NM deriving from CNR149J2, CNR137J2 and KP1 did not show any difference compared to the WT mucoid strain. Only CNR152A1-NM2 showed a different behavior, with decreased susceptibility, particularly against meropenem and ertapenem. **b**. Carbapenem susceptibility by E-test of the seven NM variants derivatives of CNR152A1. M = mucoid, NM = non-mucoid. Experiments were performed in triplicates. Error bars represent the standard error of the mean (SEM)

carbapenems by E-test in the six other independent NM variants from CNR152A1 harboring different mutations in the *cps* locus (Table 2). Consistently with what was observed for NM3, the six other NM variants showed a reduced carbapenem susceptibility. These results confirmed that the reduced susceptibility of CNR152A1 non-mucoid variants was not specific to the *wcaJ* mutant but likely related to the loss of capsule.

Capsule has been shown to play a role in resistance to antimicrobial peptides, including polymyxin B, affecting the interaction with the bacterial outer membrane [29]. Those antibiotics show mode of action and mechanisms of resistance different from ß-lactams. We measured the susceptibility levels of both the parental and the NM variants towards polymyxin B and colistin. However, we did not observe any difference between the M and the NM variant for the eight pairs (Table S2).

Discussion

Microbial populations inhabit diverse and constantly changing niches, facing oscillations between abundance of nutrients, which allows a prolific bacterial growth, and hostile environments, where individuals adopt strategies to cope with the scarcity of nutrients [30]. One of them is the phenotypic variation, where a population can switch among multiple phenotypes to survive in challenging habitats imposed, for instance, by the antibiotic pressure and the host immune system. In a scenario where multidrug resistant (MDR) clinical isolates are incessantly emerging and spreading, the adoption of such strategies from bacterial populations can further challenge their characterization in the laboratory [31]. *K. pneumoniae* can undergo phenotypic variation, switching from mucoid to non-mucoid colony aspect [32]. Hypo- or non-mucoid appearance has been associated with the loss of capsule in *Klebsiella* and different degrees of mucoidity may indicate diverse mutations affecting capsule synthesis genes [16, 17]. These colony variants might arise in vivo, but also following their isolation in the laboratory. Colony variants can be observed on solid media, but they go frequently overlooked, as they show only subtle differences. Here, by analyzing NM variants deriving from eight clinical CP*Kp*, we showed some phenotypic consequences of the capsule loss potentially contributing to NM variants selection. These phenotypic switches occurred at various frequencies in the different strains analyzed.

By using a newly developed high throughput method called TraDisort, Dorman et al. identified numerous *loci* involved in the regulatory network of capsule synthesis in *K. pneumoniae* [15]. However, here we showed that in vitro transition on solid media from M to NM variant ($n = 72$) of eight CP*Kp* clinical isolates is driven by mutations occurring in the capsule locus upon the insertion of IS elements, SNPs and deletions. In a single NM variant (CNR149J2 NM3), we identified both a mutation

inactivating *wzc*, which encodes a tyrosine-protein kinase essential for capsule biosynthesis and a mutation in the *rfaH* gene encoding a transcriptional regulator of the *cps* operon [19]. In other NM variants, the disruption of *wzc* led to a non-capsulated phenotype and the contribution of the *rfaH* mutation to the phenotype remains to be determined. Except this specific case, under the conditions we used, mutations in genes involved in this regulatory network, which would reduce capsule synthesis, do not provide a sufficient selective advantage for growth. Recently, Lee et al. observed different colony aspects (mucoid and non-mucoid) among CP*Kp* isolated successively from a single patient [16]. They showed that the within-host evolution of *K. pneumoniae* non-mucoid variants was driven by IS insertion and amino acid alterations in genes essential for capsule synthesis. Likewise, we observed that the NM phenotype among CP*Kp* clinical isolates was related to genetic events happening in the *cps* cluster, particularly targeting *wcaJ*, followed by *wzc* and *wzy* genes. These core genes are essential for capsule synthesis in *E. coli* and *Klebsiella spp.* and their disruption is associated with altered capsule polysaccharide polymerization [14, 15, 17, 33]. However, we identified among the NM variants analyzed, mutations in other genes of the *cps* operon, confirming their contribution to capsule synthesis and the selective advantage for their inactivation. For example, in the strain CNR128G5, the 11 NM variants were mutated in eight different *cps* genes. One exception is the first gene of the operon: *wzi*, as no variant harboring a mutation in this gene was observed. *Wzi* was shown to be an outer-membrane lectin contributing to the formation of the bacterial capsule [34]. Its gene inactivation will probably not lead to a metabolic advantage. However, IS insertion in this gene are predicted to have a polar effect on the downstream genes essential for capsule biosynthesis [35]. The absence of mutation in this gene might indicate a fitness cost of its inactivation under the condition used for capsule mutant selection.

Characterization of selected NM mutants unveiled a diverse landscape of mutations, with the majority (55.6%) linked to IS elements jumping into *cps* genes. Transposable elements are an important source of genetic variability. Movements of ISs are hardly detected using short-read sequencing. Therefore, this type of capsule locus inactivation might be overlooked while analyzing *K. pneumoniae* variants. Transposition is generally maintained at low level to preserve the integrity of the bacterial host genome. However, ISs can undergo bursts of transposition under stress conditions, including oxidative stress and starvation [36], which likely occurred during the prolonged incubation on TSA plates at 25 °C. In the case of KP1, the most frequent event was a thymine deletion in *wzy* (delT), occurring in 6 out of 10 NM independent variants (Table 2). These deletions occurred in a poly(T) track (nt 857–867 of the gene), which could lead to replication slippage, thus increasing the probability of frameshift errors. Similarly, we observed a high rate of frameshift mutations in KPA28006 with three adenosine deletions in *wcsM*, *wcaJ* and *wzx*, corresponding to poly-A track. Interestingly, we also isolated two variants with the same cytosine deletion. This residue is followed by a stretch of a poly-T track. These regions with stretches of nucleotides might be particularly prone to polymerase slippage. The frequency of mucoid to non-mucoid switch in these two strains was among the lowest we have observed. It is possible that the frequency of IS transposition in KP1 (1 out of 11 NM isolates) and KPA28006 (3 out of 9 NM isolates) was lower than in other strains under the condition used, revealing this mechanism of phase variation by increasing its relative frequency. On the other hand, the highest frequency of conversion from M to NM appearance was observed for CNR137J2 (more than 40% over 3-days incubation), followed by CNR152A1 and KPA28008. Notably, in the case of CNR137J2 and KPA28008, all mutants resulted from IS transposition (seven IS*1*-like insertions and one IS*903*b in CNR137J2 and five IS*1*-like insertions and one IS*903b* in KPA28008). One could hypothesize that the high rate of switching in these two strains is due to a higher rate of IS transposition and possibly to IS transposition bursts. In order to assess whether these differences could be related to different occurrence of IS elements in the eight parental strains, we estimated the number of the ISs that were responsible for a non-mucoid phenotype among the 72 isolates we analyzed (Table S3). However, we were not able to correlate the transposition frequency and the number of ISs in the parental strain. Indeed, in the strains KPA28008 and CNR137J2, which contain the smallest number of the analyzed ISs ($n = 5$), all non-mucoid mutants were predicted to result from an IS insertion. On the contrary, in KP1, which contains ten ISs, only one out of the ten non-mucoid variants resulted from an IS transposition.

Here, we also demonstrated that the simple act of picking one colony rather than another one could lead to different interpretations on the phenotype of bacterial isolates from a clinical sample. Indeed, the colony variants exhibited several distinct phenotypic properties in addition to the capsule production, like biofilm formation, autoaggregation and susceptibility to carbapenems. Those phenotypic were predicted to result from altered capsule production. However, additional mutations in some isolates might have also contributed to the observed effect. Particularly, we observed enhanced biofilm production and autoaggregation in M63/Glu for five out of eight NM variants. Higher levels of autoaggregation

are indicative of a change in cell surface [26], which here was the loss of capsule, likely unmasking other surface components contributing to autoaggregation. CNR152A1-NM2 showed the highest increase of biofilm formation and autoaggregation, as deduced from the sedimentation rate among the eight strains analyzed (< 24 h), suggesting properties impacting on cell clumping. In-depth analysis of CNR152A1 genome compared to isolates from the same STs retrieved from the National Center for Biotechnology (NCBI) revealed an IS*903b* at codon 264 disrupting *wbbM*, belonging to the antigen O biosynthesis gene cluster. It encodes a glycosyltransferase and its disruption has been shown to induce defects in LPS biosynthesis [37], increasing the electronegative charge of the bacterial cell surface. The IS insertion was also present in the CNR152A1-NM2 and in the other NM variants included in our analysis. The loss of capsule, combined with the mutation in *wbbM*, likely caused a dramatic change from a hydrophilic to a hydrophobic bacterial surface, possibly contributing to enhance the autoaggregative and biofilm formation properties. On the other hand, CNR128G5 produces a high level of biofilm on the whole and no significant difference in biofilm production was observed between NM and M variants.

We also observed a variable impact of the NM phenotype on carbapenem susceptibility. In four out of eight isolates, the capsule loss in the NM variant resulted in an increased susceptibility to meropenem, ertapenem and imipenem. This observation suggested a protection of the mucoid-capsulated phenotype under carbapenem pressure in certain strains, possibly contributing to reduced permeability of the outer membrane to these antibiotics. Interestingly, in CNR152A1, we noticed a decrease in susceptibility in the NM2 variant, particularly towards meropenem and ertapenem. This observation went true for all the NM variants of this strain, regardless the mutated gene. Markedly, loss of O-antigen expression is likely to affect the conformation and function of various surface proteins [38]. Deep rough LPS mutants, lacking the complete core region up to the 3-deoxy-d-manno-octulopyranosic acid residues, were shown to be less capable of assisting the folding, insertion, and trimerization of porins [39]. Hence, we hypothesized that the loss of capsule in the eight CNR152A1 NM variants, combined with the defects in the O-antigen, might further disturb the assembly of outer membrane proteins, resulting in a decrease in carbapenem permeability and susceptibility. Alternatively, autoaggregation and hydrophobicity by themselves might contribute to reduce carbapenem susceptibility. On the other hand, it has been reported that capsular defective strains are more susceptible to antimicrobial peptides including polymyxin B [14, 29]. However, we did not observe the same for the eight strains, possibly due to a strain- and mutation-dependent impact of the capsule loss.

Conclusions

Capsule loss is a common event, which can take place within monoclonal populations, generating heterogeneity, and it might have an impact on important phenotypic traits related to host adaptation and antimicrobial susceptibility. Given the phenotypic divergences observed between strains, the technical issues encountered to differentiate M and NM variants and to get an optimal sequencing coverage of the capsule biosynthesis region by using tagmentation for library construction, phenotypic characterization of clinical isolates should be performed carefully, especially when those display a multi-drug resistant phenotype.

Methods

Strains and growth conditions

The clinical CP*Kp* isolates used in this study were from the National Reference Centre laboratory for Carbapenemase-producing Enterobacteriaceae at the Bicêtre Hospital and are listed in Table 1, together with relevant information: origin, capsular types, ST, antibiotic resistance genes repertoire. *K. pneumoniae* ATCC CIP 53153 was used as a reference strain. Bacteria were grown in Tryptic-Soy (TS) broth or lysogeny broth (LB) and on TS agar (TSA) or LB agar (LBA) plates. Antibiotic susceptibility testing was performed on Mueller-Hinton Agar (MHA) plates. M63 minimal medium was supplemented with Glucose 0.4% (M63/Glu) to perform biofilm assay. Spent M63/Glu medium used to test autoaggregation was recovered following growth of the same isolate, centrifugation at high speed (11,000 x *g*) for 10 min and 0.22 μm filtration of the supernatant.

Isolation of non-mucoid variants and frequency of phenotypic variation

The M and NM *K. pneumoniae* variants (MVs and NMVs) can be observed on LBA although the NMVs were more accurately distinguished on TSA. We noticed that MVs typically give rise to translucent sectors after 24 h of growth at 37 °C. Appearance of NM sectors within M colonies, referred to as phenotypic switch was quantified as follows. A single mucoid colony was resuspended in normal saline to an OD_{600} of 0.1. One hundred μL of serial dilutions were plated on TSA to get c.a. 100 colonies per plate. After overnight growth, colony aspect (M or NM) was investigated optically by light contrast. The number of mucoid colonies exhibiting non-mucoid sectors was counted after 24, 48 and 72 h of incubation. The frequency of appearance of NMVs was quantified as the ratio between colonies showing NM

sectors over the total number of colonies on plate for three independent cultures.

Capsule extraction and quantification

Capsular polysaccharides were extracted and quantified using a colorimetric assay for uronic acid, a component of the *K. pneumoniae* capsule repeat unit, as described previously [25]. In parallel, serial dilutions of the bacterial culture were plated to determine the number of Colony Forming Units (CFUs). The uronic acid content was expressed in nanograms per 10^6 CFUs.

Capsule staining and microscopic visualization

Bacterial capsule was visualized by negative staining with the India Ink method, followed by counter-staining of bacterial cells with Crystal Violet as described [25]. Excess of Crystal Violet was washed away using copper sulfate 10% (wt/vol). Images were taken using a Leica DM-4 B microscope with a PL Fluotar 100x/1.32 PH3 immersion objective and photographed using the Hamamatsu ORCA Flash4.0 LT camera and the Leica Application Suite (LasX) software. The resolution was 2048 × 2048 (72 dpi). No downstream processing was made to enhance image resolution as well as any adjustment and/or manipulation.

In vitro biofilm production

The ability of the MVs and NMVs to form biofilm on polystyrene was analyzed using 96-well plates [40]. Briefly, stationary-phase cultures were diluted to OD_{600} = 0.05 in fresh M63 minimal medium supplemented with 0.4% glucose and 100 μl of this inoculum were grown for 24 h in 96-well polystyrene plates at 37 °C. Biofilm was fixed by using Bouin's solution (acetic acid 5%, formaldehyde, 9% and picric acid, 0.9% in water) and washed with water once before adding 1% (wt/vol) crystal violet. After 10 min of staining at room temperature, the plates were washed twice with water, dried at room temperature, crystal violet was solubilized by the addition of 200 μL of a solution of ethanol–acetone (80–20) and OD_{595} was determined. Results correspond to three independent experiments with four-replicates measurements.

Autoaggregation assay

Autoaggregation (i.e., cell clumping and sedimentation) was measured as previously described [41]. Mucoid isolates and their respective NMVs were grown overnight in M63 supplemented with glucose 0.4% and MgSO4 1 mM at 37 °C shaking. After centrifugation at 3000 *g* for 5 min, bacterial pellets were resuspended in 1 mL of spent M63/Glu minimal medium to get an OD_{600} ~ 0.3–0.6. The OD_{600} of the upper layer of the cultures was read after 24 h upon static incubation at room temperature by an Infinite® 200 PRO spectrophotometer. Autoaggregation percentage was expressed as: (1- OD_{600} upper layer 24 h/OD_{600} bacterial suspension at time zero) *100.

Curli/cellulase expression

Curli fibers are protease resistant and bind to Congo red (CR) and other amyloid dyes [42]. However, CR binds to other bacterial extracellular features, including cellulose [42]. We therefore assess curli/cellulose production by the Congo red assay. TS agar was supplemented with 40 μg/mL Congo red (Sigma-Aldrich) and 20 μg/mL Coomassie brilliant blue R-250 (Thermo Fisher Scientific). Plates were inoculated with drops of 5 μL of each overnight bacterial culture grown in TSB and incubated for 72 h at 37 °C after which colony morphology and color were inspected and recorded.

Carbapenem and colistin susceptibility assays

Antimicrobial susceptibility testing was performed by E-test (bioMérieux) on Mueller-Hinton (MH) agar for carbapenems, whereas colistin was tested by broth microdilution assay. Experiments were performed in triplicates. Results were interpreted according to EUCAST guidelines, as updated in 2018 (http://www.eucast.org).

Whole genome sequencing, genome assembly and variant characterization

Genomic DNA was extracted on exponentially growing *K. pneumoniae* (OD_{600} = 0.4–0.6) using the Qiagen Blood and Tissue DNeasy kit according to manufacturer's recommendations. Libraries were prepared following manufacturers' instructions by using the Illumina Flex kit based on Tn5 transposase tagmentation and the NEBNext Ultra II FS DNA Library prep kit based on random enzymatic fragmentation of genomic DNA. Whole genome sequencing was performed on Illumina NexSeq500 or HiSeq2500 platform. SPAdes [43] was used for de novo assembly and genome annotation was completed using RAST [44]. Resistome, virulome and ST were determined using Kleborate (https://github.com/katholt/Kleborate). SNPs, IS insertion and recombination events were detected by using breseq [45] using as reference contigs of the M variant and in-house scripts based on BWA [46] and GATK [47, 48]. Mutations were visually verified by using the IGV viewer [49]. IS sequences were identified in the draft genome sequences of the eight strains by BLASTN to identify IS – chromosome junctions. IS sequences were retrieved and analyzed by using the ISfinder database [50].

Statistical analysis

R version 3.6.1 (http://www.rstudio.com/) was used to construct graphs and analyze data regarding phenotypic

switch frequencies, capsule quantification, carbapenem susceptibility, biofilm formation and autoaggregation. Groups were compared using unpaired t-test. *P* values of < 0.0001 ****, < 0.001 ***, < 0.01 ** and < 0.05 * were considered significant.

Supplementary information

Supplementary information accompanies this paper at https://doi.org/10.1186/s12866-020-02007-y.

Additional file 1.

Abbreviations

CP*Kp*: Carbapenemase-producing *K. pneumoniae*; LPS: Lipopolysaccharides; CPS: Polysaccharidic capsule; K-type: Capsular-type; CC: Clonal complex; M: Mucoid; NM: Non-mucoid; IS: Insertion sequence; WGS: Whole genome sequencing; SNP: Single nucleotide polymorphism; nt: Nucleotide; TSB: Tryptic-soy broth; LB: Lysogeny broth; CFUs: Colony forming units; wt/vol: Weight/volume

Acknowledgements

The authors thank Rafael Patiño-Navarrete for his help in the bioinformatics analysis.

Authors' contributions

AC, NC, PDZ performed experiments; TN and RB collected and provided the samples for the study; AC, PG, NC, PDZ, TN and IRC analyzed the data; AC and PG designed the study; AC, IRC, RB and PG wrote the manuscript; all authors approved the manuscript prior to submission.

Funding

This work was supported by grants from the French National Research Agency (ANR-10-LABX-62-IBEID and ANR-10-LABX-33), and from the European Union's Horizon 2020 Research and Innovation Program under Grant Agreement No. 773830 (Project MedVetKlebs, One Health EJP). Adriana Chiarelli is part of the Pasteur - Paris University (PPU) International PhD Program. This project has received funding from the Institut Carnot Pasteur Microbes & Santé, and the European Union's Horizon 2020 research and innovation programme under the Marie Sklodowska-Curie grant agreement No 665807.

Availability of data and materials

Fastq files were deposited at the NCBI Sequence Read Archive (SRA) with the BioProject accession number PRJNA613777. Sequence accession numbers of the eight strains are indicated in Table 1.

Ethics approval and consent to participate

Not applicable. The eight strains are from laboratory collections without information on patient.

Consent for publication

Not applicable.

Competing interests

The authors declare that they have no competing interests.

Author details

[1]EERA Unit "Ecology and Evolution of Antibiotic Resistance", Institut Pasteur - Assistance Publique/Hôpitaux de Paris - University Paris-Saclay, Paris, France. [2]UMR CNRS 3525, 75015 Paris, France. [3]Sorbonne Université, 75015 Paris, France. [4]EA 7361 Structure, dynamic, function and expression of broad-spectrum beta-lactamases", Faculty of Medicine University Paris-Sud, University Paris-Saclay, Associated French National Reference Center for Antibiotic Resistance: Carbapenemase-producing Enterobacteriaceae, Le Kremlin-Bicêtre, France.

Received: 8 June 2020 Accepted: 12 October 2020
Published online: 27 October 2020

References

1. Wyres KL, Holt KE. *Klebsiella pneumoniae* as a key trafficker of drug resistance genes from environmental to clinically important bacteria. Curr Opin Microbiol. 2018;45:131–9.
2. Podschun R, Ullmann U. *Klebsiella* spp. as nosocomial pathogens: epidemiology, taxonomy, typing methods, and pathogenicity factors. Clin Microbiol Rev. 1998;11(4):589–603.
3. David S, Reuter S, Harris SR, Glasner C, Feltwell T, Argimon S, Abudahab K, Goater R, Giani T, Errico G, et al. Epidemic of carbapenem-resistant *Klebsiella pneumoniae* in Europe is driven by nosocomial spread. Nat Microbiol. 2019;4(11):1919–29.
4. Petrosillo N, Taglietti F, Granata G. Treatment options for colistin resistant *Klebsiella pneumoniae*: present and future. J Clin Med. 2019;8(7):934.
5. Tacconelli E, Carrara E, Savoldi A, Harbarth S, Mendelson M, Monnet DL, Pulcini C, Kahlmeter G, Kluytmans J, Carmeli Y, et al. Discovery, research, and development of new antibiotics: the WHO priority list of antibiotic-resistant bacteria and tuberculosis. Lancet Infect Dis. 2018;18(3):318–27.
6. Feldman MF, Mayer Bridwell AE, Scott NE, Vinogradov E, McKee SR, Chavez SM, Twentyman J, Stallings CL, Rosen DA, Harding CM. A promising bioconjugate vaccine against hypervirulent *Klebsiella pneumoniae*. Proc Natl Acad Sci U S A. 2019;116(37):18655–63.
7. Kabha K, Nissimov L, Athamna A, Keisari Y, Parolis H, Parolis LA, Grue RM, Schlepper-Schafer J, Ezekowitz AR, Ohman DE, et al. Relationships among capsular structure, phagocytosis, and mouse virulence in *Klebsiella pneumoniae*. Infect Immun. 1995;63(3):847–52.
8. Paczosa MK, Mecsas J. *Klebsiella pneumoniae*: going on the offense with a strong defense. Microbiol Mol Biol Rev. 2016;80(3):629–61.
9. Clements A, Gaboriaud F, Duval JF, Farn JL, Jenney AW, Lithgow T, Wijburg OL, Hartland EL, Strugnell RA. The major surface-associated saccharides of *Klebsiella pneumoniae* contribute to host cell association. PLoS One. 2008;3(11):e3817.
10. Moranta D, Regueiro V, March C, Llobet E, Margareto J, Larrarte E, Garmendia J, Bengoechea JA. *Klebsiella pneumoniae* capsule polysaccharide impedes the expression of beta-defensins by airway epithelial cells. Infect Immun. 2010;78(3):1135–46.
11. Wyres KL, Wick RR, Gorrie C, Jenney A, Follador R, Thomson NR, Holt KE. Identification of *Klebsiella* capsule synthesis loci from whole genome data. Microbial genomics. 2016;2(12):e000102.
12. Wyres KL, Gorrie C, Edwards DJ, Wertheim HF, Hsu LY, Van Kinh N, Zadoks R, Baker S, Holt KE. Extensive capsule locus variation and large-scale genomic recombination within the *Klebsiella pneumoniae* clonal group 258. Genome Biol Evol. 2015;7(5):1267–79.
13. Lin CL, Chen FH, Huang LY, Chang JC, Chen JH, Tsai YK, Chang FY, Lin JC, Siu LK. Effect in virulence of switching conserved homologous capsular polysaccharide genes from *Klebsiella pneumoniae* serotype K1 into K20. Virulence. 2017;8(5):487–93.
14. Pal S, Verma J, Mallick S, Rastogi SK, Kumar A, Ghosh AS. Absence of the glycosyltransferase WcaJ in *Klebsiella pneumoniae* ATCC13883 affects biofilm formation, increases polymyxin resistance and reduces murine macrophage activation. Microbiology. 2019;165(8):891–904.
15. Dorman MJ, Feltwell T, Goulding DA, Parkhill J, Short FL. The capsule regulatory network of *Klebsiella pneumoniae* defined by density-TraDISort. mBio. 2018;9(6):e01863–18.
16. Lee H, Shin J, Chung YJ, Baek JY, Chung DR, Peck KR, Song JH, Ko KS. Evolution of *Klebsiella pneumoniae* with mucoid and non-mucoid type colonies within a single patient. Int J Med Microbiol. 2019;309(3–4):194–8.
17. Ernst CM, Braxton JR, Rodriguez-Osorio CA, Zagieboylo AP, Li L, Pironti A, Manson AL, Nair AV, Benson M, Cummins K, et al. Adaptive evolution of virulence and persistence in carbapenem-resistant *Klebsiella pneumoniae*. Nat Med. 2020;26(5):705–11.
18. Tipton KA, Dimitrova D, Rather PN. Phase-variable control of multiple phenotypes in *Acinetobacter baumannii* strain AB5075. J Bacteriol. 2015;197(15):2593–9.
19. Bailey MJ, Hughes C, Koronakis V. RfaH and the ops element, components of a novel system controlling bacterial transcription elongation. Mol Microbiol. 1997;26(5):845–51.
20. Tato M, Coque TM, Ruiz-Garbajosa P, Pintado V, Cobo J, Sader HS, Jones RN, Baquero F, Canton R. Complex clonal and plasmid epidemiology in the first outbreak of Enterobacteriaceae infection involving VIM-1 metallo-beta-lactamase in Spain: toward endemicity? Clin Infect Dis. 2007;45(9):1171–8.

21. Monteiro J, Santos AF, Asensi MD, Peirano G, Gales AC. First report of KPC-2-producing *Klebsiella pneumoniae* strains in Brazil. Antimicrob Agents Chemother. 2009;53(1):333–4.
22. Wyres KL, Nguyen TNT, Lam MMC, Judd LM, van Vinh CN, Dance DAB, Ip M, Karkey A, Ling CL, Miliya T, et al. Genomic surveillance for hypervirulence and multi-drug resistance in invasive *Klebsiella pneumoniae* from south and Southeast Asia. Genome Med. 2020;12(1):11.
23. Stevenson G, Andrianopoulos K, Hobbs M, Reeves PR. Organization of the *Escherichia coli* K-12 gene cluster responsible for production of the extracellular polysaccharide colanic acid. J Bacteriol. 1996;178(16):4885–93.
24. Cai R, Wang G, Le S, Wu M, Cheng M, Guo Z, Ji Y, Xi H, Zhao C, Wang X, et al. Three capsular polysaccharide synthesis-related Glucosyltransferases, GT-1, GT-2 and WcaJ, are associated with virulence and phage sensitivity of Klebsiella pneumoniae. Front Microbiol. 2019;10:1189.
25. Domenico P, Schwartz S, Cunha BA. Reduction of capsular polysaccharide production in *Klebsiella pneumoniae* by sodium salicylate. Infect Immun. 1989;57(12):3778–82.
26. Trunk T, Khalil HS, Leo JC. Bacterial autoaggregation. AIMS Microbiol. 2018; 4(1):140–64.
27. Davey ME, Duncan MJ. Enhanced biofilm formation and loss of capsule synthesis: deletion of a putative glycosyltransferase in *Porphyromonas gingivalis*. J Bacteriol. 2006;188(15):5510–23.
28. Schembri MA, Blom J, Krogfelt KA, Klemm P. Capsule and fimbria interaction in *Klebsiella pneumoniae*. Infect Immun. 2005;73(8):4626–33.
29. Campos MA, Vargas MA, Regueiro V, Llompart CM, Alberti S, Bengoechea JA. Capsule polysaccharide mediates bacterial resistance to antimicrobial peptides. Infect Immun. 2004;72(12):7107–14.
30. Phillips ZN, Tram G, Seib KL, Atack JM. Phase-variable bacterial loci: how bacteria gamble to maximise fitness in changing environments. Biochem Soc Trans. 2019;47(4):1131–41.
31. Ahmad I, Karah N, Nadeem A, Wai SN, Uhlin BE. Analysis of colony phase variation switch in *Acinetobacter baumannii* clinical isolates. PLoS One. 2019; 14(1):e0210082.
32. Matatov R, Goldhar J, Skutelsky E, Sechter I, Perry R, Podschun R, Sahly H, Thankavel K, Abraham SN, Ofek I. Inability of encapsulated *Klebsiella pneumoniae* to assemble functional type 1 fimbriae on their surface. FEMS Microbiol Lett. 1999;179(1):123–30.
33. Wugeditsch T, Paiment A, Hocking J, Drummelsmith J, Forrester C, Whitfield C. Phosphorylation of Wzc, a tyrosine autokinase, is essential for assembly of group 1 capsular polysaccharides in *Escherichia coli*. J Biol Chem. 2001; 276(4):2361–71.
34. Bushell SR, Mainprize IL, Wear MA, Lou H, Whitfield C, Naismith JH. Wzi is an outer membrane lectin that underpins group 1 capsule assembly in *Escherichia coli*. Structure. 2013;21(5):844–53.
35. Rahn A, Whitfield C. Transcriptional organization and regulation of the *Escherichia coli* K30 group 1 capsule biosynthesis (*cps*) gene cluster. Mol Microbiol. 2003;47(4):1045–60.
36. Foster PL. Stress-induced mutagenesis in bacteria. Crit Rev Biochem Mol Biol. 2007;42(5):373–97.
37. Kelly SD, Clarke BR, Ovchinnikova OG, Sweeney RP, Williamson ML, Lowary TL, Whitfield C. *Klebsiella pneumoniae* O1 and O2ac antigens provide prototypes for an unusual strategy for polysaccharide antigen diversification. J Biol Chem. 2019;294(28):10863–76.
38. Klein G, Raina S. Regulated assembly of LPS, its structural alterations and cellular response to LPS defects. Int J Mol Sci. 2019;20(2):356.
39. Bolla JM, Lazdunski C, Pages JM. The assembly of the major outer membrane protein OmpF of *Escherichia coli* depends on lipid synthesis. EMBO J. 1988;7(11):3595–9.
40. O'Toole GA, Kolter R. Initiation of biofilm formation in *Pseudomonas fluorescens* WCS365 proceeds via multiple, convergent signalling pathways: a genetic analysis. Mol Microbiol. 1998;28(3):449–61.
41. Fagan RP, Smith SG. The Hek outer membrane protein of *Escherichia coli* is an auto-aggregating adhesin and invasin. FEMS Microbiol Lett. 2007;269(2): 248–55.
42. Reichhardt C, McCrate OA, Zhou X, Lee J, Thongsomboon W, Cegelski L. Influence of the amyloid dye Congo red on curli, cellulose, and the extracellular matrix in *E. coli* during growth and matrix purification. Anal Bioanal Chem. 2016;408(27):7709–17.
43. Bankevich A, Nurk S, Antipov D, Gurevich AA, Dvorkin M, Kulikov AS, Lesin VM, Nikolenko SI, Pham S, Prjibelski AD, et al. SPAdes: a new genome assembly algorithm and its applications to single-cell sequencing. J Comput Biol. 2012;19(5):455–77.
44. Aziz RK, Bartels D, Best AA, DeJongh M, Disz T, Edwards RA, Formsma K, Gerdes S, Glass EM, Kubal M, et al. The RAST server: rapid annotations using subsystems technology. BMC Genomics. 2008;9:75.
45. Deatherage DE, Barrick JE. Identification of mutations in laboratory-evolved microbes from next-generation sequencing data using breseq. Methods Mol Biol. 2014;1151:165–88.
46. Langmead B: Aligning short sequencing reads with Bowtie. Current protocols in bioinformatics 2010, Chapter 11:Unit 11.17.
47. McKenna A, Hanna M, Banks E, Sivachenko A, Cibulskis K, Kernytsky A, Garimella K, Altshuler D, Gabriel S, Daly M, et al. The genome analysis toolkit: a MapReduce framework for analyzing next-generation DNA sequencing data. Genome Res. 2010;20(9):1297–303.
48. Patino-Navarrete R, Rosinski-Chupin I, Cabanel N, Gauthier L, Takissian J, Madec JY, Hamze M, Bonnin RA, Naas T, Glaser P. Stepwise evolution and convergent recombination underlie the global dissemination of carbapenemase-producing *Escherichia coli*. Genome Med. 2020;12(1):10.
49. Robinson JT, Thorvaldsdottir H, Winckler W, Guttman M, Lander ES, Getz G, Mesirov JP. Integrative genomics viewer. Nat Biotechnol. 2011;29(1):24–6.
50. Siguier P, Perochon J, Lestrade L, Mahillon J, Chandler M. ISfinder: the reference Centre for bacterial insertion sequences. Nucleic Acids Res. 2006; 34(Database issue):D32–6.

Publisher's Note

ARTICLE II

Heteroresistance of KPC producing *Klebsiella pneumoniae* results of three subpopulations associated with a broad range of mutations

Adriana Chiarelli, Nicolas Cabanel, Isabelle Rosinski-Chupin, Thomas Obadia, Thierry Naas, Rémy A. Bonnin, Philippe Glaser

Clinical isolates of *K. pneumoniae* producing carbapenemase (CPKp) often show MICs below the clinical breakpoints, thereby complicating their detection. Moreover, some of them exhibit carbapenem heteroresistance (HR), i.e., growing colonies within the inhibition halo formed by the antibiotic disk or gradient strip. There is general acceptance that HR refers to the occurrence of a range of susceptibilities to an antibiotic within seemingly isogenic bacteria populations. Yet, inconsistency among methodologies used to investigate HR has challenged the understanding of this phenomenon. Attempts to provide some clarity in this field have been made by some research groups, but mechanisms mediating HR remain blurry or suggests multiple pathways.

Altogether, these observations paved the way for my PhD project, which aimed at assessing the frequency and diversity of HR among KPC-Kp clinical isolates, and eventually elucidating the mechanism driving the heterogeneous response to carbapenems. One major hypothesis was the existence of subpopulations with distinct physiological characteristics, whose emergence is facilitated by the progressive inactivation of the carbapenem drug by the carbapenemase.

In this regard, we collected 62 KPC-Kp clinical isolates, complemented with 20 additional *K. pneumoniae* with other carbapenemases and six without any for comparison. First, I investigated the levels of carbapenem resistance (R) and HR among the collected isolates by Etest. R levels were diverse, and HR was prevalent among KPC-Kp, particularly towards IMP, and poorly observed with other CP producers or totally absent in non-CP isolates.

Consistently with former findings, we observed HR majorly with IMP compared to MEM, reason why we next thought to focus solely on this carbapenem drug. Hence, we selected a subset of isolates showing varying HR profile by Etest for Population Analysis Profiling (PAP), considered as the reference method for HR quantification. Yet, besides providing information of the frequency of survival towards IMP, the PAP method does not elucidate the identity of surviving populations. Furthermore, when looking at the different studies addressing HR that use PAP, experimental conditions seem arbitrary, and this might impact on the interpretation of the phenotype.

After reviewing the literature, searching for diverse techniques that could be helpful for our purposes and several attempts to purify the surviving fraction of cells for further characterization (e.g., recovery of surviving cells upon removal of residual carbapenemase as

well as carbapenem from the growth medium where cells were exposed overtime to IMP, FACS and microscopy on agarose pads), I finally selected the ScanLag method for quantification of the dynamics of bacterial response challenged with high dose of carbapenems. This setup allowed us to observe heterogeneity of growth at single-colony level and, notably, differences among KPC-Kp isolates in the frequency and modalities of survival to high concentration of IMP. One isolate was selected for further analysis due to its highly HR pattern by Etest, subsequently confirmed with the PAP.

Colony characterization by susceptibility testing and comparative whole genome analysis with the parental isolate gave us the opportunity to reveal that the HR phenotype - in the specific case of KPC-Kp, is nonetheless a mixture of resistant, tolerant and heterotolerant (persisters) cells, where the early detection of persisters is likely due to the rapid hydrolysis of IMP driven by KPC, together with its instability.

Heteroresistance of KPC producing *Klebsiella pneumoniae* results of three subpopulations associated with a broad range of mutations

[1,2,3]Adriana Chiarelli, [1,2]Nicolas Cabanel, [1,2]Isabelle Rosinski-Chupin, [4]Thomas Obadia
[1,5]Thierry Naas, [1,5]Rémy A. Bonnin, [1,2]Philippe Glaser*

[1]Joint research Unit EERA « Evolution and Ecology of Resistance to Antibiotics », Institut Pasteur-APHP-University Paris-Saclay, [2]CNRS UMR3525, 75015, Paris, France. [3]Sorbonne Université, Paris, France. [4]Bioinformatics and Biostatistics Hub, Institut Pasteur, USR 3756, CNRS, Paris, France. [5]UMR1184 Team RESIST, Faculty of Medicine University Paris-Sud, University Paris-Saclay, French National Reference Center for Antibiotic Resistance: Carbapenemase producing Enterobacteriaceae, Le Kremlin-Bicêtre, France

* Corresponding author: Philippe GLASER,
Institut Pasteur, 28 Rue du Dr Roux, 75724 Paris Cedex 15, Tel + 33 1 45 68 89 96 –
E-mail: pglaser@pasteur.fr

ABSTRACT

Carbapenemase producing *Klebsiella pneumoniae* (CPKp) have disseminated globally and represent a major threat in hospitals with few therapeutic options and a high mortality rates. *K. pneumoniae* producing the carbapenemase KPC (KPC-Kp) frequently show heteroresistance (HR), with colonies typically growing in the inhibition zone of agar-based AST. This may result in clinical isolates classified as susceptible by antibiotic susceptibility testing (AST), but showing high failure rates during imipenem or meropenem treatment of infections. HR might also represent a first step towards resistance. By analysing a set of 82 CPKp, we showed that HR is, as expected, frequent among KPC-Kp and specific to these isolates compared to those producing other carbapenemases (VIM, NDM or OXA-48). In order to characterize the surviving population, we used the ScanLag setup to track the emergence of colonies at 8-fold the imipenem minimal inhibitory concentration. By analysing the distribution of colony time of appearance for six clinical isolates, we were able to discriminate two patterns of distribution: a Gaussian-like distribution of early appearing colonies, the growth of which is slightly delayed compared to colonies in the absence of antibiotics, and a long tail of late appearing colonies. The two populations were predicted to result from tolerance and persistence mechanisms, respectively. In addition, a subset of colonies showed a slower growth rate. To characterize these populations, we determined the genome sequence of 332 colonies. Among these colonies, 78% (n= 246 did not show any genetic alteration. In the other 25% (n=84), we identified a broad range of genetic events, including gene loss, DNA amplification and point mutations. The predicted impact of these mutations is in agreement with an heterogeneous population encompassing not only tolerant and persistent cells, but also resistant bacteria. Resistance resulted from alteration of functions affecting the cell wall and, in particular, the outer membrane permeability, yet not affecting the bacterial growth, and from mutations in the Krebs cycle and cellular respiration leading to small colony variants. Altogether, these data revealed the complexity of imipenem HR among KPC-Kp isolates.

INTRODUCTION

Antibiotic resistance represents a global health concern, strongly driven by inappropriate use or overuse of antibiotics and promoted by the lack of new effective molecules. Several bacterial pathogens evolved multi-drug resistance (MDR), seriously impairing their clinical management. Carbapenem-resistant *Enterobacterales* (CRE), including *Klebsiella pneumoniae*, were listed by the World Health Organization as critical priority pathogens for which there is an urgent need to develop new antibiotics (1). Carbapenem resistance may be the result of the production of an extended-spectrum ß-lactamase (ESBL) or a cephalosporinase associated to decreased permeability (due to mutations in porin genes and/or upregulation of efflux pumps) or to the production of specific carbapenem-hydrolysing β-lactamases (carbapenemases) (2). Carbapenemase-producing *K. pneumoniae* (CPKp) is one of the most feared nosocomial pathogen worldwide (3). Among the clinically relevant carbapenemases detected in *K. pneumoniae* clinical isolates, KPC enzymes are endemic in some areas and have been associated with high mortality rates and treatment failure (4). However, treatment effectiveness is extremely dependent on the accurate measurement of carbapenem minimum inhibitory concentration (MIC) (5), and MIC determination is often challenged by the variable resistance levels shown by CPKp, especially those producing the class A carbapenemase KPC (KPC-Kp) (4).

A further challenge is represented by heteroresistance (HR) towards carbapenems. Heteroresistance broadly describes heterogeneous susceptibility levels to an antibiotic within seemingly isogenic bacterial populations. This “bet-hedging” survival strategy confers long-term fitness benefit to populations in constantly fluctuating environments (6). In addition, as resistance is often a stepwise evolution process, such heterogeneity may precede genetic changes and thus accelerate resistance development in the population (7). The ambiguity in the use of the term HR has been blearing its exact meaning. In addition, the lack of standardized methodologies to characterize HR precluded the comparison among studies and thus, a general understanding of the phenomenon (8). To correctly identify mechanism driving HR in a bacterial population, aspects such as the origin and clonality of resistant subpopulations, the stability of the observed phenotype and the resistance levels of the subpopulations should be considered (9). However, multiple factors can influence the interpretation of the phenotype, including bacterial species, inoculum density, type of antibiotic and presence of drug-inactivating enzymes. Population Analysis profiling (PAP) is generally considered as the gold-

standard method and adopted by most of the studies HR issue, although following different parameters. There is general consensus that an isolate can be defined as HR whether it shows subpopulations at ≥8 × MIC of the main cell population (9).

Heteroresistance has been largely reported among *K. pneumoniae* isolates towards colistin (10) (11) and, to a minor extent, to carbapenems (12-15). Heteroresistance to carbapenems was mostly observed among KPC-Kp (15, 16) (14). However, mechanisms mediating carbapenem HR in *K. pneumoniae* remain poorly investigated. Heteroresistant KPC-Kp strains survival upon exposure to high bactericidal concentrations of imipenem (IMP) resulted from the emergence of subpopulations with decreased expression of the major outer membrane porin, OmpK36 (16). Survival might be favoured in the first place by IMP degradation driven by KPC released into the culture medium and high level of resistance among the subpopulations was shown to result from adaptive changes in response to stress first induced by the ß-lactam (17).

Here, we aimed at characterizing carbapenem HR in CPKp clinical isolates and identifying metabolic and regulatory pathways underlying the diversity of susceptibility levels to high doses of carbapenems. We characterized a collection of 82 CPKp isolates by phenotypic and genomic analyses. A subset of HR *K. pneumoniae* isolates was further selected to infer the dynamics of bacterial response to high doses of IMP at single colony level (18). By performing phenotypic and genomic analysis of the surviving subpopulations, we showed that HR to imipenem is a complex phenomenon, which encompasses different strategies adopted by bacterial populations to survive drug exposure, namely tolerance, persistence and resistance. In particular, this approach allowed to reveal a broad diversity of genetic alterations in diverse pathways, contributing to the observed phenotypes.

MATERIALS AND METHODS

***Klebsiella pneumoniae* isolates, media and growth conditions.** The isolates analysed in this work and their main characteristics are listed in Table S1. It includes 62 KPC-Kp clinical isolates and for comparison, 20 isolates expressing other carbapenemases (OXA-48, n=3; VIM-1, n=11; NDM-1, n=3; isolates co-carrying two carbapenemases, n=3) and six isolates not carrying any carbapenemase gene as control. Bacteria were grown in Mueller-Hinton (MH), Tryptic-Soy Broth (TSB) or Lysogeny broth (LB) and on Tryptic-Soy agar (TSA) or LB agar (LBA) plates. Antibiotic susceptibility testings (AST) were performed by Etest (Biomerieux) on Mueller-Hinton Agar (MHA) plates inoculated by flood with 2 ml of bacterial culture (10^6 bacteria/ml) and following manufacturer recommendations. Heteroresistance was determined

according to the number of colonies (>3) identified in the inhibition zone after 16-20 hours of incubation at 37 °C.

Population Analysis Profiling (PAP). Heteroresistance was quantified by PAP, following spreading on agar plate of either stationary phase (SP) bacterial cultures (overnight culture, ON) or exponentially growing bacteria (ON culture diluted 1000 times in TSB and incubated at 37°C until it reached an OD_{600}~0.3-0.4). Bacterial cultures were serially diluted in saline buffer and 100 µl of dilution at OD_{600} of 0.01 (an estimate of 10^7 bacteria/ml) were spread evenly using the automatic plater EasySpiral (Interscience) on freshly prepared TSA plates containing IMP at 4-fold, 8-fold and 10-fold the MIC of each isolate, as determined by Etest. The plates were incubated at 37 °C, and colonies were counted at 24 and 48 hours. The proportion of surviving colonies per each IMP concentration was calculated compared to the number of CFUs as determined on medium without IMP. Experiment were performed in triplicates.

ScanLag assay, data analysis and surviving colonies characterization. The ScanLag analysis was carried out as described above for PAP analysis. The ScanLag setup was built as described previously (18), but adapted to our purposes: approximately 1-3 x 10^6 cells from mid-EP or SP cultures were spread onto TSA plates supplemented with IMP. Colony tracking was carried out every 20 minutes for 48-hours at 37 °C. Time of appearance (ToA) and colony growth rates were estimated by running MATLAB scripts publicly available at https://github.com/iosonofabio/scanlag (19).

Colony ToA distributions were analysed by using the R package *mixtools* (20). We applied a two-component mixture model to the ToA distributions of both untreated populations and those surviving IMP exposure using expectation–maximization (EM) algorithm by the *normalmixEM* function. Per each N group, parameters µ (estimated ToA means per each components), Σ (the estimated standard deviations) and λ (the estimated mixing weights, corresponding to the initial proportion of colonies, expressed in %) were used to analyse and quantitatively compare subpopulations across the selected isolates. The delay in growth of IMP exposed populations compared to untreated colonies, hereto referred to as "Lag time extension", was quantified as the ratio of mean ToA of N1 cells (first appearing population on IMP plates) over the mean ToA of untreated colonies. The "persister" fraction was estimated using thresholds as previously described (21). Briefly, colonies were considered as deriving from persister cells if they appeared later than three standard deviations away from the mean of N1 ($ToA > \mu_{N1}+3\Sigma_{N1}$).

Persisters frequencies over the whole populations were calculated per each isolate; data were then visualized using the *ggplot2* (22).

Isolation of colonies from subpopulations with decreased susceptibility. Surviving colonies were selected from IMP-containing plates, re-isolated on media containing the same IMP concentration and, in parallel, on drug free media. On the next day, colonies were picked from IMP plates or from plates without IMP if the colony did not grow on the IMP plate and incubated in TSB without antibiotic until mid-exponential phase was reached. The cultures were then used for AST by Etest and DNA extraction for further genome sequencing.

Whole-genome sequencing and analysis. Genomic DNAs were extracted by using the DNeasy Blood & Tissue Kit (QIAGEN). *K. pneumoniae* genomes were sequenced by using the Illumina HiSeq2500 or NextSeq500 platform, with 100- and 75-nucleotides (nt) paired-end reads respectively. Libraries of *K. pneumoniae* clinical isolates were constructed by using the Nextera XT kit (Illumina) and libraries of CNR146C9 clones selected during ScanLag experiments by using NEBNext Ultra II FS DNA Library prep kit, which provide a more even genome coverage (23). Paired-end reads were assembled into contigs with SPAdes 3.9.0 (24). The complete genome sequence of CNR146C9 was determined by using the long-read PacBio technology. Accurate consensus reads obtained from raw reads with pbccs (https://github.com/nlhepler/pbccs) were assembled with Canu (25). The assembly was polished with Circulator (26) and manually corrected by mapping Illumina reads with Breseq 0.33.2 (27). Variants compared to CNR146C9 complete genome sequence were identified by using Breseq (27). Missing regions and recombination events were identified by analysing the "Unassigned missing coverage evidence" and "Unassigned new junction evidence" sections of the Breseq outputs respectively. Polymorphisms were visually verified by using the viewer Tablet (28). Genome sequences were annotated with Prokka 1.14.5 (29) and analysed for MLST and ARG content by using Kleborate (30) and Resfinder 4.0.1 (31). Plasmid incompatibility groups were identified by using PlasmidFinder 2.1 (32). Copy number variation was estimated by counting the number of reads per gene and comparing with number of Illumina reads of the parental strain CNR146C9 by using the DESSeq2 R Package (33).

Statistical analyses. All statistical tests and graphical representations were performed using R 4.0.3 with R studio 1.3.1093 (34). To visualize whether there was any significant difference in

survival between exponentially growing and stationary phase bacterial culture for the PAP and between the different subpopulations in the ScanLag experiments, boxplots were created with ggplot2 (22) and statistical assessment between groups was performed by Student's t-test using the "stat_compare_means" in the R package ggpubr, which yielded the P values (https://rpkgs.datanovia.com/ggpubr/index.html).

Availability of data. Sequence data for the clinical isolates have been deposited at DDBJ/EMBL/GenBank (Bioproject pending). CNR146C9 WGS was deposited with the following accession numbers: **pending**. Biosamples for the Illumina sequence data are listed in Table S1.

RESULTS

Diversity of resistance and prevalence of heteroresistance among KPC-Kp. In order to characterize HR among KPC-producing *K. pneumoniae*, we collected 62 KPC-Kp clinical isolates. For comparison, we included 20 isolates expressing other carbapenemases and six isolates without any carbapenemase as control (Table S1). WGS analysis revealed that the KPC-Kp isolates belong to 16 STs, with ST512 being the most prevalent (n = 19), followed by ST101 (n = 10) and ST258 (n = 8). Thirteen different capsular types were identified, with KL107 being the most represented type (n = 24) and mostly associated with ST512. In addition to the carbapenemase genes, the 82 CPKp isolates show a diversity of resistome and porin mutations (Table S1). Defects in the major porin genes (*ompK35* and *ompK36*) were detected in 66% of isolates (n = 54/82) and, among them, 33% (n = 18/54) co-harboured an ESBL gene. In agreement with previous studies, CPKp ST512 isolates shared a truncated *ompK35* sequence and a G134D135 duplication that constricts the porin channel of OmpK36, previously shown to yield similar resistance levels as if the porin was lost (35). Likewise, CPKp ST258 isolates exhibited a truncated *ompK35* sequence and, two of them had the same *ompK36* GD duplication. The ten ST101 CPKp isolates shared a frameshift mutation in *ompK35* and nine of them also had a TD or GD duplication in *ompK36* (Table S1).

The susceptibility levels to IMP and MEM were determined by Etest, as the broth microdilution method is affected by carbapenem degradation (36). The carbapenemase-producing isolates exhibited a broad range of MIC, from 0,125 to >32 mg/L to MEM and 0,25 to >32 mg/L to IMP respectively (Fig. 1A, Table S1). For both carbapenems breakpoints are < 1 mg/L for susceptible (S) and >4 mg/L for resistant (R). All the IMP R isolates (n = 18) exhibited defects in outer membrane (OM) permeability and 89% (n=16/18) showed altered sequences of both *ompK35* and *ompK36*. All MEM R isolates (n = 37) but one showed at least one mutation in

ompK35, with 86% having both *omp* genes disrupted (n = 32). A minority of MEM R isolates (8/37) and IMP R isolates (4/18) carries a ESBL gene. This observation suggested that higher carbapenem MICs did not result of the expression of an ESBL in the KPC-Kp isolates we have analysed.

The Etest allows also a preliminary screen for HR. We first evaluated HR based on the appearance of colonies within the inhibition halo induced by the antibiotic gradient strip (Fig. 1B). We referred to HR as the occurrence of at least 5 colonies within the inhibition halo. Isolates with 3 or 4 colonies were defined as "moderately HR" and isolates with less than 3 colonies in the halo were classified as "non HR" (Fig 1A). Isolates showing full contact with the Etest gradient strip (IMP, n = 3; MEM, n = 29) for which HR could not be detected (Fig 1B), were excluded from the analysis.

Of the KPC-Kp isolates, 73% (n = 43/59) and 51% (n = 17/33) showed HR or moderate HR to IMP and MEM, respectively (Table S1). A higher rate of IMP HR were detected for isolates otherwise classified as susceptible based on their MIC (77.8%) or intermediate (80%) compared to resistant ones (66.7%). In the case of MEM, HR was more frequent with isolates classified as intermediate (58.3%), followed by susceptible ones (47%) (Fig 1C). IMP HR was slightly more prevalent among isolates harbouring the $bla_{\text{KPC-3}}$ compared to those carrying the $bla_{\text{KPC-2}}$ (53.5% and 46.5%, respectively). Conversely, the proportion of MEM HR isolates was higher among isolates carrying $bla_{\text{KPC-2}}$ relative to those harbouring $bla_{\text{KPC-3}}$ (70.6% and 29.4%, respectively) (Fig 1D).

These results showed that our set of isolates harbouring bla_{KPC} exhibited a broad range of resistance and HR levels. Using the same criteria, HR was also detected by Etest, although to a minor extent, among NDM-producing *K. pneumoniae* (n = 3/5 HR to IMP 2/5 HR to MEM), but was not observed among the VIM- and OXA- isolates (Table S1).

KPC-Kp isolates show subpopulations growing at high imipenem doses. Based on MIC values and HR data, we selected 13 CPKp isolates (7 KPC-Kp, 2 NDM-Kp, 2 OXA-Kp and 2 VIM-KP) to quantify IMP HR by PAP and to characterize isolates' response to IMP concentrations 4-, 8- and 10-fold their MICs, as determined by Etest (Table S1). To evaluate the impact of the growth phase on the survival of subpopulations to IMP, bacterial cultures in exponential (EP) and stationary phase (SP) were tested. According to the definition of HR, we confirmed HR for isolates showing colonies at least at IMP 8xMIC. After setting the significance threshold to 10 colonies on plate (10^2 CFU/ml), we identified HR, to varying degrees, in four KPC-Kp isolates: CNR146C9, CNR121E10, KP H15-21-6 and BIC-1 (Fig 2).

250 The highest proportion of surviving colonies at 8- and 10-fold MIC of IMP was recorded for
251 CNR121E10, followed by CNR146C9, thus confirming their HR profile displayed by Etest.
252 Interestingly, KP H15-21-6 was not HR by Etest, but it showed surviving subpopulations by
253 PAP. On the other hand, although NDM isolates showed a HR-like pattern by Etest, they did
254 not show HR by PAP assay. VIM- and OXA-isolates showed scarce or none ability to grow at
255 least at 8xMIC IMP, in agreement with absent HR profile by Etest. Significant differences
256 between EP and SP inoculum were observed for 4 out of 13 isolates at 8-fold MIC (Fig 2). We
257 observed a higher number of colonies with SP inoculum for the two KPC-Kp isolates with the
258 highest HR rate: CNR146C9 and CNR121E10. We observed a similar trend for the VIM-1
259 producing isolate CNR206A5 but the opposite for the other VIM-1 isolate (KP_{VIM-1}). These
260 data suggested a strain-specific ability to cope differently with high doses of IMP, according to
261 the physiological state of the bacterial population.
262
263 **Subpopulation growth dynamics**. Differences in colony size were noticed on medium
264 supplemented with 8xMIC IMP for CNR146C9, CNR121E10, Kp H15-21-6 and BIC-1,
265 indicating an heterogeneous growth of surviving subpopulations in the presence of IMP. To
266 better characterize the dynamics with which subpopulations survive exposure to high IMP
267 concentrations, we used the ScanLag system (18) to monitor growth of individual colonies from
268 these isolates in the presence of IMP. For comparison, we included in our analysis the two
269 KPC-Kp isolates showing scarce or none HR (CNR149B2 and CNR152H4). For these two
270 isolates, colony behaviour was investigated at 4xMIC IMP, as CFU numbers at 8xMIC were
271 below the detection threshold (less or equal than 10^2 CFU/ml). Imipenem MICs for the six
272 selected KPC-Kp isolates ranged from 0,25 to 1,5 mg/L (Table S1).
273 By using ScanLag, we quantified the distribution of colony time of appearance (ToA) of the six
274 isolates over 48 hours onto drug-free and IMP-containing media (Fig. 3). With the drug free
275 condition, we observed a narrow normal distribution of ToA for all the isolates, with mean
276 values ranging from 426,3 to 518,1 minutes (Table S2, Fig 3a; green bars). By contrast, the
277 distribution of colony ToA onto media supplemented with IMP was heterogeneous and
278 exhibited a tail of various lengths, particularly visible in CNR146C9, CNR152H4, CNR121E10
279 (Fig 3A, red bars). Based on this distribution, we assumed the presence of two subpopulations:
280 an early appearing population N1 corresponding to the main peak of colony ToA distribution,
281 and N2 including the late-appearing colonies. In order to characterize this heterogeneity, we
282 attempt to fit the data to a two-component mixed model using ToA as index. We were able to
283 quantify the proportions of the N1 and N2 subpopulations across the isolates and the

heterogeneous delay in growth of the N1 population relative to the untreated colonies (Fig 3b, Table S2). In particular, N1 subpopulation of isolates CNR149B2, Kp H15-21-6 and BIC-1 showed an earlier appearance compared to the three other isolates with LE <2 compared to a LE ≥ 2 (Fig 3D, green boxplots). By considering as persisters the colonies exhibiting a delay more than three standard deviations away from the mean of the main peak distribution (subpopulation N1) as previously proposed (21), we estimated their frequency in the six isolates. The highest persister rate in exponential phase was observed for CNR146C9, whereas BIC-1 exhibited the lowest frequency (Fig 3E and Table S2).

To estimate the influence of the bacterial growth phase on the rate of survival and, in particular, on the frequency of the two subpopulations, we tracked the colony ToA following spreading of stationary phase cultures of the six isolates in the drug-free and IMP-supplemented agar media. Since SP cultures have been shown to be more tolerant to ß-lactams (37), we expected to observe an extended delay in growth for SP cultures exposed to IMP. However, by quantifying the LE of N1 subpopulations, we could detect a significantly longer delay only for CNR149B2 and Kp H15-21-6 in SP compared to EP. In addition, we did not detect any significant difference in the proportions of persisters between the EP and SP phase, except for CNR146C9, which showed a lower occurrence of persisters in SP (Fig 3E, Table S2)..

Overall, we observed heterogeneous growth resumption among the selected isolates when exposed to high concentrations of IMP (4xMIC and 8xMIC), which indicated the co-existence of at least two distinct phenotypes in the surviving populations. The diversity of delay in growth (lag time extension) and proportions of the subpopulations N1 and N2 were strain-specific, likely due to the genomic background of the isolates.

Genetic heterogeneity associated with the observed heteroresistance. Heteroresistance refers to a phenotypically heterogeneous subpopulation within a seemingly isogenic population. However, increased survival might be also linked to genetic events. We selected CNR146C9 for in-depth genetic analysis of the HR populations. Based on the ToA and colony growth rates as visualized by ScanLag (Fig 3A), we classified surviving colonies according to three patterns: A, B and C. Pattern A included all colonies showing wild-type growth rates and belonging to population N1; pattern B indicated colonies showing reduced growth rates and variable ToA, and pattern C included colonies showing wild-type growth rates but delayed and variable ToA, thus belonging to population N2.

To obtain a high quality reference genome, we determined CNR146C9 whole genome sequence by combining long- and short-read sequencing. CNR146C9 hosts two plasmids carrying *bla*$_{CTX}$-

318 $_{M\text{-}15}$ and $bla_{KPC\text{-}3}$, of 237,007 bp and 110,489 bp, respectively and a circular 52,608 bp-long
319 extrachromosomal phage, previously reported in *K. pneumoniae* ST307 isolates (38) (Table
320 S3). A total of 332 colonies were analysed: 167 of pattern A (Table S4), 29 of pattern B (Table
321 S5) and 136 of pattern C (Table S6). Colonies were submitted to WGS just after isolation and
322 IMP and MEM MIC determination by Etest using the same culture. Ninety-three colonies
323 showed at least one genetic modification, including single-nucleotide variations (SNVs),
324 insertions, deletions of bases, plasmid/phage loss and amplification. In addition to the loss of
325 entire or part of mobile genetic elements (MGEs), and to three large DNA region
326 amplifications, genome mutations affected 54 loci affecting different cellular processes (Table
327 S4, S5 and S6).
328 For most of the A-type colonies (128/167), we did not detect any genetic change. These colonies
329 exhibited MIC values for MEM and IMP and an HR profile determined by Etest similar to the
330 parental strain CNR146C9. Forty-one A-isolates showed genetic alterations (Table S4). Most
331 of them were not associated with a decreased susceptibility (63%). The most recurrent event
332 was the loss of the 52,608 bp extrachromosomal phage. One ICE and part of the *tra* region from
333 the CTX-M-15 plasmid were also lost. Point mutations were also detected among those colonies
334 and affecting different functions like a nonsense mutation in *lysS* encoding one of the two tRNA
335 synthase gene or a mutation in *rpsC* encoding the ribosomal protein S3. Some of these diverse
336 genetic events might have been selected and contributed to IMP survival.
337 On the other hand, 15 colonies showed a decreased susceptibility to IMP and MEM ranging
338 from 1,5 mg/L to >32 mg/L. Strikingly, all mutations detected in these colonies except one
339 were associated with alterations of the cell envelope. Mutations leading to the highest MICs
340 affected the OM permeability, with three clones mutated in *ompK36*. However, non-canonical
341 mutations affecting the Bam pathway of insertion of outer membrane proteins (OMP) into the
342 OM (39) were also selected. Three clones showed a truncated *bamB* gene, one was mutated in
343 *bamA* (N448Y), which is essential, and one isolate showed an IS*Kpn25* insertion six bp
344 upstream of the start codon of the *surA* gene encoding the major chaperon molecule from the
345 periplasmic chaperon network contributing to the translocation of OMP across the periplasm
346 (40). A second class of mutations affected LPS biosynthesis, with three clones mutated in
347 different functions related to this process. Three mutations occurred in regulatory systems
348 affecting cell wall components. AC90 carried two mutations in the *cpxAR* locus encoding a two
349 component regulatory system (TCS) sensing OM stresses (41, 42): a four codons deletion (pos.
350 20 to 23) in the sensor *cpxA*, present in 100% of the reads and a R205W mutation in *cpxR*
351 present in 95% of the reads. This clone is heterogeneous with dominant large colonies, mutated

in *cpxR* and *cpxA* and few highly resistant small colonies, only mutated in *cpxA* (Table S4). AC50 was mutated in *comR* encoding a TetR/AcrR family transcriptional regulator, regulating the expression of *ldtC*, which encodes an OM protein induced under different stress conditions (43). AC151 was mutated in *slyA* (*kvrA*), coding for a pleiotropic regulator of the MarR family that regulates capsule synthesis in *K. pneumoniae* and its loss-of-function downregulates *ompK35* and *ompK36* expression (44). In the strain AC376, we observed a 89,584 bp duplication encompassing the *dcw* locus encoding major functions for cell wall synthesis and cell division (Fig. S1). Interestingly, this isolate showed a 16-fold decrease of IMP susceptibility but almost no effect on MEM susceptibility.

The only mutation associated with reduced susceptibility but not affecting the cell envelope occurred in the *lipA* gene, involved in lipoyl cofactor biosynthesis. Lipoyl is a cofactor of pyruvate and 2-ketoglutarate dehydrogenases, key enzymes of glycolysis and the tricarboxylic acid (TCA) cycle. This metabolic mutation reminds the type of mutations from the B pattern (see below).

Twenty-one out of the 29 B pattern colonies analysed showed an increased MIC for both antibiotics. Some isolates might have been misclassified as pattern B, as they did not phenotypically differentiate from the parental strains (Table S5). We identified mutations in 27 isolates (Table S5). None of the mutations involved genes affected among pattern A colonies. Indeed, 67 % of the mutations occurred in genes with metabolic functions. The most recurrent mutations affected respiration, the coenzyme Q synthesis genes *ubiA* (n=2)*, ubiB* (n=2)*, ubiD* and *ispA* (n=3), heme biosynthesis (*hemA*) and the TCA cycle (a deletion encompassing *lpdA* and *aceF*; *icd*, encoding isocitrate dehydrogenase (n=2) and *acnB*, encoding the aconitate hydratase (n=2)). One isolate showed inactivation of the gene *ptsI* from the central phosphotransferase system (PTS), contributing to carbon source import and catabolic regulation. These mutants exhibited small colony variant (SCV) phenotype and increased resistance under aerobic conditions. However, these phenotypic traits were reversed for respiratory and TCA mutant under anaerobiosis, confirming the causality of these mutations for the phenotype (Table S5).

Two mutations affected lipid metabolism: *pgpC* encoding a phosphatidylglycerophosphatase C and *hldE,* encoding a bifunctional kinase/adenylyltransferase involved in the inner core LPS biosynthesis (45). One isolate mutated in *cysB* showed an increased MICs only towards IMP. Interestingly, *cysB* mutation is the major cause of mecillinam resistance in clinical isolates of *E. coli* (46). One isolate (AC171) mutated in the $tRNA^{Ser}$(gct) encoding gene showed a moderate decrease in susceptibility to both carbapenems, but strongly affected growth, possibly

due to an effect on protein synthesis. Globally, pattern B corresponded to resistant clones with mutations in *K. pneumoniae* core resistome and associated with decreased growth rate.

Unlike colonies from pattern A and B, none of the pattern C colonies arising late on the plate showed a significant increase in the MICs to IMP or MEM. Most of the colonies did not show any detectable genetic modification (n=117/136, 86%). Unexpectedly, ten colonies showed an increased susceptibility to the two carbapenems due to the loss of the pKPC plasmid (Table S6). These observations were in agreement with colonies resulting from persistent cells escaping imipenem bactericidal effect. As observed for pattern A colonies, four pattern C colonies showed loss of the phage, whereas one clone (AC158-C) lost an integrated prophage. In one isolate (AC362-C), we observed a 3-fold copy number increase of a 51 kb long region of the pCTX-M plasmid bracketed by two IS*5075*. This genomic island contains numerous adaptive functions for glycogen biosynthesis, lactose catabolism, the Fe(3+) dicitrate transport system (*fec* locus) and a glutathione transport system (38). Increased expression of these genes might have contributed to the enhanced survival as persistent cell. Two colonies showed intergenic mutations, while one non-sense mutation inactivated the type VI secretion system protein TssG. Whether these mutations have an impact on the persistent phenotype remain to be determined.

DISCUSSION

Heteroresistance to IMP represents a critical issue in the management of KPC-Kp isolates in the clinic. Indeed, the reduced susceptibility to IMP and MICs conferred by the KPC carbapenemase may remain below the breakpoint for susceptibility/resistance (1 mg/L), as we observed in the set of isolates we have analysed. Such MICs are theoretically compatible with IMP usage, but with a high risk of resistance selection and treatment escape (47). By analysing a collection of 62 KPC-Kp clinical isolates with a broad range of carbapenem susceptibility levels, we showed that HR towards IMP and MEM was prevalent and specific to KPC isolates when compared to isolates producing other carbapenemases like VIM or OXA. Among KPC-Kp isolates, we observed a higher rate of HR to IMP compared to MEM. These two carbapenems share similar mode of action by targeting mainly PBP2, but also binding to PBP1a PBP1b. In addition, MEM shows a higher affinity to PBP3, explaining differences in the morphological impact of those two carbapenems on *E. coli* cells (48). On the other hand, IMP is a smaller molecule than MEM and shows a rapid influx through the OM (49). These different properties might also explain the diverse impacts of mutations we selected on the susceptibility levels to the two antibiotics (Tables SX, Y and Z). Under laboratory conditions, IMP is less

stable than MEM and is spontaneously degraded (49, 50), a key factor for the development of HR in carbapenemase-producing bacteria.

HR has been defined as bacterial population growing at 8x the MIC (9). In our PAP analyses, at this antibiotic concentration, frequency of survival ranged from 5,33 x 10^{-6} to 1,82 x 10^{-4} in EP and from 3,95 x 10^{-5} to 4,76 x 10^{-4} in SP, preventing their harvesting and limiting the use of microscopy for single cell analysis on agarose-pad or microfluidics device such as the mother machine (51). Previous studies addressing HR in KPC-Kp were performed in bulk, following addition of IMP at concentrations higher than the MIC leading to the selection of resistant mutants in the porin gene *ompK36* (16, 17). Here, we have applied the ScanLag system (18) to analyse the individual fate of surviving bacteria forming colonies on plates with IMP at 8xMIC or 4xMIC. For the six KPC-Kp isolates, ScanLag revealed a bimodal profile of appearance of the colonies in the presence of IMP: first a Gaussian peak delayed compared to the appearance of colonies not exposed to IMP followed by a tail of late appearing colonies. In addition to the delayed time of appearance, some colonies showed a slower growth rate. Overall, these results revealed an heterogeneous surviving population. Compared to other antibiotics, a specific parameter of HR to ß-lactams in ß-lactamase producing bacteria is the degradation of the antibiotic in the medium. As estimated by ScanLag, the first Gaussian peak of the surviving populations N1 included colonies with variable lag time extension compared to colonies grown in the absence of IPM but for most of them a normal growth rates. This is consistent with what has been defined as tolerant by adjusting lag time (52). Similarly, the late appearing colonies (N2) in the tail of the distribution, growing under conditions where the antibiotic is degraded would result from the regrowth of persister cells (21, 52). In agreement with these hypotheses, the vast majority of colonies from N1 and N2 populations reproduced the same susceptibility and HR phenotype as the parental strains. Comparisons of the six clinical isolates showed different profiles and effects of plating EP or SP bacteria (Fig. 3E), which would correspond to different levels of tolerance to IMP and persistence. It revealed a contribution of the genomic context to drug survival which remains to be characterized. As characterized in experimental models of evolution (53, 54), these features might have been selected in synergy with the selection of antibiotic resistance following drug treatments.

One limitation of ScanLag is the absence of information on the first generations before the appearance of a visible colony. The observed delay might be related to an extended lag phase or to a transient slow growth phase reducing susceptibility. We speculated that combining genomic and phenotypic analyses of surviving colonies at 8x MIC might provide additional information on surviving populations. Most of the clones from profile A and C (showing similar

454 growth as the parental strain) did not show any genetic events, which is in agreement with
455 tolerance and persistence mechanisms, respectively. The frequent loss of pKPC plasmid in ten
456 of the C-isolates and the restoration of carbapenem susceptibility suggested that these colonies
457 arose from persistent cells. Indeed, no plasmid loss was detected among 200 colonies of
458 CNR146C9 growing on antibiotic-free medium. pKPC carries functions contributing to its
459 stability including a *vapBC* family toxin/antitoxin (TA) locus. VapC toxins inhibit translation
460 by an RNAse activity (55). In *E. coli*, the VapBC TA system was previously reported to
461 contribute to increased rate of persistence (56) and a *vapB* mutant was associated with an
462 extension of lag-time and higher drug tolerance in *E.coli* exposed to intermittent high doses of
463 ampicillin (52). We hypothesise that the loss of pKPC might lead to an activation of VapC
464 resulting from the instability of VapB and a growth arrest contributing to the persistent state.
465 Therefore, pKPC loss would be under positive selection in the set-up we have used.
466 Interestingly, loss of the KPC-plasmid was previously observed in clinical KPC-Kp isolates
467 (57). Nevertheless, we could not rule out the possibility that the antibiotic stress contributed
468 also to plasmid loss. Among the diverse mutations identified not affecting IMP MIC, some
469 might have occurred by chance. However, they might also have been selected as contributing
470 to persistence or to an increased tolerance like mutation in the lysine tRNA synthetase lysS or
471 in the serine tRNA GCU.
472 In addition to mutants with similar MICs as the parental strains, we observed an extremely
473 broad range of mutations leading to increased MIC towards IMP, and in most cases also to
474 MEM. Resistant colonies could be classified according to their fitness based on their growth
475 rate as determined by ScanLag. Most isolates showing the less affected fitness (pattern A), were
476 affected in OM permeability. These mutations affected the porin *ompK36*, but also the Bam
477 system and the major chaperon involved in the insertion of OMP in the OM. We also observed
478 co-lateral effects of these mutations such as a hypermucoid phenotype for the *bamA* mutant.
479 Some mutations like regulatory mutants and mutations affecting LPS biosynthesis also likely
480 indirectly affected the OM permeability. On the other hand, mutations from the B pattern
481 showed a strong fitness cost and were reminiscent of small colony variants (SCV). SCV have
482 been described in a broad range of species and are frequently associated with a decreased
483 antibiotic susceptibility (58). However, there are only few reports of SCV in *K. pneumoniae*: in
484 a bone and joint infection (59) and associated with colistin HR in biofilm (60). In both cases,
485 the genetic bases for the SCV phenotype were not identified. As reported in other species, most
486 mutations we have characterized affected aerobic respiration (quinone and heme biosynthesis)
487 and the central metabolism (TCA cycle and glycolysis). Interestingly, both the slow growth and

488 the increased MICs were fully or partially reversed in anaerobic conditions (Table S5). The
489 combination of high resistance in the presence of oxygen and normal growth in its absence
490 might contribute to the selection of such mutation during treatment. However, due to their slow
491 growth under laboratory conditions, they might have been overlooked during diagnosis.
492 The increased MICs observed among HR colonies were shown to be frequently unstable and
493 lost following passages in antibiotic-free medium (9). For different bacteria / antibiotic pairs,
494 HR has been shown to result mainly from genomic amplification (61) which could revert by
495 homologous recombination. Here, we identified only three cases of amplification. The
496 duplication of the CTX-M-15 plasmid region carrying fitness functions might favour bacterial
497 survival and be selected among colonies from the C-pattern (persistent-like). The two other
498 amplifications affected chromosomal regions of colonies from A profile. In the strain AC376,
499 we observed a 89,584 bp duplication encompassing the *dcw* locus encoding major functions for
500 cell wall synthesis and cell division. The duplication corresponded to an ectopic copy/paste of
501 the region at position 688,936 and was stable (Fig. S1). The insertion was located in the *ygiW*
502 - *qseBC* intergenic region within *ygiW* ribosome binding site (RBS). Therefore the increased
503 resistance might result of the two events: genes duplication and modification of the expression
504 of *ygiW* or *qseBC*. In E. coli, QseBC is a pleiotropic TCS regulating mobility and biofilm
505 formation (62, 63). Interestingly, AC376 showed a 16-fold decrease of IMP susceptibility but
506 almost no effect on MEM susceptibility. This observation is in agreement with a previous study
507 showing that amplification of the *ftsQAZ* genes, part of the *dcw* locus, led to decreased
508 susceptibility to mecillinam, an antibiotic targeting exclusively PBP2 (64). Indeed, both IMP
509 and MEM have a high affinity to PBP2, but MEM has also some further affinity to PBP3 (48).
510 In this case, the amplification and the phenotype were stable.
511 For mutations leading to a high fitness cost, we observed reversion of the growth defect and of
512 the increased MICs. A typical case was strain AC90 from the A pattern, which showed a
513 decreased MIC compared to the parental strain and was mutated in both *cpxA* and in *cpxR*. The
514 *cpxA* mutation would have been first selected, leading to an hyperactivation of CpxR and in
515 turn among other effects to an over expression of *acrB*, *acrD* and *eefB* efflux systems genes
516 and a repression of the porin gene *ompK36* (41). The resulting decreased susceptibility to
517 carbapenems and aminoglycosides is associated with a high fitness cost. The secondary
518 mutation in *cpxR*, leading to an increased susceptibility compared to the parental strain,
519 suppresses the effect of the *cpxA* mutation and compensates for the high cost of the primary
520 mutation.
521

CONCLUSION

HR to IMP in KPC-Kp results from of a combination of the different means to escape bactericidal antibiotics: tolerance, persistence and resistance. The inter-strain variation is possibly due to the different genetic backgrounds, thus leading to different frequency of HR across the clinical isolates we analysed. The analysis of HR on solid media compared to liquid culture allows to address the diversity of phenotypes and genotypes of surviving bacteria. Although the majority of colonies did not show any genetic change compared to the parental strains, we selected mutations in a very broad range of functions considerably extending our knowledge of *K. pneumoniae* intrinsic ß-lactam resistome. We hypothesized that mutations affecting these functions might also contribute to IMP treatment failure in patients infected by KPC-Kp isolates.

ACKNOLEDGEMENTS

This work was supported by grants from the French National Research Agency (ANR-10-LABX-62-IBEID). Adriana Chiarelli is part of the Pasteur - Paris University (PPU) International PhD Program, with funding from the Institut Carnot Pasteur Microbes & Santé, and the European Union's Horizon 2020 research and innovation programme under the Marie Sklodowska-Curie grant agreement No 665807.

The authors thank Virgile Andrani and Gregory Bath for discussion on HR, Laurence Ma from the Institut Pasteur Biomics platform (C2RT, Institut Pasteur, Paris, France, supported by France Génomique, ANR-10-INBS-09-09 and IBISA) for her help in Illumina sequencing. We are grateful to Pr. Raymond Ruimy for providing two KPC-Kp isolates.

BIBLIOGRAPHY

1. Tacconelli E, Carrara E, Savoldi A, Harbarth S, Mendelson M, Monnet DL, Pulcini C, Kahlmeter G, Kluytmans J, Carmeli Y, Ouellette M, Outterson K, Patel J, Cavaleri M, Cox EM, Houchens CR, Grayson ML, Hansen P, Singh N, Theuretzbacher U, Magrini N. 2018. Discovery, research, and development of new antibiotics: the WHO priority list of antibiotic-resistant bacteria and tuberculosis. Lancet Infect Dis 18:318-327.
2. Nordmann P, Dortet L, Poirel L. 2012. Carbapenem resistance in Enterobacteriaceae: here is the storm! Trends Mol Med 18:263-72.
3. Munoz-Price LS, Poirel L, Bonomo RA, Schwaber MJ, Daikos GL, Cormican M, Cornaglia G, Garau J, Gniadkowski M, Hayden MK, Kumarasamy K, Livermore DM, Maya JJ, Nordmann P, Patel JB, Paterson DL, Pitout J, Villegas MV, Wang H,

Woodford N, Quinn JP. 2013. Clinical epidemiology of the global expansion of *Klebsiella pneumoniae* carbapenemases. Lancet Infect Dis 13:785-96.
4. Nordmann P, Cuzon G, Naas T. 2009. The real threat of *Klebsiella pneumoniae* carbapenemase-producing bacteria. Lancet Infect Dis 9:228-36.
5. Kowalska-Krochmal B, Dudek-Wicher R. 2021. The Minimum Inhibitory Concentration of Antibiotics: Methods, Interpretation, Clinical Relevance. Pathogens 10.
6. Dewachter L, Fauvart M, Michiels J. 2019. Bacterial Heterogeneity and Antibiotic Survival: Understanding and Combatting Persistence and Heteroresistance. Mol Cell 76:255-267.
7. Bódi Z, Farkas Z, Nevozhay D, Kalapis D, Lázár V, Csörgő B, Nyerges Á, Szamecz B, Fekete G, Papp B, Araújo H, Oliveira JL, Moura G, Santos MAS, Székely T, Jr., Balázsi G, Pál C. 2017. Phenotypic heterogeneity promotes adaptive evolution. PLoS Biol 15:e2000644.
8. El-Halfawy OM, Valvano MA. 2015. Antimicrobial heteroresistance: an emerging field in need of clarity. Clin Microbiol Rev 28:191-207.
9. Andersson DI, Nicoloff H, Hjort K. 2019. Mechanisms and clinical relevance of bacterial heteroresistance. Nat Rev Microbiol 17:479-496.
10. Band VI, Satola SW, Smith RD, Hufnagel DA, Bower C, Conley AB, Rishishwar L, Dale SE, Hardy DJ, Vargas RL, Dumyati G, Kainer MA, Phipps EC, Pierce R, Wilson LE, Sorensen M, Nilsson E, Jordan IK, Burd EM, Farley MM, Jacob JT, Ernst RK, Weiss DS. 2021. Colistin Heteroresistance Is Largely Undetected among Carbapenem-Resistant *Enterobacterales* in the United States. mBio 12.
11. Bardet L, Baron S, Leangapichart T, Okdah L, Diene SM, Rolain JM. 2017. Deciphering Heteroresistance to Colistin in a *Klebsiella pneumoniae* Isolate from Marseille, France. Antimicrob Agents Chemother 61.
12. Tan K, Nguyen J, Nguyen K, Huse HK, Nieberg PH, Wong-Beringer A. 2020. Prevalence of the carbapenem-heteroresistant phenotype among ESBL-producing Escherichia coli and Klebsiella pneumoniae clinical isolates. J Antimicrob Chemother 75:1506-1512.
13. López-Camacho E, Paño-Pardo JR, Sotillo A, Elías-López C, Martínez-Martínez L, Gómez-Gil R, Mingorance J. 2019. Meropenem heteroresistance in clinical isolates of OXA-48-producing *Klebsiella pneumoniae*. Diagn Microbiol Infect Dis 93:162-166.
14. Nodari CS, Ribeiro VB, Barth AL. 2015. Imipenem heteroresistance: high prevalence among Enterobacteriaceae *Klebsiella pneumoniae* carbapenemase producers. J Med Microbiol 64:124-126.
15. Pournaras S, Kristo I, Vrioni G, Ikonomidis A, Poulou A, Petropoulou D, Tsakris A. 2010. Characteristics of meropenem heteroresistance in *Klebsiella pneumoniae* carbapenemase (KPC)-producing clinical isolates of *K. pneumoniae*. J Clin Microbiol 48:2601-4.
16. Adams-Sapper S, Nolen S, Donzelli GF, Lal M, Chen K, Justo da Silva LH, Moreira BM, Riley LW. 2015. Rapid induction of high-level carbapenem resistance in heteroresistant KPC-producing Klebsiella pneumoniae. Antimicrob Agents Chemother 59:3281-9.
17. Adams-Sapper S, Gayoso A, Riley LW. 2018. Stress-Adaptive Responses Associated with High-Level Carbapenem Resistance in KPC-Producing *Klebsiella pneumoniae*. J Pathog 2018:3028290.
18. Levin-Reisman I, Gefen O, Fridman O, Ronin I, Shwa D, Sheftel H, Balaban NQ. 2010. Automated imaging with ScanLag reveals previously undetectable bacterial growth phenotypes. Nat Methods 7:737-9.

19. Levin-Reisman I, Fridman O, Balaban NQ. 2014. ScanLag: high-throughput quantification of colony growth and lag time. J Vis Exp doi:10.3791/51456.
20. Benaglia T, Chauveau D, Hunter DR, Young DS. 2010. mixtools: An R Package for Analyzing Mixture Models. Journal of Statistical Software 32.
21. Levin-Reisman I, Balaban NQ. 2016. Quantitative Measurements of Type I and Type II Persisters Using ScanLag. Methods Mol Biol 1333:75-81.
22. Wickham HS, Berlin, 2009). 2009. ggplot2: Elegant Graphics for Data Analysis. Springer, Berlin.
23. Chiarelli A, Cabanel N, Rosinski-Chupin I, Zongo PD, Naas T, Bonnin RA, Glaser P. 2020. Diversity of mucoid to non-mucoid switch among carbapenemase-producing *Klebsiella pneumoniae*. BMC Microbiol 20:325.
24. Bankevich A, Nurk S, Antipov D, Gurevich AA, Dvorkin M, Kulikov AS, Lesin VM, Nikolenko SI, Pham S, Prjibelski AD, Pyshkin AV, Sirotkin AV, Vyahhi N, Tesler G, Alekseyev MA, Pevzner PA. 2012. SPAdes: a new genome assembly algorithm and its applications to single-cell sequencing. J Comput Biol 19:455-77.
25. Koren S, Walenz BP, Berlin K, Miller JR, Bergman NH, Phillippy AM. 2017. Canu: scalable and accurate long-read assembly via adaptive k-mer weighting and repeat separation. Genome Res 27:722-736.
26. Hunt M, Silva ND, Otto TD, Parkhill J, Keane JA, Harris SR. 2015. Circlator: automated circularization of genome assemblies using long sequencing reads. Genome Biol 16:294.
27. Deatherage DE, Barrick JE. 2014. Identification of mutations in laboratory-evolved microbes from next-generation sequencing data using breseq. Methods Mol Biol 1151:165-88.
28. Milne I, Stephen G, Bayer M, Cock PJ, Pritchard L, Cardle L, Shaw PD, Marshall D. 2013. Using Tablet for visual exploration of second-generation sequencing data. Brief Bioinform 14:193-202.
29. Seemann T. 2014. Prokka: rapid prokaryotic genome annotation. Bioinformatics 30:2068-9.
30. Wyres KL, Nguyen TNT, Lam MMC, Judd LM, van Vinh Chau N, Dance DAB, Ip M, Karkey A, Ling CL, Miliya T, Newton PN, Lan NPH, Sengduangphachanh A, Turner P, Veeraraghavan B, Vinh PV, Vongsouvath M, Thomson NR, Baker S, Holt KE. 2020. Genomic surveillance for hypervirulence and multi-drug resistance in invasive *Klebsiella pneumonia*e from South and Southeast Asia. Genome Med 12:11.
31. Bortolaia V, Kaas RS, Ruppe E, Roberts MC, Schwarz S, Cattoir V, Philippon A, Allesoe RL, Rebelo AR, Florensa AF, Fagelhauer L, Chakraborty T, Neumann B, Werner G, Bender JK, Stingl K, Nguyen M, Coppens J, Xavier BB, Malhotra-Kumar S, Westh H, Pinholt M, Anjum MF, Duggett NA, Kempf I, Nykäsenoja S, Olkkola S, Wieczorek K, Amaro A, Clemente L, Mossong J, Losch S, Ragimbeau C, Lund O, Aarestrup FM. 2020. ResFinder 4.0 for predictions of phenotypes from genotypes. J Antimicrob Chemother doi:10.1093/jac/dkaa345.
32. Carattoli A, Zankari E, Garcia-Fernandez A, Voldby Larsen M, Lund O, Villa L, Moller Aarestrup F, Hasman H. 2014. In silico detection and typing of plasmids using PlasmidFinder and plasmid multilocus sequence typing. Antimicrob Agents Chemother 58:3895-903.
33. Varet H, Brillet-Guéguen L, Coppée JY, Dillies MA. 2016. SARTools: A DESeq2- and EdgeR-Based R Pipeline for Comprehensive Differential Analysis of RNA-Seq Data. PLoS One 11:e0157022.
34. Racine JS. 2012. RStudio: A Platform-Independent IDE for R and Sweave. Journal of Applied Econometrics 27:167-172.

35. Fajardo-Lubian A, Ben Zakour NL, Agyekum A, Qi Q, Iredell JR. 2019. Host adaptation and convergent evolution increases antibiotic resistance without loss of virulence in a major human pathogen. PLoS Pathog 15:e1007218.
36. Steward CD, Mohammed JM, Swenson JM, Stocker SA, Williams PP, Gaynes RP, McGowan JE, Jr., Tenover FC. 2003. Antimicrobial susceptibility testing of carbapenems: multicenter validity testing and accuracy levels of five antimicrobial test methods for detecting resistance in Enterobacteriaceae and Pseudomonas aeruginosa isolates. J Clin Microbiol 41:351-8.
37. Anderl JN, Zahller J, Roe F, Stewart PS. 2003. Role of nutrient limitation and stationary-phase existence in *Klebsiella pneumoniae* biofilm resistance to ampicillin and ciprofloxacin. Antimicrob Agents Chemother 47:1251-6.
38. Villa L, Feudi C, Fortini D, Brisse S, Passet V, Bonura C, Endimiani A, Mammina C, Ocampo AM, Jimenez JN, Doumith M, Woodford N, Hopkins K, Carattoli A. 2017. Diversity, virulence, and antimicrobial resistance of the KPC-producing *Klebsiella pneumoniae* ST307 clone. Microb Genom 3:e000110.
39. Hagan CL, Silhavy TJ, Kahne D. 2011. β-Barrel membrane protein assembly by the Bam complex. Annu Rev Biochem 80:189-210.
40. Denoncin K, Schwalm J, Vertommen D, Silhavy TJ, Collet JF. 2012. Dissecting the Escherichia coli periplasmic chaperone network using differential proteomics. Proteomics 12:1391-401.
41. Srinivasan VB, Vaidyanathan V, Mondal A, Rajamohan G. 2012. Role of the two component signal transduction system CpxAR in conferring cefepime and chloramphenicol resistance in *Klebsiella pneumoniae* NTUH-K2044. PLoS One 7:e33777.
42. Vogt SL, Raivio TL. 2012. Just scratching the surface: an expanding view of the Cpx envelope stress response. FEMS Microbiol Lett 326:2-11.
43. Zhang XS, García-Contreras R, Wood TK. 2007. YcfR (BhsA) influences *Escherichia coli* biofilm formation through stress response and surface hydrophobicity. J Bacteriol 189:3051-62.
44. Dulyayangkul P, Wan Nur Ismah WAK, Douglas EJA, Avison MB. 2020. Mutation of kvrA Causes OmpK35 and OmpK36 Porin Downregulation and Reduced Meropenem-Vaborbactam Susceptibility in KPC-Producing *Klebsiella pneumoniae*. Antimicrob Agents Chemother 64.
45. Kneidinger B, Marolda C, Graninger M, Zamyatina A, McArthur F, Kosma P, Valvano MA, Messner P. 2002. Biosynthesis pathway of ADP-L-glycero-beta-D-manno-heptose in Escherichia coli. J Bacteriol 184:363-9.
46. Thulin E, Sundqvist M, Andersson DI. 2015. Amdinocillin (Mecillinam) resistance mutations in clinical isolates and laboratory-selected mutants of *Escherichia coli*. Antimicrob Agents Chemother 59:1718-27.
47. Bassetti M, Peghin M. 2020. How to manage KPC infections. Ther Adv Infect Dis 7:2049936120912049.
48. Sumita Y, Fukasawa M, Okuda T. 1990. Comparison of two carbapenems, SM-7338 and imipenem: affinities for penicillin-binding proteins and morphological changes. J Antibiot (Tokyo) 43:314-20.
49. Zhanel GG, Wiebe R, Dilay L, Thomson K, Rubinstein E, Hoban DJ, Noreddin AM, Karlowsky JA. 2007. Comparative review of the carbapenems. Drugs 67:1027-52.
50. Nickolai DJ, Lammel CJ, Byford BA, Morris JH, Kaplan EB, Hadley WK, Brooks GF. 1985. Effects of storage temperature and pH on the stability of eleven beta-lactam antibiotics in MIC trays. J Clin Microbiol 21:366-70.

51. Wang P, Robert L, Pelletier J, Dang WL, Taddei F, Wright A, Jun S. 2010. Robust growth of Escherichia coli. Curr Biol 20:1099-103.
52. Fridman O, Goldberg A, Ronin I, Shoresh N, Balaban NQ. 2014. Optimization of lag time underlies antibiotic tolerance in evolved bacterial populations. Nature 513:418-21.
53. Levin-Reisman I, Brauner A, Ronin I, Balaban NQ. 2019. Epistasis between antibiotic tolerance, persistence, and resistance mutations. Proc Natl Acad Sci U S A 116:14734-14739.
54. Levin-Reisman I, Ronin I, Gefen O, Braniss I, Shoresh N, Balaban NQ. 2017. Antibiotic tolerance facilitates the evolution of resistance. Science 355:826-830.
55. Winther KS, Gerdes K. 2011. Enteric virulence associated protein VapC inhibits translation by cleavage of initiator tRNA. Proc Natl Acad Sci U S A 108:7403-7.
56. Gerdes K, Maisonneuve E. 2012. Bacterial persistence and toxin-antitoxin loci. Annu Rev Microbiol 66:103-23.
57. Jousset AB, Bonnin RA, Takissian J, Girlich D, Mihaila L, Cabanel N, Dortet L, Glaser P, Naas T. 2020. Concomitant carriage of KPC-producing and non-KPC-producing *Klebsiella pneumoniae* ST512 within a single patient. J Antimicrob Chemother 75:2087-2092.
58. Proctor RA, von Eiff C, Kahl BC, Becker K, McNamara P, Herrmann M, Peters G. 2006. Small colony variants: a pathogenic form of bacteria that facilitates persistent and recurrent infections. Nat Rev Microbiol 4:295-305.
59. Ronde-Oustau C, Lustig S, Dupieux C, Ferry T. 2017. Implant-associated ESBL-*Klebsiella pneumonia* producing small colony variant bone and joint infection in a healthy 40-year-old man. BMJ Case Rep 2017.
60. Silva A, Sousa AM, Alves D, Lourenço A, Pereira MO. 2016. Heteroresistance to colistin in Klebsiella pneumoniae is triggered by small colony variants sub-populations within biofilms. Pathog Dis 74.
61. Nicoloff H, Hjort K, Levin BR, Andersson DI. 2019. The high prevalence of antibiotic heteroresistance in pathogenic bacteria is mainly caused by gene amplification. Nat Microbiol 4:504-514.
62. Sperandio V, Torres AG, Kaper JB. 2002. Quorum sensing *Escherichia coli* regulators B and C (QseBC): a novel two-component regulatory system involved in the regulation of flagella and motility by quorum sensing in E. coli. Mol Microbiol 43:809-21.
63. González Barrios AF, Zuo R, Hashimoto Y, Yang L, Bentley WE, Wood TK. 2006. Autoinducer 2 controls biofilm formation in *Escherichia coli* through a novel motility quorum-sensing regulator (MqsR, B3022). J Bacteriol 188:305-16.
64. Vinella D, Cashel M, D'Ari R. 2000. Selected amplification of the cell division genes *ftsQ-ftsA-ftsZ* in *Escherichia coli*. Genetics 156:1483-92.

FIGURE LEGENDS

Fig 1. Diversity of resistance and heteroresistance among 62 KPC-KP clinical isolates. A. Carbapenem susceptibility levels of CPKp isolates. SIR = Susceptible/Intermediate/Resistant (S: MIC ≤ 1 mg/L; I: 1 mg/L < MIC ≤ 4 mg/L; R: MIC > 4 mg/L). Dark grey for imipenem (IMP) and light grey for meropenem (MEM); **B**. Visualization of the HR profiles by Etest. Three different categories were distinguished; HR, Moderate HR and No HR. Isolates that showed full contact with the antibiotic strip were excluded from further analyses; **C**. Occurrence of HR among KPC-Kp isolates. Dark grey for IMP and light grey for MEM. Yes stands for HR and moderate HR isolate and No for its absence; **D.** Association between HR profile and the type of KPC carbapenemase. Red bar stands for KPC-2 and green for KPC-3. The percentage within the bar was only indicated when higher in one KPC variant compared to the other.

Fig 2. Population analysis profiling (PAP) of 13 CPKp clinical isolates. Results were expressed in CFU/ml. 0 correspond to untreated population. 4-FOLD, 8-FOLD, 10-FOLD stand for four, eight and ten times the concentration of IMP relative to the MIC of the isolate as determined by Etest. Isolate names are indicated at the top of each chart. Data were calculated from at least three independent experiments. **p*-values ranging from 0.011 to 0.047; ** *p*-value ranging from 0.002 to 0.0044; *** *p*-value = 0.00053; ****p-value = 4,6 x 10^{-6};

Fig 3. Heterogeneous survival of KPC-Kp to high concentrations of IMP as detected by ScanLag. Colony appearance time was monitored every 20 minute over 48-hours incubation on plate. ToA = Time of Appearance; CDF = cumulative distribution function; Lag time extension = delay in growth relative to untreated colonies; EP = exponential phase, SP = stationary phase; N1 = subpopulation 1 (the first apearing peak of ToA distributions) and N2 = subpopulation 2 (colonies forming the tails of ToA distributions). **A**. Histograms of single-colony time of appearances from EP cultures. Green bars represent colonies appearing on drug-free media, whereas red bars indicate colonies growing onto IMP-containing agar plates. The data are an overlap of at least three independent replicates per each isolate and each condition. **B**. Same data as in A) but shown as a CDF of ToA. Represented as such, ToA distributions data provide information on the delay in growth of each isolate relative to the untreated cells. **C**. Fit of two-mixture component model to the distributions of ToA per each isolates in EP. In orange, population 1 (N1), and in blue population 2 (N2). The representation is an overlap of at least

three independent replicates per each isolate and each condition. Estimated parameters of each subgroup per each replicate are given in Table S2. Note that, for BIC-1, the model failed to fit a normal distribution to the tail. **D.** Comparison of Lag Time Extension (LE) of N1 subpopulations relative to drug-free condition from the six isolates between EP and SP cultures. Only significant differences were highlighted (* corresponds to p-value = 0.033 , ** corresponds to p-value = 0.0025). LE was calculated as the mean ToA value of N1 subpopulation over the mean ToA value of untreated population. **E**. Frequency of subpopulations calculated according to the methodology previously proposed (21) from at least three replicates (data are available in Table S2). All the colonies appearing after the cutoff value (calculated as ToA > $\mu+3\Sigma$, where μ= estimated ToA mean for N1 and Σ = estimated standard deviations) are defined as persisters. Frequency of colonies appearing before the cutoff (ToA < $\mu+3\Sigma$) are shown in the left panel. Frequencies were calculated as the proportion of CFU/ml of each subpopulation over the total number of CFU/ml of the initial inoculum.

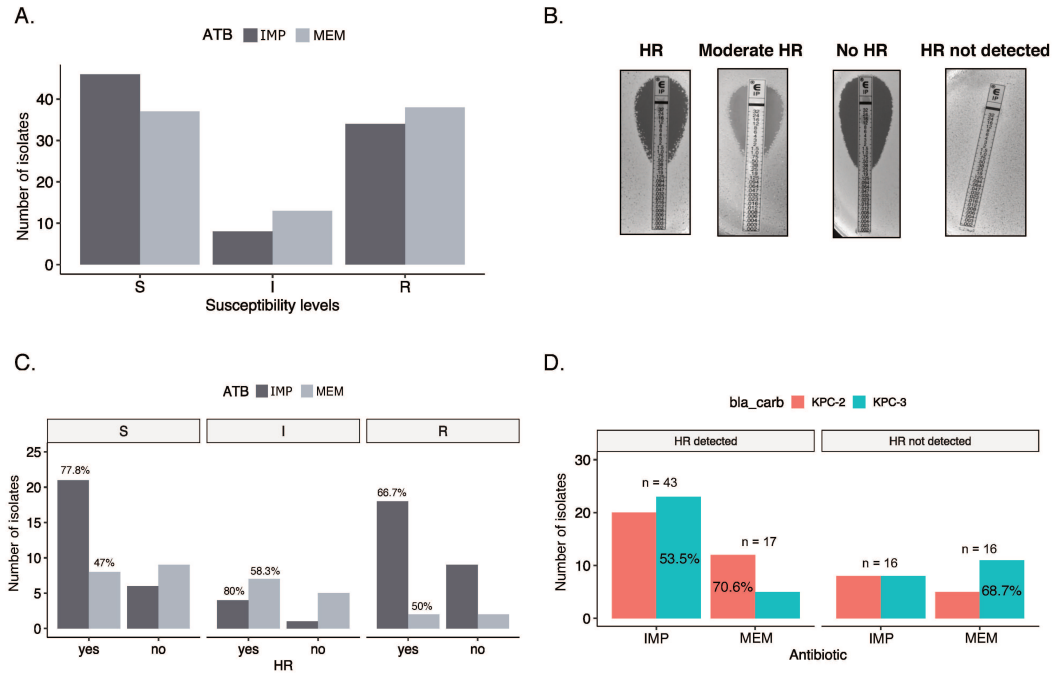
A.
ATB IMP MEM
Number of isolates
Susceptibility levels
S
I
R
B.
HR
Moderate HR
No HR
HR not detected
C.
ATB IMP MEM
S
I
R
77.8%
47%
80%
58.3%
66.7%
50%
yes
no
HR
D.
bla_carb KPC-2 KPC-3
HR detected
HR not detected
n = 43
53.5%
n = 17
70.6%
n = 16
n = 16
68.7%
IMP
MEM
Antibiotic

Fig.1

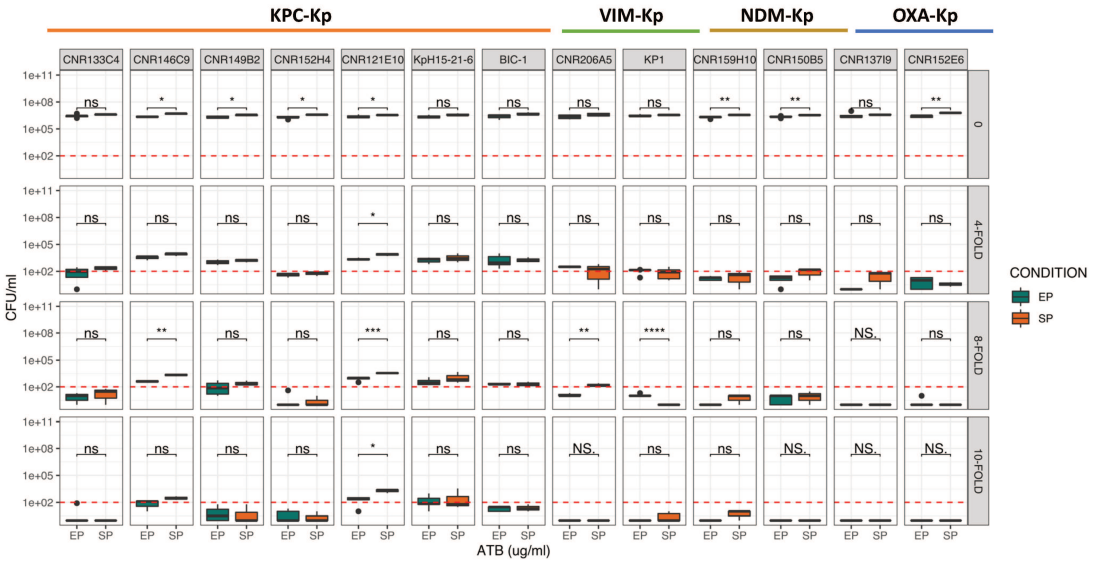
KPC-Kp
VIM-Kp
NDM-Kp
OXA-Kp
CNR133C4
CNR146C9
CNR149B2
CNR152H4
CNR121E10
KpH15-21-6
BIC-1
CNR206A5
KP1
CNR159H10
CNR150B5
CNR137I9
CNR152E6
CFU/ml
0
4-FOLD
8-FOLD
10-FOLD
CONDITION
EP
SP
ATB (ug/ml)

Fig.2

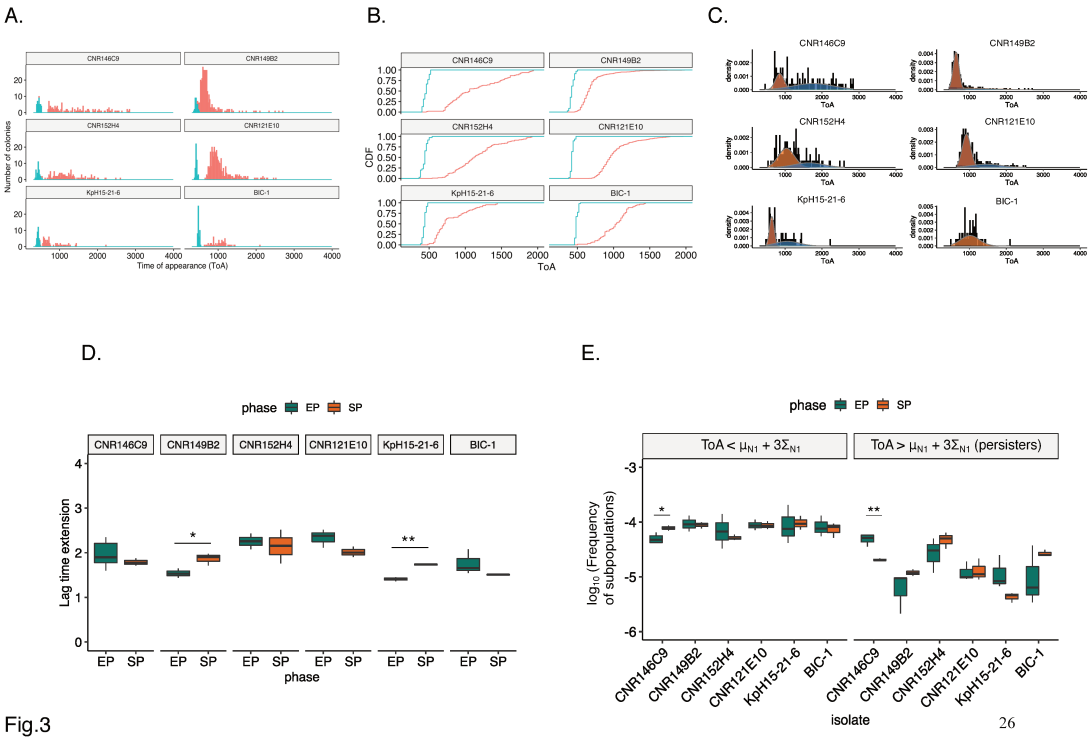
A.
B.
C.
CNR146C9
CNR149B2
CNR152H4
CNR121E10
KpH15-21-6
BIC-1
Number of colonies
Time of appearance (ToA)
CDF
ToA
density
D.
E.
phase
EP
SP
Lag time extension
ToA < μN1 + 3ΣN1
ToA > μN1 + 3ΣN1 (persisters)
log10 (Frequency of subpopulations)
isolate

Fig.3

SUPPLEMENTARY MATERIAL

Table S1. *Klebsiella pneumoniae* isolates analyzed in this study. (Excel file)

Genome sequences were annotated by using Kleborate. For HR, 0, 1 and 2 mean not HR by Etest, weakly HR and HR respectively. MIC for IMP and MEM were determined by Etest not considering HR colonies. Isolates coloured in green were analysed by PAP and those in blue by PAP and by ScanLag. Antibiotic abreviations are as follow: AGly, aminoglycoside; Col, colistin, Fcyn, fosfomycin, Flq fluoroquinolone, MLS, Macrolide, lincosamide and streptogramin; Phe, phenicol, Rif, rifamycin, Sul, sulphonamide; Tet, tetracycline, Tmt, trimethoprime, Bla, ß-lactamase.

Table S2. Ssummary of ScanLag quantittative values (Excel file)

*The value indicates the mean of Time of Appearance (ToA) for at least three replicates. $N = type of population. N0 = untreated; N1 = treated, corresponding to the Gaussian peak; N2 = treated, corresponding to late appearing colonies

&Parameters estimated by fitting the data to the two-component mixture model. λ = Estimated percentage per each group; μ = mean ToA value; Σ = standard deviation.

Table S3: CNR146C9 chromosome, plasmids and antibiotic resistance genes

		Chromosome	pCTX-M-15	pKPC	Circular phage
replicon			IncFIB/IncFII	IncFIB(pQil) /IncFII	Phage
size (base pairs)		5,351,626	237,007	110,489	52608
ARG	Aminoglycoside		aac(6')-Ib-cr aac(3)-IIa aph(3'')-Ib aph(6)-Id		
	ß-lactam	*bla*$_{SHV-28}$*	*bla*$_{TEM-1B}$ *bla*$_{OXA-1}$ *bla*$_{CTX-M-15}$	*bla*$_{TEM-1A}$ *bla*$_{KPC-3}$ *bla*$_{OXA-9}$	
	Fluoroquinolone	*oqxA* *oqxB*	*qnrB1*		
	Fosfomycin	*fosA*			
	Phenicol		*catB2*		
	Sulfonamide		*sul2*		
	Trimethoprim		*dfrA14*		

* SHV-28 like;

Table S4. Genetic events among pattern A colonies

Colony	[&]Genetic events	Gene, name, orientation and annotation	Category	[$#]IMP	[$#]MEM
AC150-A	pCTXM; tra region deletion		Loss of genetic material	0.5	0.75
AC179-A	pCTXM; tra region deletion		Loss of genetic material	0.5	0.75
AC176-A	pCTXM; tra region deletion		Loss of genetic material	0.5	0.75
AC8-A	Loss of the circular phage		Loss of genetic material	0.5	0.75
AC-143-A	Loss of the circular phage		Loss of genetic material	0.5	1
AC-15-A	Loss of the circular phage IS*Kpn25* insertion	Intergenic, tRNA-Asp/dnaQ ← (DNA polymerase III subunit epsilon 23% of the reads)	Loss of genetic material Protein synthesis/DNA replication	0.5	0.75
AC-16-A	Loss of the circular phage Circularization of an integrated prophage - pos: 1493 - 1533 kb (29% of the reads)		Loss of genetic material	0.5	1
AC-18-A	Loss of the circular phage		Loss of genetic material	0.5	1
AC-24-A	Loss of the circular phage		Loss of genetic material	0.5	1
AC200-A	Loss of the circular phage		Loss of genetic material	0.5	1
AC216-A	Loss of the circular phage		Loss of genetic material	0.75	1
AC239-A	Loss of the circular phage		Loss of genetic material	0.75	1
AC318-A	Loss of the circular phage		Loss of genetic material	0.5	0.75
AC340-A	Loss of the circular phage		Loss of genetic material	0.5	0.75
AC4-A	Loss of the circular phage		Loss of genetic material	0.75	0.5
AC309-A	A -> G; intergenic, synonymous	JGOJPJMA_03113	Unknown	0.75	1
AC196-A	W77C (TGG→TGC	JGOJPJMA_03620 → Membrane protein of unknown function, upstream the *ramA* regulatory gene	Unknown	0.5	0.5
AC244-A	G107G (GGT→GGG)	*argP_3* ← LysR regulatory protein	Other function	0.75	1
AC6-A	K2E (AAA→GAA)	*ompC* → Porin OmpK36	Outer membrane	>32	>32
AC149-A	L305P (CTG→CCG)	*ompC* → Porin OmpK36	Outer membrane	>32	>32
AC1-A	T259P (ACC→CCC)	*ompC* → Porin OmpK36	Outer membrane	>32	>32
AC175-A	N448Y (AAC→TAC)	*bamA* ← Outer membrane protein assembly factor	Outer membrane	>32	>32
AC88-A	+T, coding coding (656/1179 nt)	*bamB* → Outer membrane protein assembly factor	Outer membrane	6	8
AC148-A	Q381* (CAG→TAG)	*bamB* → Outer membrane protein assembly factor	Outer membrane	4	6
AC294-A	32 bp duplication (582/1179 nt);	*bamB* → Outer membrane protein assembly factor	Outer membrane	6	8
AC50-A	T55I (ACC→ATC)	*comR* → regulator of *ycfS* (OMP)	Outer membrane (regulator)	1.5	2
AC90-A	Δ12 bp	*cpxA* → Sensor Histidine Kinase, cell envelope stress response	Outer membrane (regulator)	0.38 [$](12)	0.5 [$](3)
	R205W (CGG→TGG)	*cpxR* → *Regulator,* cell envelope stress response	Outer membrane (regulator)		

AC-72-A	intergenic (+49/‑6);intergenic (+149/+1658)	*lptD/surA* (*surA* encodes a chaperon); *JGOJPJMA_05345/xerC_4*	Outer membrane	3	6
AC41-A	Δ10 bp	*JGOJPJMA_01704* → upstream *rfbD* dTDP-4-dehydrorhamnose reductase	LPS biosynthesis	2	2
AC-14-A	P148L (CCC→CTC)	*cdh* → CDP-diacylglycerol pyrophosphatase	LPS biosynthesis	1	0.75
AC18b-A	A54P (GCC→CCC)	*lpxC* ← UDP-3-O-acyl-N-acetylglucosamine deacetylase	LPS biosynthesis	0.75	0.5
AC-57-A	K186K (AAA→AAG)	*pglA* → *mixed reads Glycosyl transferase*	LPS biosynthesis operon	0.5	1
AC151-A	V64E (GTG→GAG)	*slyA (kvrA)* → Pleiotropic transcriptional regulator	capsule production (regulator)	3	1.5
AC161-A	D203E (GAT→GAG);	*JGOJPJMA_01692 pglI* → Glycosyl transferase caspsule operon	Capsule	0.75	1
	D93H (GAC→CAC)	*ndmA* → Methylxanthine N1‑demethylase NdmA 2Fe-2S-binding protein	Metabolism		
AC376-A	chromosomal amplification 4389225 – 4478809	amplification of a region including the *dcw* locus	Cell envelope	16	0.75
AC201-A	C79Y (TGC→TAC)	*lipA* → Lipoyl synthase	Central metabolism	4	2
AC67-A	Δ48 bp	*trpA* → tryptophan synthase gene	Metabolism	0.75	1
AC24-A	E381* (GAA→TAA);	*lysS* → Lys tRNA ligase	Protein synthesis	0.5	0.75
	D93H (GAC→CAC)	*JGOJPJMA_03417* →	Unknown		
AC207-A	Q226E (CAG→GAG)	*rpsC* →	Protein synthesis	0.5	1
AC-114-A	Amplification between posittion 3148 kb and 3617 kb Kb(2 ISKpn1)			0.75	1.5

Only isolates showing a genetic defect or modified MICs to IMP or MEM are shown. [&]As determined by Breseq. [#]MIC in mg/L, [$]MIC of the isolate only mutated in *cpxA*

Table S5. Genetic events among pattern B colonies

Colony	[&]Genetic events	Gene, name, orientation and annotation	Category	[$#]IMP	[$#]MEM
AC-91-B	V45G (GTG→GGG)	*hemA* → *Glutamyl-tRNA reductase*	Respiration	32 (3)	6 (2)
AC-125-B	D191A (GAT→GCT)	*ubiA* ← 4-hydroxybenzoate octaprenyltransferase	Respiration	8 (1,5)	4 (1)
AC192-B	(AGCGCC)2→1 in coding (372‑377/867 nt)	*ubiA* ←*4-hydroxybenzoate octaprenyltransferase*	Respiration	8 (0.5)	3 (0.5)
AC26-B	D93H (GAC→CAC);	*JGOJPJMA_03417* → Unknown	Unknown	SLOW GROWING	SLOW GROWING
	Δ10 bp coding (776‑785/1641 nt	*ubiB* ← Probable protein kinase	Respiration		
AC301-B	Δ131 bp	*ubiB* ← Probable protein kina*se*	Respiration	6 (0.5)	2 (0.75)
AC167-B	+C; coding (555/900 nt)	*ispA* → Farnesyl diphosphate synthase	Respiration	6 (0.5)	2 (0.25)
AC19-B	Δ42 bp coding (483‑524/900 nt)	*ispA* → Farnesyl diphosphate synthase	Respiration	6 (0.5)	2 (0.25)
AC20-B	Δ42 bp coding (483‑524/900 nt)	*ispA* → Farnesyl diphosphate synthase	Respiration	6 (0.5)	2 (0.25)
AC169-B	W158* (TGG→TAG)	*ubiD* → 3-octaprenyl-4-hydroxybenzoate carboxy-lyase	Respiration	8 (0.5)	4 (0.25)
AC289-B	L147Q (CTG→CAG)	*hldE* → bi-functional enzyme LPS	LPS	4(2)	4 (2)
AC78-B	(T)8_9;	*tuaB* → flippase	Capsul	1.5	1.5
AC413-B	(G)6→5 (deletion of one base) in coding	*acnB* ← Aconitate hydratase B	Central metabolism	12 (0.38)	2 (0.38)
AC-17-B	A516V (GCC→GTC)	*acnB* ← Aconitate hydratase B	Central	>32 (0.5)	8 (1)
AC-53-B	Δ4,660 bp at pos 4,417,453	deletion of *JGOJPJMA_04159, JGOJPJMA_0416, lpdA, Dihydrolipoyl dehydrogenase, aceF Dihydrolipoyllysine-residue*	Central metabolism	4 (0.38)	2 (0.25)
AC428-B	Δ12 bp	*icd* ← isocitrate dehydrogenase TCA	Central	6 (0.5)	1 (0.25)
AC208-B	Δ1 bp coding (3/1251 nt)	*icd* ← *isocitrate dehydrogenase TCA*	Central	8 (0.38)	4 (0.25)
AC202-B	coding (1136/1728 nt) duplication of 8 codons	*ptsI* ← PEP‑protein phosphotransferase enzyme 1	central metabolism	1 (0.38)	2 (0.25)
AC366-B	R345P (CGT→CCT)	*fbaA_1* fructose bi-phosphate aldolase	Central	0.5	0.75
AC23-B	D93H (GAC→CAC);	*JGOJPJMA_03417* → Unknown	Unknown	4	0.5
	Q30L (CAG→CTG)	*cysB* ← Transcriptional regulator	AA Metabolism -		
AC234-B	L335Q (CTG→CAG)	*malP_6* →	Sugar	0.75	0.75
AC17-B	P203L (CCT→CTT)	*pgpC* →	Membrane	>32	6
AC315-B	Δ1 bp	*polB* DNA polymerase II	DNA synthesis	0.38	0.5
AC274-B	L309Q (CTG→CAG)	*frlB_2* Glucose lysine‑6‑phosphate	Sugar	0.75	0.75
AC246-B	E312K (GAA→AAA)	*purM* ← Phosphoribosylformylglycinamidine	Nucleotide metabolism	0.75	0.5
AC171-B	C→A,	*JGOJPJMA_01085* → tRNAser(gct)	Protein	2	2
AC195-B	C->T; intergenic (+22/‑3)	*nlpA* → Lipoprotein 28 / → JGOJPJMA_00080 unknown		4	2
AC35-B	none detected			3	4

Only isolates showing a genetic defect or modified MICs to IMP or MEM are shown. [&]As determined by Breseq. [#]MIC in mg/L, [$]MIC in anaerobic conditions.

Table S6. Genetic events among pattern C colonies

Colony	[&]Genetic events	Gene, name, orientation and annotation	Category	[#]IMP	[#]MEM
AC-86-C	Loss of pKPC		Loss of genetic material	0.19	0.023
AC127-C	Loss of pKPC		Loss of genetic material	0.19	0.023
AC133-C	Loss of pKPC		Loss of genetic material	0.19	0.023
AC218-C	Loss of pKPC		Loss of genetic material	0.19	0.023
AC266-C	Loss of pKPC		Loss of genetic material	0.19	0.023
AC417-C	Loss of pKPC		Loss of genetic material	0.19	0.023
AC418-C	Loss of pKPC		Loss of genetic material	0.19	0.023
AC420-C	Loss of pKPC		Loss of genetic material	0.19	0.023
AC421-C	Loss of pKPC		Loss of genetic material	0.19	0.023
AC-76-C	Loss of pKPC		Loss of genetic material	0.19	0.023
	M217I (ATG→ATT)	*dhaR* → regulator	Central metabolism	0.19	0.023
	N375D (AAC→GAC)	JGOJPJMA_05212 → unknown	Unknown	0.19	0.023
AC378-C	Loss of the circular phage		Loss of genetic material	0.5	0.75
AC160-C	Loss of the circular phage		Loss of genetic material	0.5	0.75
AC272-C	Loss of the circular phage		Loss of genetic material	0.5	0.75
AC331-C	Loss of the circular phage		Loss of genetic material	0.5	0.75
AC327-C	C→T intergenic (‑22/+11)2	JGOJPJMA_04049 tRNA-Asp ← / ← dnaQ (DNA polymerase III	Protein synthesis/DNA synthesis	0.5	0.75
AC362-C	pCTXM: amplification	amplification between two IS*5075* at 26.731 kb to 75986 Include the glycogen synthase operon, the *fec*	Adaptive function	0.5	0.75
AC158-C	N196T (AAC→ACC)	JGOJPJMA_05425 ← hypotethical	Unknown	0.5	0.75
	Δ39,533 bp (chromosomal prophage) at pos 1,493,544		Loss of genetic material	0.5	0.75
AC211-C	T->C; intergenic (‑247/+183)	thpA_2 ←ABC transporter / ← JGOJPJMA_03681	Sugar metabolism	0.5	1
AC126-C	W252* (TGG→TAG)	JGOJPJMA_01977 → type VI secretion system TssG	Adaptive function	0.5	0.75

Only isolates showing a genetic defect or modified MICs to IMP or MEM are shown. [&]As determined by Breseq

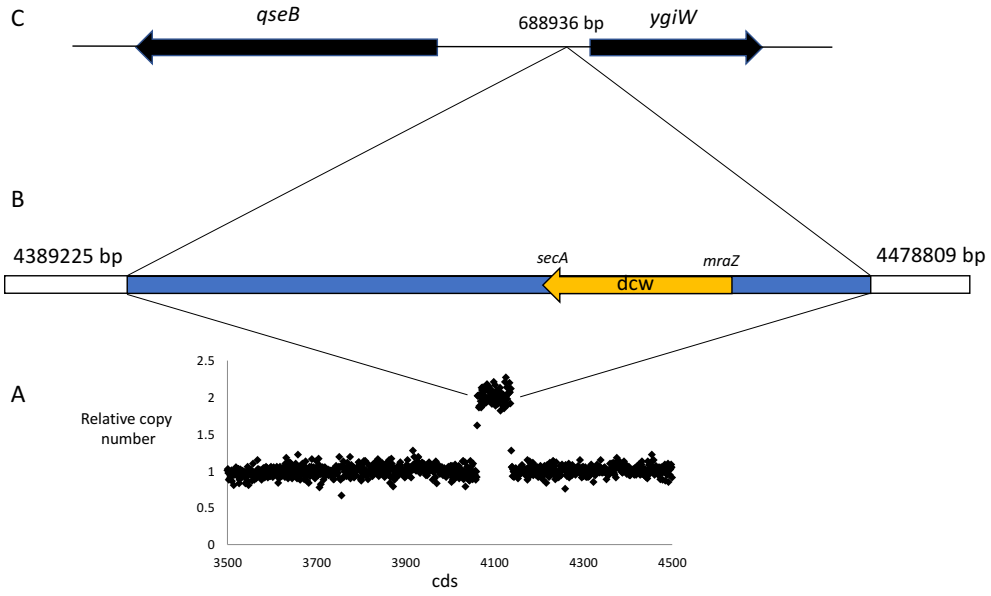

Fig. S1: *Duplication of a 89584 bp region in strain AC 376*. A. Relative copy number estimate compared to the parental stain CNR146C9 based on the count of number of reads per gene. B. Duplicated region in blue. It contains as remarkable *loci* the division and cell wall (dcw) locus in orange, C. Insertion site of the duplicated copy 11 bp upstream *ygiW* with a 5 bp (GAGAA) duplication. *ygiW* expression is activated by the two component regulatory system QseBC. Limits of the duplicated region and insertion sites were deduced from chimeric reads as identified by using Breseq.

V. Discussion

When I applied for the PhD fellowship at the Institut Pasteur, heteroresistance (HR) was to me a fascinating yet complex (and rather mysterious) topic. I was surprised by the diversity of notions attributed to HR, the lack of defined methods for its characterization and how this complex phenomenon involving multiple bacterial species, several antibiotics, and diverse mechanisms has been generalized. Two published reviews (Andersson et al., 2019; El-Halfawy and Valvano, 2015) have helped to shed light on the field.

In *Klebsiella pneumoniae*, HR is widely observed with last-resort drugs such as colistin and carbapenems; while for colistin there are some reports available, identifying mutations responsible for the high resistance levels, for carbapenem HR few cases have been reported and most of them only describe the phenomenon. Authors often mention that carbapenem HR in *K. pneumoniae* is mostly observed with carbapenemase-producing (CPKp), and more specifically, with KPC-Kp isolates (Nodari et al., 2015).

With my PhD project, we aimed at investigating whether HR towards carbapenems was a frequent phenomenon among CPKp clinical isolates, with the hope of shedding light on aspects that might contribute to treatment failure. CPKp are mainly found in hospitals, thus people who get infected with these isolates are often immunocompromised. Ensuring a correct pathogen identification and diagnosis is then fundamental to reduce mortality rates and promote positive treatment outcome. The HR phenotype might challenge the classification of susceptibility levels and lead to inappropriate treatment choices, later responsible for inefficacy of antibiotics in the patient.

When we collected the CPKp clinical isolates, the first goal was to assess the purity of these isolates, to avoid misinterpretation of susceptibility levels and thus HR, due to contamination. In the beginning, while screening these isolates, I noticed heterogeneous colony appearance for some of them, which, at first, I had considered as result of a contamination; however, when I finalized the screening, I realized that this heterogeneity was frequent among the collected isolates. This observation prompted me to go further in the characterization of these diverse colony variants, which overall would appear either as translucent non-mucoid or opaque mucoid (Figure 20).

Since the main objective of my PhD project was to characterize heterogeneity of resistance among CPKp and possibly, to unveil the underlying mechanistic reasons, I hypothesized that such variation on plate might be one factor contributing to HR to carbapenems.

However, the model we chose to investigate was rather challenging, due to the possible contribution to the phenotype of multiple aspects such as the hydrolysing activity of the carbapenemase (not only in the periplasmic space, but also upon release in the culture medium), instability of the IMP and inoculum size, in addition to putative genetic and non-

genetic survival strategies adopted by the bacteria to survive. HR is mainly visualized in agar-based cultures, thus the use of ScanLag appeared as the best compromise to investigate HR in CPKp clinical isolates. By monitoring the dynamics bacterial growth of KPC-Kp with high concentrations of IMP at single colony level, we revealed heterogeneity in the surviving subpopulations, encompassing different strategies known to counteract the bactericidal activity of drugs.

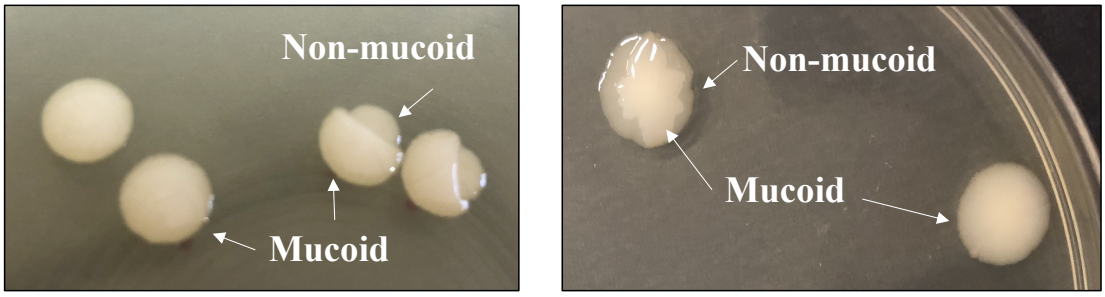

Figure 20. Examples of the two colony variants appearing on the same plate.

Colony heterogeneity denotes frequent variation in capsule content among CPKp mainly due to capsule genes inactivation

Microbial populations are often encountering a multitude of diverse niches in the environment and within the host. To cope with challenging conditions, specialized bacterial structures together with genetic and non-genetic strategies contributing to phenotypic diversification and maximizing the likelihood of survival. Among the specialized structures that bacteria use to defend themselves from external aggressions, the capsule (CPS) is a major defence mechanism (Bengoechea and Sa Pessoa, 2019). Half of the bacterial species produces capsules (Rendueles et al., 2017), which provide protection from host immune system and antibiotic exposure and thereby supports survival in challenging environments. A great portion of these cell-surface polysaccharides is produced via the Wzx/Wzy-dependent assembly pathway. The genes responsible for capsule synthesis are organized into an operon, with conserved functions and organization and a diverse repertoire of glycosyltransferase genes (Wyres et al., 2016). Different serotypes – corresponding to the combination of different units of oligosaccharides – have been characterized, even within the same species, resulting of a remarkable genetic diversity of the capsule loci. Species encoding multiple capsules were shown to have larger environmental breadths than other species (Rendueles et al., 2017). The wide diversity of capsules observed amongst *K. pneumoniae* isolates might thus indicate the broad flexibility of this species complex and the potential to adapt to various niches and increase its host range.

CPS production is also dependent on the bacterial physiological state. The highest *in vitro* amount of CPS is produced during the early logarithmic phase, whereas aged bacterial cultures have been associated with the emergence of non-capsulated clones (Mengistu et al.,

1994). Typically, the switches from mucoid to non-mucoid colony aspect are indicative of variation in the CPS production. Under laboratory conditions, clinical isolates of *K. pneumoniae* may exhibit heterogeneous colony aspect, depending on medium, time and temperature of incubation (Tipton et al., 2015). If overlooked, these mixed variants may be stored and transferred across clinical laboratories, ultimately leading to phenotypic misinterpretations of clinical isolates.

The use of solid media in the routine laboratory practice is still invaluable, cost-effective, and easy to perform. Compared to liquid cultures, where the bulk populations' response to different agents can be assessed quite efficiently, solid media provide the advantage of detecting phenotypic variations that may suggest heterogeneity within seemingly isogenic populations. Indeed, by meticulously observing colony formation on solid media, we could predict diversity within the CPKp populations. By monitoring bacterial cultures on solid media for a three-days period, we showed that *in vitro* switch from mucoid to non-mucoid colony appearance across eight clinical CPKp isolates occurred at various frequencies, depending on the isolate. The simple observation of heterogeneous colony aspect thus prompted me in pursuing further with our analysis, which integrated phenotypic characterization of the colony variants and whole genome sequencing.

We showed that this phenotypic diversity resulted from alterations in the CPS content, mostly relying on mutations occurring at the capsule (*cps*) locus, despite the complex regulatory network of capsule synthesis identified in *K. pneumoniae* (Dorman et al., 2018; Mike et al., 2021). The sole detection of mutations occurring at the *cps* locus may be explained by a selective advantage for growth provided by these alterations under our experimental conditions. Similar to what we observed, extended incubation of *K. pneumoniae* species complex isolates in rich laboratory media (LB) led to the appearance of spontaneous non-capsulated mutants (Buffet et al., 2021). Conversely, capsule production was selected for in poor media, providing a significant fitness advantage. These findings, together with ours, suggest that maintenance of CPS *in vitro* is dependent on nutritional availability. The assembly of the extracellular layer is energy-consuming, and it involves genes from several essential cellular processes including Tricarboxylic Acid Cycle (TCA cycle), pyruvate metabolism, and cellular energetics (Mike et al., 2021). Therefore, producing a capsule may pose a fitness disadvantage in more stringent environments, where the cellular energy is deployed for ensuring bacterial survival.

Capsule production is definitely an advantageous trait for *K. pneumoniae* clinical isolates during an infection, especially in the case of invasive infections (Ernst et al., 2020). Nevertheless, capsules were reported to be more abundant among environmental isolates rather than among pathogenic bacteria (Rendueles et al., 2017), suggesting that the capsule might support the persistence of bacterial populations across various environmental niches but differential CPS expression might occur in the host.

In our study, the most targeted genes in the *cps* operon were *wcaJ*, followed by *wzc* and *wzy* genes. Yet, we observed a diverse landscape of mutations, most of them linked to insertion

sequences (IS) jumping within *cps* genes. Transposable elements are ubiquitously distributed across living organisms and they represent an important source of genetic variability in response to environmental changes. Transposition rates are usually low (Nagy and Chandler, 2004). However, ISs can undergo bursts of transposition in response to various stresses, including temperature shifts and starvation (Foster, 2007), which likely occurred during the prolonged incubation on Tryptic-Soy Agar (TSA) plates at 25 °C. During incubation on solid media, bacteria are more likely to undergo shifts in nutrient availability, eventually leading to starvation. Furthermore, the structural organization of a colony allows the overgrowth of evolved sectors. Therefore, the likelihood of activating the stress response and/or enhancing the overall mutation rate is higher. The enhanced transposition rate under stress conditions may represent a general adaptive strategy conferring a growth advantage during unfavourable times through continuous genome rearrangements.

In our isolates, the highest frequency of conversion from mucoid to non-mucoid appearance was driven by transposition of IS elements including IS*1*-like and IS*903b* types. Non-capsulated variants from the isolate CNR137J2 mostly resulted from IS*1* insertion in *wcaJ* gene. IS*1* elements are highly abundant in facultative anaerobic Gram Negative and significantly associated with resistance genes. For instance, IS*1* transposition into the *bgi* locus of *E. coli* occurs preferentially in stationary phase (Hall, 1998). A plausible explanation for our observation would be that the prolonged incubation led to nutritional deprivation, which in turn activated the IS*1* transcription. To test our assumption, we could quantify the transcription level of IS*1* transposase gene by RT-PCR in optimal growth *versus* unfavourable growth conditions.

Out of 72 non-mucoid variants characterized, 12.5% (n = 9) showed a IS*903b* element disrupting diverse *cps* genes. In *E. coli*, enhanced transposition of IS*903b* occurs in late stages of colony growth of nutrient-starved cells, likely in response to the cellular environment (Coros et al., 2005). Factors such as *dam* methylation and nucleoid-associated proteins (e.g., H-NS) can affect IS*903* transposition rates. In addition, mutations in genes involved in DNA metabolism, proteolysis, regulation, and metabolism also elevate IS*903b* transposition rate. Three out of seven non-mucoid variants from *K. pneumoniae* CNR152A1 showed an IS*903b* insertion in *cps* genes. Possibly, this isolate harbours mutations in such cellular pathways that lead to enhanced likelihood of transposition. A meticulous investigation of its genome is required to clarify this aspect.

Movements of ISs are hardly detected using short-read sequencing. In addition, the library preparation protocols for genome sequencing may be determining. Indeed, when using the Illumina Nextera technology, based on tagmentation of genomic DNA, consisting of a simultaneous cleavage and addition of adaptors by a modified Tn*5* transposase, we noticed extremely low or no coverage of the capsule operon (Figure 21), likely due to the high richness of AT segments within the *cps* region. Hence, this complicated the detection of any genetic event, including IS transpositions. The coverage was significantly improved by replacing the

Nextera technology with NEBNext® Ultra™ II DNA Library Prep Kit for Illumina® (Figure 21), which was then used for the sequencing of the published non-capsulated variants.

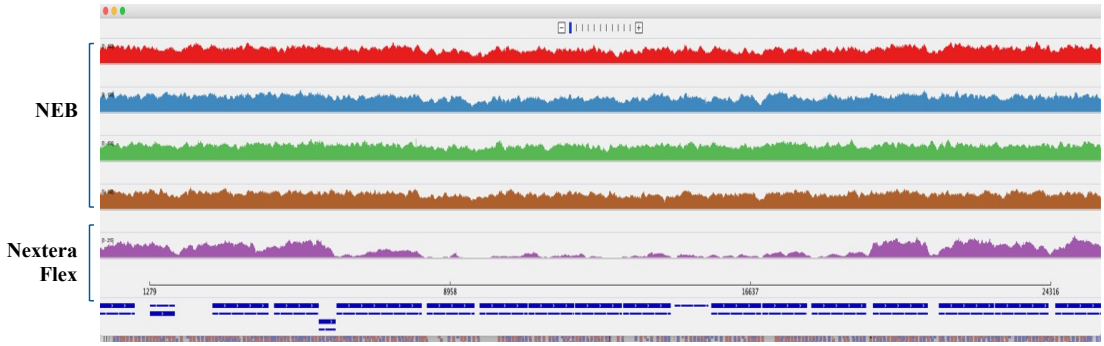

Figure 21. Comparison of coverage of the *cps* region in NM variants from the same isolate obtained with the two different kits for library preparation (upper part: four NM variants sequenced upon using NEB for library preparation *versus* bottom part: NM variant from the same isolate but obtained with Nextera Flex). Alignments of the BAM files were performed through Integrative Genomics Viewer (IGV).

This allowed to visualize the high occurrence of indels in *cps* genes containing AT-rich DNA stretches [(poly(A) or poly(T)], likely resulting from polymerase slippages during DNA replication ultimately leading to frameshift errors. The *cps* loci with the poly(nt) tracts may be considered as hypermutable loci, which, under stressful conditions, generate heterogeneity and contribute to evolutionary success of bacterial populations.

However, it remains an open question whether the accumulation of mutations within the *cps* region provides any benefit from an evolutionary perspective. Intuitively, the co-existence of distinct phenotypes within the same bacterial population may represent a strategy to thrive in challenging environments. Preliminary evidence suggests that, albeit frequent, the loss of capsule is a transient event. Hence, non-capsulated isolates tend to disappear over time, either because counter-selected or due to re-acquisition of functional capsules by conjugation (Buffet et al., 2021). In addition, capsule deficiency allows bacterial cells to become more permissive for conjugation (Buffet et al., 2021). In a scenario where multidrug resistant (MDR) clinical isolates are incessantly emerging and disseminating, being more incline to gain virulence and resistance determinants, often carried by large conjugative plasmids, might constitute an advantage, making non-capsulated variants optimal and transient vector for antibiotic resistance.

In addition to altered capsule production, the colony variants exhibited differences in biofilm formation, autoaggregation and susceptibility to carbapenems. Although at this stage we cannot rule out the contribution of additional mutations in some isolates to the observed divergences, our findings suggest that capsule loss might confer an advantage in colonization due to enhanced biofilm production and autoaggregation. Consistently, capsule-deficiency in *K. pneumoniae* isolates resulted from alterations in *cps* genes was associated with higher biofilm formation and better invasion of bladder epithelial cells (Ernst et al., 2020).

As the general objective was to characterize HR, I hypothesized that colony heterogeneity contributed to the HR phenotype. By performing AST, we measured a significant *increase in susceptibility* to MEM, ETP and IMP in 50% of isolates when losing the capsule, suggesting a protective role of this extracellular layer from carbapenems. Interestingly, the non-mucoid variants derived from the CNR152A1 isolate showed a *decreased susceptibility*, particularly towards MEM and ETP. Loss of O-antigen expression in this isolate might have affected the function of surface proteins important for the entry of carbapenems (Klein and Raina, 2019). Presumably, the loss of capsule in the strain already defective for O-antigen production might have further disturbed the assembly of outer membrane proteins (OMPs), thereby decreasing carbapenem permeability. Consistently, Ernst *et al*., also showed that last resort-drugs such as MEM/Vaborbactam and colistin do not kill intracellular non-capsulated, carbapenem-resistant *K. pneumoniae* from bladder epithelial cells (Ernst et al., 2020).

Capsule loss is a common event that contributes to generate heterogeneity within monoclonal populations, mostly resulted from insertion of transposable elements and indels occurring at *cps* genes. As we have seen in the Introduction, bacteria can use different strategies to adapt to environmental changes, including standing genetic variation at hypermutable loci (also referred to as contingency loci). Examples of such loci are genes involved in the biosynthesis of capsule polysaccharide (Lukácová et al., 2008). Hence, we speculate that variation of capsule content through alterations in *cps* genes (possibly hypermutable) may represent an adaptive mechanism facilitating the survival of *K. pneumoniae* in challenging environments. Therefore, we think that our work contributed to improve the understanding of a successful pathogen like *K. pneumoniae*. Finally, given the phenotypic divergences, caution should be used in the characterization of clinical isolates, especially when those display a multi-drug resistant phenotype, to avoid misinterpretations and misclassifications.

Heterogeneity of resistance to imipenem among KPC-Kp is multifactorial

Carbapenem resistant Enterobacterales (CRE) are known to exhibit variable degrees of resistance to carbapenems according to level of carbapenemase expression and concurrent presence of other mechanisms of carbapenem resistance. KPC-Kp may display low levels of carbapenem resistance, often within the range of susceptibility (≤1 mg/L), as observed for the collected isolates we have analysed and elsewhere (Cury et al., 2020). Therefore, detection of KPC-Kp is not always straightforward. Owing to this difficulty, carbapenem susceptibility breakpoints keep on changing in recent times. Carbapenem MIC values ≤4 mg/L for KPC-Kp isolates allow the clinical use of carbapenems with low mortality rates (Daikos and Markogiannakis, 2011). Therefore, accurate carbapenem MIC measurement is essential to establish treatment regimens using carbapenems (Fattouh et al., 2015).

The HR profile poses a further challenge in the laboratory diagnosis and clinical management of KPC-Kp isolates. In our work, we demonstrated that HR towards two clinically relevant carbapenem drugs, IMP and MEM is prevalent among KPC-Kp clinical isolates, as

previously suggested (Adams-Sapper et al., 2015; Nodari et al., 2015; Pournaras et al., 2010) and greatly observed with IMP compared to MEM. The specificity of HR profile *in vitro* to IMP may stem from the different properties of the two carbapenems. Although both drugs primarily bind to PBP2, MEM, unlike IMP, simultaneously bind to PBP3 as well, likely potentiating its bactericidal activity. In addition, MEM is a "bulky" carbapenem due to its larger size, whereas IMP is a smaller, "nonbulky" molecule, showing a rapid influx through the OM (Zhanel et al., 2007). IMP is also less stable than MEM under laboratory conditions and it is spontaneously degraded (Nickolai et al., 1985; Zhanel et al., 2007).

HR is an ancient observation that dates back to 1947. However, it is still a blurry and poorly understood phenomenon, and its clinical relevance has been a matter of debate. Attempts to draw up a general definition yet considering various drugs, different bactericidal mechanisms, and several bacterial species have possibly oversimplified a complex phenomenon. Furthermore, the lack of standardized methodologies for HR characterization accounts for the a great variability of results across diverse studies (El-Halfawy and Valvano, 2015). Commonly, HR is referred to as the ability of populations to grow at concentrations of the drug at least eightfold higher than their MIC (Andersson et al., 2019). Yet, when looking at the different research studies on HR, it is unclear which MIC is taken into consideration. Indeed, multiple factors influence the value of MIC and reproducibility of results. Among those, the size of the inoculum is crucial when ß-lactams are assayed. Variable carbapenem MICs can be obtained for carbapenemase-producing (CP) strains depending on the system used for their determination (Antonelli et al., 2019), thus choosing one method over another may have an impact on classification of isolates. According to CLSI guidelines[32], MIC results should be interpreted not later than 18 hours after inoculation. However, what we read after this incubation period is the result of a complex interplay of several factors, overlooking minor but significant variations in the susceptibility pattern of individual bacteria that could be an alarm bell for the future emergence of resistance. In addition, the classic endpoint MIC estimation by broth microdilution (BMD) tends to overestimate the MIC values for carbapenems more than agar-based methods (Antonelli et al., 2019), likely due to the progressive inactivation of the drug by the carbapenemase or instability of the drug that favours the emergence of subpopulations.

Surprisingly, all these factors are rarely discussed across studies on HR. Given their influence on determination of susceptibility levels of CP isolates and the discrepancies among different methods, we believe that specifying which MIC is used as reference for further characterization of HR is crucial.

Population Analysis Profiling (PAP) is a time-consuming assay broadly used to confirm the HR phenotype preliminary detected by Etest. In our study, PAP was performed on 13 CPKp

[32]Clinical and Laboratory Standards Institute (CLSI). Performance Standards for Antimicrobial Susceptibility Testing. 27th ed. CLSI supplement M100 (ISBN 1-56238-804-5 [Print]; ISBN 1-56238-805-3 [Electronic]). Clinical and Laboratory Standards Institute, 950 West Valley Road, Suite 2500, Wayne, Pennsylvania 19087 USA, 2017.

isolates using the MIC determined by E-test as reference. HR is mainly characterized by agar-based methods (Etest and Population Analysis Profiling, PAP); thus, it sounds reasonable to use the MIC by Etest as a reference for HR investigation. The PAP analysis we performed confirmed the specificity of HR to KPC-producing isolates, but we could not explain the reasons behind that. Several factors might contribute to this specificity:

(i) *The complexity of KPC expression.* Typically, the *bla*$_{KPC}$ is embedded within a 10-kb mobile transposon (Tn*4401*), which is frequently located on conjugative plasmids (Naas et al., 2008). The seven different isoforms of Tn*4401* are distinguished based on deletions occurring in the noncoding region upstream of *bla*$_{KPC}$, which contains three putative promoters (P1, P2, P3), but only P1 and P2 contribute to KPC expression (Naas et al., 2012). Given this complex regulation, it is possible that heterogeneous expression of KPC occurs, contributing to variable kinetics of carbapenem hydrolysis that could explain various susceptibility levels of a bacterial populations, as shown for CTX-M-15 in *E. coli* (X. Wang et al., 2014).

(ii) *The kinetics of degradations.* The degradation of the carbapenem drug, specifically IMP, is likely a key factor in the emergence of HR. β-lactam antibiotics are hydrolysed via a two-step model involving acylation and deacylation. IMP possesses a bicyclic core, with a β-lactam ring fused to a pyrroline ring. The rate of hydrolysis of the carbapenem depends on the conformational change of the acyl-enzyme complex and the class of carbapenemase. Carbapenem degradation was suggested to be favoured when the pyrroline ring is in the enamine (2-pyrroline) (Δ^2) conformation, which may rapidly tautomerize to the (S)-Δ^1 and (R)-Δ^1 products in a time-dependent manner. The tautomerization has been proposed to inhibit drug hydrolysis (Lohans et al., 2019). Serine β-lactamases (SBLs) like KPC-2 and KPC-3 efficiently hydrolyse carbapenems by rapidly reducing tautomerization or by facilitating the reconversion of the Δ^1 epimers back to the Δ^2 form. Metallo β-lactamases (MBLs) require zinc ion to be active and rely on a different reaction mechanism. Hydrolysis of IMP leads to accumulation of an anionic intermediate with an already cleaved carbon-nitrogen bond. This intermediate can either undergo protonation at N-1 yielding the Δ^2 tautomer, that once released in solution tautomerizes rapidly to its Δ^1 form, or remain inside the enzyme pocket, that would favour the stereospecific protonation at C-2. On the other hand, the scarce hydrolytic activity of Class D like OXA-48 might stem from the different mechanism of IMP degradation, where the isomerization of carbapenem gives rise to β-lactones that can tautomerize in solution, thus inhibiting or slowing down the hydrolysis.

As shown in Table II, KPC-3 and NDM-1 show the highest K_{cat} values for IMP, suggesting a rapid drug turnover (a fast deacylation step) at high concentration of IMP. OXA-48 and VIM-1, instead, show low steady-state K_{cat} values for IMP, suggesting a slow deacylation rate, consistently with the possible re-tautomerization of β-lactones in solution. The faster drug degradation in KPC-isolates may anticipate the regrowth of dormant subpopulations and the appearance of HR profile on solid media. However, although showing a rapid IMP turnover (high K_{cat} values), NDM-1 isolates were rarely reported to exhibit HR. Although the number of NDM isolates was too little in our collection to draw conclusion, we observed, for the few of

them, HR by Etest which was not further confirmed by PAP analysis, as reported for *Providencia rettgeri* (Zavascki et al., 2014). The NDM has been shown to be a lipoprotein anchored to the outer membrane of Gram-negative bacteria, which is secreted in outer membrane vesicles (OMVs), ultimately ensuring the carbapenemase stability in the extracellular space (González et al., 2016). The wide diversity of catalytic efficiency for IMP hydrolysis across different studies (Table II) might be due to the variable expression of NDM depending on its cellular localization. In addition, NDM-1, under conditions of Zn (II) deprivation, is poorly stable compared to other NDM variants (Bahr et al., 2018). The MHA cation adjusted used for AST is a rich medium with high Zn (II) content, which, however, does not reflect the in vivo conditions, where host immune factors like calprotectin sequester zinc ions. In our PAP experiments, variations in zinc concentration might have occurred and affected the stability of the NDM-1 protein in the extracellular space, resulting in poor degradation of IMP when released in the medium. Assuming that the IMP degradation is a key factor for HR profile and knowing that other NDM variants are more stable to zinc deprivation, it would be interesting to characterize carbapenem HR among other NDM-isolates.

(iii) *Disulphide bonds of KPC.* Class A enzymes, unlike the other β-lactamases, contain a disulphide bridge between Cys69 and Cys238, which is essential for maintaining the structural integrity of the enzyme active site and crucial for carbapenem hydrolysis (Naas et al., 2016). It is possible that this specific structural property of class A carbapenemase contributes to their stability when released in the culture medium and to the HR phenotype in KPC-Kp isolates.

Parameter[a]	KPC-2	KPC-3	OXA-48	NDM-1	VIM-1
K_{cat} (s^{-1})	15[b]; 15[c]; 20[d]; 31[e]	45[b]; 45[c]; 41[f]	4.8[g]; 2[f]; 6.7	238[h]; 600[i]; 59[l]; 20[m]	0.2[c]; 2[n]
K_m (μM)	51[b]; 51[c]; 21[d]; 90[e]	23[b]; 23[c]; 88[f]	13[g]; 13[f]; 5.3	65[h]; 78[i]; 123[l]; 94[m]	1.5[c]; 1.5[n]
K_{cat}/K_m (s^{-1} μM^{-1})	0.3[b]; 0.3[c]; 0.95[d]; 0.34[e]	1.9[b]; 1.9[c] 0.46[f]	0.37[g]; 0.15[f]; 0.13	3.71[h]; 7.6[i]; 0.48[l]; 0.21[m]	0.13[c]; 0.75[n]

Table II. [a]The parameters were retrieved by available publications. K_{cat} = turnover number, it describes how many molecules of substrate are converted by the enzyme per unit time; K_m = indicates the substrate concentration needed to achieve a half-maximum enzyme velocity; K_{cat}/K_m = describes the catalytic efficiency of the enzyme. List of references: [b](Alba et al., 2005); [c](Docquier et al., 2003); [d](D. Wang et al., 2014); [e](Queenan and Bush, 2007); [f](Walther-Rasmussen and Høiby, 2006); [g](Docquier et al., 2009); [h](Sun et al., 2018); [i](Makena et al., 2015a); [l] (Tada et al., 2014); [m](Yong et al., 2009); [n](Franceschini et al., 2000).

Heterogeneous survival of HR KPC-Kp isolates to high doses of imipenem

Initially, my main hypothesis on reasons behind the HR pattern was the emergence of subpopulations surviving the IMP treatment owing to three possible strategies:

(i) *Indirect resistance*: a fraction of carbapenem susceptible cells manage to survive the IMP exposure as, upon cell lysis, the released KPC carbapenemase still exhibits hydrolytic activity,

which carries on the progressive inactivation of the antibiotic. Accordingly, our observations on restored carbapenem susceptibility upon capsule loss suggested a contribution of CPS switch to HR.

(ii) *Resistant mutants*: since these are clinical strains, it is plausible that previous antibiotic exposure selected for mutations, which, once exposed again to the antibiotic, have been selected for and emerged in the inhibition halo of the drug.

(iii) *Tolerance/heterotolerance (persistence)*: the whole isolate or only a fraction of cells can endure in the presence of IMP as result of decreased growth rate or growth suppression, which protect cells from bacterial killing by IMP. Normal growth rate or growth resumption are then restored when the drug is removed, which is naturally the case of CPKp with IMP.

After several attempts to recover the fraction of surviving subpopulations, e.g., by cell sorting with FACS using propidium iodide to discriminate between viable and dead cells, or in liquid culture upon removal of the spent medium containing released carbapanemase and residuals of the drug, I finally discovered the ScanLag setup (Levin-Reisman et al., 2010). This system seemed promising to test the subpopulation hypothesis and, eventually, to understand the dynamics with which those survive exposure to high IMP concentrations. After installing the system in our laboratory with the help of my colleague Nicolas Cabanel, we could monitor the time of appearance and the growth rates of individual colonies from a subset of KPC-Kp isolates.

However, *all that glitters is not gold*. While setting up the experimental conditions, we realized that multiple factors would affect the outcome of the assay. Among them, the bacterial inoculum size, instability of imipenem during storage at both -20/-80 °C and room temperature, as well as during incubation on plate, uneven spreading of the bacterial culture, uneven distribution of the drug in the medium, would lead to artifacts and affect the reproducibility of the results obtained. Finally, by using the spiralling system to ensure uniform spreading of the bacterial culture with approximately 10^6 cells final on plate, freshly prepared IMP stock solution and IMP-containing plates any time the experiment was performed, I could reduce the variability among replicates and successfully apply the ScanLag setup for HR investigation of KPC-Kp isolates.

The system allowed us to detect a heterogeneous colony growth resumption, distributed in a bimodal manner over time. Overall, by fitting the data on time of appearance (ToA) for each colony to a two-component mixture model, we could distinguish two subgroups: a main one including the colonies exhibiting wild-type (WT) growth rates and similar times of appearance, thus distributed in a Gaussian-like manner, followed by a tail including late-appearing colonies. The tail as measured by ScanLag was suggestive of persister cells (Levin-Reisman and Balaban, 2016). In addition, a fraction of cells showed reduced growth rate. Overall, we observed an inter-strain variation and diverse effects of bacterial growth phase, likely due to the genomic context, which will need to be carefully analysed.

In KPC-Kp, the delayed appearance of colonies is reminiscent of the Post-Antibiotic Effect (PAE), defined as the delay of bacterial growth after short exposure to antibiotics. Of all ß-

lactams, carbapenems are the only members producing significant PAE with Gram Negative organisms. The molecular mechanism behind carbapenem PAE is undetermined, but one hypothesis is the selection of slow-growing subpopulations in the exposed bacteria. In the specific case of CP bacteria, drug clearance over time might create the optimal conditions for otherwise dormant subpopulations to emerge with different delays.

A broad landscape of mutations behind heterogeneous survival of KPC-Kp to imipenem

The observed delay might stem from an extended lag phase or a transient slow growth reducing susceptibility. To gain more information on the subpopulations contributing to the HR phenotype we combined genomic and phenotypic analyses of surviving colonies at 8xMIC. For our purposes, I selected one isolate based on the HR profile and genomic features. The chosen isolate, CNR149C9, belongs to ST307, an emerging high-risk clone that possesses the *lacZYI* operon, the Fec-like iron (III) dicitrate and the glutathione ABC-transport systems, the urea transport system and the cluster for glycogen synthesis, all features that may contribute to its adaptation to various niches (Villa et al., 2017). This isolate was highly HR compared to other isolates and it showed a high proportion of late growing colonies.
Most of the colonies appearing within the first Gaussian peak did not show genetic alteration and reproduced the same susceptibility and HR phenotypes as the parental strain but were delayed in time, in agreement with what has been defined tolerance by lag time optimization (Fridman et al., 2014). Nevertheless, a fraction of them showed a decreased MIC to IMP and in most cases to MEM and mutations, mostly in genes involved in cell wall synthesis and OM permeability. In addition to mutations already known to affect carbapenem susceptibility, e.g., *ompK36* (Adams-Sapper et al., 2015), we observed alterations the OMP BamA, whose inhibition impedes correct OMP folding, conferring antibiotic resistance (Hart et al., 2019). Mutants in outer membrane proteins (OMPs) showed shorter PAE with IMP (Majcherczyk et al., 1994). Consistently, the isolates mutated in the porins had a shorter delay in growth compared to the rest of emerging colonies. Interestingly, loss of the extra chromosomal phage was frequent among early appearing colonies. As previously reported (Knudsen et al., 2016), the loss of phage might have resulted from antibiotic-induced stress response or, alternatively, provide an increased drug tolerance. Similarly, the large deletion of the *tra* region within the plasmid harbouring $bla_{\text{CTX-M-15}}$ may have provided a growth advantage during IMP exposure. In fact, the *tra* genes encode proteins involved in conjugal transfer and pilus assembly, two processes that require energy and numerous envelope components (Wilkins and Frost, 2002). A comparison of the antibiotic tolerance and an analysis of the lag phase in these different isolates might allow to confirm those hypotheses.

HR was previously shown to result mainly from DNA amplification involving *loci* conferring decreased susceptibility to antibiotics in a fraction of cells (Andersson et al., 2019; Nicoloff et al., 2019). Here, we identified only three cases of genomic amplification, two of which were associated with an increased MIC. An interesting case is the amplification of the

region of the CTX-M-15 plasmid encompassing the *lac* operon, which was suggested to favour bacterial survival in stressful condition (Villa et al., 2017) and was detected in a colony predicted to result from persisters regrowth. On the other hand, one isolate showed amplification of the region encompassing the *dcw* locus, encoding major functions for cell wall synthesis and cell division. This isolate exhibited higher resistance to IMP than MEM, with a peculiar double halo in the zone of IMP inhibition (Figure 22a). The different impact on resistance might be explained by the ability of MEM to bind to PBP3, in addition to PBP2, like IMP (Sumita et al., 1990).

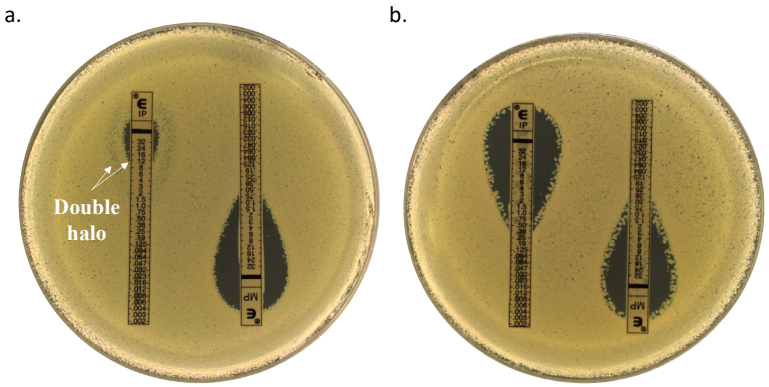

Figure 22. a) Picture of Etest on the isolate showing the amplification of the region encompassing the *dcw* locus. The double halo was only noticed for IMP and not for MEM, b) Picture of Etest on the isolate showing the *polB* mutation. A strong HR phenotype is obtained for both IMP and MEM.

Colonies appearing after the defined cut-off, as suggested by the team of Nathalie Balaban (Levin-Reisman and Balaban, 2016), were defined as persisters. None of these colonies showed increased carbapenem MICs and mutations in the intrinsic resistome, consistently with the definition of persistence. Interestingly, among them, 7% had lost the pKPC plasmid and restored susceptibility to IMP. Here, the emergence of colonies that had lost the resistance pattern is favoured by the progressive inactivation of the drug and by mechanisms conferring a persister-like profile, which allowed survival otherwise not possible. Plasmid loss is generally a rare event in bacterial population. The higher frequency of plasmid elimination herein observed might have resulted from errors in replication/segregation due to stress of IMP exposure and/or nutrient level in the medium before plating. Moreover, this KPC plasmid carries a *vapBC* toxin/antitoxin (TA) locus. VapBC is one of the largest families of type II TA systems, which have been associated with bacterial persistence (Winther and Gerdes, 2012). Mutation of *vapB* antitoxin (inversion of 26 bp or V5E mutation) in *E. coli* strains exposed to intermittent high doses of ampicillin resulted in extended lag phase by ScanLag and higher drug tolerance (Fridman et al., 2014). This phenotype likely resulted from an increased activity of the VapC toxin as it was reverted by the deletion of the *vapBC* locus. In *K. pneumoniae*, expression of the toxin VapC was associated with slower cell growth and a decrease in cell viability, fully restored by the expression of VapB (Kang et al., 2020). It is plausible to imagine that the loss of pKPC led to disappearance of the unstable antitoxin VapB, thereby resulting in

transient activation of the toxin VapC that alters protein translation, ultimately contributing to persistence of a fraction of cells.

We detected a broad range of mutations among colonies associated with persistence and tolerance with no or a small effect on IMP MIC. For example, mutations affecting protein synthesis in tRNA genes, tRNA synthetase and a ribosomal protein. These mutations might have been occurred serendipitously. However, they might also have been selected for better survival in the presence of the antibiotics or to increase the rate of dormancy. This analysis provides therefore unique opportunities to identify novel functions associated with *K. pneumoniae* survival in the presence of carbapenems.

In addition, ScanLag also allowed to identify colonies emerging at various time points and showing decreased growth rate. These colonies showed features of carbapenem resistant small colony variants (SCVs) with mutations in the core genome. SCV has been extensively studied in Gram positive bacteria (*S. aureus*) and other Gram-negative bacteria (*E. coli* and *P. aeruginosa*), but surprisingly, despite its clinical importance, only two reports exist on SCVs in *K. pneumoniae* (Ronde-Oustau et al., 2017; Silva et al., 2016). Hence, to the best of our knowledge, our pioneering study has elucidated genetic bases of carbapenem resistant SCVs in *K. pneumoniae*. As reported for other species, most of the SCVs detected were defective in central metabolism (TCA cycle and glycolysis) and respiration (heme and ubiquinone synthesis), thus explaining the extremely slow growth rate under aerobic conditions. How metabolism contributes to ß-lactam susceptibility is still a matter of debate. It seems unlikely that the increased resistance would be only due to a decreased growth rate. Indeed, under anaerobic condition, the parental strain showed a reduced growth rate compared to aerobic condition but similar MICs for IMP and MEM. Under anaerobic conditions, isolates mutated in metabolic pathways showed wild-type growth rates and susceptibility patterns. Interestingly, under aerobic conditions, we noticed for some mutants the appearance of large colonies, suggesting the occurrence of compensatory mutations reverting the phenotype. This was frequently observed, for instance, for the isocitrate dehydrogenase *icd* mutant (AC208), whereas no large colony were detected among the *hemA* (AC91) or *ubiA* mutant (AC125). Further analysis of these pseudo-revertants by WGS and phenotyping might provide additional clues on the reason for the increased MIC in those strains.

In the routine laboratory investigations, SCVs may be difficult to detect in patient samples due to their pinpoint morphology, slow growth, and late appearance during routine diagnostic, therefore leading to inappropriate treatment choice. *In vivo* treatment with carbapenem may thus select for these variants, ultimately leading to treatment escape and causing recurrent and chronic infections without their isolation in the hospital laboratory.

We also detected mutants for L-cysteine (*cysB*) and L-tryptophan (*trpA*) metabolism. These mutations might result in response to external perturbations and sustain the pathogen adaptation and survival across diverse niches. Interestingly, non-functional *cysB* was shown to alter the expression of several genes in *E. coli* and to confer resistance to mecillinam by

upregulating the PBP1b protein and its activator LpoB (Thulin and Andersson, 2019). In the light of these findings, it would be worth to quantify the expression level of PBPs in our *cysB* mutant, grown with- and without cysteine.

Three evolved clones showed a mutation in *ispA* gene. In *B. subtilis*, alteration of *ispA* gene was shown to stabilize the L-form growth (Kawai et al., 2019). L-forms are cell wall deficient bacteria widely reported in Gram positive bacteria. In Gram Negatives, these cells are named spheroplasts. As mentioned in the Introduction, IMP targets mainly PBP2, thus leading to transient spheroplast morphology. Spheroplasts formation has been associated with increased tolerance towards beta-lactams drugs (Cross et al., 2019; Westblade et al., 2020). In contrast to L-form, spheroplasts do not divide in the presence of antibiotic and revert to rod-shape only upon drug removal. In our experiments, it is possible that the degradation of IMP allowed the reversion of spheroplasts to rod-shaped bacteria for most of the surviving colonies, except for the mutants in *ispA*, which stabilized the cell-wall deficient shape, thereby providing resistance to cell-wall targeting agents. Microscopic observation of these mutants would help clarifying their morphology.

Finally, one isolate (AC315) showed a nonsense mutation in the *polB* gene, encoding the DNA polymerase II (Pol II), which plays an important role in f DNA repair. Pol II is regulated by the SOS system to DNA damage in *Escherichia coli*. PolB null mutants may have a higher mutation rate and being inclined to evolve adaptive mutations (Foster et al., 1995). Interestingly, this mutant exhibits a hyper HR phenotype by Etest (Figure 22b). One could hypothesize that the absence of *polB* facilitates the emergence of adaptive mutations in the presence of carbapenem, thereby generating heterogeneity of susceptibility within the population. Future functional studies will help to characterize the *polB* null mutant and further elucidate its role in HR to carbapenems.

VI. Concluding remarks and future perspectives

The study on capsule switch taught us the importance of meticulously identify colony aspect divergences while screening clinical isolates because picking one colony over another can make a difference in the pathogen characterization. Caution should be then used to avoid the storage and transfer of mixed clinical samples that might be subsequently misclassified. Although we ruled out the contribution of capsule switch to HR in the subset of CPKp isolates analyzed, we cannot exclude that this phenotypic diversification might have different effect on susceptibility according to the isolate under investigation and *in vivo*. In support of that, among the eight CPKp isolates selected, one showed higher resistance levels to carbapenems upon capsule loss, regardless the *cps* gene affected.

Furthermore, HR seems to be a multifaceted phenomenon, which can vary based on the species analyzed, type of antibiotic and of resistance mechanisms. Attempts to provide a general definition of HR have disregarded its complexity. Certainly, the understanding of HR has been challenged by the lack of consistency in methodologies applied to characterize such phenomenon. In our work, we could overcome the technical difficulty of investigating HR by using ScanLag, a simple yet powerful tool, which allowed us to identify heterogeneity in the surviving populations. Although this system has been already used elsewhere for HR characterization, e.g., in *Candida albicans*, our study is, to the best of our knowledge, the first report adopting ScanLag in CPKp. We believe that this system could provide substantial help in assessing heterogeneity of clinical isolates in various conditions. The combination with genomics-based approach, then, allowed us to uncover additional mechanisms associated with HR.

By characterizing several clinical isolates, we have provided a clarification, if not a full elucidation of what HR implies in the specific case of CPKP isolates, where multiple factors are contributing to their heterogenous survival in the presence of carbapenems. Among them, the progressive drug-enzyme inactivation, especially when the already unstable IMP is used, seems pivotal in revealing subpopulations with a distinct physiology. This model is clinically relevant, as during treatment *K. pneumoniae* will encounter variable concentrations of antibiotics in the different body sites.

We showed that HR to IMP in KPC-Kp is a complex phenomenon, which results from at least three different strategies know to contribute to treatment escape, namely tolerance, persistence, and resistance. Inter-strain variations led to different frequency of HR, likely due to strain-specific genomic features. Remarkably, albeit occurring in only a fraction of the surviving populations, the mutations identified were extremely diverse and affecting multiple pathways. We speculate that these mutations could be also selected during *in vivo* treatment with carbapenems.

Although these two studies conducted during my PhD describe two distinct strategies to generate heterogeneity in the population, a common observation is the capacity of *K. pneumoniae* to rapidly develop adaptive responses, which will provide a growth advantage in adverse conditions, ultimately promoting survival and persistence in the environment in the host. We have showed that CPKp populations, when challenged with nutrient deficiency or high doses of imipenem, undergo phenotypic diversification. Such heterogeneity is reflected by the emergence of two distinct colony variants on solid media upon limited nutrient availability, driven by mutations in the hypermutable genes encoding the capsule layer affecting various phenotypic properties and/or upon exposure to high concentrations of imipenem, by altering their growth rate and colony appearance following metabolic alterations and defects in the cell envelope and outer membrane permeability.

This first study for the EERA Unit on heterogeneity of *K. pneumoniae* populations, and more specifically, on HR, persistence, and tolerance, allowed to build up a collection of mutant strains derived from a single clinical KPC-Kp isolate, opening numerous perspectives for future research, such as: (a) Uncovering the mechanism by which tolerant cells can maintain normal growth in the presence of IMP and clarifying whether this mechanism causes differential gene expression. My current hypothesis involves the transient formation of non-dividing spheroplasts, which could either be stabilized by further mutations or revert to rod-shape due to the inactivation of the drug occurring very rapidly, (b) Mathematical models to describe crucial parameters of HR in CPKp, including kinetics of antibiotic degradation, carbapenemase activity and delay in growth, (c) I have observed both by PAP and by ScanLag differences among MDR clinical isolates. This provides an opportunity to test the hypothesis that tolerance and persistence contribute to the selection of resistant isolates. One first experiment would be to analyze the phenotype of isolates susceptible to multiple drugs following introduction of the KPC plasmid. Additionally, since HR has been suggested to be antecedent to resistance, experimental evolution with intermittent exposure to high doses of carbapenems of the isolates showing mutations but no change in the MIC would provide information on their contribution to resistance, (d) Analysis of the diversity of the loci identified through our work among the genome sequence of *K. pneumoniae* isolates publicly available and correlation with the presence of specific ARGs, namely the *bla* genes.

VII. Annex

Article 1

Bonnin *et al*. Emerg Infect Dis 2020

Emergence of New Non–Clonal Group 258 High-Risk Clones among *Klebsiella pneumoniae* Carbapenemase–Producing *K. pneumoniae* Isolates, France

Rémy A. Bonnin, Agnès B. Jousset, Adriana Chiarelli, Cécile Emeraud, Philippe Glaser, Thierry Naas, Laurent Dortet

The worldwide spread of *Klebsiella pneumoniae* carbapenemase–producing *Klebsiella pneumoniae* (KPC-*Kp*) isolates was reported to be caused by dissemination of 1 clonal complex (i.e., clonal group [CG] 258, which includes sequence types [STs] 258 and 512). We conducted whole-genome sequencing and epidemiologic analysis of all KPC-*Kp* isolates in France in 2018 and found that new successful high-risk clones of ST147, ST307, ST231, and ST383 are now the main drivers of bla_{KPC} genes. The bla_{KPC} genes were mostly carried by Tn*4401a* and Tn*4401d* structures and a new non–Tn*4401* element. Our epidemiologic investigations showed that the emergence of these non-CG258 KPC-*Kp* isolates in France was linked to dissemination of these clones from Portugal. Thus, KPC-*Kp* epidemiology has changed in Europe, at least in several non–KPC-endemic countries of western Europe, such as France and Portugal, where CG258 is not the most prevalent clone.

In *Klebsiella pneumoniae* bacteria, resistance to carbapenems results in 2 main mechanisms: the production of an extended spectrum β-lactamase or plasmid-borne cephalosporinase associated with a decrease in permeability of the outer membrane (especially through alteration of OmpK35 and OmpK36 porins), or the production of a carbapenemase (*1*,*2*). In France, these carbapenemases are Ambler's class A KPC enzymes; class B metallo-β-lactamases of NDM-, VIM- and, to a lesser extent, IMP-type; and Ambler's class D oxacillinases of OXA-48–like type (*3*,*4*).

K. pneumoniae carbapenemase (KPC) was first identified in United States in the early 2000s (*5*). Since then, this carbapenemase has spread and has become endemic in several countries, including the United States, Israel, Greece, China, and Italy. It has also been sporadically described in many countries of Europe (*1*). The worldwide spread of KPC has been linked to the dissemination of a main clone of *K. pneumoniae* (sequence type [ST] 258) and a single-locus variant (ST512) (*6*). In Asia (especially China), ST11, another single-locus variant of ST258, is mostly reported among bla_{KPC}-harboring *K. pneumoniae* isolates (*7*). In addition, a recently published study, conducted by the EUSCAPE working group in 2013 in Europe, revealed that the spread of carbapenemase-producing *K. pneumoniae* was driven by only a few clones (*8*). The most prevalent carbapenemase was KPC (45.5% [311/684 isolates]), and 72.7% (229/311) of KPC-producing *K. pneumoniae* (KPC-*Kp*) belong to the same clonal group (CG) 258, including ST258 and ST512. Whole-genome sequencing (WGS) analysis has suggested that ST258 and ST512 KPC-*Kp* spread out in Europe from 2 KPC-endemic countries: Greece (ST258) and Italy (ST512) (*6*,*9*–*11*). However, that study described the epidemiology of KPC in Europe in 2013, whereas the aim of our study was to describe the genomic characteristics of KPC isolates from a more recent period.

Author affiliations: Institut Pasteur–Assistance Publique/Hôpitaux de Paris–University Paris Sud, Paris, France (R.A. Bonnin, A.B. Jousset, A. Chiarelli, C. Emeraud, T. Naas, L. Dortet); Faculty of Medicine University Paris-Sud, University Paris–Saclay, Le Kremlin-Bicêtre, France (R.A. Bonnin, A.B. Jousset, C. Emeraud, T. Naas, L. Dortet); National Reference Center for Antibiotic Resistance: Carbapenemase Producing *Enterobacteriaceae*, Le Kremlin-Bicêtre, (R.A. Bonnin, A.B. Jousset, C. Emeraud, T. Naas, L. Dortet); Assistance Publique/Hôpitaux de Paris, Bicêtre Hospital, Le Kremlin-Bicêtre (A.B. Jousset, C. Emeraud, T. Naas, L. Dortet)

DOI: https://doi.org/10.3201/eid2606.191517

Analysis of the genetic context of bla_{KPC} has revealed that this gene is mostly localized into a class 2 transposon named Tn*4401* (*12*). Several variants of this Tn*4401* (Tn*4401a* through Tn*4401i*) have been reported with deletions upstream of bla_{KPC} within the promoter region (*13*,*14*). Consequently, expression of bla_{KPC} genes is complex and might involve different promoters, depending on the specific genetic environment and bacterial species. The 2 main promoters are named P1, which is in the vicinity of bla_{KPC}, and P2, a hybrid promoter located partly in the inverted repeat right of IS*Kpn7* (*15*). In rare cases, bla_{KPC} genes have been described in genetic structure not related to Tn*4401* and are named non–Tn*4401* elements (NTE) (*16*). However, in NTE, the expression of bla_{KPC} is mediated by other promoters. Our study aimed to deeply characterize the epidemiology of KPC-*Kp* circulating in France in 2018.

Material and Methods

Strains Collections and Culture Conditions

We included all KPC-*Kp* sent to France's National Reference Center for Antimicrobial Resistance during January 1–December 31, 2018. As previously described, we used isolates that were recovered from clinical and screening specimens and sent on a voluntary basis by any type of laboratory related to any health facility, such as private and public hospitals, nursing homes, and community laboratories (*3*,*4*). These laboratories were located throughout France, including overseas territories. KPC-*Kp* recovered by the National Reference Center for Antimicrobial Resistance represent ≈85%–90% of the KPC-*Kp* infection cases reported to the French Public Health Agency (R.A. Bonnin, L. Dortet, unpub. data). The collection used for WGS analysis represents a total of 63 nonduplicate isolates recovered from rectal screening (n = 45), urine (n = 12), blood cultures (n = 1), wound infections (n = 2), and respiratory samples (n = 2) and 1 isolate for which no recovery site information was available. Because the aim of the study was to evaluate the genetic diversity of KPC producers, we discarded from further analysis any duplicate isolates or isolates recovered from the same patient.

Antimicrobial Susceptibility Testing and Carbapenemase Detection

We performed antimicrobial susceptibility testing by using the disc diffusion method on Mueller-Hinton agar (Bio-Rad, https://www.bio-rad.com) and interpreted results according to European Committee on Antimicrobial Susceptibility Testing guidelines as updated in 2018 (http://www.eucast.org). We determined MICs for colistin by using broth microdilution (Sensititer Thermofisher, https://www.thermofisher.com). We performed carbapenemase detection by using Rapidec Carba NP (bioMérieux, https://www.biomerieux.com), followed by immunochromatographic detection of the carbapenemase enzyme using NG-Carba5 test (NG Biotech, https://ngbiotech.com).

WGS and Bioinformatic analysis

We sequenced all KPC-*Kp* isolates by using Illumina technology as previously described (*17*). We extracted total DNA from colonies by using the Ultraclean Microbial DNA Isolation Kit (MO BIO Laboratories, https://www.mobio.com) according to the manufacturer's instructions. We prepared the DNA library as previously described (*17*) and performed de novo assembly and read mappings by using CLC Genomics Workbench 12.0 (QIAGEN, https://www.qiagen.com). We identified the acquired antimicrobial resistance genes by using Resfinder 3.1 (https://cge.cbs.dtu.dk/services/ResFinder/) and the CARD database (https://card.mcmaster.ca). We annotated the genomes by using RAST (*18*). We performed phylogenic analysis by using CSIphylogeny 1.4 (https://cge.cbs.dtu.dk/services/CSIPhylogeny) and visualized the genomes by using FigTree 1.4.3 (http://tree.bio.ed.ac.uk/software/figtree). We performed sequences alignments by using ClustalW (https://www.genome.jp/tools-bin/clustalw). We analyzed single-nucleotide polymorphisms (SNPs) on the whole genome by using CSIphylogeny V1.4 with parameters as follows: select minimum depth at SNP position at 10×, minimum distance between SNPs at 10 bp, and minimum SNP quality score of 30.

We constructed the genetic contexts by using de novo assembly or by mapping with reference genomes from GenBank and verified by in-house PCR as previously described (*17*). We analyzed plasmid contents of clinical isolates by using PlasmidFinder 2.1 to search for the replicase gene and by conducting manual searches for genes showing homology with the replicase gene.

Results

Low Prevalence of KPC Producers among Carbapenem-Resistant *K. pneumoniae* in France

In 2018, a total of 3,931 carbapenem-resistant *Enterobacteriaceae* were collected, including 1,259 carbapenem-resistant *K. pneumoniae*, among which 1,010 were carbapenemase producers. OXA-48-like enzymes were the most prevalent carbapenemases (69.4%), followed by NDM (17.1%); 37 isolates (3.7%) had a

combination of both of these carbapenemases. KPC enzymes represent only 3.0% of all carbapenemases, corresponding to 6.8% (69 isolates, including 6 duplicated isolates) of all carbapenemase produced by *K. pneumoniae*. KPC also was produced by 13 non–*K. pneunomiae*, including 5 KPC-2 producers (2 *Escherichia coli*, 1 *Klebsiella oxytoca*, 1 *Enterobacter cloacae*, and 1 *Citrobacter koseri*) and 8 KPC-3 producers (5 *E. coli*, 1 *C. freundii*, 1 *E. cloacae*, and 1 *K. aerogenes*). Accordingly, *K. pneumoniae* is the most prevalent species (84.1%) among KPC producers.

Antimicrobial-Susceptibility of KPC-*Kp*

Susceptibility testing revealed that all KPC-*Kp* were resistant to all broad-spectrum cephalosporins (ceftazidime, cefotaxime, cefepime) and monobactam (Figure 1). All KPC-*Kp* were resistant to ertapenem. According to European Committee on Antimicrobial Susceptibility Testing breakpoints, 62.1% (41/66) KPC-*Kp* isolates remained susceptible to imipenem and 30.3% (20/66) to meropenem (Figure 1). Ceftazidime/avibactam (98.5% susceptibility) and colistin (92.2%) remained the most potent agents (Figure 1,

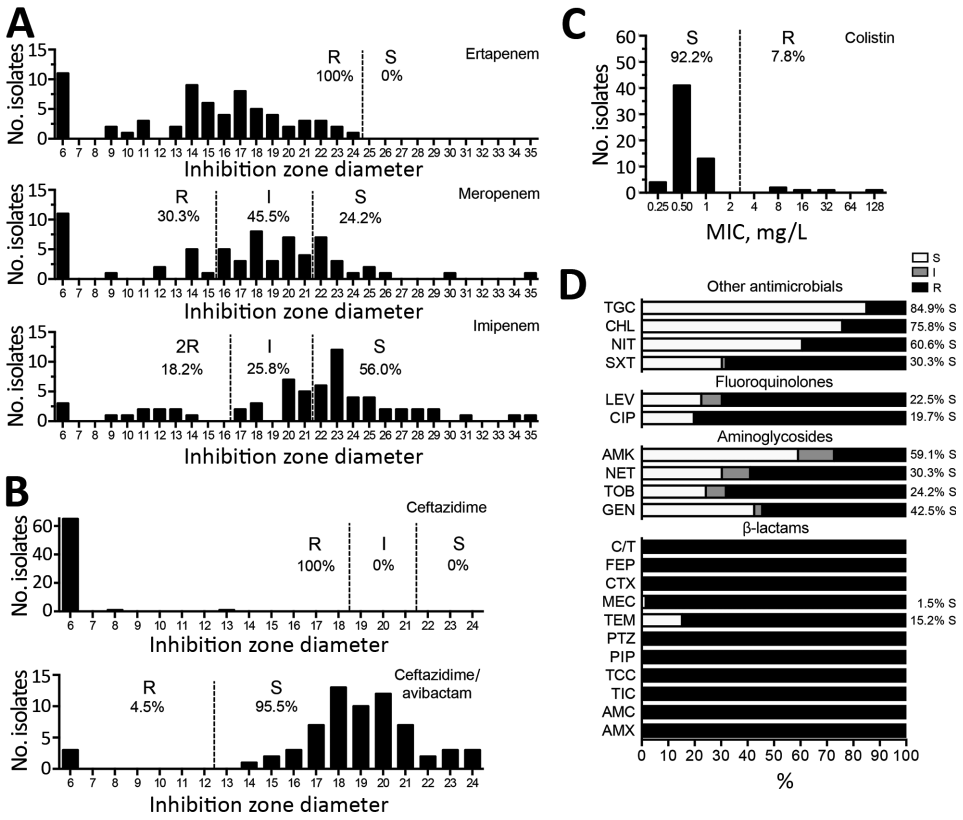

Figure 1. Susceptibility testing of *Klebsiella pneumoniae* carbapenemase–producing *K. pneumoniae* isolates, France, 2018. A) Antimicrobial susceptibility to carbapenems tested by using the disc diffusion method and interpreted according to European Committee on Antimicrobial Susceptibility Testing guidelines (http://www.eucast.org). B) Susceptibility to ceftazidime or ceftazidime/avibactam combination. C) MICs for colistin as determined by broth microdilution. D) Percentage of susceptibility to other antibiotic families. Where percentage of resistance is <100%, percentage of susceptible isolates is indicated. AMC, amoxicillin/clavulanate; AMK, amikacin; AMX, amoxicillin; CIP, ciprofloxacin; CHL, chloramphenicol; C/T, ceftolozane/tazobactam; CTX, cefotaxime; FEP, cefepime; GEN, gentamicin; I, intermediate; LEV, levofloxacin; MEC, mecillinam; NET, netilmicin; NIT, nitrofurane; PIP, piperacillin; PTZ, piperacillin/tazobactam; R, resistant; S, susceptible; TCC, ticarcillin/clavulanate; TEM, temocillin; TGC, tigecycline; TIC, ticarcillin.

panels B and C). However, we identified 1 isolate resistant to ceftazidime/avibactam but susceptible to carbapenems (Figure 1). This isolate produces a new variant of KPC, named KPC-39, that has been reported to possess increased ceftazidime catalytic activity but also to have concomitantly lost its carbapenemase activity (*19*). Among other antimicrobial families, 84.9% KPC-*Kp* isolates were susceptible to tigecycline, 30.3% to sulfamethoxazole/trimethoprim, and 19.7% to ciprofloxacin (Figure 1, panel D). Resistance to aminoglycosides varied from 40.9% for amikacin to 75.8% for tobramycin.

bla_{KPC} Variants and Associated Acquired Resistance Genes

We performed WGS on 63 nonduplicate KPC-*Kp* isolates and identified their resistomes by using Illumina technology. In this collection, 44 isolates possessed the bla_{KPC-3} gene (69.8%), and 18 (28.5%) possessed the bla_{KPC-2} gene. One isolate harbored a novel single-nucleotide variant of bla_{KPC-3}, bla_{KPC-39} (Figure 1, panel B). Two isolates produced 2 carbapenemases, including 1 isolate coharboring bla_{KPC-2} and bla_{VIM-1} and another 1 coharboring bla_{KPC-2} and bla_{NDM-4} (Figure 2). We identified additional antimicrobial-resistance determinants in all isolates (Appendix 1, https://wwwnc.cdc.gov/EID/article/26/6/19-1517-App1.xlsx). Approximately 46% of the KPC-*Kp* isolates carried an extended spectrum β-lactamase encoding gene, including 22 isolates harboring $bla_{CTX-M-15}$; 4 isolates coharboring $bla_{CTX-M-14}$ and $bla_{CTX-M-15}$; and 3 isolates with $bla_{CTX-M-14}$, $bla_{CTX-M-3}$, or $bla_{CTX-M-65}$. The other acquired β-lactam resistance determinants encoded for the narrow-spectrum β-lactamases OXA-9 and TEM-1. To decipher quinolone resistance, we analyzed the presence of plasmid-mediated resistance determinants and known mutations in gyrase and topoisomerases (*20*–*22*). Resistance to quinolones was mediated by either mutation in gyrase *gyrA* affecting the residues S83 (p.S83I, n = 42; p.S83F, n = 7; and p.S83Y, n = 2) or D87 (p.D87N, n = 7; p.D87G, n = 3; and p.D87A, n = 2) or *parC* affecting the residues p.S80 (p.S80I, n = 51) or the production of *Qnr* (Qnr66-like, QnrB6, or QnrS1). Aminoglycoside resistance was caused by the production of the 16S RNA methylase RmtB (n = 7) or an aminoglycoside-modifying enzyme (encoding by *aac(3')-IIa, aadA1, aadA2, aac(6')-Ib-cr, or strA/strB*). Colistin resistance (n = 5) resulted systematically in chromosome-encoded resistance with alteration of the *mgrB* gene. In these isolates, 2 possessed a nonsense substitution (p.Q30*), 1 missense involved in colistin resistance (p.C27W) (*23*), an IS*Kpn26*-like inserted (with direct repeats [DRs] of 4 bp: TTAA), and a missense mutation leading to the disappearance of the start codon. No isolate had plasmid-encoded resistance *mcr*-1.

Genetic Diversity of KPC-*Kp*

Phylogenetic analysis revealed that the 63 KPC-*Kp* belonged to 15 different clones (STs) circulating in France (Figure 2; Appendix 1). Although many studies have asserted that CG258 is responsible for the spread of bla_{KPC} (*6*,*8*–*11*), in our collection, only 8 isolates (12.7%) belonged to CG258 (4 each for ST258 and ST512). Furthermore, epidemiologic investigations revealed no link between these isolates (Figure 2). Because KPC is not widely disseminated in France, we did not expect to observe such clonal diversity. Indeed, the epidemiology of KPC in France is not comparable to what was reported in nearby countries in Europe where KPC is endemic, such as Greece and Italy, and where the spread of $bla_{KPC-2/-3}$ is clearly linked to CG258 (*24*,*25*). Among the 8 isolates we identified that belonged to CG258, 3 were recovered from patients with travel history in Greece (isolate 175C3 and isolate 177H5) and Italy (isolate 160C2). In France, the 3 most prevalent clones are ST307 (with 15 isolates), ST147 (12 isolates), and ST13 (7 isolates). By using the 21 SNP cutoff value proposed by David et al. to identity a single hospital outbreak caused by a ST258 and ST512 cluster (*8*), we identified that the ST307 clone was overrepresented because of an outbreak that included 11 isolates (Figure 2; Appendix 2, https://wwwnc.cdc.gov/EID/article/26/6/19-1517-App2.pdf). However, this ST307 also included 4 isolates that were not related to this outbreak, such as the 195I4 strain, which was isolated from a patient who traveled in Crete (Greece) and possesses an additional carbapenemase-encoding gene (bla_{NDM-4}). The second most prevalent clone, ST147, seemed to have disseminated upon distinct events (Appendix 2). Most of the ST147 isolates have been recovered from different areas with no epidemiologic link between the patients (Figure 2). A link with Portugal has been identified for most (9/11) patients infected or colonized with a KPC-3–producing *K. pneumoniae* of ST147 (Figure 2). The same link with Portugal was observed for 4 patients infected or colonized with a KPC-3–producing *K. pneumoniae* of ST231. Strains from ST383 represented a small outbreak for which cross contamination was evidenced (<20 SNPs between 4 isolates [Appendix 2]). One isolate (171J7) was distantly related to other clones and corresponded to *K. variicola*. KPC-2-producing *K. pneumoniae* isolates of ST11 were predominantly linked to patients who had a history of travel in Asia (China and Vietnam), where this ST is known to be the main vector of bla_{KPC} dissemination.

Diversity of Genetic Vehicle Involved in Spread of *bla*$_{KPC}$

Analysis of the close genetic context of *bla*$_{KPC}$ highlighted diversity in the genetic structures at the origin of the acquisition of the carbapenemase-encoding gene. The well-known Tn*4401a* (in 29 isolates) and Tn*4401d* (in 26 isolates) were the most prevalent structures identified (Figure 2 and 3; Appendix 1). The KPC-*Kp* of the 2 main clones ST307 and ST147, *bla*$_{KPC}$, is carried on Tn*4401a* in ST307 and Tn*4401d* in ST147. Two unrelated isolates (ST11–167I9 and the *K. variicola* 171J7 isolate) harbored *bla*$_{KPC}$ in the Tn*4401b* isoform. In the remaining 6 isolates (ST273–171J9, ST147–199D1, ST1788–189B3,

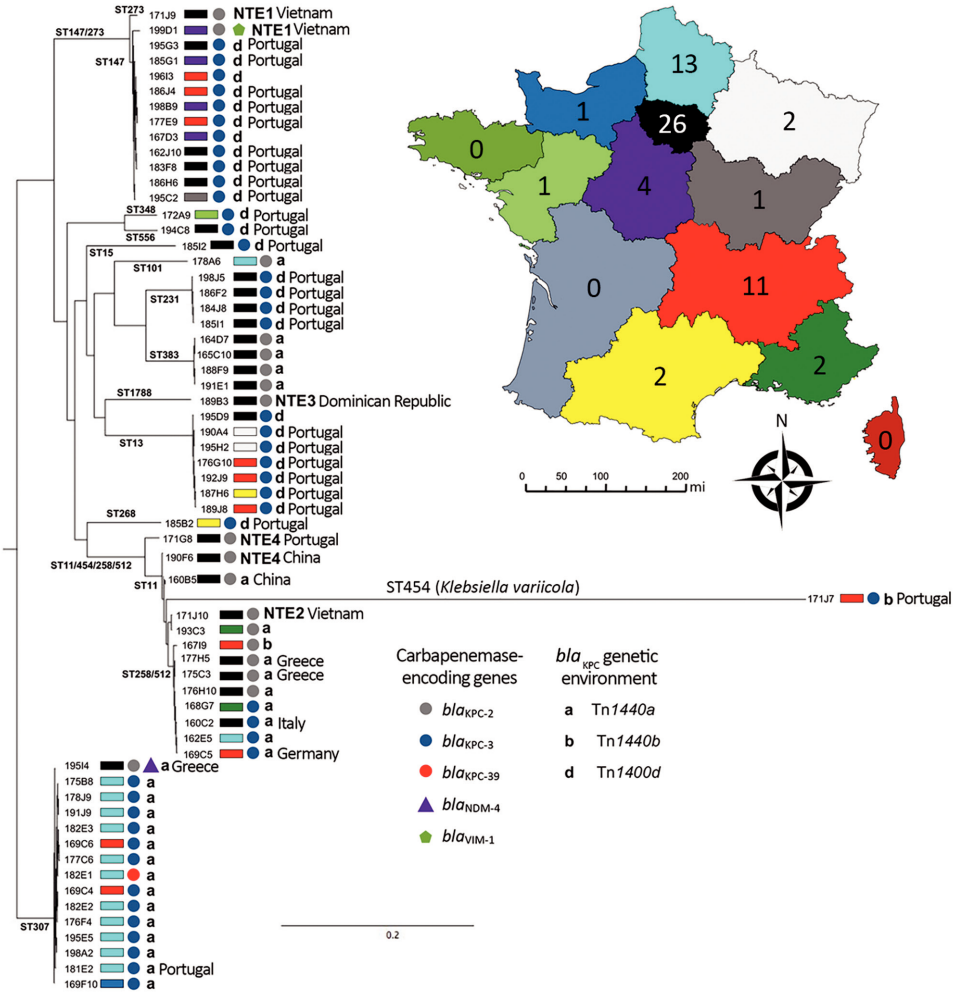

Figure 2. Phylogenetic analysis of *Klebsiella pneumoniae* carbapenemase–producing *K. pneumoniae* isolates, France, 2018. STs are indicated on the branches of the tree. Colored circles, triangles, or pentagons indicate carbapenemase type. Colored rectangles indicate region where isolates were recovered, as indicated on inset map; numbers on map indicate number of isolates. Genetic context indicated by isoform of Tn*4401* or NTE. Labels indicate links with foreign countries. Scale bar on tree indicates the number of single-nucleotide polymorpisms per position of common sequences. NTE, non-Tn*4401* element; ST, sequence type.

ST11–171G8, ST11–190F6, and ST11–171J10), bla_{KPC-2} is localized in an NTE element (Figures 2, 3). Although 3 isolates belonged to ST11, they displayed 200–800 SNPs of differences along their core genome, indicating that they were unrelated (Appendix 2). The links with 3 different countries (Portugal for ST11–171G8, China for ST11–190F6, and Vietnam for ST11–171J10) are consistent with this unrelatedness. Analysis of NTE elements revealed 4 different structures even if common features were observed (Figure 3). For instance, the presence of a fragment of IS*Kpn6* downstream of bla_{KPC} and a copy of IS*Kpn27* upstream were always present (Figure 3). DRs of TATAGG bracketing IS*Kpn27* indicated a transposition process that occurred inside the resolvase gene of Tn*3*. Immediately upstream of bla_{KPC-2} (74 bp), the presence of the inverted repeat right of Tn*3* is present in all NTE, indicating that all these structures were related. However, the NTE differed by the size of the deletions that are present between IS*Kpn27* and bla_{KPC-2} (from 280 bp in NTE-190F6 to 940 bp in NTE-199D1). We could observe a remnant of bla_{TEM-1} in longer structures, but it was not functional anymore. Analysis of the 4 NTE revealed that in NTE-199D1, several copies of IS*26* bracketed the whole structure, indicating that this IS might be involved in its acquisition by transposition or a recombination event. IS*26* has been recently demonstrated to be able to transpose and thus create a class I transposon by targeting another copy of IS*26* (*26*). NTE-171J10 is inserted in the *fip* gene of IncN-type plasmids with the presence of DRs surrounding the NTE-171J0 (Figure 3). The *fip* gene has already been demonstrated to be an integration hot spot in IncN-type plasmids (*27*,*28*). DRs as well as putative inverted repeats of Tn*3*-family transposon are present at the integration site (Figure 3). Moreover, the presence of the complete Tn*3* transposase gene indicated that NTE-171J10 might be functional. In NTE-189B3, a new class I transposon carrying a protein of unknown function has been identified. DRs bracketed IS*Apu1* and IS*Apu2*, indicating a transposition process mediated by these close insertion sequences (Figure 3).

Discussion

In France, KPC producers (84.1% of *K. pneumoniae*) represent only 6.8% of all carbapenemase producers,

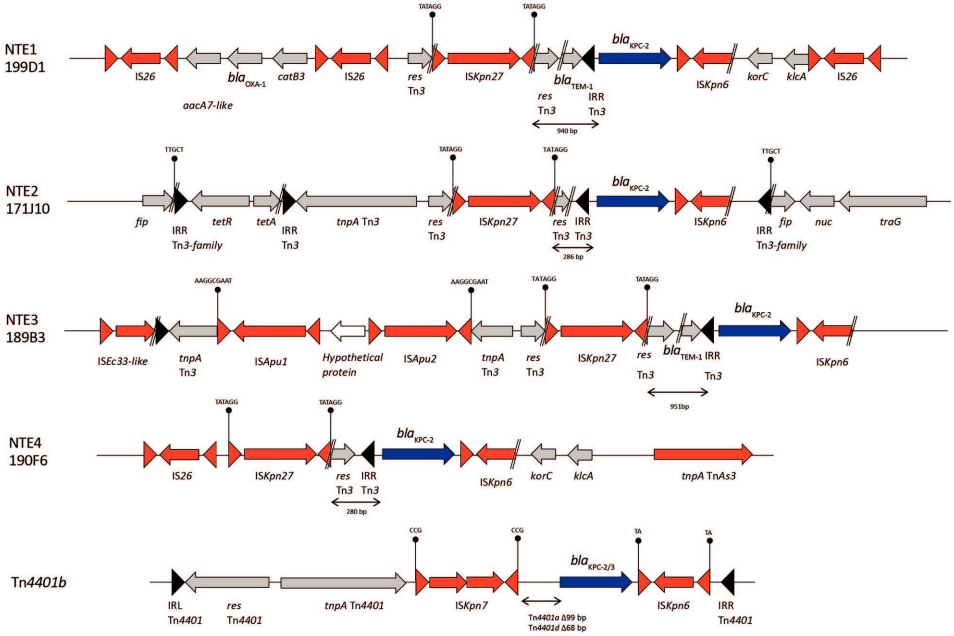

Figure 3. Analysis of genetic context of bla_{KPC} genes in *Klebsiella pneumoniae* carbapenemase–producing *K. pneumoniae* isolates, France, 2018. Different isoforms of NTE and Tn*4401* are represented. Inverted repeat sequences are indicated by triangles. Direct repeats are indicated by vertical lines. Genes are represented by arrows. NTE, non-Tn*4401* element.

far away from the global 72.7% found in Europe in 2013 (*8*). This relatively low prevalence of KPC producers in France compared with OXA-48–like and NDM producers has been reported since 2012 (*3*,*4*,*29*). We demonstrated unexpected clonal diversity among KPC-*Kp* isolated in France. A few overrepresented clones were identified (i.e., ST307, ST147, ST231, and ST13). However, ST307 was involved in a regional outbreak, whereas ST147 and ST13 were identified in different parts of France. Most of the patients colonized or infected with KPC-*Kp* had a clear link with Portugal, where these 4 STs were recently described to be the more prevalent (*30*,*31*). The KPC-2–producing *K. pneumoniae* isolates identified in France were predominantly recovered from patients with a history of travel in Greece (ST258) or Asia (ST11).

Regarding antimicrobial susceptibility of KPC-*Kp* in France, the relative high susceptibility to imipenem (30.3%) and meropenem to a lesser extent (18.2%) are in agreement with previous reports from Italy, where ST512 is highly prevalent (26.6% susceptibility to meropenem) (*32*). Conversely, data from the United States and Taiwan indicated that KPC-*Kp* are more resistant to carbapenems in those parts of the world, where ST258 is more prevalent (*33*,*34*).

Altogether, our results indicate that the KPC-*Kp* epidemiology has changed in Europe during the past 5 years. In 2018, ST258 and ST512 *K. pneumoniae* were no longer the main drivers of KPC resistance, at least in several non–KPC-endemic countries of western Europe, such as France and Portugal (*30*,*31*). KPC-*Kp* epidemiology also appears to have begun changing in some countries, such as Italy and Colombia, where CG-258 KPC-*Kp* was previously known to be endemic. This change is indicated by the reported emergence of ST307 and ST273 KPC-*Kp* in Sicilia (Italy) (*35*) and ST307 and ST14 KPC-*Kp* in Colombia (*36*). This change in the global epidemiology of KPC-*Kp* might have an effect on the identification of these carbapenemase producers with the molecular methods dedicated to the identification of GC258 *K. pneumoniae* (*37*,*38*).

In addition, our study highlights the dissemination of bla_{KPC} genes in high-risk clones of *K. pneumoniae* (ST307 and ST147), genetic features that might provide an advantage in adaptation to the hospital environment and the human host (*39*). These clones already convey several antimicrobial-resistance genes, including genes encoding other carbapenemases of NDM and OXA-48–like types (*40*,*41*). Accordingly, we might now fear the emergence of ST307 and ST147 high-risk clones of *K. pneumoniae* that can co-produce multiple carbapenemases. A recent study demonstrated the importance of ST307 in the dissemination of $bla_{OXA-181}$ in South Africa (*42*). In that study, >600 isolates belonging to ST307 were recovered and analyzed, and the results demonstrated the importance of this clone as a carrier of carbapenemase genes in all continents. Another study used Bayesian analysis to demonstrate that ST307 emerged in the mid-1990s (*43*). ST307 had been strongly associated with the diffusion of $bla_{CTX-M-15}$ (*43*) and now is associated with the dissemination of carbapenemase genes (*42*).

In conclusion, we found that the epidemiology of KPC-*Kp* has changed in Europe, in particular, with emergence of non–CG258 KPC-*Kp* isolates in France, linked to dissemination from Portugal. This change in epidemiology has to be considered by microbiologists because a few diagnostic assays specifically designed for the identification of ST-258 KPC-*Kp* isolates will not be able to detect non–CG258 KPC-*Kp* isolates.

This work was funded in part by the University Paris-Sud, France. L.D., T.N., and R.A.B. are members of the Laboratory of Excellence in Research on Medication and Innovative Therapeutics, which is supported by a grant from France's National Research Agency (grant no. ANR-10-LABX-33).

About the Author

Dr. Bonnin is an associate professor in Medical Microbiology at the University of Paris-Sud Medical School and a member of the Associated National Reference Center for Carbapenemase-Producing Enterobacteriaceae. His research focuses on bacterial genomes and transcriptomes with a special interest in mobile genetic elements and evolution.

References

1. Munoz-Price LS, Poirel L, Bonomo RA, Schwaber MJ, Daikos GL, Cormican M, et al. Clinical epidemiology of the global expansion of *Klebsiella pneumoniae* carbapenemases. Lancet Infect Dis. 2013;13:785–96. https://doi.org/10.1016/S1473-3099(13)70190-7
2. Tzouvelekis LS, Markogiannakis A, Psichogiou M, Tassios PT, Daikos GL. Carbapenemases in *Klebsiella pneumoniae* and other *Enterobacteriaceae*: an evolving crisis of global dimensions. Clin Microbiol Rev. 2012;25:682–707. https://doi.org/10.1128/CMR.05035-11
3. Dortet L, Cuzon G, Nordmann P. Dissemination of carbapenemase-producing *Enterobacteriaceae* in France, 2012. J Antimicrob Chemother. 2014;69:623–7. https://doi.org/10.1093/jac/dkt433
4. Dortet L, Cuzon G, Ponties V, Nordmann P. Trends in carbapenemase-producing *Enterobacteriaceae*, France, 2012 to 2014. Euro Surveill. 2017;22:22. https://doi.org/10.2807/1560-7917.ES.2017.22.6.30461
5. Nordmann P, Cuzon G, Naas T. The real threat of *Klebsiella pneumoniae* carbapenemase-producing bacteria. Lancet Infect Dis. 2009;9:228–36. https://doi.org/10.1016/S1473-3099(09)70054-4
6. Cuzon G, Naas T, Truong H, Villegas MV, Wisell KT, Carmeli Y, et al. Worldwide diversity of *Klebsiella pneumoniae*

that produce β-lactamase bla_{KPC-2} gene. Emerg Infect Dis. 2010;16:1349–56. https://doi.org/10.3201/eid1609.091389
7. Fu P, Tang Y, Li G, Yu L, Wang Y, Jiang X. Pandemic spread of bla $_{KPC-2}$ among *Klebsiella pneumoniae* ST11 in China is associated with horizontal transfer mediated by IncFII-like plasmids. Int J Antimicrob Agents. 2019;54:117–24. https://doi.org/10.1016/j.ijantimicag.2019.03.014
8. David S, Reuter S, Harris SR, Glasner C, Feltwell T, Argimon S, et al.; EuSCAPE Working Group; ESGEM Study Group. Epidemic of carbapenem-resistant *Klebsiella pneumoniae* in Europe is driven by nosocomial spread. Nat Microbiol. 2019;4:1919–29. https://doi.org/10.1038/s41564-019-0492-8
9. Chmelnitsky I, Shklyar M, Hermesh O, Navon-Venezia S, Edgar R, Carmeli Y. Unique genes identified in the epidemic extremely drug-resistant KPC-producing *Klebsiella pneumoniae* sequence type 258. J Antimicrob Chemother. 2013;68:74–83. https://doi.org/10.1093/jac/dks370
10. Fortini D, Villa L, Feudi C, Pires J, Bonura C, Mammina C, et al. Double copies of *bla*(KPC-3):Tn*4401a* on an IncX3 plasmid in *Klebsiella pneumoniae* successful clone ST512 from Italy. Antimicrob Agents Chemother. 2015;60:646–9. https://doi.org/10.1128/AAC.01886-15
11. Kitchel B, Rasheed JK, Patel JB, Srinivasan A, Navon-Venezia S, Carmeli Y, et al. Molecular epidemiology of KPC-producing *Klebsiella pneumoniae* isolates in the United States: clonal expansion of multilocus sequence type 258. Antimicrob Agents Chemother. 2009;53:3365–70. https://doi.org/10.1128/AAC.00126-09
12. Naas T, Cuzon G, Villegas MV, Lartigue MF, Quinn JP, Nordmann P. Genetic structures at the origin of acquisition of the β-lactamase bla_{KPC} gene. Antimicrob Agents Chemother. 2008;52:1257–63. https://doi.org/10.1128/AAC.01451-07
13. Araújo BF, Royer S, Campos PA, Ferreira ML, Gonçalves IR, Machado LG, et al. Insights into a novel Tn*4401* deletion (Tn*4401i*) in a multidrug-resistant *Klebsiella pneumoniae* clinical strain belonging to the high-risk clonal group 258 producing KPC-2. Int J Antimicrob Agents. 2018;52:525–7. https://doi.org/10.1016/j.ijantimicag.2018.08.011
14. Naas T, Cuzon G, Truong HV, Nordmann P. Role of IS*Kpn7* and deletions in bla_{KPC} gene expression. Antimicrob Agents Chemother. 2012;56:4753–9. https://doi.org/10.1128/AAC.00334-12
15. Girlich D, Bonnin RA, Jousset A, Naas T. Promoter characterization and expression of the bla_{KPC-2} gene in *Escherichia coli*, *Pseudomonas aeruginosa* and *Acinetobacter baumannii*. J Antimicrob Chemother. 2017;72:1597–601. https://doi.org/10.1093/jac/dkx044
16. Chen L, Mathema B, Chavda KD, DeLeo FR, Bonomo RA, Kreiswirth BN. Carbapenemase-producing *Klebsiella pneumoniae*: molecular and genetic decoding. Trends Microbiol. 2014;22:686–96. https://doi.org/10.1016/j.tim.2014.09.003
17. Girlich D, Bonnin RA, Bogaerts P, De Laveleye M, Huang DT, Dortet L, et al. Chromosomal amplification of the bla_{OXA-58} carbapenemase gene in a *Proteus mirabilis* clinical isolate. Antimicrob Agents Chemother. 2017;61:61.
18. Aziz RK, Bartels D, Best AA, DeJongh M, Disz T, Edwards RA, et al. The RAST Server: rapid annotations using subsystems technology. BMC Genomics. 2008;9:75. https://doi.org/10.1186/1471-2164-9-75
19. Jousset AB, Oueslati S, Creton E, Cotellon E, Sauvadet A, Emeraud C, et al. Resistance to ceftazidime-avibactam in a *Klebsiella pneumoniae* clinical isolate due to the production of KPC-39, a single amino-acid variant of KPC-3. Presented at: 29th European Congress of Clinical Microbiology and Infectious Diseases; Amsterdam, the Netherlands; 2019 April 13–16.
20. Ruiz J, Goñi P, Marco F, Gallardo F, Mirelis B, Jimenez De Anta T, et al. Increased resistance to quinolones in *Campylobacter jejuni*: a genetic analysis of *gyrA* gene mutations in quinolone-resistant clinical isolates. Microbiol Immunol. 1998;42:223–6. https://doi.org/10.1111/j.1348-0421.1998.tb02274.x
21. Vila J, Ruiz J, Goñi P, De Anta MT. Detection of mutations in *par*C in quinolone-resistant clinical isolates of *Escherichia coli*. Antimicrob Agents Chemother. 1996;40:491–3. https://doi.org/10.1128/AAC.40.2.491
22. Vila J, Ruiz J, Marco F, Barcelo A, Goñi P, Giralt E, et al. Association between double mutation in *gyrA* gene of ciprofloxacin-resistant clinical isolates of *Escherichia coli* and MICs. Antimicrob Agents Chemother. 1994;38:2477–9. https://doi.org/10.1128/AAC.38.10.2477
23. Poirel L, Jayol A, Nordmann P. Polymyxins: antibacterial activity, susceptibility testing, and resistance mechanisms encoded by plasmids or chromosomes. Clin Microbiol Rev. 2017;30:557–96. https://doi.org/10.1128/CMR.00064-16
24. Conte V, Monaco M, Giani T, D'Ancona F, Moro ML, Arena F, et al.; AR-ISS Study Group on Carbapenemase-Producing K. pneumoniae. Molecular epidemiology of KPC-producing *Klebsiella pneumoniae* from invasive infections in Italy: increasing diversity with predominance of the ST512 clade II sublineage. J Antimicrob Chemother. 2016;71:3386–91. https://doi.org/10.1093/jac/dkw337
25. Gartzonika K, Rossen JWA, Sakkas H, Rosema S, Priavali E, Friedrich AW, et al. Identification of a KPC-9-producing *Klebsiella pneumoniae* ST258 cluster among KPC-2-producing isolates of an ongoing outbreak in northwestern Greece: a retrospective study. Clin Microbiol Infect. 2018;24:558–60. https://doi.org/10.1016/j.cmi.2017.12.007
26. Harmer CJ, Hall RM. IS*26*-mediated formation of transposons carrying antibiotic resistance genes. MSphere. 2016;1:1. https://doi.org/10.1128/mSphere.00038-16
27. Gauthier L, Dortet L, Jousset AB, Mihaila L, Golse N, Naas T, et al. Molecular characterization of plasmid-encoded Tripoli MBL 1 (TMB-1) in *Enterobacteriaceae*. J Antimicrob Chemother. 2019;74:42–7.
28. Poirel L, Bonnin RA, Nordmann P. Analysis of the resistome of a multidrug-resistant NDM-1-producing *Escherichia coli* strain by high-throughput genome sequencing. Antimicrob Agents Chemother. 2011;55:4224–9. https://doi.org/10.1128/AAC.00165-11
29. Lee CR, Lee JH, Park KS, Kim YB, Jeong BC, Lee SH. Global dissemination of carbapenemase-producing *Klebsiella pneumoniae*: epidemiology, genetic context, treatment options, and detection methods. Front Microbiol. 2016;7:895. https://doi.org/10.3389/fmicb.2016.00895
30. Aires-de-Sousa M, Ortiz de la Rosa JM, Gonçalves ML, Pereira AL, Nordmann P, Poirel L. Epidemiology of carbapenemase-producing *Klebsiella pneumoniae* in a hospital, Portugal. Emerg Infect Dis. 2019;25:1632–8. https://doi.org/10.3201/eid2509.190656
31. Rodrigues C, Bavlovič J, Machado E, Amorim J, Peixe L, Novais Â. KPC-3-producing *Klebsiella pneumoniae* in Portugal linked to previously circulating non-CG258 lineages and uncommon genetic platforms (Tn*4401d*-IncFIA and Tn*4401d*-IncN). Front Microbiol. 2016;7:1000. https://doi.org/10.3389/fmicb.2016.01000
32. Cojutti P, Sartor A, Bassetti M, Scarparo C, Pea F. Is meropenem MIC increase against KPC-producing *Klebsiella pneumoniae* correlated with increased resistance rates against other antimicrobials with Gram-negative activity? J Glob Antimicrob Resist. 2018;14:238–41. https://doi.org/10.1016/j.jgar.2018.05.005

33. Chiu SK, Ma L, Chan MC, Lin YT, Fung CP, Wu TL, et al. Carbapenem nonsusceptible *Klebsiella pneumoniae* in Taiwan: dissemination and increasing resistance of carbapenemase producers during 2012–2015. Sci Rep. 2018;8:8468. https://doi.org/10.1038/s41598-018-26691-z
34. Kaiser RM, Castanheira M, Jones RN, Tenover F, Lynfield R. Trends in *Klebsiella pneumoniae* carbapenemase-positive *K. pneumoniae* in US hospitals: report from the 2007–2009 SENTRY Antimicrobial Surveillance Program. Diagn Microbiol Infect Dis. 2013;76:356–60. https://doi.org/10.1016/j.diagmicrobio.2013.03.032
35. Bonura C, Giuffrè M, Aleo A, Fasciana T, Di Bernardo F, Stampone T, et al.; MDR-GN Working Group. An update of the evolving epidemic of bla_{KPC} carrying *Klebsiella pneumoniae* in Sicily, Italy, 2014: emergence of multiple non-ST258 clones. PLoS One. 2015;10:e0132936. https://doi.org/10.1371/journal.pone.0132936
36. Ocampo AM, Chen L, Cienfuegos AV, Roncancio G, Chavda KD, Kreiswirth BN, et al. A two-year surveillance in five Colombian tertiary care hospitals reveals high frequency of non-CG258 clones of carbapenem-resistant *Klebsiella pneumoniae* with distinct clinical characteristics. Antimicrob Agents Chemother. 2015;60:332–42. https://doi.org/10.1128/AAC.01775-15
37. Chen L, Chavda KD, Mediavilla JR, Zhao Y, Fraimow HS, Jenkins SG, et al. Multiplex real-time PCR for detection of an epidemic KPC-producing *Klebsiella pneumoniae* ST258 clone. Antimicrob Agents Chemother. 2012;56:3444–7. https://doi.org/10.1128/AAC.00316-12
38. Yu F, Lv J, Niu S, Du H, Tang YW, Pitout JDD, et al. Multiplex PCR analysis for rapid detection of *Klebsiella pneumoniae* carbapenem-resistant (sequence type 258 [ST258] and ST11) and hypervirulent (ST23, ST65, ST86, and ST375) strains. J Clin Microbiol. 2018;56:56. https://doi.org/10.1128/JCM.00731-18
39. Villa L, Feudi C, Fortini D, Brisse S, Passet V, Bonura C, et al. Diversity, virulence, and antimicrobial resistance of the KPC-producing *Klebsiella pneumoniae* ST307 clone. Microb Genom. 2017;3:e000110. https://doi.org/10.1099/mgen.0.000110
40. Potel C, Ortega A, Martínez-Lamas L, Bautista V, Regueiro B, Oteo J. Interspecies transmission of the bla_{OXA-48} gene from a *Klebsiella pneumoniae* high-risk clone of sequence type 147 to different *Escherichia coli* clones in the gut microbiota. Antimicrob Agents Chemother. 2017;62:62. https://doi.org/10.1128/AAC.01699-17
41. Turton J, Davies F, Turton J, Perry C, Payne Z, Pike R. Hybrid resistance and virulence plasmids in "high-risk" clones of *Klebsiella pneumoniae*, including those carrying bla_{NDM-5}. Microorganisms. 2019;7:7. https://doi.org/10.3390/microorganisms7090326
42. Lowe M, Kock MM, Coetzee J, Hoosien E, Peirano G, Strydom K-A, et al. *Klebsiella pneumoniae* ST307 with $bla_{OXA-181}$, South Africa, 2014–2016. Emerg Infect Dis. 2019;25:739–47. https://doi.org/10.3201/eid2504.181482
43. Wyres KL, Hawkey J, Hetland MAK, Fostervold A, Wick RR, Judd LM, et al. Emergence and rapid global dissemination of CTX-M-15-associated *Klebsiella pneumoniae* strain ST307. J Antimicrob Chemother. 2019;74:577–81. https://doi.org/10.1093/jac/dky492

Address for correspondence: Laurent Dortet, Service de Bactériologie-Hygiène, Hôpital de Bicêtre, 78 rue du Général Leclerc, 94275 Le Kremlin-Bicêtre CEDEX, France; email: laurent.dortet@aphp.fr

Article II

Cabanel *et al*. bioRxiv 2021

Evolution of VIM-1 producing *Klebsiella pneumoniae* isolates from a hospital outbreak reveals the genetic bases of the loss of the urease-positive identification character

[1,2,]Nicolas Cabanel, [1,2,#]Isabelle Rosinski-Chupin, [1,2,3,#]Adriana Chiarelli,[1,2,#]Tatana Botin, [4]Marta Tato, [4]Rafael Canton and [1,2]Philippe Glaser*

[1]EERA Unit "Evolution and Ecology of Resistance to Antibiotics", Institut Pasteur-Assistance Publique/Hôpitaux de Paris - University Paris-Saclay, Paris, France
[2]UMR CNRS 3525, 75015, Paris France
[3]Sorbonne Université, 75015, Paris, France
[4]Servicio de Microbiología, Hospital Universitario Ramón y Cajal and Instituto Ramón y Cajal de Investigación Sanitaria (IRYCIS), Madrid, Spain.

#Contributed equally to this work

*Corresponding author:
Philippe GLASER,
Institut Pasteur, 28 Rue du Dr Roux, 75724 Paris Cedex 15,
Tel + 33 1 45 68 89 96 - E-mail: pglaser@pasteur.fr

Running title: Urease deficiency in *K. pneumoniae*

ABSTRACT

Outbreaks of carbapenemase producing *Klebsiella pneumoniae* (CP*Kp*) represent a major threat for hospitals. We molecularly characterized the first outbreak of VIM-1 producing *K. pneumoniae* in Spain, that raised fears about the spread of this strain or of the plasmid carrying $bla_{\text{VIM-1}}$. Through in-depth genomic analysis of 18 isolates recovered between October 2005 and September 2007, we show that 17 ST39 isolates were clonal, whereas the last isolate had acquired the VIM-1 plasmid from the epidemic clone. The index isolate carried 31 antibiotic resistance genes (ARGs) and was resistant to almost all antibiotics tested. Later isolates further gained mutations in efflux pumps regulators *ramR* and *opxR*, deletion of *mgrB* (colistin resistance) and frameshift mutations in *ompK36* (ß-lactam resistance) likely selected by antibiotic usage. Comparison with publicly available genome sequences and literature review revealed no sign of dissemination of this CP*Kp* strain. However, the VIM-1 plasmid was found in diverse *Enterobacterales* species, although restricted to Spain. One isolate became urease negative following IS*5075* transposition into *ureC*. Analysis of 9755 *K. pneumoniae* genomes showed the same *ureC*::IS*5075* insertion in 14.1% of the isolates and explained why urease activity is a variable identification trait for *K pneumoniae*. Transposition into *ureC* results from the similarity of its 3'-end and the terminal inverted repeats of Tn*21* like transposons, the targets of IS*5075* and related ISs. As these transposons frequently carry ARGs, this might explain the frequent chromosomal invasion by these ISs and *ureC* inactivation in multidrug resistant isolates.

IMPORTANCE

Evolution of multidrug resistant bacterial pathogens occurs at multiple scales, in the patient, locally in the hospital or more globally. Some mutations or gene acquisitions, for instance in response to antibiotic treatment, may be restricted to a single patient due to their high fitness cost. However, some events are more general. By analyzing the evolution of a hospital acquired multidrug resistant *K. pneumoniae* strain producing the carbapenemase VIM-1, we showed a likely environmental source in the hospital and identified mutations contributing to a further decrease in antibiotic susceptibility. By combining the genomic analysis of this outbreak with literature data and genome sequences available in databases, we showed that the VIM-1 plasmid has been acquired by different *Enterobacterales* but is only endemic in Spain. We also discovered that urease loss in *K. pneumoniae* results from the specific transposition of an IS element into the *ureC* gene and was more frequent in fluoroquinolone resistant isolates and carrying a carbapenemase gene.

INTRODUCTION

Klebsiella pneumoniae is responsible for a broad range of diseases including pneumonia, blood stream and urinary tract infections, mostly in health-care facilities. *K. pneumoniae* isolates are frequently resistant to multiple antibiotics and contribute to the dissemination of antibiotic resistance genes (ARGs) (1, 2). Carbapenems are among the last resort drugs to treat infections due to multidrug resistant (MDR) *K. pneumoniae* isolates expressing extended spectrum ß-lactamases (ESBL). From the end of the 20th century onwards, the emergence and dissemination of carbapenemase producing *K. pneumoniae* (CP*Kp*) resulting in high mortality rates is becoming a major public health threat. CP*Kp* hospital outbreaks are particularly feared with patient-to-patient transmission or transmission from the hospital environments to patient. Recently, a broad genomic study on CP*Kp* from 244 hospitals in 32 countries across Europe confirmed the existence of dominant lineages responsible for hospital outbreaks (3). In this study, the most prevalent multi locus sequence typing (MLST) types (STs) were from the Clonal Group (CG) 258, including ST258, 512, 340, 437 and 11, expressing the carbapenemase KPC (1, 3). Other prominent CP*Kp* STs are ST307 (4) and ST101 (5). However, the molecular epidemiology of CP*Kp* is different between countries (6) and a large proportion of CP*Kp* isolates belongs to diverse and rare STs denoting relevance of local epidemiology.

In 2007, we reported the first case of a hospital outbreak involving CP*Kp* isolates producing the VIM-1 carbapenemase in a hospital in Madrid, Spain (7, 8). During the same period, *Escherichia coli, Klebsiella oxytoca* and *Enterobacter cloacae* isolates also producing VIM-1 were identified in the same hospital (7). Pulsed field gel electrophoresis (PFGE) of *K. pneumoniae* isolates showed that they were likely clonal (8). This observation raised questions about the risk of endemicity of this clone and of the plasmid carrying $bla_{\text{VIM-1}}$ (7).

Whole genome sequencing (WGS) is becoming instrumental to decipher hospital outbreaks and to characterize transmission (9). Point mutations and small indels, particularly those leading to gene inactivation or contributing to antibiotic resistance are the main focus of genomic epidemiology studies. Other events, and in particular the mobility of insertion sequences (IS), more difficult to identify by short read sequencing, are frequently set asides. In this work, we have analyzed the evolution of the VIM-1 producing *K. pneumoniae* isolates from the outbreak (7, 8). In addition to mutations selected by antibiotics used in the hospital, we observed a diversity in ARGs and plasmid contents and mobility of transposable elements: a Group 2 intron and three ISs, IS*26*, IS*5075* and IS*421*. In one isolate, IS*5075* transposed into the *ure* operon encoding the urease subunits and led to a urease defective phenotype. By analyzing 9755 publicly available *K. pneumoniae* genome sequences we show that this insertion is frequent, explaining why some *K. pneumoniae* isolates display a urease negative phenotype. Furthermore, through a literature survey and the analysis of publicly available genome sequences, we did not find any evidence of further dissemination of this VIM-1 producing

strain. On the other hand, the *bla*$_{VIM-1}$ plasmid has broadly disseminated across *Enterobacterales* species but so far has only been isolated in Spain.

RESULTS

Genomic characterization of the outbreak isolates.

Illumina WGS of the 18 isolates and *in silico* MLST showed that the 17 first isolates (KP$_{VIM}$1-17) sharing the same PFGE profile belong to ST39 and the last isolate (KP$_{VIM}$18) to ST45 (Table S1). ST45 represents 1.5% (n=161) of the 10,515 genomes retrieved from NCBI (July. 2020). ST39 is less frequent, with only 38 other genome sequences, including seven isolates carrying carbapenemase genes (*bla*$_{KPC-3}$, n=3; *bla*$_{KPC-2}$, n=2; *bla*$_{NDM-1}$, n=2) but none *bla*$_{VIM-1}$. In order to characterize the strain responsible for the outbreak and to identify genetic events occurring during its evolution, we determined the complete genome sequence of the first isolate, KP$_{VIM}$1. KP$_{VIM}$1 chromosome is 5,351,626 base pairs (bp) long. It hosts four plasmids of 227,556 bp (pKP1-1), 110,924 bp (pKP1-2), 76,065 bp (pKP1-3) and 80,027 bp (pKP1-4) (Table S2). The chromosome and plasmids pKP1-1, 2 and 3 carry 31 ARGs (Table S2). Those ARGs target all major classes of antibiotics used against Gram negative bacteria. The porin gene *ompK*35 is interrupted by a non-sense mutation at codon 230. In agreement with the ARG content, KP$_{VIM}$1 is highly resistant to almost all antibiotics tested, remaining susceptible to only fluoroquinolones, tigecycline, and colistin and exhibiting an intermediate phenotype to amikacin, imipenem, meropenem and ertapenem (Fig. S1).

The *bla*$_{VIM-1}$ gene is carried by a gene cassette inserted in a type-1 integron expressing six ARGs in addition to *bla*$_{VIM-1}$ (*aacA4*, *dfrB1*, *ant1*, *cat*, *emrE* and *sul1*) carried by plasmid pKP1-3 (Fig. 1). BLASTN search using the nucleotide sequence of this plasmid against the contigs of KP$_{VIM}$18 showed 100% identity over its entire length, except a 1722 bp region containing a *catA* gene and missing in KP$_{VIM}$18. The VIM-1 plasmid was therefore likely transferred in the hospital from the outbreak strain to the ST45 *K. pneumoniae* isolate. Plasmid pKP1-3 belongs to IncL/M type. Comparison with complete plasmid sequences showed that pKP1-3 is more than 99.9% identical over 89% of its length to pKP1050-3b carrying *bla*$_{VIM-1}$ from a pan-drug resistant *K. pneumoniae* isolated in June 2016 in a hospital in Madrid (Fig. 1) (10). Both plasmids are highly similar to a *bla*$_{VIM-1}$ carrying plasmid from a *Salmonella* Typhimurium isolated in Spain in 2014 (11) and from *Klebsiella oxytoca* strains isolated in Madrid in 2016 (12). Recently, a closely related plasmid was identified in 28 *Serratia marcescens* VIM-1 producing isolates recovered in our hospital as KP$_{VIM}$1 between September 2016 and December 2018 (13). We identified by BLASTN search ten additional *K. pneumoniae* isolates carrying a plasmid closely related to pKP1-3, among the 85 *K. pneumoniae* genome sequences containing *bla*$_{VIM-1}$ of the 10,515 *K. pneumoniae* genome sequences from the NCBI (Table S3). Strikingly these isolates from four different STs were also all isolated in Spain between 2010 and 2016. Therefore, IncL/M plasmids

carrying bla_{VIM-1} likely arose in Spain following the insertion of a type 2 integron and disseminated locally only but were recurrently isolated in Spain between 2005 and 2018.

These plasmids are closely related to the broadly distributed IncL/M plasmid pOXA48 carrying the bla_{OXA-48} carbapenemase gene (10) (Fig. 1). pKP1-3 shows only seven SNPs over 57,386 conserved bp with pOXA-48_1639, the closest relative identified at the NCBI (accession number LR025105.1). BLASTN search against the NCBI database showed that one SNP was specific to all characterized IncL/M VIM-1 plasmids, whereas for the six other positions, two different allelic forms could be identified: one shared by pOXA-48_1639 and other pOXA-48 plasmids, the other by pKP1-3 and IncL/M plasmids carrying other resistance genes. Therefore, these two plasmids share a very recent common ancestor which acquired either Tn*1999* (14) carrying bla_{OXA-48} or an integron carrying bla_{VIM-1}.

Intra-hospital evolution of the ST39 lineage follows different paths associated with modifications of antibiotic susceptibility.

On the basis of the variants identified, we reconstructed the evolutionary path of the 17 ST39 isolates (Fig. 2A). In total, we identified 64 SNPs (59 in the chromosome and five in the plasmids), and seven short indels, five of which leading to a frameshift in coding frames (Table S4). Ancestral genotype for each polymorphism was predicted by parsimony based on BLASTN comparisons with complete *K. pneumoniae* genomes sequences at the NCBI. The first isolate, $KP_{VIM}1$, shows six SNPs compared to the reconstructed sequence of the last common ancestor (LCA) of the 17 isolates. We next analyzed the root to tip number of chromosomal SNPs according to the time of isolation. Despite the duration of the outbreak over 24 months, we did not observe a strong temporal correlation (Fig. 2B).

We identified three large chromosomal deletions: a 6.3 kb deletion encompassing *mgrB*, a 600 bp deletion of a type 6 secretion system (T6SS) immunity phospholipase A1-binding lipoprotein and a 55.4 kb deletion corresponding to the excision of an Integrated and Conjugative Element. Five large deletions in pKP1-1 and pKP1-2 led to the loss of clusters of ARGs (Table S2 and S4) in agreement with modifications of the antibiotic susceptibility profiles (Table S3).

Several genetic events were likely selected in response to antibiotic use in the hospital. The deletion of the *mgrB* gene led to colistin resistance in $KP_{VIM}17$ (Fig. S1). The same isolate was highly resistant to all ß-lactams including carbapenems due to the inactivation of the second major porin gene, *ompK*36, by a non-sense mutation leading to a stop codon at position 125. In addition, we identified three mutations disrupting *oqxR* and *ramR* genes encoding repressors of efflux systems. *oqxR* was inactivated by an IS*26* insertion in $KP_{VIM}12$ and $KP_{VIM}13$ whereas *ramR* was inactivated by a non-sense mutation in $KP_{VIM}14$ and by a frameshift mutation in $KP_{VIM}7$ and $KP_{VIM}8$. In agreement with previous comparisons of mutants of *oqxR* and *ramR* (15, 16, 17, 18), we observed a stronger decrease in the susceptibility to fluoroquinolones in the isolates mutated in *oqxR* ($KP_{VIM}12$ and $KP_{VIM}13$) and a

stronger decrease in tigecycline susceptibility in the isolates mutated in *ramR* (KP_{VIM}7, 8 and 14). In the case of KP_{VIM}14, the mutation in *ramR* likely compensates the loss of the *qnrA1* gene for fluoroquinolone susceptibility. The five isolates also showed a decreased susceptibility to cefepime and cefoxitin (Fig S2). To assess if there was any fitness cost associated with the increased resistance observed, we followed bacterial growth of these isolates in LB at 37°C. We observed in all four mutated isolates a decreased growth rate compared to KP_{VIM}1. The effect was more pronounced for Kp_{VIM}17 defective in both *mgrB* and *ompK36* which showed a 17% increase of generation time (Fig. 3).

Diversity of cryptic plasmid content.

In the course of the epidemic strain evolution, we also observed changes in plasmid content (Fig. 2). Plasmid pKp1-4 is a IncFII type, which is present in the first isolate KP_{VIM}1 and in three of the last isolates of the outbreak (KP_{VIM}11, 16, 17), reflecting its stability. This plasmid mainly codes for maintenance functions (toxin antitoxin systems, colicin B production and partition) and conjugative functions. BLASTN search against bacterial genome sequences showed that pKp1-4 is almost identical (99.7% identities over its entire length) to plasmid pEC14III (accession number KU932028.1) from an *E. coli* strain isolated in Finland. We also identified three plasmids specific to the lineage KP_{VIM}3 to KP_{VIM}8 (Fig. 2). These six isolates share a 34,017 bp-long, linear plasmid (pKP3-5) flanked by two 695 bp-long terminal inverted repeats (TIR). Unlike most linear plasmids described in *K. pneumoniae*, pKP3-5 is unrelated to phages. No adaptive functions were recognized, unlike in a similar linear plasmid pBSSB1 from *Salmonella* Typhi that encodes a flagellin structural gene (19). Search among *K. pneumoniae* genomes revealed 19 isolates carrying putative linear plasmids closely similar to pKP3-5 (>90% identities over 90% of the length). The two other plasmids are small high copy number plasmids: pKP3-6 (2811 bp) and pKP3-7 (3861 bp) that are present in strains KP_{VIM}3 to 6 and KP_{VIM}3 to 8 respectively (table S2 and Fig. 2). No adaptive functions were predicted in these two plasmids. For these three plasmids, we could not determine whether they were gained in the common ancestor of the KP_{VIM}3 to KP_{VIM}8 clade or lost by other isolates.

Insertion of IS*5075* into *ureC* is responsible for a urease negative phenotype in one isolate of the outbreak.

In addition to IS*26* insertion in *oqxR*, we identified nine transpositions of mobile genetic elements: two insertions of a class 2 intron named *Kl.pn.I5* (20), and two and five transpositions of IS*421* and IS*5075* respectively (Fig. 2). Compared to the other isolates, KP_{VIM}14 was characterized by an IS*5075* inserted three codons upstream of the stop codon of the *ureC* gene encoding the urease catalytic subunit (Fig. 4A). This insertion led to a *ureC* - IS*5075* transposase gene fusion. It might also have a polar effect on

197 the expression of the downstream genes of the operon: *ureE*, *ureF* and *ureG*. Accordingly, the
198 $KP_{VIM}14$ isolate was urease negative, whereas all other isolates from the outbreak were urease positive
199 (Fig. 4B). IS*5075,* like its close relative IS*4321,* is known to transpose into the TIR of Tn*21* and of
200 related transposons of the Tn*3* family (21). Tn*3* family transposons are abundant and diverse (22).
201 They are vectors of heavy metal resistance and ARGs (21). The 17 ST39 isolates harbor three copies
202 of IS*5075* inserted in a pKP1-2 Tn*3* family transposon, just after the initiation codon of a pKP1-1 gene
203 coding for a EAL motif protein and upstream a chromosomal permease gene (Fig 4A). Four
204 independent and identical transposition events of IS*5075* also occurred in the TIR of a Tn*3* family
205 transposon carried by pKP1-3, in $KP_{VIM}5$, $KP_{VIM}9$, $KP_{VIM}12$ and $KP_{VIM}15$ (Fig. 2A). Based on the
206 conservation of the insertion sites of IS*5075* we proposed a 13 bp consensus sequence for the IS*5075*
207 transposition site (Fig. 4A).
208
209 **Urease negative phenotypes are prevailing in several *K. pneumoniae* MDR lineages.**
210 Urea hydrolysis is an identification trait of *K. pneumoniae* in clinical microbiology laboratories.
211 However, earlier reports have shown that 5% of *K. pneumoniae* isolates are urease negative (23). In
212 order to determine whether this phenotype was due to similar IS*5075* transposition, we analyzed the
213 *ureC* gene in 9755 *K. pneumoniae* genomes quality filtered from the 10,515 genome sequences
214 retrieved from the NCBI (Table S5). BLASTN search showed that an IS*5075* or a similar IS was
215 inserted at the same position in 1380 isolates (14.1%) (Table 1). Search for other insertions or
216 frameshifts in *ureC* did not reveal other frequent mutations putatively responsible for a urease
217 deficiency.
218 To determine whether the insertion of IS*5075* into *ureC* preferentially occurred under specific genetic
219 backgrounds, we analyzed the 45 *K. pneumoniae* STs with at least 20 isolates (Fig. 5). We observed
220 that IS*5075* urease inactivation occurred throughout the species with variable frequencies. In seven
221 STs, all with less than 100 isolates, no insertion was observed. On the other hand, we observed a high
222 proportion of *ureC*::IS*5075* isolates in some STs like ST11 (884 out of 1603) and ST340 (18 out of 77
223 isolates) from the clonal group (CG) 258 and ST14 (58 out of 174). On the other hand, the two-other
224 dominant CG258 STs, ST258 and ST512, showed lower insertion frequencies of 6.9% and 4.1%
225 respectively.
226 As several of the STs associated with a higher frequency of *ureC*::IS*5075* include major MDR
227 lineages, we next analyzed the distribution of IS insertions in *ureC* in relation with antibiotic
228 resistance. As markers of antibiotic resistance, we considered mutations in fluoroquinolone resistance
229 (FQR) determinants, presence of carbapenemase genes and the number of ARGs among the 9755
230 *K. pneumoniae* genomes sequences (Table S5). Among these genome sequences, 62% were mutated in
231 *gyrA* and/or *parC* quinolone resistance-determining regions (QRDR), 53% carried carbapenemase

genes, and the average number of ARG was 9.33, revealing a strong bias towards MDR isolates (Table 1). Despite this bias, *ureC*::IS*5075* isolates appeared as even more resistant, with an average number of 12.5 ARGs compared to 8.8 in the remaining isolates, 94% of the isolates showing mutations in *gyrA* and/or *parC* and 86.4% carrying a carbapenemase gene (Table 1). To determine whether the insertion in *ureC* was associated with a global expansion of IS*5075* and related ISs, we estimated the copy number of these ISs in the different isolates (Table 1). Isolates with an IS insertion in *ureC* showed in average a 4-fold higher copy number of IS*5075* and related ISs than the remaining isolates (5 *vs*. 1.31). On the other hand, more than half of the isolates with an intact *ureC* genes did not carry a single IS*5075* copy (4334 out of 8375).

In a given ST a high frequency of *ureC*::IS*5075* isolates might result from frequent transposition events or from the expansion of lineages carrying the insertion. To discriminate between these two possibilities, we performed a whole genome phylogeny focusing on ST11, ST14 and ST258. ST11 was the most abundant ST among the genome sequences retrieved from the NCBI (16.4% of all isolates). Except two isolates WT for *gyrA* and *parC*, all ST11 isolates were predicted to be FQR (Fig. 6). The two most populated lineages belong to the K-types KL64 (n=622) and KL47 (n=463). These closely related lineages share the same three mutations in QRDR regions (ParC-80I, GyrA-83I, GyrA-87G) and carry the carbapenemase gene $bla_{\text{KPC-2}}$. Analysis of IS*5075* insertions in *ureC* showed an uneven distribution, mostly associated with these two lineages. In the KL64 clade, the IS insertion is ancestral, as it was present in all except six isolates (in pink). In the KL47 clade, two different situations were noted: an ancestral transposition event in the LCA of a specific sublineage, with the 138 isolates from this clade showing an IS*5075* in *ureC* (clade colored in red); a relatively high frequency of insertion in the other isolates of the clade (85 out of 324, 26%) likely resulting from multiple sporadic transposition events. Out of the two clades, the frequency of insertion is much lower (8.5%). All over the ST11 phylogeny, insertion in the *ureC* gene was associated with a higher copy number of IS*5075* with on average 5 copies compared to 1.7 in ST11 isolates with a WT *ureC* gene. Altogether these results show that the high proportion of ST11 isolates mutated in *ureC* results in a large part from the dissemination of two clades showing a high number of IS*5075* copies. The situation was similar among ST14 isolates, as all but one isolate (n=58) mutated in *ureC* belonged to a single FQR lineage suggesting that transposition occurred in the LCA of the lineage (in blue, Fig. S2). Isolates of this lineage also showed a high IS*5075* copy-number (n=5.1). In ST258, isolates were characterized by a lower frequency of IS insertion in *ureC* (6.9%). Most of the ST258 isolates cluster in two lineages expressing two different capsule operons of K-type KL106 and KL107 and associated mostly with the carbapenemase genes $bla_{\text{KPC-2}}$ and $bla_{\text{KPC-3}}$ respectively (24). In contrast to what was observed in ST11 and ST14, no expansion of a large *ureC*::IS*5075* clade occurred (Fig. S3). All but two isolates with the insertion in *ureC* belonged to the KL107 lineage. Strikingly, this clade was characterized by an higher

copy number of IS*5075* of 2.17 (5.24 for *ureC*::IS*5075* isolates) compared to only 0.12 for the KL106 lineage. Therefore, a major driver for insertion into *ureC* is the presence of an IS*5075* or a related IS and its active transposition.

DISCUSSION:

Whole genome sequencing has revolutionized molecular epidemiology and its use in outbreak analysis has contributed to decipher the path of pathogen transmission (25). Here, we investigated the first outbreak due to a VIM-1 producing *K. pneumoniae* in Spain (7, 8). The strain was extensively drug resistant and belongs to an uncommon ST (ST39). Based on available genomic data, we showed that the strain pre-existed in the hospital prior to the identification of the first isolate in October 2005. Furthermore, the weak temporal signal in the evolution (Fig. 2B) indicated a likely environmental reservoir in the hospital, which agrees with epidemiological data (7). Molecular clock for *K. pneumoniae* evolution have been estimated between 1.4 (26), 1.9 (27) and 3.65 (28) mutations/10^6bp/year. Here, the rate of SNPs/10^6bp/year is on the lower range (n=0.87). Growth as a biofilm compared to planktonic growth has been related to a greater diversity due to its structured organization, but a lower mutation rate due to a reduced number of generations (29). The diversity observed, the duration of the outbreak and the small number of SNPs agree with a biofilm source of the isolates. In line with this observation, we observed biofilm production of all the isolates but to variable levels (Fig. S4).

During the 2-year evolution of the strain, we observed variations in the antibiotic resistance profile. This was due on the one hand to the loss of ARGs (Table S4). On the other hand, mutations leading to the increased expression of efflux pumps or to a decreased drug permeation, and subsequently to a decreased susceptibility to some antibiotics, were selected. However, these mutations led to a fitness cost (Fig. 3), which might explain their limited expansion in the hospital.

By combining genomic analysis of the strain responsible for the outbreak with global genomic information retrieved from the NCBI and data from the literature, we were able to draw more general conclusions related to the risk associated with the outbreak strain and the VIM-1 plasmid. Likewise, we were able to identify the main reason for urease deficiency among *K. pneumoniae* isolates. Following the identification of the first VIM-1 isolates in Spain, their dissemination was a matter of concern (7). Although we showed that one single ST39 clone, except for one isolate, was responsible for the outbreak, we did not identify any new occurrence of this strain or of a ST39 isolate carrying $bla_{\text{VIM-1}}$ based on bibliographical survey and on the analysis of more than 10,000 *K. pneumoniae* genome sequences publicly available. Therefore, this clone seems to be restricted to the hospital where it was isolated. Conversely, we showed that the plasmid carrying $bla_{\text{VIM-1}}$ has disseminated among various *Enterobacterales* species. Transfers occurred probably in the hospital context, as suggested in

the case of a *S. typhimurium* isolate (11). Similarly, we showed the transmission of the VIM-1 plasmid between *K. pneumoniae* isolates in the course of the outbreak. We previously predicted similar transfers between *K. pneumoniae* and *E. coli* based on plasmid typing and size determination (7). This IncL/M plasmid is closely related to the broadly disseminated pOXA48. Our mutation analysis strongly suggests independent gain of a carbapenemase gene by very similar plasmid backbones showing only seven SNPs over 57,386 bp. In agreement with this hypothesis, the first OXA-48 plasmid was detected in Spain in 2009 (30) four years after the first VIM-1 isolate of the hospital outbreak (7).

Strikingly, IncL/M VIM-1 plasmids were until now only reported in Spain. A recent study on plasmids encoding VIM-1 from broad origins showed that among the 28 plasmids analyzed, nine were from IncL/M type (31). These nine plasmids were related to pKP1-3 and were from *K. pneumoniae*, *E. hormaechei* and *E. cloacae* and all from Spain. The limited dissemination of the VIM-1 plasmid might be due to the conjunction of different factors including: a lower conjugation efficiency than pOXA-48 plasmids, a fitness cost restricting its dissemination to environments characterized by strong selective pressures, such as the hospital, or a specificity in antibiotic prescription in Spain. Comparing IncL/M VIM-1 and OXA-48 plasmids provides a model system to study two closely related plasmids with two different spreading destinies.

Urease is considered in many bacterial species as a virulence factor beyond its contribution in harnessing urea as a nitrogen source (32). Urease participates in the adaptation to acidic conditions in a broad range of human pathogens, including *Helicobacter pylori* (33), *Yersinia enterocolytica* (34) and *Proteus mirabilis* (35). Urease is considered as a potential target for the development of new antibacterial drugs against enteric bacteria including *K. pneumoniae* (36). In *K. pneumoniae*, the urease has been shown to contribute to gastrointestinal colonization (37). However, a significant proportion of *K. pneumoniae* isolates are urease negative. Here, we showed that the inactivation of the operon is due to the transposition into the *ureC* gene of IS*5075* or of related ISs, like IS*4321*sharing the same specificity. Urease inactivation can be observed in both carriage isolates and isolates associated with clinical symptoms. For instance, we identified a cluster of eight IS*5075*::*ureC* ST340 isolates from a single institution (Fig. S5). These isolates were recovered from three patients, from urinary tract infections, blood culture, cerebrospinal fluid and fecal carriage (38).

Among *ureC*::IS*5075* isolates, we observed a higher prevalence of *gyrA* and *parC* mutations and of carbapenemase genes and more generally, a higher number of ARGs compared to *ureC* WT isolates (Table 1). This was partly due to a small number of MDR lineages mutated in *ureC*, such as those of ST11 and ST14, which represent 68% of the *ureC*::IS*5075* isolates (Fig 6 and Fig. S2). Nevertheless, this higher prevalence remained true even after removing ST11 and ST14 isolates (Table 1). IS insertions in *ureC* were also associated with a four-fold increase in IS*5075* copies, resulting from

337 additional transposition events (Table 1). This expansion of IS*5075* in some genetic backgrounds
338 might be a relatively recent event. Indeed, 44% of the isolates did not carry a single IS*5075* copy,
339 despite the high number of ARGs in the genomes we have analyzed. Indeed, IS*5075* most frequent
340 targets are the conserved TIR of transposons related to Tn*21*, which are ARG vectors and frequently
341 carried by conjugative plasmids as in the case of pKP1-2 (21, 22). This insertion specificity represents
342 a safe harbor for these ISs, as it does not incur fitness costs and ensures their dissemination. The
343 insertion into *ureC* results from the high similarity between its last codons and TIRs of Tn*21* and is
344 likely accidental. Therefore, the higher frequency of *ureC* inactivation in some MDR lineages might
345 merely be a consequence of a more frequent acquisition of Tn*3* family transposons carrying IS*5075*.
346 However, we cannot completely dismiss the possibility that the loss of urease activity might provide
347 MDR *K. pneumoniae* isolates with a selective advantage under some circumstances. This seems rather
348 unlikely, as other *ureC* inactivation events, including transpositions of other IS, would have been
349 expected in that case and we did not detect such events. Overall, IS*5075* transposition into
350 *K. pneumoniae ureC* gene represents a perfect example of chromosomal colonization by IS elements
351 carried by plasmids and leading to a homoplasic loss of function.
352
353 **Material and methods**
354
355 **Bacterial strains, growth conditions and antibiotic susceptibility testing.** VIM-1-producing
356 *K. pneumoniae* isolates were collected from 2005 through 2008 at Ramon y Cajal University Hospital
357 in Madrid, Spain (8) (tableS1). Colistin Minimum Inhibitory Concentration (MIC) was determined in
358 Mueller Hinton (MH) broth as recommended by the Clinical & Laboratory Standards Institute
359 guidelines (CLSI) (39). Susceptibility against 33 other antibiotics (Fig. S1) was evaluated by disk
360 diffusion on MH agar according to the CLSI guidelines (39). Fitness was determined by growth
361 curve analysis with an automatic spectrophotometer Tecan Infinite M200 during 24 hours in LB.
362 Wells were inoculated with overnight cultures at an OD_{600} of 0.001. OD_{600} was measured every
363 ten minutes. Background was determined as the average value of the OD_{600} of the three first time
364 points. Doubling time was determined between OD_{600} 0.005 and 0.03, where an almost perfect fit
365 with an exponential growth was observed.
366
367 **Genome sequencing and sequences analysis.** *K. pneumoniae* genomes were sequenced by using
368 the Illumina HiSeq2500 platform, with 100-nucleotides paired-end reads. Libraries were
369 constructed by using the Nextera XT kit (Illumina). Reads were assembled with SPAdes 3.9.0 (40).
370 The complete genome sequence of strain $KP_{VIM}1$ was determined by using the long-read PacBio
371 technology (Macrogen, Seoul, Korea). Reads were assembled with the RS_HGAP_Assembly.3

372 protocol (41) and with Canu (42). The consensus sequence was polished with Quiver (41) and
373 manually corrected by mapping Illumina reads with Breseq 0.33.2 (43). Variants compared to
374 $KP_{VIM}1$ were identified by using Breseq (43). Genome sequences were annotated with Prokka 1.14.5
375 (44) and analyzed for MLST and ARG content by using Kleborate (45) and Resfinder 4.0.1 (46).
376 Plasmid incompatibility groups were identified by using PlasmidFinder 2.1 (47). Directionality of
377 mutations was determined as previously described by performing BLASTN comparisons against
378 publicly available *K. pneumoniae* genomes (48).
379
380 **Analysis of publicly available genome sequences.** *K. pneumoniae* genome assemblies (n=10,515)
381 were downloaded from the NCBI (July 2020) with Batch Entrez (49). Genome sequences with more
382 than 200 contigs of more than 500 nt were filtered out. Sixty genome sequences (Bioproject
383 PRJNA510003) for which the contig ends corresponding to repeated sequences have been trimmed
384 were removed from the analysis. In total, we analyzed IS*5075* insertions in 9755 genome sequences
385 (Table S5). Phylogenetic analysis was performed by using Parsnp 1.1.2 (50). Recombination regions
386 were visually identified as regions with a higher SNP density by using Gingr (50) and removed from
387 the reference genome sequence (ST11: strain FDAARGOS_444, CP023941.1; ST14: strain 11,
388 CP016923.1; ST258: strain BIC-1, NZ_CP022573.1; ST340: strain EuSCAPE_RS081,
389 GCA_902155965.1_18858_1_51). Insertion of IS*5075* and of related ISs in *ureC* was identified by
390 BLASTN search using as query sequence the junction sequence detected in the $KP_{VIM}14$ isolate
391 encompassing 20 nt of the *ureC* gene and 20 nt of IS*5075* (E-value of $1e^{-10}$ as threshold). The integrity
392 of *ureC* was tested by tBLASTN using the UreC protein sequence from $KP_{VIM}1$ as query. Copy
393 number of IS*5075* and of closely related ISs was estimated by counting BLASTN hits (100% identity
394 over the entire length), using the first 17 nucleotides of IS*5075* sequence as query. Phylogenetic trees
395 were visualized by using iTOL (51).
396
397 **Phenotypic analyses.** Urease detection test was carried out with urea-indole medium (BIORAD)
398 according to the manufacturer's instructions. Biofilm formation capacity was measured by the
399 microtiter plate assay as previously described (52). *K. pneumoniae* strain LM21 (53) was used as a
400 positive control.
401
402 **Statistical analysis.** The significance of the differences in frequencies of IS insertions in *ureC* was
403 determined by using the Chi-square test. The significance of differences in IS*5075* copy numbers and
404 in ARGs numbers was determined by the Wilcoxon Rank sum tests. Both tests were performed by
405 using standard libraries contained within the R statistics package (http://www.R-project.org/).
406 Statistical significances of growth rate differences were tested with a Student's t-test.

Availability of data. All sequence data have been deposited at DDBJ/EMBL/GenBank (Bioproject PRJEB41835) with the following accession numbers: LR991401, $KP_{VIM}1$ chromosome and plasmids; LR991487, plasmid pKP1-5, LR991544, plasmid pKP1-6; LR991565, plasmid pKP1-7. Biosamples for the Illumina sequence data are listed in Table S1.

Acknowledgments

This work was supported by grants from the French National Research Agency (ANR-10-LABX-62-IBEID), and from the European Union's Horizon 2020 Research and Innovation Program under Grant Agreement No. 773830 (Project MedVetKlebs, One Health EJP). Adriana Chiarelli is part of the Pasteur - Paris University (PPU) International PhD Program, with funding from the Institut Carnot Pasteur Microbes & Santé, and the European Union's Horizon 2020 research and innovation programme under the Marie Sklodowska-Curie grant agreement No 665807.

The authors thank Rafael Patiño-Navarrete for his help in the bioinformatics analysis and Laurence Ma from the Institut Pasteur Biomics platform for her help in Illumina sequencing.

References

1. Wyres KL, Holt KE. 2018. *Klebsiella pneumoniae* as a key trafficker of drug resistance genes from environmental to clinically important bacteria. Curr Opin Microbiol 45:131-139.
2. Navon-Venezia S, Kondratyeva K, Carattoli A. 2017. *Klebsiella pneumoniae*: a major worldwide source and shuttle for antibiotic resistance. FEMS Microbiol Rev 41:252-275.
3. David S, Reuter S, Harris SR, Glasner C, Feltwell T, Argimon S, Abudahab K, Goater R, Giani T, Errico G, Aspbury M, Sjunnebo S, Feil EJ, Rossolini GM, Aanensen DM, Grundmann H. 2019. Epidemic of carbapenem-resistant *Klebsiella pneumoniae* in Europe is driven by nosocomial spread. Nat Microbiol 4:1919-1929.
4. Wyres KL, Hawkey J, Hetland MAK, Fostervold A, Wick RR, Judd LM, Hamidian M, Howden BP, Lohr IH, Holt KE. 2019. Emergence and rapid global dissemination of CTX-M-15-associated *Klebsiella pneumoniae* strain ST307. J Antimicrob Chemother 74:577-581.
5. Roe CC, Vazquez AJ, Esposito EP, Zarrilli R, Sahl JW. 2019. Diversity, Virulence, and Antimicrobial Resistance in Isolates From the Newly Emerging *Klebsiella pneumoniae* ST101 Lineage. Front Microbiol 10:542.
6. Bonnin RA, Jousset AB, Chiarelli A, Emeraud C, Glaser P, Naas T, Dortet L. 2020. Emergence of New Non-Clonal Group 258 High-Risk Clones among *Klebsiella pneumoniae* Carbapenemase-Producing *K. pneumoniae* Isolates, France. Emerg Infect Dis 26:1212-1220.
7. Tato M, Coque TM, Ruiz-Garbajosa P, Pintado V, Cobo J, Sader HS, Jones RN, Baquero F, Canton R. 2007. Complex clonal and plasmid epidemiology in the first outbreak of Enterobacteriaceae infection involving VIM-1 metallo-beta-lactamase in Spain: toward endemicity? Clin Infect Dis 45:1171-8.

8. Tato M, Morosini M, Garcia L, Alberti S, Coque MT, Canton R. 2010. Carbapenem Heteroresistance in VIM-1-producing *Klebsiella pneumoniae* isolates belonging to the same clone: consequences for routine susceptibility testing. J Clin Microbiol 48:4089-93.
9. Snitkin ES, Zelazny AM, Thomas PJ, Stock F, Henderson DK, Palmore TN, Segre JA. 2012. Tracking a hospital outbreak of carbapenem-resistant *Klebsiella pneumoniae* with whole-genome sequencing. Sci Transl Med 4:148ra116.
10. Lazaro-Perona F, Sotillo A, Troyano-Hernaez P, Gomez-Gil R, de la Vega-Bueno A, Mingorance J. 2018. Genomic path to pandrug resistance in a clinical isolate of *Klebsiella pneumoniae*. Int J Antimicrob Agents 52:713-718.
11. Sotillo A, Munoz-Velez M, Santamaria ML, Ruiz-Carrascoso G, Garcia-Bujalance S, Gomez-Gil R, Mingorance J. 2015. Emergence of VIM-1-producing *Salmonella enterica* serovar Typhimurium in a paediatric patient. J Med Microbiol 64:1541-3.
12. Perez-Vazquez M, Oteo-Iglesias J, Sola-Campoy PJ, Carrizo-Manzoni H, Bautista V, Lara N, Aracil B, Alhambra A, Martinez-Martinez L, Campos J. 2019. Characterization of Carbapenemase-Producing *Klebsiella oxytoca* in Spain, 2016-2017. Antimicrob Agents Chemother 63.
13. Pérez-Viso B, Hernández-García M, Ponce-Alonso M, Morosini MI, Ruiz-Garbajosa P, Del Campo R, Cantón R. 2020. Characterization of carbapenemase-producing *Serratia marcescens* and whole-genome sequencing for plasmid typing in a hospital in Madrid, Spain (2016-18). J Antimicrob Chemother doi:10.1093/jac/dkaa398.
14. Poirel L, Bonnin RA, Nordmann P. 2012. Genetic features of the widespread plasmid coding for the carbapenemase OXA-48. Antimicrob Agents Chemother 56:559-62.
15. Nicolas-Chanoine MH, Mayer N, Guyot K, Dumont E, Pagès JM. 2018. Interplay Between Membrane Permeability and Enzymatic Barrier Leads to Antibiotic-Dependent Resistance in *Klebsiella Pneumoniae*. Front Microbiol 9:1422.
16. Hentschke M, Wolters M, Sobottka I, Rohde H, Aepfelbacher M. 2010. *ramR* mutations in clinical isolates of *Klebsiella pneumoniae* with reduced susceptibility to tigecycline. Antimicrob Agents Chemother 54:2720-3.
17. Bialek-Davenet S, Lavigne JP, Guyot K, Mayer N, Tournebize R, Brisse S, Leflon-Guibout V, Nicolas-Chanoine MH. 2015. Differential contribution of AcrAB and OqxAB efflux pumps to multidrug resistance and virulence in *Klebsiella pneumoniae*. J Antimicrob Chemother 70:81-8.
18. Wan Nur Ismah WAK, Takebayashi Y, Findlay J, Heesom KJ, Avison MB. 2018. Impact of OqxR loss of function on the envelope proteome of *Klebsiella pneumoniae* and susceptibility to antimicrobials. J Antimicrob Chemother 73:2990-2996.
19. Baker S, Hardy J, Sanderson KE, Quail M, Goodhead I, Kingsley RA, Parkhill J, Stocker B, Dougan G. 2007. A novel linear plasmid mediates flagellar variation in *Salmonella Typhi*. PLoS Pathog 3:e59.
20. Candales MA, Duong A, Hood KS, Li T, Neufeld RA, Sun R, McNeil BA, Wu L, Jarding AM, Zimmerly S. 2012. Database for bacterial group II introns. Nucleic Acids Res 40:D187-90.
21. Partridge SR, Hall RM. 2003. The IS*1111* family members IS*4321* and IS*5075* have subterminal inverted repeats and target the terminal inverted repeats of Tn*21* family transposons. J Bacteriol 185:6371-84.
22. Nicolas E, Lambin M, Dandoy D, Galloy C, Nguyen N, Oger CA, Hallet B. 2015. The Tn*3*-family of Replicative Transposons. Microbiol Spectr 3(4):MDNA3-0060-2014.
23. Farmer JJ, 3rd, Davis BR, Hickman-Brenner FW, McWhorter A, Huntley-Carter GP, Asbury MA, Riddle C, Wathen-Grady HG, Elias C, Fanning GR, et al. 1985. Biochemical identification of new species and biogroups of Enterobacteriaceae isolated from clinical specimens. J Clin Microbiol 21:46-76.
24. Wyres KL, Holt KE. 2016. Klebsiella pneumoniae Population Genomics and Antimicrobial-Resistant Clones. Trends Microbiol 24:944-956.

25. Quainoo S, Coolen JPM, van Hijum S, Huynen MA, Melchers WJG, van Schaik W, Wertheim HFL. 2017. Whole-Genome Sequencing of Bacterial Pathogens: the Future of Nosocomial Outbreak Analysis. Clin Microbiol Rev 30:1015-1063.
26. Jousset AB, Bonnin RA, Rosinski-Chupin I, Girlich D, Cuzon G, Cabanel N, Frech H, Farfour E, Dortet L, Glaser P, Naas T. 2018. 4.5 years within-patient evolution of a colistin resistant KPC-producing *Klebsiella pneumoniae* ST258. Clin Infect Dis doi:10.1093/cid/ciy293.
27. Mathers AJ, Stoesser N, Sheppard AE, Pankhurst L, Giess A, Yeh AJ, Didelot X, Turner SD, Sebra R, Kasarskis A, Peto T, Crook D, Sifri CD. 2015. *Klebsiella pneumoniae* carbapenemase (KPC)-producing *K. pneumoniae* at a single institution: insights into endemicity from whole-genome sequencing. Antimicrob Agents Chemother 59:1656-63.
28. Stoesser N, Giess A, Batty EM, Sheppard AE, Walker AS, Wilson DJ, Didelot X, Bashir A, Sebra R, Kasarskis A, Sthapit B, Shakya M, Kelly D, Pollard AJ, Peto TE, Crook DW, Donnelly P, Thorson S, Amatya P, Joshi S. 2014. Genome sequencing of an extended series of NDM-producing *Klebsiella pneumoniae* isolates from neonatal infections in a Nepali hospital characterizes the extent of community- versus hospital-associated transmission in an endemic setting. Antimicrob Agents Chemother 58:7347-57.
29. Santos-Lopez A, Marshall CW, Scribner MR, Snyder DJ, Cooper VS. 2019. Evolutionary pathways to antibiotic resistance are dependent upon environmental structure and bacterial lifestyle. Elife 8:e47612
30. Pitart C, Solé M, Roca I, Fàbrega A, Vila J, Marco F. 2011. First outbreak of a plasmid-mediated carbapenem-hydrolyzing OXA-48 beta-lactamase in *Klebsiella pneumoniae* in Spain. Antimicrob Agents Chemother 55:4398-401.
31. Matsumura Y, Peirano G, Bradford PA, Motyl MR, DeVinney R, Pitout JDD. 2018. Genomic characterization of IMP and VIM carbapenemase-encoding transferable plasmids of Enterobacteriaceae. J Antimicrob Chemother 73:3034-3038.
32. Rutherford JC. 2014. The emerging role of urease as a general microbial virulence factor. PLoS Pathog 10:e1004062.
33. Eaton KA, Brooks CL, Morgan DR, Krakowka S. 1991. Essential role of urease in pathogenesis of gastritis induced by *Helicobacter pylori* in gnotobiotic piglets. Infect Immun 59:2470-5.
34. De Koning-Ward TF, Robins-Browne RM. 1995. Contribution of urease to acid tolerance in *Yersinia enterocolitica*. Infect Immun 63:3790-5.
35. Rózalski A, Sidorczyk Z, Kotełko K. 1997. Potential virulence factors of *Proteus* bacilli. Microbiol Mol Biol Rev 61:65-89.
36. Benoit SL, Schmalstig AA, Glushka J, Maier SE, Edison AS, Maier RJ. 2019. Nickel chelation therapy as an approach to combat multi-drug resistant enteric pathogens. Sci Rep 9:13851.
37. Maroncle N, Rich C, Forestier C. 2006. The role of *Klebsiella pneumoniae* urease in intestinal colonization and resistance to gastrointestinal stress. Res Microbiol 157:184-93.
38. Gorrie CL, Mirceta M, Wick RR, Judd LM, Wyres KL, Thomson NR, Strugnell RA, Pratt NF, Garlick JS, Watson KM, Hunter PC, McGloughlin SA, Spelman DW, Jenney AWJ, Holt KE. 2018. Antimicrobial-Resistant *Klebsiella pneumoniae* Carriage and Infection in Specialized Geriatric Care Wards Linked to Acquisition in the Referring Hospital. Clin Infect Dis 67:161-170.
39. Anonymous. Clinical and Laboratory Standards Institute (CLSI). Performance Standards for Antimicrobial Susceptibility Testing, Twenty-Seventh Informational Supplement, M100-S25 edition. Clinical and Laboratory Standards Institute, Wayne, PA.
40. Bankevich A, Nurk S, Antipov D, Gurevich AA, Dvorkin M, Kulikov AS, Lesin VM, Nikolenko SI, Pham S, Prjibelski AD, Pyshkin AV, Sirotkin AV, Vyahhi N, Tesler G, Alekseyev MA,

Pevzner PA. 2012. SPAdes: a new genome assembly algorithm and its applications to single-cell sequencing. J Comput Biol 19:455-77.

41. Chin CS, Alexander DH, Marks P, Klammer AA, Drake J, Heiner C, Clum A, Copeland A, Huddleston J, Eichler EE, Turner SW, Korlach J. 2013. Nonhybrid, finished microbial genome assemblies from long-read SMRT sequencing data. Nat Methods 10:563-9.
42. Koren S, Walenz BP, Berlin K, Miller JR, Bergman NH, Phillippy AM. 2017. Canu: scalable and accurate long-read assembly via adaptive k-mer weighting and repeat separation. Genome Res 27:722-736.
43. Deatherage DE, Barrick JE. 2014. Identification of mutations in laboratory-evolved microbes from next-generation sequencing data using breseq. Methods Mol Biol 1151:165-88.
44. Seemann T. 2014. Prokka: rapid prokaryotic genome annotation. Bioinformatics 30:2068-9.
45. Wyres KL, Nguyen TNT, Lam MMC, Judd LM, van Vinh Chau N, Dance DAB, Ip M, Karkey A, Ling CL, Miliya T, Newton PN, Lan NPH, Sengduangphachanh A, Turner P, Veeraraghavan B, Vinh PV, Vongsouvath M, Thomson NR, Baker S, Holt KE. 2020. Genomic surveillance for hypervirulence and multi-drug resistance in invasive *Klebsiella pneumonia*e from South and Southeast Asia. Genome Med 12:11.
46. Bortolaia V, Kaas RS, Ruppe E, Roberts MC, Schwarz S, Cattoir V, Philippon A, Allesoe RL, Rebelo AR, Florensa AF, Fagelhauer L, Chakraborty T, Neumann B, Werner G, Bender JK, Stingl K, Nguyen M, Coppens J, Xavier BB, Malhotra-Kumar S, Westh H, Pinholt M, Anjum MF, Duggett NA, Kempf I, Nykäsenoja S, Olkkola S, Wieczorek K, Amaro A, Clemente L, Mossong J, Losch S, Ragimbeau C, Lund O, Aarestrup FM. 2020. ResFinder 4.0 for predictions of phenotypes from genotypes. J Antimicrob Chemother doi:10.1093/jac/dkaa345.
47. Carattoli A, Zankari E, Garcia-Fernandez A, Voldby Larsen M, Lund O, Villa L, Moller Aarestrup F, Hasman H. 2014. In silico detection and typing of plasmids using PlasmidFinder and plasmid multilocus sequence typing. Antimicrob Agents Chemother 58:3895-903.
48. Almeida A, Villain A, Joubrel C, Touak G, Sauvage E, Rosinski-Chupin I, Poyart C, Glaser P. 2015. Whole-Genome Comparison Uncovers Genomic Mutations between Group B Streptococci Sampled from Infected Newborns and Their Mothers. J Bacteriol 197:3354-66.
49. Sayers EW, Karsch-Mizrachi I. 2016. Using GenBank. Methods Mol Biol 1374:1-22.
50. Treangen TJ, Ondov BD, Koren S, Phillippy AM. 2014. The Harvest suite for rapid core-genome alignment and visualization of thousands of intraspecific microbial genomes. Genome Biol 15:524.
51. Letunic I, Bork P. 2019. Interactive Tree Of Life (iTOL) v4: recent updates and new developments. Nucleic Acids Res 47:W256-w259.
52. O'Toole GA, Kolter R. 1998. Initiation of biofilm formation in *Pseudomonas fluorescens* WCS365 proceeds via multiple, convergent signalling pathways: a genetic analysis. Mol Microbiol 28:449-61.
53. Favre-Bonte S, Joly B, Forestier C. 1999. Consequences of reduction of *Klebsiella pneumoniae* capsule expression on interactions of this bacterium with epithelial cells. Infect Immun 67:554-61.

Figure Legends

Fig. 1. *Comparison of pKP1-3, pKp1050-3 and pOXA-48. 1*: A. Comparison of plasmids pKp1-3 and pKp1050-3 (Accession: CP023419.1) carrying bla_{VIM-1} and of pOXA-48_1639 carrying bla_{OXA-48} (Accession: LR025105.1). pOXA48_1639 was chosen as it was the closest relative to pKp1-3. Grey areas between ORFs denote nucleotide identities with a gradient representing 99% (light grey) to 100% (dark grey) identity. In red are represented identities of an inverted region. Genes are indicated by arrows with a color code as in the figure key. Antibiotic resistance genes are numbered as follows, 1: *catA1*; 2 and 4: *msrE_1*; 3 and 5: *mph*E; 6: bla_{VIM-1}; 7: *aac*A4_2; 8: *dfr*B1 9: *ant*1_2; 10: *cat*_2; 11: *emr*E; 12: *fol*P_4; 13: bla_{OXA-48}. B. Analysis of the SNPs detected between pKP1-3 and pOXA-48_1639. Occurrence of SNP among publicly available IncL/M plasmids ware identified by BLASTN. SNPs position in pKp1-3 are indicated in the first line. Mut. indicates that the mutation is specific to IncL/M VIM-1 plasmids. For other positions, plasmids with the pKp1-3 allele or the pOXA-48_1639 allele are indicated in the second and third line respectively. pSCH909 carries bla_{OXA-10} and bla_{TEM-1}, but no carbapenemase gene.

Fig. 2. *Hospital evolution of the* K. pneumoniae *ST39 VIM-1 producing strain*. **A.** Phylogeny of the 17 isolates reconstructed by maximum parsimony. Numbers next to branches indicate the number of chromosomal SNPs in the corresponding branch. Presence of plasmids are indicated by colored points and transposition events by triangles. IS*26* insertion in *oqxR* occurred in the common ancestor of $KP_{VIM}12$ and $KP_{VIM}13$. **B.** Root to tip representation of the number of chromosomal SNPs according to the time (in days) following the isolation of the first isolate $KP_{VIM}1$. The trendline equation and the correlation coefficient are indicated on the graph.

Fig. 3. *Growth and generation times of isolates with decreased antibiotic susceptibility*. **A.** Growth of $KP_{VIM}1$ and of four isolates mutated in a repressor of efflux pumps ($KP_{VIM}8$, $KP_{VIM}12$ and $KP_{VIM}14$) or in *mgrB* and *ompK36* ($KP_{VIM}17$) was followed by using an automatic plate reader. Background was subtracted as described in the Material and methods section. During the first 90 minutes, the OD_{600} was below 0.0015 and its quantification is noisy. B. Box plot representation for 10 replicates of the generation times of the five isolates quantified in early exponential phase 2.5 hours following the start of the culture (OD_{600} between 0.005 and 0.04). Statistical significances were tested with a Student's t-test. ****, $P \leq 0{,}0001$; n.s. non-significant.

Fig. 4. *Urease inactivation following IS*5075 *transposition*. **A.** Sequence alignment of the sites targeted by IS*5075* among KP_{VIM} isolates. In blue, targets of transposition events occurring during the outbreak: *ureC* in $KP_{VIM}14$ and pKP1-3 Tn*21* in $KP_{VIM}5$, $KP_{VIM}9$, $KP_{VIM}12$ and $KP_{VIM}15$. The green triangles correspond to IS*5075* insertion sites. In red are indicated conserved bases. Stop and start codons are

underlined. B. Urease activity test of the 17 ST39 isolates. The number of each KP_{VIM} isolate is indicated on the well. A pink color of the indole reaction reveals a urease positive phenotype.

Fig. 5. *Distribution of IS*5075 *insertions in* ureC *among* K. pneumoniae *isolates*. Occurrence of IS*5075* insertion among the 45 STs with at least 20 isolates among 9755 *K. pneumoniae* genome sequences retrieved from the NCBI. Phylogeny was reconstructed using Parsnp (50) and by using a representative isolate from each ST. The tree was rooted according to David et al. (3). Blue bars indicate the % of isolates with an insertion in *ureC* (upper scale) and red dashes the number of isolates in the corresponding ST (lower scale)

Fig. 6: *Core genome phylogeny of* K. pneumoniae *ST11 isolates*. Phylogeny was obtained by using Parsnp (50) considering 1603 genomes passing the quality threshold. K-type, mutations in *gyrA* and *parC* QRDR, carbapenemase genes, $bla_{CTX\text{-}M}$ genes, copy-number of IS*5075* and related ISs and IS insertion in *ureC* are annotated by circles from inside to outside as indicated in the figure key (left). The *ureC* deficient KL64 lineage is in pink. The KL47 lineage is in blue and the *ureC* deficient sublineage in red. The two *gyrA*/*parC* WT isolates were used as outgroups to root the tree. The tree was visualized by using iTOL (51).

Table 1: Comparison of *ureC*::IS*5075* and *ureC* WT *K. pneumoniae* isolates for antibiotic resistance features and ARG and IS copy numbers.

		All	*ureC* WT	*ureC*::IS*5075*	$^{\$}$P values
$^{\#}$Number of isolates	All isolates	$^{\#}$9755	8375	1380 $^{@}$(14.1%)	
	Minus ST11 ST14	7978	7540	438 $^{@}$(5.4%)	
gyrA or *parC* QRDR mutated	All isolates	6062	4763 $^{\$}$(55.9%)	1299 $^{\&}$(94%)	1e-153
	Minus ST11 ST14	4367	4009 $^{\$}$(53.2%)	358 $^{\&}$(81.7%)	3e-31
Carbapenemase gene	All isolates	5146	3953 $^{\$}$(47.2%)	1193 $^{\&}$(86.4%)	6.3e-161
	Minus ST11 ST14	3677	3393 $^{\$}$(45%)	284 $^{\&}$(64.8%)	8.4e-16
Carbapenemase gene and *gyrA* or *parC* mutated	All isolates	4549	3376 $^{\$}$(40.3%)	1173 $^{\&}$(85%)	2.2e-208
	Minus ST11 ST14	3093	2829 $^{\$}$(36.5%)	264 $^{\&}$(60.2%)	3.3e-21
Average number of IS*5075* and related IS	All isolates	1.82	1.31	5	0
	Minus ST11 ST14	1.45	1.27	5,11	4.2e-207
Average ARGs number	All isolates	9.33	8.81	12.5	4.3e-101
	Minus ST11 ST14	8.7	8.51	11.74	1.6e-23

$^{\#}$After filtering out 760 genome sequences out of the 10,515 sequences retrieved from the NCBI. $^{@}$% of isolates with an IS insertion in *ureC*. $^{\$}$% of *ureC* WT isolates mutated in QRDR and/or carrier of carbapenemase genes. $^{\&}$% of *ureC*::IS*5075* isolates mutated in QRDR and/or carrier of carbapenemase genes. $^{\$}$Significance of the difference between *ureC*::IS*5075* and *ureC* as determined by the Chi-square or the Wilcoxon Rank sum statistical tests.

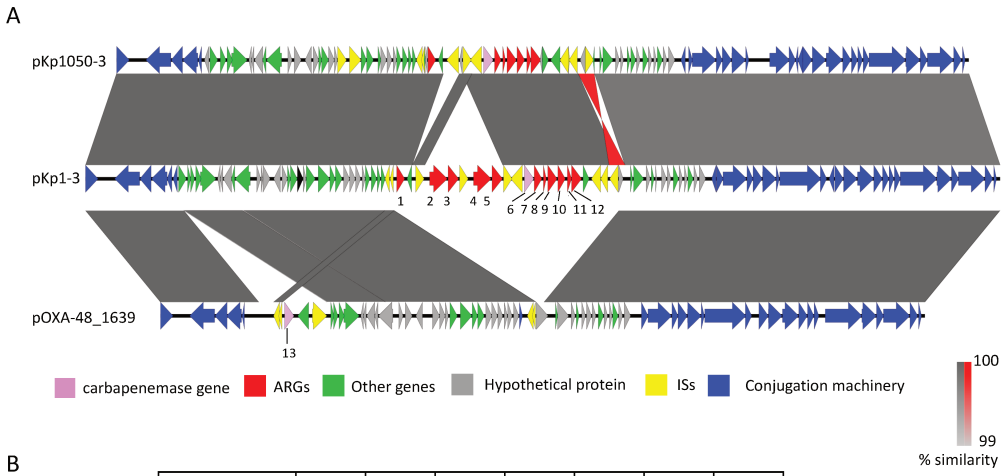

B

Position (pKp1-3)	11114	1937	15148	49053	50205	61124	75189
pKp1-3	Mut.	*Serratia marcescens*, SCH909 plasmid pSCH909 (CP063239.1)					
pOXA-48_1639	pOXA-48 plasmids						

Fig. 1.

20

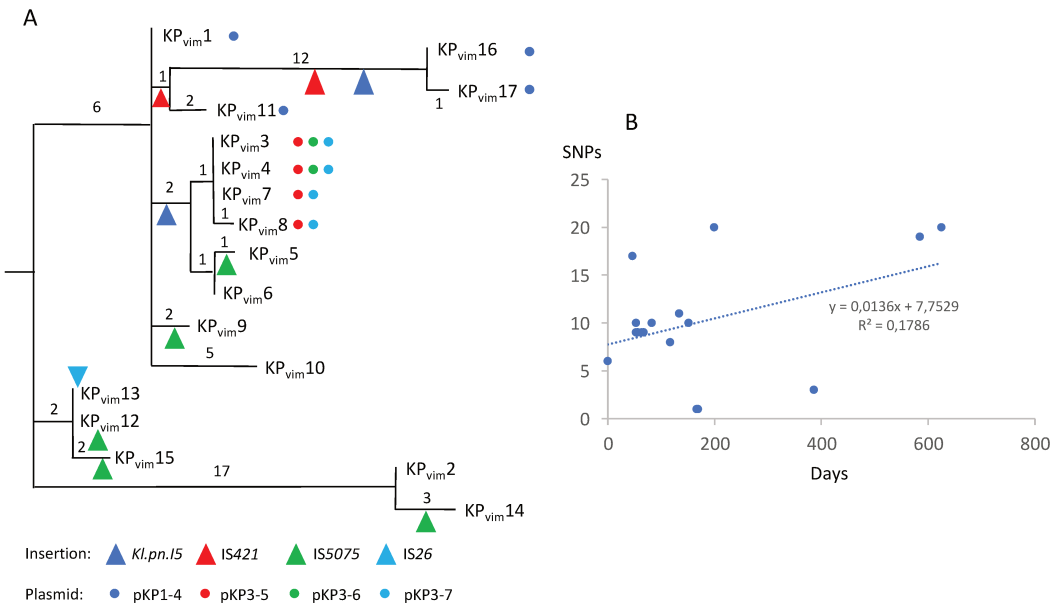

Fig. 2.

21

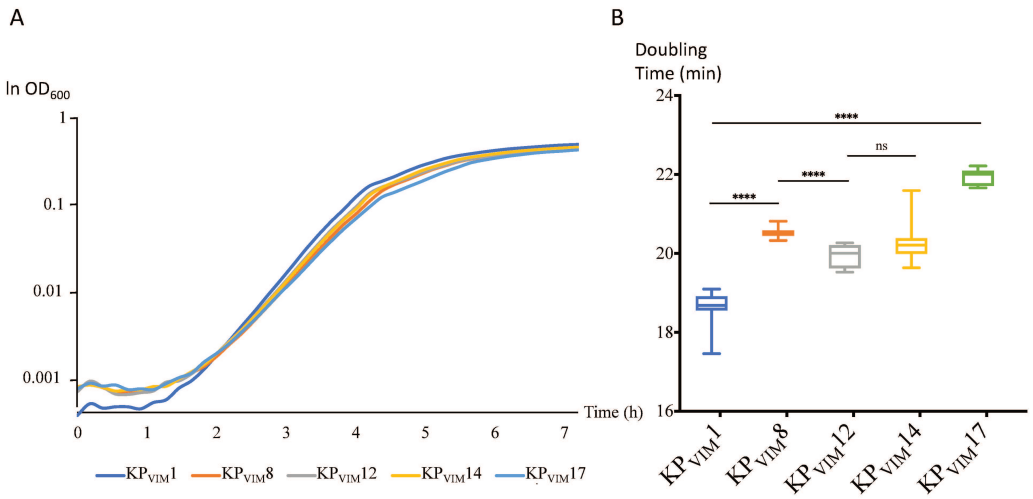
A
ln OD600
1
0.1
0.01
0.001
0
1
2
3
4
5
6
7
Time (h)
KPVIM1
KPVIM8
KPVIM12
KPVIM14
KPVIM17
B
Doubling
Time (min)
24
22
20
18
16
****
****
****
ns
KPVIM1
KPVIM8
KPVIM12
KPVIM14
KPVIM17

Fig. 3.

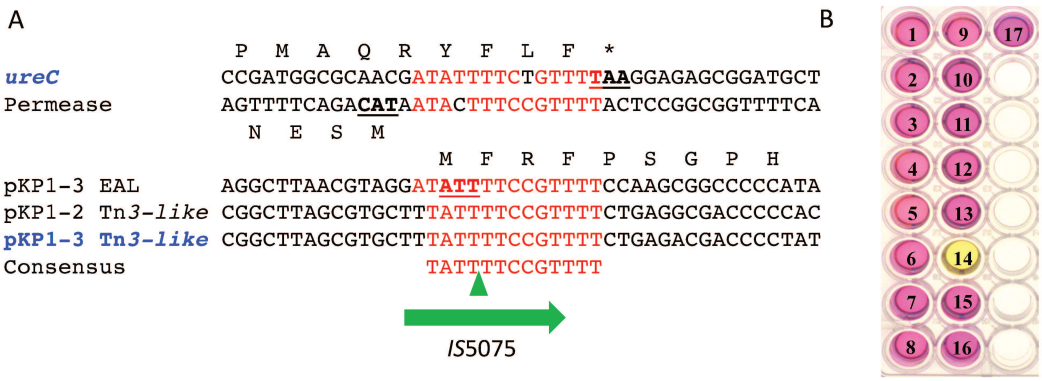
A
P M A Q R Y F L F *
ureC CCGATGGCGCAACGATATTTTCTGTTTTAAGGAGAGCGGATGCT
Permease AGTTTTCAGACATAATACTTTCCGTTTTACTCCGGCGGTTTTCA
N E S M
M F R F P S G P H
pKP1-3 EAL AGGCTTAACGTAGGATATTTTCCGTTTTCCAAGCGGCCCCCATA
pKP1-2 Tn3-like CGGCTTAGCGTGCTTTATTTTCCGTTTTCTGAGGCGACCCCCAC
pKP1-3 Tn3-like CGGCTTAGCGTGCTTTATTTTCCGTTTTCTGAGACGACCCCTAT
Consensus TATTTTCCGTTTT
IS5075
B
1
9
17
2
10
3
11
4
12
5
13
6
14
7
15
8
16

Fig. 4.

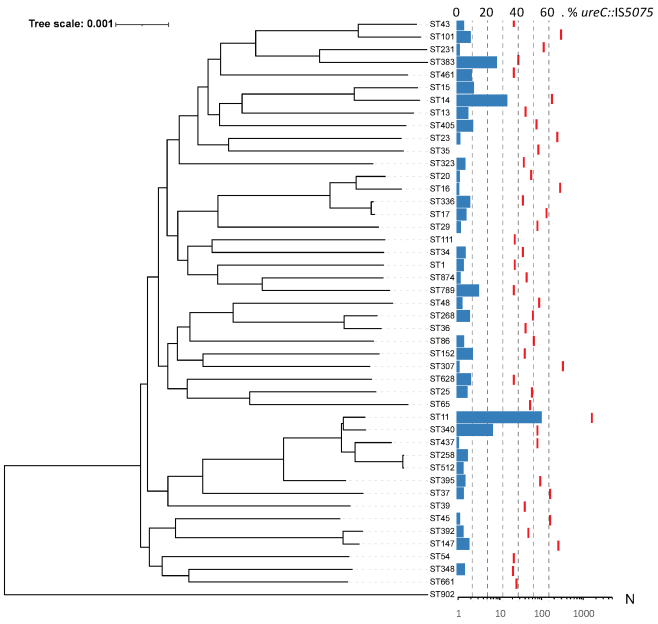
Tree scale: 0.001
0
20
40
60
. % ureC::IS5075
ST43
ST101
ST231
ST383
ST461
ST15
ST14
ST13
ST405
ST23
ST35
ST323
ST20
ST16
ST336
ST17
ST29
ST111
ST34
ST1
ST874
ST789
ST48
ST268
ST36
ST86
ST152
ST307
ST628
ST25
ST65
ST11
ST340
ST437
ST258
ST512
ST395
ST37
ST39
ST45
ST392
ST147
ST54
ST348
ST661
ST902
N
1
10
100
1000

Fig. 5.

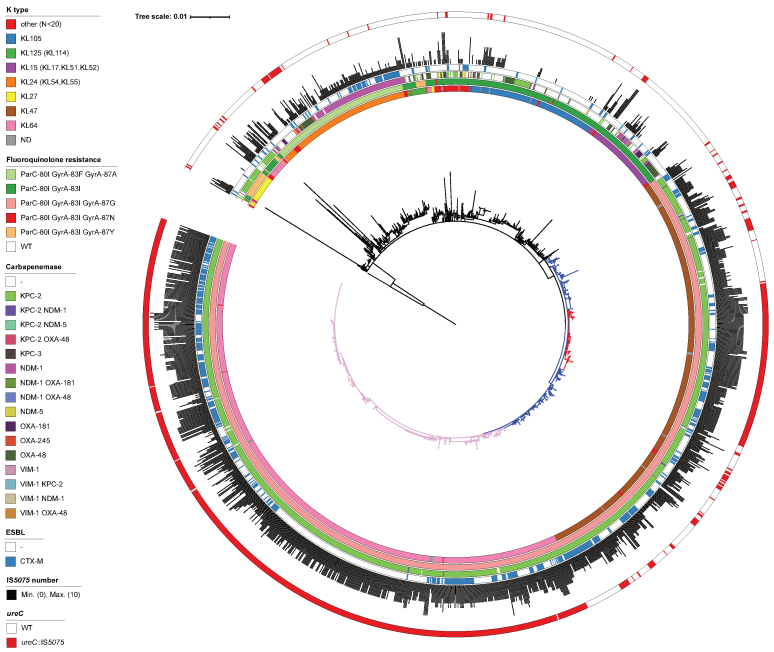
K type
other (N<20)
KL105
KL125 (KL114)
KL15 (KL17,KL51,KL52)
KL24 (KL54,KL55)
KL27
KL47
KL64
ND
Fluoroquinolone resistance
ParC-80I GyrA-83F GyrA-87A
ParC-80I GyrA-83I
ParC-80I GyrA-83I GyrA-87G
ParC-80I GyrA-83I GyrA-87N
ParC-80I GyrA-83I GyrA-87Y
WT
Carbapenemase
-
KPC-2
KPC-2 NDM-1
KPC-2 NDM-5
KPC-2 OXA-48
KPC-3
NDM-1
NDM-1 OXA-181
NDM-1 OXA-48
NDM-5
OXA-181
OXA-245
OXA-48
VIM-1
VIM-1 KPC-2
VIM-1 NDM-1
VIM-1 OXA-48
ESBL
-
CTX-M
IS5075 number
Min. (0), Max. (10)
ureC
WT
ureC::IS5075
Tree scale: 0.01

Fig. 6.

VIII. References

- Abeles, R.H., Maycock, A.L., 1976. Suicide enzyme inactivators. Acc. Chem. Res. 9, 313–319. https://doi.org/10.1021/ar50105a001
- Abokhalil, R.N., Elkhatib, W.F., Aboulwafa, M.M., Hassouna, N.A., 2020. Persisters of Klebsiella pneumoniae and Proteus mirabilis: A Common Phenomenon and Different Behavior Profiles. Curr Microbiol 77, 1233–1244. https://doi.org/10.1007/s00284-020-01926-3
- Abraham, E.P., Chain, E., 1988. An enzyme from bacteria able to destroy penicillin. 1940. Rev Infect Dis 10, 677–678.
- Abshire, K.Z., Neidhardt, F.C., 1993. Growth rate paradox of Salmonella typhimurium within host macrophages. J Bacteriol 175, 3744–3748. https://doi.org/10.1128/jb.175.12.3744-3748.1993
- Acar, J.F., Courvalin, P., Chabbert, Y.A., 1970. Methicillin-resistant staphylococcemia: bacteriological failure of treatment with cephalosporins. Antimicrob Agents Chemother (Bethesda) 10, 280–285.
- Adams-Sapper, S., Gayoso, A., Riley, L.W., 2018. Stress-Adaptive Responses Associated with High-Level Carbapenem Resistance in KPC-Producing Klebsiella pneumoniae. J Pathog 2018, 3028290. https://doi.org/10.1155/2018/3028290
- Adams-Sapper, S., Nolen, S., Donzelli, G.F., Lal, M., Chen, K., Justo da Silva, L.H., Moreira, B.M., Riley, L.W., 2015. Rapid induction of high-level carbapenem resistance in heteroresistant KPC-producing Klebsiella pneumoniae. Antimicrob Agents Chemother 59, 3281–3289. https://doi.org/10.1128/AAC.05100-14
- Adler, A., Ben-Dalak, M., Chmelnitsky, I., Carmeli, Y., 2015. Effect of Resistance Mechanisms on the Inoculum Effect of Carbapenem in Klebsiella pneumoniae Isolates with Borderline Carbapenem Resistance. Antimicrob Agents Chemother 59, 5014–5017. https://doi.org/10.1128/AAC.00533-15
- Aertsen, A., Michiels, C.W., 2005. Diversify or die: generation of diversity in response to stress. Crit Rev Microbiol 31, 69–78. https://doi.org/10.1080/10408410590921718
- Alam, M.R., Donabedian, S., Brown, W., Gordon, J., Chow, J.W., Zervos, M.J., Hershberger, E., 2001. Heteroresistance to vancomycin in Enterococcus faecium. J Clin Microbiol 39, 3379–3381. https://doi.org/10.1128/jcm.39.9.3379-3381.2001
- Alba, J., Ishii, Y., Thomson, K., Moland, E.S., Yamaguchi, K., 2005. Kinetics study of KPC-3, a plasmid-encoded class A carbapenem-hydrolyzing beta-lactamase. Antimicrob Agents Chemother 49, 4760–4762. https://doi.org/10.1128/AAC.49.11.4760-4762.2005
- Alexander, H.E., Leidy, G., 1947a. MODE OF ACTION OF STREPTOMYCIN ON TYPE b HEMOPHILUS INFLUENZAE: II. NATURE OF RESISTANT VARIANTS. J Exp Med 85, 607–621. https://doi.org/10.1084/jem.85.6.607
- Alexander, H.E., Leidy, G., 1947b. The present status of treatment for influenzal meningitis. Am J Med 2, 457–466. https://doi.org/10.1016/0002-9343(47)90091-0
- Allen, B.L., Gerlach, G.F., Clegg, S., 1991. Nucleotide sequence and functions of mrk determinants necessary for expression of type 3 fimbriae in Klebsiella pneumoniae. Journal of Bacteriology 173, 916–920. https://doi.org/10.1128/JB.173.2.916-920.1991
- Allison, C., Coleman, N., Jones, P.L., Hughes, C., 1992. Ability of Proteus mirabilis to invade human urothelial cells is coupled to motility and swarming differentiation. Infect Immun 60, 4740–4746. https://doi.org/10.1128/IAI.60.11.4740-4746.1992

- Alvarez, D., Merino, S., Tomás, J.M., Benedí, V.J., Albertí, S., 2000. Capsular polysaccharide is a major complement resistance factor in lipopolysaccharide O side chain-deficient Klebsiella pneumoniae clinical isolates. Infect Immun 68, 953–955. https://doi.org/10.1128/iai.68.2.953-955.2000
- Amábile-Cuevas, C.F., 2013. Antibiotic resistance: from Darwin to Lederberg to Keynes. Microb Drug Resist 19, 73–87. https://doi.org/10.1089/mdr.2012.0115
- Amanatidou, E., Matthews, A.C., Kuhlicke, U., Neu, T.R., McEvoy, J.P., Raymond, B., 2019. Biofilms facilitate cheating and social exploitation of β-lactam resistance in Escherichia coli. npj Biofilms Microbiomes 5, 36. https://doi.org/10.1038/s41522-019-0109-2
- Ambler, R.P., 1980. The structure of beta-lactamases. Philos Trans R Soc Lond B Biol Sci 289, 321–331. https://doi.org/10.1098/rstb.1980.0049
- Anderson, S.E., Sherman, E.X., Weiss, D.S., Rather, P.N., 2018. Aminoglycoside Heteroresistance in Acinetobacter baumannii AB5075. mSphere 3. https://doi.org/10.1128/mSphere.00271-18
- Andersson, D.I., Hughes, D., 2009. Gene amplification and adaptive evolution in bacteria. Annu Rev Genet 43, 167–195. https://doi.org/10.1146/annurev-genet-102108-134805
- Andersson, D.I., Jerlström-Hultqvist, J., Näsvall, J., 2015. Evolution of new functions de novo and from preexisting genes. Cold Spring Harb Perspect Biol 7. https://doi.org/10.1101/cshperspect.a017996
- Andersson, D.I., Nicoloff, H., Hjort, K., 2019. Mechanisms and clinical relevance of bacterial heteroresistance. Nat Rev Microbiol 17, 479–496. https://doi.org/10.1038/s41579-019-0218-1
- Antonelli, A., Coppi, M., Camarlinghi, G., Parisio, E.M., Nardone, M., Riccobono, E., Giani, T., Mattei, R., Rossolini, G.M., 2019. Variable performance of different commercial systems for testing carbapenem susceptibility of KPC carbapenemase-producing Escherichia coli. Clinical Microbiology and Infection 25, 1432.e1-1432.e4. https://doi.org/10.1016/j.cmi.2019.08.005
- Aono, R., Yamasaki, M., Tamura, G., 1979. High and selective resistance to mecillinam in adenylate cyclase-deficient or cyclic adenosine 3',5'-monophosphate receptor protein-deficient mutants of Escherichia coli. J Bacteriol 137, 839–845. https://doi.org/10.1128/JB.137.2.839-845.1979
- Aranega-Bou, P., George, R.P., Verlander, N.Q., Paton, S., Bennett, A., Moore, G., TRACE Investigators' Group, 2019. Carbapenem-resistant Enterobacteriaceae dispersal from sinks is linked to drain position and drainage rates in a laboratory model system. J Hosp Infect 102, 63–69. https://doi.org/10.1016/j.jhin.2018.12.007
- Arnoldini, M., Vizcarra, I.A., Peña-Miller, R., Stocker, N., Diard, M., Vogel, V., Beardmore, R.E., Hardt, W.-D., Ackermann, M., 2014. Bistable expression of virulence genes in salmonella leads to the formation of an antibiotic-tolerant subpopulation. PLoS Biol 12, e1001928. https://doi.org/10.1371/journal.pbio.1001928
- Baba, T., Ara, T., Hasegawa, M., Takai, Y., Okumura, Y., Baba, M., Datsenko, K.A., Tomita, M., Wanner, B.L., Mori, H., 2006. Construction of Escherichia coli K-12 in-frame, single-gene knockout mutants: the Keio collection. Mol Syst Biol 2, 2006.0008. https://doi.org/10.1038/msb4100050
- Bagley, S.T., 1985. Habitat association of Klebsiella species. Infect Control 6, 52–58. https://doi.org/10.1017/s0195941700062603
- Bahr, G., Vitor-Horen, L., Bethel, C.R., Bonomo, R.A., González, L.J., Vila, A.J., 2018. Clinical Evolution of New Delhi Metallo-β-Lactamase (NDM) Optimizes Resistance under Zn(II) Deprivation. Antimicrob Agents Chemother 62. https://doi.org/10.1128/AAC.01849-17
- Balaban, N.Q., Helaine, S., Lewis, K., Ackermann, M., Aldridge, B., Andersson, D.I., Brynildsen, M.P., Bumann, D., Camilli, A., Collins, J.J., Dehio, C., Fortune, S., Ghigo, J.-M., Hardt, W.-D., Harms, A., Heinemann, M., Hung, D.T., Jenal, U., Levin, B.R., Michiels, J., Storz, G., Tan, M.-W.,

Tenson, T., Van Melderen, L., Zinkernagel, A., 2019. Definitions and guidelines for research on antibiotic persistence. Nat Rev Microbiol 17, 441–448. https://doi.org/10.1038/s41579-019-0196-3

- Balaban, N.Q., Merrin, J., Chait, R., Kowalik, L., Leibler, S., 2004. Bacterial persistence as a phenotypic switch. Science 305, 1622–1625. https://doi.org/10.1126/science.1099390
- Balouiri, M., Sadiki, M., Ibnsouda, S.K., 2016. Methods for in vitro evaluating antimicrobial activity: A review. J Pharm Anal 6, 71–79. https://doi.org/10.1016/j.jpha.2015.11.005
- Band, V.I., Satola, S.W., Burd, E.M., Farley, M.M., Jacob, J.T., Weiss, D.S., 2018a. Carbapenem-Resistant Klebsiella pneumoniae Exhibiting Clinically Undetected Colistin Heteroresistance Leads to Treatment Failure in a Murine Model of Infection. mBio 9, e02448-17. https://doi.org/10.1128/mBio.02448-17
- Band, V.I., Weiss, D.S., 2019. Heteroresistance: A cause of unexplained antibiotic treatment failure? PLoS Pathog 15, e1007726. https://doi.org/10.1371/journal.ppat.1007726
- Baquero, F., Martínez, J.-L., 2017. Interventions on Metabolism: Making Antibiotic-Susceptible Bacteria. mBio 8. https://doi.org/10.1128/mBio.01950-17
- Barber, M., 1964. Naturally Occurring Methicillin-Resistant Staphylococci. Journal of General Microbiology 35, 183–190. https://doi.org/10.1099/00221287-35-2-183
- Bardet, L., Baron, S., Leangapichart, T., Okdah, L., Diene, S.M., Rolain, J.-M., 2017. Deciphering Heteroresistance to Colistin in a Klebsiella pneumoniae Isolate from Marseille, France. Antimicrob. Agents Chemother. 61. https://doi.org/10.1128/AAC.00356-17
- Barrett, F.F., McGehee, R.F., Finland, M., 1968. Methicillin-resistant Staphylococcus aureus at Boston City Hospital. Bacteriologic and epidemiologic observations. N Engl J Med 279, 441–448. https://doi.org/10.1056/NEJM196808292790901
- Barrett, R.D.H., Schluter, D., 2008. Adaptation from standing genetic variation. Trends Ecol Evol 23, 38–44. https://doi.org/10.1016/j.tree.2007.09.008
- Barrick, J.E., Lenski, R.E., 2009. Genome-wide mutational diversity in an evolving population of Escherichia coli. Cold Spring Harb Symp Quant Biol 74, 119–129. https://doi.org/10.1101/sqb.2009.74.018
- Barrick, J.E., Yu, D.S., Yoon, S.H., Jeong, H., Oh, T.K., Schneider, D., Lenski, R.E., Kim, J.F., 2009. Genome evolution and adaptation in a long-term experiment with Escherichia coli. Nature 461, 1243–1247. https://doi.org/10.1038/nature08480
- Beceiro, A., Maharjan, S., Gaulton, T., Doumith, M., Soares, N.C., Dhanji, H., Warner, M., Doyle, M., Hickey, M., Downie, G., Bou, G., Livermore, D.M., Woodford, N., 2011. False extended-spectrum {beta}-lactamase phenotype in clinical isolates of Escherichia coli associated with increased expression of OXA-1 or TEM-1 penicillinases and loss of porins. J Antimicrob Chemother 66, 2006–2010. https://doi.org/10.1093/jac/dkr265
- Bengoechea, J.A., Sa Pessoa, J., 2019. Klebsiella pneumoniae infection biology: living to counteract host defences. FEMS Microbiol Rev 43, 123–144. https://doi.org/10.1093/femsre/fuy043
- Bergmiller, T., Andersson, A.M.C., Tomasek, K., Balleza, E., Kiviet, D.J., Hauschild, R., Tkačik, G., Guet, C.C., 2017. Biased partitioning of the multidrug efflux pump AcrAB-TolC underlies long-lived phenotypic heterogeneity. Science 356, 311–315. https://doi.org/10.1126/science.aaf4762
- Besier, S., Smaczny, C., von Mallinckrodt, C., Krahl, A., Ackermann, H., Brade, V., Wichelhaus, T.A., 2007. Prevalence and clinical significance of Staphylococcus aureus small-colony variants in cystic fibrosis lung disease. J Clin Microbiol 45, 168–172. https://doi.org/10.1128/JCM.01510-06

- Betteridge, T., Merlino, J., Natoli, J., Cheong, E.Y.-L., Gottlieb, T., Stokes, H.W., 2013. Plasmids and bacterial strains mediating multidrug-resistant hospital-acquired infections are coresidents of the hospital environment. Microb Drug Resist 19, 104–109. https://doi.org/10.1089/mdr.2012.0104
- Bialek-Davenet, S., Criscuolo, A., Ailloud, F., Passet, V., Jones, L., Delannoy-Vieillard, A.-S., Garin, B., Le Hello, S., Arlet, G., Nicolas-Chanoine, M.-H., Decré, D., Brisse, S., 2014. Genomic definition of hypervirulent and multidrug-resistant Klebsiella pneumoniae clonal groups. Emerg Infect Dis 20, 1812–1820. https://doi.org/10.3201/eid2011.140206
- Bialek-Davenet, S., Lavigne, J.-P., Guyot, K., Mayer, N., Tournebize, R., Brisse, S., Leflon-Guibout, V., Nicolas-Chanoine, M.-H., 2015. Differential contribution of AcrAB and OqxAB efflux pumps to multidrug resistance and virulence in Klebsiella pneumoniae. Journal of Antimicrobial Chemotherapy 70, 81–88. https://doi.org/10.1093/jac/dku340
- Bigger, JosephW., 1944. TREATMENT OF STAPHYLOCOCCAL INFECTIONS WITH PENICILLIN BY INTERMITTENT STERILISATION. The Lancet 244, 497–500. https://doi.org/10.1016/S0140-6736(00)74210-3
- Black, D.S., Kelly, A.J., Mardis, M.J., Moyed, H.S., 1991. Structure and organization of hip, an operon that affects lethality due to inhibition of peptidoglycan or DNA synthesis. J Bacteriol 173, 5732–5739. https://doi.org/10.1128/jb.173.18.5732-5739.1991
- Blair, J.M.A., Webber, M.A., Baylay, A.J., Ogbolu, D.O., Piddock, L.J.V., 2015. Molecular mechanisms of antibiotic resistance. Nat Rev Microbiol 13, 42–51. https://doi.org/10.1038/nrmicro3380
- Blake, K.L., O'Neill, A.J., 2013. Transposon library screening for identification of genetic loci participating in intrinsic susceptibility and acquired resistance to antistaphylococcal agents. J Antimicrob Chemother 68, 12–16. https://doi.org/10.1093/jac/dks373
- Bleriot, I., Blasco, L., Delgado-Valverde, M., Gual de Torella, A., Ambroa, A., Fernandez-Garcia, L., Lopez, M., Oteo-Iglesias, J., Wood, T.K., Pascual, A., Bou, G., Fernandez-Cuenca, F., Tomas, M., 2020. Mechanisms of Tolerance and Resistance to Chlorhexidine in Clinical Strains of Klebsiella pneumoniae Producers of Carbapenemase: Role of New Type II Toxin-Antitoxin System, PemIK. Toxins (Basel) 12. https://doi.org/10.3390/toxins12090566
- Blin, C., Passet, V., Touchon, M., Rocha, E.P.C., Brisse, S., 2017. Metabolic diversity of the emerging pathogenic lineages of Klebsiella pneumoniae. Environ Microbiol 19, 1881–1898. https://doi.org/10.1111/1462-2920.13689
- Blumberg, P.M., Strominger, J.L., 1974. Interaction of penicillin with the bacterial cell: penicillin-binding proteins and penicillin-sensitive enzymes. Bacteriol Rev 38, 291–335.
- Blumer, J.L., 1997. Meropenem: evaluation of a new generation carbapenem. Int J Antimicrob Agents 8, 73–92. https://doi.org/10.1016/s0924-8579(96)00347-0
- Bódi, Z., Farkas, Z., Nevozhay, D., Kalapis, D., Lázár, V., Csörgő, B., Nyerges, Á., Szamecz, B., Fekete, G., Papp, B., Araújo, H., Oliveira, J.L., Moura, G., Santos, M.A.S., Székely, T., Balázsi, G., Pál, C., 2017. Phenotypic heterogeneity promotes adaptive evolution. PLoS Biol 15, e2000644. https://doi.org/10.1371/journal.pbio.2000644
- Bonnin, R.A., Jousset, A.B., Chiarelli, A., Emeraud, C., Glaser, P., Naas, T., Dortet, L., 2020. Emergence of New Non–Clonal Group 258 High-Risk Clones among Klebsiella pneumoniae Carbapenemase–Producing K. pneumoniae Isolates, France. Emerg. Infect. Dis. 26, 1212–1220. https://doi.org/10.3201/eid2606.191517

- Bonnin, R.A., Poirel, L., Carattoli, A., Nordmann, P., 2012. Characterization of an IncFII plasmid encoding NDM-1 from Escherichia coli ST131. PLoS One 7, e34752. https://doi.org/10.1371/journal.pone.0034752
- Bonura, C., Giuffrè, M., Aleo, A., Fasciana, T., Di Bernardo, F., Stampone, T., Giammanco, A., MDR-GN Working Group, Palma, D.M., Mammina, C., 2015. An Update of the Evolving Epidemic of blaKPC Carrying Klebsiella pneumoniae in Sicily, Italy, 2014: Emergence of Multiple Non-ST258 Clones. PLoS One 10, e0132936. https://doi.org/10.1371/journal.pone.0132936
- Borg, M.A., Scicluna, E.A., 2002. Over-the-counter acquisition of antibiotics in the Maltese general population. Int J Antimicrob Agents 20, 253–257. https://doi.org/10.1016/s0924-8579(02)00194-2
- Botelho-Nevers, E., Gouriet, F., Lepidi, H., Couvret, A., Amphoux, B., Dessi, P., Raoult, D., 2007. Chronic nasal infection caused by Klebsiella rhinoscleromatis or Klebsiella ozaenae: two forgotten infectious diseases. Int J Infect Dis 11, 423–429. https://doi.org/10.1016/j.ijid.2006.10.005
- Botsford, J.L., Harman, J.G., 1992. Cyclic AMP in prokaryotes. Microbiol Rev 56, 100–122.
- Boucher, H.W., Talbot, G.H., Bradley, J.S., Edwards, J.E., Gilbert, D., Rice, L.B., Scheld, M., Spellberg, B., Bartlett, J., 2009. Bad bugs, no drugs: no ESKAPE! An update from the Infectious Diseases Society of America. Clin Infect Dis 48, 1–12. https://doi.org/10.1086/595011
- Bowker, K.E., Holt, H.A., Reeves, D.S., MacGowan, A.P., 1996. Bactericidal activity, post antibiotic effect and modified controlled effective regrowth time of meropenem at high concentrations. J Antimicrob Chemother 38, 1055–1060. https://doi.org/10.1093/jac/38.6.1055
- Boyd, S.E., Livermore, D.M., Hooper, D.C., Hope, W.W., 2020. Metallo-β-Lactamases: Structure, Function, Epidemiology, Treatment Options, and the Development Pipeline. Antimicrob Agents Chemother 64. https://doi.org/10.1128/AAC.00397-20
- Bradley, J.S., Armstrong, J., Arrieta, A., Bishai, R., Das, S., Delair, S., Edeki, T., Holmes, W.C., Li, J., Moffett, K.S., Mukundan, D., Perez, N., Romero, J.R., Speicher, D., Sullivan, J.E., Zhou, D., 2016. Phase I Study Assessing the Pharmacokinetic Profile, Safety, and Tolerability of a Single Dose of Ceftazidime-Avibactam in Hospitalized Pediatric Patients. Antimicrob Agents Chemother 60, 6252–6259. https://doi.org/10.1128/AAC.00862-16
- Braun, S.D., Monecke, S., Thürmer, A., Ruppelt, A., Makarewicz, O., Pletz, M., Reißig, A., Slickers, P., Ehricht, R., 2014. Rapid Identification of Carbapenemase Genes in Gram-Negative Bacteria with an Oligonucleotide Microarray-Based Assay. PLoS ONE 9, e102232. https://doi.org/10.1371/journal.pone.0102232
- Brauner, A., Fridman, O., Gefen, O., Balaban, N.Q., 2016. Distinguishing between resistance, tolerance and persistence to antibiotic treatment. Nat Rev Microbiol 14, 320–330. https://doi.org/10.1038/nrmicro.2016.34
- Brauner, A., Shoresh, N., Fridman, O., Balaban, N.Q., 2017. An Experimental Framework for Quantifying Bacterial Tolerance. Biophys J 112, 2664–2671. https://doi.org/10.1016/j.bpj.2017.05.014
- Brisse, S., Verhoef, J., 2001. Phylogenetic diversity of Klebsiella pneumoniae and Klebsiella oxytoca clinical isolates revealed by randomly amplified polymorphic DNA, gyrA and parC genes sequencing and automated ribotyping. Int J Syst Evol Microbiol 51, 915–924. https://doi.org/10.1099/00207713-51-3-915
- Brunson, D.N., Maldosevic, E., Velez, A., Figgins, E., Ellis, T.N., 2019. Porin loss in Klebsiella pneumoniae clinical isolates impacts production of virulence factors and survival within macrophages. International Journal of Medical Microbiology 309, 213–224. https://doi.org/10.1016/j.ijmm.2019.04.001

- Buffet, A., Rocha, E.P.C., Rendueles, O., 2021. Nutrient conditions are primary drivers of bacterial capsule maintenance in Klebsiella. Proc. R. Soc. B. 288, 20202876. https://doi.org/10.1098/rspb.2020.2876
- Buijs, J., Dofferhoff, A.S.M., Mouton, J.W., van der Meer, J.W.M., 2006. Pathophysiology of in-vitro induced filaments, spheroplasts and rod-shaped bacteria in neutropenic mice. Clin Microbiol Infect 12, 1105–1111. https://doi.org/10.1111/j.1469-0691.2006.01503.x
- Bulik, C.C., Fauntleroy, K.A., Jenkins, S.G., Abuali, M., LaBombardi, V.J., Nicolau, D.P., Kuti, J.L., 2010. Comparison of meropenem MICs and susceptibilities for carbapenemase-producing Klebsiella pneumoniae isolates by various testing methods. J Clin Microbiol 48, 2402–2406. https://doi.org/10.1128/JCM.00267-10
- Bush, K., 2015. A resurgence of β-lactamase inhibitor combinations effective against multidrug-resistant Gram-negative pathogens. Int J Antimicrob Agents 46, 483–493. https://doi.org/10.1016/j.ijantimicag.2015.08.011
- Cano, V., March, C., Insua, J.L., Aguiló, N., Llobet, E., Moranta, D., Regueiro, V., Brennan, G.P., Millán-Lou, M.I., Martín, C., Garmendia, J., Bengoechea, J.A., 2015. Klebsiella pneumoniae survives within macrophages by avoiding delivery to lysosomes. Cell Microbiol 17, 1537–1560. https://doi.org/10.1111/cmi.12466
- Cantón, R., Coque, T.M., 2006. The CTX-M beta-lactamase pandemic. Curr Opin Microbiol 9, 466–475. https://doi.org/10.1016/j.mib.2006.08.011
- Carniel, E., 2001. The Yersinia high-pathogenicity island: an iron-uptake island. Microbes Infect 3, 561–569. https://doi.org/10.1016/s1286-4579(01)01412-5
- Caroff, N., Espaze, E., Gautreau, D., Richet, H., Reynaud, A., 2000. Analysis of the effects of -42 and -32 ampC promoter mutations in clinical isolates of Escherichia coli hyperproducing ampC. J Antimicrob Chemother 45, 783–788. https://doi.org/10.1093/jac/45.6.783
- Carrie, C., Walewski, V., Levy, C., Alexandre, C., Baleine, J., Charreton, C., Coche-Monier, B., Caeymaex, L., Lageix, F., Lorrot, M., Klosowski, S., Hess, L., Zafer, O., Gaudelus, J., Pinquier, D., Carbonnelle, E., Cohen, R., de Pontual, L., 2019. Klebsiella pneumoniae and Klebsiella oxytoca meningitis in infants. Epidemiological and clinical features. Arch Pediatr 26, 12–15. https://doi.org/10.1016/j.arcped.2018.09.013
- Carvalhaes, C.G., Cayo, R., Visconde, M.F., Barone, T., Frigatto, E.A.M., Okamoto, D., Assis, D.M., Juliano, L., Machado, A.M.O., Gales, A.C., 2014. Detection of carbapenemase activity directly from blood culture vials using MALDI-TOF MS: a quick answer for the right decision. Journal of Antimicrobial Chemotherapy 69, 2132–2136. https://doi.org/10.1093/jac/dku094
- Cassini, A., Högberg, L.D., Plachouras, D., Quattrocchi, A., Hoxha, A., Simonsen, G.S., Colomb-Cotinat, M., Kretzschmar, M.E., Devleesschauwer, B., Cecchini, M., Ouakrim, D.A., Oliveira, T.C., Struelens, M.J., Suetens, C., Monnet, D.L., Burden of AMR Collaborative Group, 2019. Attributable deaths and disability-adjusted life-years caused by infections with antibiotic-resistant bacteria in the EU and the European Economic Area in 2015: a population-level modelling analysis. Lancet Infect Dis 19, 56–66. https://doi.org/10.1016/S1473-3099(18)30605-4
- Cassini, A., Plachouras, D., Eckmanns, T., Abu Sin, M., Blank, H.-P., Ducomble, T., Haller, S., Harder, T., Klingeberg, A., Sixtensson, M., Velasco, E., Weiß, B., Kramarz, P., Monnet, D.L., Kretzschmar, M.E., Suetens, C., 2016. Burden of Six Healthcare-Associated Infections on European Population Health: Estimating Incidence-Based Disability-Adjusted Life Years through a Population Prevalence-Based Modelling Study. PLoS Med 13, e1002150. https://doi.org/10.1371/journal.pmed.1002150

- Castanheira, M., Deshpande, L.M., Mendes, R.E., Canton, R., Sader, H.S., Jones, R.N., 2019. Variations in the Occurrence of Resistance Phenotypes and Carbapenemase Genes Among Enterobacteriaceae Isolates in 20 Years of the SENTRY Antimicrobial Surveillance Program. Open Forum Infect Dis 6, S23–S33. https://doi.org/10.1093/ofid/ofy347
- Cavicchioli, R., Ripple, W.J., Timmis, K.N., Azam, F., Bakken, L.R., Baylis, M., Behrenfeld, M.J., Boetius, A., Boyd, P.W., Classen, A.T., Crowther, T.W., Danovaro, R., Foreman, C.M., Huisman, J., Hutchins, D.A., Jansson, J.K., Karl, D.M., Koskella, B., Mark Welch, D.B., Martiny, J.B.H., Moran, M.A., Orphan, V.J., Reay, D.S., Remais, J.V., Rich, V.I., Singh, B.K., Stein, L.Y., Stewart, F.J., Sullivan, M.B., van Oppen, M.J.H., Weaver, S.C., Webb, E.A., Webster, N.S., 2019. Scientists' warning to humanity: microorganisms and climate change. Nat Rev Microbiol 17, 569–586. https://doi.org/10.1038/s41579-019-0222-5
- Cerqueira, G.C., Earl, A.M., Ernst, C.M., Grad, Y.H., Dekker, J.P., Feldgarden, M., Chapman, S.B., Reis-Cunha, J.L., Shea, T.P., Young, S., Zeng, Q., Delaney, M.L., Kim, D., Peterson, E.M., O'Brien, T.F., Ferraro, M.J., Hooper, D.C., Huang, S.S., Kirby, J.E., Onderdonk, A.B., Birren, B.W., Hung, D.T., Cosimi, L.A., Wortman, J.R., Murphy, C.I., Hanage, W.P., 2017. Multi-institute analysis of carbapenem resistance reveals remarkable diversity, unexplained mechanisms, and limited clonal outbreaks. Proc Natl Acad Sci USA 114, 1135–1140. https://doi.org/10.1073/pnas.1616248114
- Chain, E., Florey, H.W., Gardner, A.D., Heatley, N.G., Jennings, M.A., Orr-Ewing, J., Sanders, A.G., 2005. THE CLASSIC: penicillin as a chemotherapeutic agent. 1940. Clin Orthop Relat Res 439, 23–26. https://doi.org/10.1097/01.blo.0000183429.83168.07
- Chambers, H.F., 1997. Methicillin resistance in staphylococci: molecular and biochemical basis and clinical implications. Clin Microbiol Rev 10, 781–791. https://doi.org/10.1128/CMR.10.4.781-791.1997
- Chambers, H.F., Hartman, B.J., Tomasz, A., 1985. Increased amounts of a novel penicillin-binding protein in a strain of methicillin-resistant Staphylococcus aureus exposed to nafcillin. J Clin Invest 76, 325–331. https://doi.org/10.1172/JCI111965
- Chand, M.S., MacArthur, C.J., 1997. Primary atrophic rhinitis: a summary of four cases and review of the literature. Otolaryngol Head Neck Surg 116, 554–558. https://doi.org/10.1016/s0194-5998(97)70311-5
- Chatterjee, I., Kriegeskorte, A., Fischer, A., Deiwick, S., Theimann, N., Proctor, R.A., Peters, G., Herrmann, M., Kahl, B.C., 2008. In vivo mutations of thymidylate synthase (encoded by thyA) are responsible for thymidine dependency in clinical small-colony variants of Staphylococcus aureus. J Bacteriol 190, 834–842. https://doi.org/10.1128/JB.00912-07
- Chen, L., Lin, J., Lu, H., Zhang, Xiucai, Wang, C., Liu, H., Zhang, Xiaoxiao, Li, J., Cao, J., Zhou, T., 2020. Deciphering colistin heteroresistance in Acinetobacter baumannii clinical isolates from Wenzhou, China. J Antibiot 73, 463–470. https://doi.org/10.1038/s41429-020-0289-2
- Chen, L., Mathema, B., Pitout, J.D.D., DeLeo, F.R., Kreiswirth, B.N., 2014. Epidemic Klebsiella pneumoniae ST258 is a hybrid strain. mBio 5, e01355-01314. https://doi.org/10.1128/mBio.01355-14
- Chen, M., Li, Y., Li, S., Tang, L., Zheng, J., An, Q., 2016. Genomic identification of nitrogen-fixing Klebsiella variicola, K. pneumoniae and K. quasipneumoniae. J Basic Microbiol 56, 78–84. https://doi.org/10.1002/jobm.201500415
- Chen, Y., Hu, D., Zhang, Q., Liao, X.-P., Liu, Y.-H., Sun, J., 2017. Efflux Pump Overexpression Contributes to Tigecycline Heteroresistance in Salmonella enterica serovar Typhimurium. Front Cell Infect Microbiol 7, 37. https://doi.org/10.3389/fcimb.2017.00037

- Chen, Y.-T., Lin, J.-C., Fung, C.-P., Lu, P.-L., Chuang, Y.-C., Wu, T.-L., Siu, L.K., 2014. KPC-2-encoding plasmids from Escherichia coli and Klebsiella pneumoniae in Taiwan. Journal of Antimicrobial Chemotherapy 69, 628–631. https://doi.org/10.1093/jac/dkt409
- Cheruvanky, A., Stoesser, N., Sheppard, A.E., Crook, D.W., Hoffman, P.S., Weddle, E., Carroll, J., Sifri, C.D., Chai, W., Barry, K., Ramakrishnan, G., Mathers, A.J., 2017. Enhanced Klebsiella pneumoniae Carbapenemase Expression from a Novel Tn4401 Deletion. Antimicrob Agents Chemother 61, e00025-17, e00025-17. https://doi.org/10.1128/AAC.00025-17
- Chmelnitsky, I., Shklyar, M., Hermesh, O., Navon-Venezia, S., Edgar, R., Carmeli, Y., 2013. Unique genes identified in the epidemic extremely drug-resistant KPC-producing Klebsiella pneumoniae sequence type 258. J Antimicrob Chemother 68, 74–83. https://doi.org/10.1093/jac/dks370
- Chmelnitsky, I., Shklyar, M., Leavitt, A., Sadovsky, E., Navon-Venezia, S., Ben Dalak, M., Edgar, R., Carmeli, Y., 2014. Mix and match of KPC-2 encoding plasmids in Enterobacteriaceae-comparative genomics. Diagnostic Microbiology and Infectious Disease 79, 255–260. https://doi.org/10.1016/j.diagmicrobio.2014.03.008
- Chung, H.S., Yao, Z., Goehring, N.W., Kishony, R., Beckwith, J., Kahne, D., 2009. Rapid beta-lactam-induced lysis requires successful assembly of the cell division machinery. Proc Natl Acad Sci U S A 106, 21872–21877. https://doi.org/10.1073/pnas.0911674106
- Churcher, G.M., 1968. A screening test for the detection of methicillin-resistant staphylococci. J Clin Pathol 21, 213–217. https://doi.org/10.1136/jcp.21.2.213
- Claessen, D., Errington, J., 2019. Cell Wall Deficiency as a Coping Strategy for Stress. Trends in Microbiology 27, 1025–1033. https://doi.org/10.1016/j.tim.2019.07.008
- Clancy, C.J., Chen, L., Hong, J.H., Cheng, S., Hao, B., Shields, R.K., Farrell, A.N., Doi, Y., Zhao, Y., Perlin, D.S., Kreiswirth, B.N., Nguyen, M.H., 2013. Mutations of the ompK36 porin gene and promoter impact responses of sequence type 258, KPC-2-producing Klebsiella pneumoniae strains to doripenem and doripenem-colistin. Antimicrob Agents Chemother 57, 5258–5265. https://doi.org/10.1128/AAC.01069-13
- Clarivet, B., Grau, D., Jumas-Bilak, E., Jean-Pierre, H., Pantel, A., Parer, S., Lotthé, A., 2016. Persisting transmission of carbapenemase-producing Klebsiella pneumoniae due to an environmental reservoir in a university hospital, France, 2012 to 2014. Euro Surveill. 21. https://doi.org/10.2807/1560-7917.ES.2016.21.17.30213
- Colwell, C.A., 1946. Small Colony Variants of Escherichia coli. J Bacteriol 52, 417–422. https://doi.org/10.1128/JB.52.4.417-422.1946
- Cook, M., Molto, E., Anderson, C., 1989. Fluorochrome labelling in Roman period skeletons from Dakhleh Oasis, Egypt. Am J Phys Anthropol 80, 137–143. https://doi.org/10.1002/ajpa.1330800202
- Coros, A.M., Twiss, E., Tavakoli, N.P., Derbyshire, K.M., 2005. Genetic evidence that GTP is required for transposition of IS903 and Tn552 in Escherichia coli. J Bacteriol 187, 4598–4606. https://doi.org/10.1128/JB.187.13.4598-4606.2005
- Correia, F.F., D'Onofrio, A., Rejtar, T., Li, L., Karger, B.L., Makarova, K., Koonin, E.V., Lewis, K., 2006. Kinase activity of overexpressed HipA is required for growth arrest and multidrug tolerance in Escherichia coli. J Bacteriol 188, 8360–8367. https://doi.org/10.1128/JB.01237-06
- Cortés, G., Alvarez, D., Saus, C., Albertí, S., 2002. Role of lung epithelial cells in defense against Klebsiella pneumoniae pneumonia. Infect Immun 70, 1075–1080. https://doi.org/10.1128/iai.70.3.1075-1080.2002
- Cowan, S.T., Steel, K.J., Shaw, C., Duguid, J.P., 1960. A classification of the Klebsiella group. J Gen Microbiol 23, 601–612. https://doi.org/10.1099/00221287-23-3-601

- Craig, W.A., 2003. Basic pharmacodynamics of antibacterials with clinical applications to the use of beta-lactams, glycopeptides, and linezolid. Infect Dis Clin North Am 17, 479–501. https://doi.org/10.1016/s0891-5520(03)00065-5
- Cross, T., Ransegnola, B., Shin, J.-H., Weaver, A., Fauntleroy, K., VanNieuwenhze, M.S., Westblade, L.F., Dörr, T., 2019. Spheroplast-Mediated Carbapenem Tolerance in Gram-Negative Pathogens. Antimicrob Agents Chemother 63. https://doi.org/10.1128/AAC.00756-19
- Curtis, N.A., Orr, D., Ross, G.W., Boulton, M.G., 1979. Affinities of penicillins and cephalosporins for the penicillin-binding proteins of Escherichia coli K-12 and their antibacterial activity. Antimicrob Agents Chemother 16, 533–539. https://doi.org/10.1128/aac.16.5.533
- Cury, A.P., Girardello, R., Duarte, A.J. da S., Rossi, F., 2020. KPC-producing Enterobacterales with uncommon carbapenem susceptibility profile in Vitek 2 system. International Journal of Infectious Diseases 93, 118–120. https://doi.org/10.1016/j.ijid.2020.01.016
- Cushnie, T.P.T., O'Driscoll, N.H., Lamb, A.J., 2016. Morphological and ultrastructural changes in bacterial cells as an indicator of antibacterial mechanism of action. Cell Mol Life Sci 73, 4471–4492. https://doi.org/10.1007/s00018-016-2302-2
- Cuzon, G., Naas, T., Truong, H., Villegas, M.V., Wisell, K.T., Carmeli, Y., Gales, A.C., Venezia, S.N., Quinn, J.P., Nordmann, P., 2010. Worldwide diversity of Klebsiella pneumoniae that produce beta-lactamase blaKPC-2 gene. Emerging Infect. Dis. 16, 1349–1356. https://doi.org/10.3201/eid1609.091389
- Dabos, L., Rodriguez, C.H., Nastro, M., Dortet, L., Bonnin, R.A., Famiglietti, A., Iorga, B.I., Vay, C., Naas, T., 2020. LMB-1 producing Citrobacter freundii from Argentina, a novel player in the field of MBLs. Int J Antimicrob Agents 55, 105857. https://doi.org/10.1016/j.ijantimicag.2019.11.014
- Daikos, G.L., Markogiannakis, A., 2011. Carbapenemase-producing Klebsiella pneumoniae: (when) might we still consider treating with carbapenems? Clin Microbiol Infect 17, 1135–1141. https://doi.org/10.1111/j.1469-0691.2011.03553.x
- Das, G., Varshney, U., 2006. Peptidyl-tRNA hydrolase and its critical role in protein biosynthesis. Microbiology (Reading) 152, 2191–2195. https://doi.org/10.1099/mic.0.29024-0
- David, S., Cohen, V., Reuter, S., Sheppard, A.E., Giani, T., Parkhill, J., European Survey of Carbapenemase-Producing Enterobacteriaceae (EuSCAPE) Working Group, ESCMID Study Group for Epidemiological Markers (ESGEM), Rossolini, G.M., Feil, E.J., Grundmann, H., Aanensen, D.M., 2020. Integrated chromosomal and plasmid sequence analyses reveal diverse modes of carbapenemase gene spread among Klebsiella pneumoniae. Proc Natl Acad Sci U S A 117, 25043–25054. https://doi.org/10.1073/pnas.2003407117
- David, S., Reuter, S., Harris, S.R., Glasner, C., Feltwell, T., Argimon, S., Abudahab, K., Goater, R., Giani, T., Errico, G., Aspbury, M., Sjunnebo, S., EuSCAPE Working Group, ESGEM Study Group, Feil, E.J., Rossolini, G.M., Aanensen, D.M., Grundmann, H., 2019. Epidemic of carbapenem-resistant Klebsiella pneumoniae in Europe is driven by nosocomial spread. Nat Microbiol 4, 1919–1929. https://doi.org/10.1038/s41564-019-0492-8
- Davidson, C.J., Surette, M.G., 2008. Individuality in bacteria. Annu Rev Genet 42, 253–268. https://doi.org/10.1146/annurev.genet.42.110807.091601
- Davies, J., Davies, D., 2010. Origins and evolution of antibiotic resistance. Microbiol Mol Biol Rev 74, 417–433. https://doi.org/10.1128/MMBR.00016-10
- Davis, R.T., Brown, P.D., 2020. spoT-mediated stringent response influences environmental and nutritional stress tolerance, biofilm formation and antimicrobial resistance in Klebsiella pneumoniae. APMIS 128, 48–60. https://doi.org/10.1111/apm.13006

- Dean, M.A., Olsen, R.J., Long, S.W., Rosato, A.E., Musser, J.M., 2014. Identification of point mutations in clinical Staphylococcus aureus strains that produce small-colony variants auxotrophic for menadione. Infect Immun 82, 1600–1605. https://doi.org/10.1128/IAI.01487-13
- Delcour, A.H., 2009. Outer membrane permeability and antibiotic resistance. Biochim Biophys Acta 1794, 808–816. https://doi.org/10.1016/j.bbapap.2008.11.005
- Diancourt, L., Passet, V., Verhoef, J., Grimont, P.A.D., Brisse, S., 2005. Multilocus sequence typing of Klebsiella pneumoniae nosocomial isolates. J Clin Microbiol 43, 4178–4182. https://doi.org/10.1128/JCM.43.8.4178-4182.2005
- Docquier, J.-D., Calderone, V., De Luca, F., Benvenuti, M., Giuliani, F., Bellucci, L., Tafi, A., Nordmann, P., Botta, M., Rossolini, G.M., Mangani, S., 2009. Crystal structure of the OXA-48 beta-lactamase reveals mechanistic diversity among class D carbapenemases. Chem Biol 16, 540–547. https://doi.org/10.1016/j.chembiol.2009.04.010
- Docquier, J.-D., Lamotte-Brasseur, J., Galleni, M., Amicosante, G., Frère, J.-M., Rossolini, G.M., 2003. On functional and structural heterogeneity of VIM-type metallo-beta-lactamases. J Antimicrob Chemother 51, 257–266. https://doi.org/10.1093/jac/dkg067
- Domingues, I.L., Gama, J.A., Carvalho, L.M., Dionisio, F., 2017. Social behaviour involving drug resistance: the role of initial density, initial frequency and population structure in shaping the effect of antibiotic resistance as a public good. Heredity (Edinb) 119, 295–301. https://doi.org/10.1038/hdy.2017.33
- Dorman, M.J., Feltwell, T., Goulding, D.A., Parkhill, J., Short, F.L., 2018. The Capsule Regulatory Network of Klebsiella pneumoniae Defined by density-TraDISort. mBio 9. https://doi.org/10.1128/mBio.01863-18
- Dortet, L., Cuzon, G., Ponties, V., Nordmann, P., 2017. Trends in carbapenemase-producing Enterobacteriaceae, France, 2012 to 2014. Euro Surveill 22. https://doi.org/10.2807/1560-7917.ES.2017.22.6.30461
- Dortet, L., Poirel, L., Nordmann, P., 2014. Worldwide dissemination of the NDM-type carbapenemases in Gram-negative bacteria. Biomed Res Int 2014, 249856. https://doi.org/10.1155/2014/249856
- Dragoš, A., Kiesewalter, H., Martin, M., Hsu, C.-Y., Hartmann, R., Wechsler, T., Eriksen, C., Brix, S., Drescher, K., Stanley-Wall, N., Kümmerli, R., Kovács, Á.T., 2018. Division of Labor during Biofilm Matrix Production. Curr Biol 28, 1903-1913.e5. https://doi.org/10.1016/j.cub.2018.04.046
- Drancourt, M., Bollet, C., Carta, A., Rousselier, P., 2001. Phylogenetic analyses of Klebsiella species delineate Klebsiella and Raoultella gen. nov., with description of Raoultella ornithinolytica comb. nov., Raoultella terrigena comb. nov. and Raoultella planticola comb. nov. Int J Syst Evol Microbiol 51, 925–932. https://doi.org/10.1099/00207713-51-3-925
- Drawz, S.M., Bonomo, R.A., 2010. Three decades of beta-lactamase inhibitors. Clin Microbiol Rev 23, 160–201. https://doi.org/10.1128/CMR.00037-09
- Drusano, G., 1997. Meropenem: laboratory and clinical data. Clin Microbiol Infect 3 Suppl 4, S51–S59.
- Du, D., Wang-Kan, X., Neuberger, A., van Veen, H.W., Pos, K.M., Piddock, L.J.V., Luisi, B.F., 2018. Multidrug efflux pumps: structure, function and regulation. Nat Rev Microbiol 16, 523–539. https://doi.org/10.1038/s41579-018-0048-6
- Eagle, H., 1948. A Paradoxical Zone Phenomenon in the Bactericidal Action of Penicillin in Vitro. Science 107, 44–45. https://doi.org/10.1126/science.107.2767.44

- Edlund, T., Grundström, T., Normark, S., 1979. Isolation and characterization of DNA repetitions carrying the chromosomal beta-lactamase gene of Escherichia coli K-12. Mol Gen Genet 173, 115–125. https://doi.org/10.1007/BF00330301
- Edlund, T., Normark, S., 1981. Recombination between short DNA homologies causes tandem duplication. Nature 292, 269–271. https://doi.org/10.1038/292269a0
- Egger, M., Kurath, S., Strenger, V., Grisold, A., Schlenke, P., Rosskopf, K., Krakowitzky, P., Lackner, H., Schwinger, W., Urban, C., 2017. Klebsiella Oxytoca Bacteremia Induced Septic Shock following Platelet Transfusion. Klin Padiatr 229, 304–305. https://doi.org/10.1055/s-0043-116850
- El-Halfawy, O.M., Valvano, M.A., 2015. Antimicrobial heteroresistance: an emerging field in need of clarity. Clin Microbiol Rev 28, 191–207. https://doi.org/10.1128/CMR.00058-14
- Engel, H., Mika, M., Denapaite, D., Hakenbeck, R., Mühlemann, K., Heller, M., Hathaway, L.J., Hilty, M., 2014. A low-affinity penicillin-binding protein 2x variant is required for heteroresistance in Streptococcus pneumoniae. Antimicrob Agents Chemother 58, 3934–3941. https://doi.org/10.1128/AAC.02547-14
- Ernst, C.M., Braxton, J.R., Rodriguez-Osorio, C.A., Zagieboylo, A.P., Li, L., Pironti, A., Manson, A.L., Nair, A.V., Benson, M., Cummins, K., Clatworthy, A.E., Earl, A.M., Cosimi, L.A., Hung, D.T., 2020. Adaptive evolution of virulence and persistence in carbapenem-resistant Klebsiella pneumoniae. Nat Med. https://doi.org/10.1038/s41591-020-0825-4
- Evans, B.A., Amyes, S.G.B., 2014. OXA β-lactamases. Clin Microbiol Rev 27, 241–263. https://doi.org/10.1128/CMR.00117-13
- Evans, T.J., 2015. Small colony variants of Pseudomonas aeruginosa in chronic bacterial infection of the lung in cystic fibrosis. Future Microbiol 10, 231–239. https://doi.org/10.2217/fmb.14.107
- Ezraty, B., Vergnes, A., Banzhaf, M., Duverger, Y., Huguenot, A., Brochado, A.R., Su, S.-Y., Espinosa, L., Loiseau, L., Py, B., Typas, A., Barras, F., 2013. Fe-S cluster biosynthesis controls uptake of aminoglycosides in a ROS-less death pathway. Science 340, 1583–1587. https://doi.org/10.1126/science.1238328
- Fajardo, A., Martínez-Martín, N., Mercadillo, M., Galán, J.C., Ghysels, B., Matthijs, S., Cornelis, P., Wiehlmann, L., Tümmler, B., Baquero, F., Martínez, J.L., 2008. The neglected intrinsic resistome of bacterial pathogens. PLoS One 3, e1619. https://doi.org/10.1371/journal.pone.0001619
- Fajardo-Lubián, A., Ben Zakour, N.L., Agyekum, A., Qi, Q., Iredell, J.R., 2019. Host adaptation and convergent evolution increases antibiotic resistance without loss of virulence in a major human pathogen. PLoS Pathog 15, e1007218. https://doi.org/10.1371/journal.ppat.1007218
- Fattouh, R., Tijet, N., McGeer, A., Poutanen, S.M., Melano, R.G., Patel, S.N., 2015. What Is the Appropriate Meropenem MIC for Screening of Carbapenemase-Producing Enterobacteriaceae in Low-Prevalence Settings? Antimicrob Agents Chemother 60, 1556–1559. https://doi.org/10.1128/AAC.02304-15
- Fernández, L., Hancock, R.E.W., 2012. Adaptive and mutational resistance: role of porins and efflux pumps in drug resistance. Clin Microbiol Rev 25, 661–681. https://doi.org/10.1128/CMR.00043-12
- Ferreira, G.F., Santos, D.A., 2017. Heteroresistance and fungi. Mycoses 60, 562–568. https://doi.org/10.1111/myc.12639
- Fisher, J.F., Mobashery, S., 2014. The sentinel role of peptidoglycan recycling in the β-lactam resistance of the Gram-negative Enterobacteriaceae and Pseudomonas aeruginosa. Bioorg Chem 56, 41–48. https://doi.org/10.1016/j.bioorg.2014.05.011
- Fitzpatrick, A.W.P., Llabrés, S., Neuberger, A., Blaza, J.N., Bai, X.-C., Okada, U., Murakami, S., van Veen, H.W., Zachariae, U., Scheres, S.H.W., Luisi, B.F., Du, D., 2017. Structure of the MacAB-TolC

ABC-type tripartite multidrug efflux pump. Nat Microbiol 2, 17070. https://doi.org/10.1038/nmicrobiol.2017.70

- Fleming, A., 1980. Classics in infectious diseases: on the antibacterial action of cultures of a penicillium, with special reference to their use in the isolation of B. influenzae by Alexander Fleming, Reprinted from the British Journal of Experimental Pathology 10:226-236, 1929. Rev Infect Dis 2, 129–139.
- Fletcher, S., 2015. Understanding the contribution of environmental factors in the spread of antimicrobial resistance. Environ Health Prev Med 20, 243–252. https://doi.org/10.1007/s12199-015-0468-0
- Foster, P.L., 2007. Stress-induced mutagenesis in bacteria. Crit Rev Biochem Mol Biol 42, 373–397. https://doi.org/10.1080/10409230701648494
- Foster, P.L., Gudmundsson, G., Trimarchi, J.M., Cai, H., Goodman, M.F., 1995. Proofreading-defective DNA polymerase II increases adaptive mutation in Escherichia coli. Proc Natl Acad Sci U S A 92, 7951–7955. https://doi.org/10.1073/pnas.92.17.7951
- Founou, R.C., Founou, L.L., Essack, S.Y., 2017. Clinical and economic impact of antibiotic resistance in developing countries: A systematic review and meta-analysis. PLoS One 12, e0189621. https://doi.org/10.1371/journal.pone.0189621
- Franceschini, N., Caravelli, B., Docquier, J.D., Galleni, M., Frère, J.M., Amicosante, G., Rossolini, G.M., 2000. Purification and biochemical characterization of the VIM-1 metallo-beta-lactamase. Antimicrob Agents Chemother 44, 3003–3007. https://doi.org/10.1128/aac.44.11.3003-3007.2000
- Fridman, O., Goldberg, A., Ronin, I., Shoresh, N., Balaban, N.Q., 2014. Optimization of lag time underlies antibiotic tolerance in evolved bacterial populations. Nature 513, 418–421. https://doi.org/10.1038/nature13469
- Fung, C.-P., Chang, F.-Y., Lee, S.-C., Hu, B.-S., Kuo, B.I.-T., Liu, C.-Y., Ho, M., Siu, L.K., 2002. A global emerging disease of Klebsiella pneumoniae liver abscess: is serotype K1 an important factor for complicated endophthalmitis? Gut 50, 420–424. https://doi.org/10.1136/gut.50.3.420
- Gaibani, P., Campoli, C., Lewis, R.E., Volpe, S.L., Scaltriti, E., Giannella, M., Pongolini, S., Berlingeri, A., Cristini, F., Bartoletti, M., Tedeschi, S., Ambretti, S., 2018. In vivo evolution of resistant subpopulations of KPC-producing Klebsiella pneumoniae during ceftazidime/avibactam treatment. Journal of Antimicrobial Chemotherapy 73, 1525–1529. https://doi.org/10.1093/jac/dky082
- Gardner, A., West, S.A., Griffin, A.S., 2007. Is bacterial persistence a social trait? PLoS One 2, e752. https://doi.org/10.1371/journal.pone.0000752
- Garriss, G., Waldor, M.K., Burrus, V., 2009. Mobile antibiotic resistance encoding elements promote their own diversity. PLoS Genet 5, e1000775. https://doi.org/10.1371/journal.pgen.1000775
- Gefen, O., Chekol, B., Strahilevitz, J., Balaban, N.Q., 2017. TDtest: easy detection of bacterial tolerance and persistence in clinical isolates by a modified disk-diffusion assay. Sci Rep 7, 41284. https://doi.org/10.1038/srep41284
- Gefen, O., Gabay, C., Mumcuoglu, M., Engel, G., Balaban, N.Q., 2008. Single-cell protein induction dynamics reveals a period of vulnerability to antibiotics in persister bacteria. Proceedings of the National Academy of Sciences 105, 6145–6149. https://doi.org/10.1073/pnas.0711712105
- Geiger, T., Kästle, B., Gratani, F.L., Goerke, C., Wolz, C., 2014. Two small (p)ppGpp synthases in Staphylococcus aureus mediate tolerance against cell envelope stress conditions. J Bacteriol 196, 894–902. https://doi.org/10.1128/JB.01201-13
- George, A.M., Hall, R.M., Stokes, H.W., 1995. Multidrug resistance in Klebsiella pneumoniae: a novel gene, ramA, confers a multidrug resistance phenotype in Escherichia coli. Microbiology (Reading) 141 (Pt 8), 1909–1920. https://doi.org/10.1099/13500872-141-8-1909

- Gera, K., Roshan, R., Varma-Basil, M., Shah, A., 2015. Chronic pneumonia due to Klebsiella oxytoca mimicking pulmonary tuberculosis. Pneumonol Alergol Pol 83, 383–386. https://doi.org/10.5603/PiAP.2015.0061
- Gerdes, K., Maisonneuve, E., 2012. Bacterial persistence and toxin-antitoxin loci. Annu Rev Microbiol 66, 103–123. https://doi.org/10.1146/annurev-micro-092611-150159
- Germain, E., Castro-Roa, D., Zenkin, N., Gerdes, K., 2013. Molecular Mechanism of Bacterial Persistence by HipA. Molecular Cell 52, 248–254. https://doi.org/10.1016/j.molcel.2013.08.045
- Giani, T., Pini, B., Arena, F., Conte, V., Bracco, S., Migliavacca, R., AMCLI-CRE Survey Participants, Pantosti, A., Pagani, L., Luzzaro, F., Rossolini, G.M., 2013. Epidemic diffusion of KPC carbapenemase-producing Klebsiella pneumoniae in Italy: results of the first countrywide survey, 15 May to 30 June 2011. Euro Surveill. 18.
- Gillings, M.R., 2013. Evolutionary consequences of antibiotic use for the resistome, mobilome and microbial pangenome. Front Microbiol 4, 4. https://doi.org/10.3389/fmicb.2013.00004
- Girgis, H.S., Harris, K., Tavazoie, S., 2012. Large mutational target size for rapid emergence of bacterial persistence. Proc Natl Acad Sci U S A 109, 12740–12745. https://doi.org/10.1073/pnas.1205124109
- Girlich, D., Poirel, L., Nordmann, P., 2013. Comparison of the SUPERCARBA, CHROMagar KPC, and Brilliance CRE screening media for detection of Enterobacteriaceae with reduced susceptibility to carbapenems. Diagnostic Microbiology and Infectious Disease 75, 214–217. https://doi.org/10.1016/j.diagmicrobio.2012.10.006
- Girlich, D., Poirel, L., Nordmann, P., 2009. CTX-M expression and selection of ertapenem resistance in Klebsiella pneumoniae and Escherichia coli. Antimicrob Agents Chemother 53, 832–834. https://doi.org/10.1128/AAC.01007-08
- Godinez, W.J., Chan, H., Hossain, I., Li, C., Ranjitkar, S., Rasper, D., Simmons, R.L., Zhang, X., Feng, B.Y., 2019. Morphological Deconvolution of Beta-Lactam Polyspecificity in E. coli. ACS Chem. Biol. 14, 1217–1226. https://doi.org/10.1021/acschembio.9b00141
- Gogarten, J.P., Townsend, J.P., 2005. Horizontal gene transfer, genome innovation and evolution. Nat Rev Microbiol 3, 679–687. https://doi.org/10.1038/nrmicro1204
- Gomez, M.J., Neyfakh, A.A., 2006. Genes involved in intrinsic antibiotic resistance of Acinetobacter baylyi. Antimicrob Agents Chemother 50, 3562–3567. https://doi.org/10.1128/AAC.00579-06
- González, L.J., Bahr, G., Nakashige, T.G., Nolan, E.M., Bonomo, R.A., Vila, A.J., 2016. Membrane anchoring stabilizes and favors secretion of New Delhi metallo-β-lactamase. Nat Chem Biol 12, 516–522. https://doi.org/10.1038/nchembio.2083
- Gorrie, C.L., Mirceta, M., Wick, R.R., Edwards, D.J., Thomson, N.R., Strugnell, R.A., Pratt, N.F., Garlick, J.S., Watson, K.M., Pilcher, D.V., McGloughlin, S.A., Spelman, D.W., Jenney, A.W.J., Holt, K.E., 2017. Gastrointestinal Carriage Is a Major Reservoir of Klebsiella pneumoniae Infection in Intensive Care Patients. Clin. Infect. Dis. 65, 208–215. https://doi.org/10.1093/cid/cix270
- Gorrie, C.L., Mirceta, M., Wick, R.R., Judd, L.M., Wyres, K.L., Thomson, N.R., Strugnell, R.A., Pratt, N.F., Garlick, J.S., Watson, K.M., Hunter, P.C., McGloughlin, S.A., Spelman, D.W., Jenney, A.W.J., Holt, K.E., 2018. Antimicrobial-Resistant Klebsiella pneumoniae Carriage and Infection in Specialized Geriatric Care Wards Linked to Acquisition in the Referring Hospital. Clinical Infectious Diseases 67, 161–170. https://doi.org/10.1093/cid/ciy027
- Graham, D.W., Ashton, W.T., Barash, L., Brown, J.E., Brown, R.D., Canning, L.F., Chen, A., Springer, J.P., Rogers, E.F., 1987. Inhibition of the mammalian beta-lactamase renal dipeptidase

(dehydropeptidase-I) by (Z)-2-(acylamino)-3-substituted-propenoic acids. J Med Chem 30, 1074–1090. https://doi.org/10.1021/jm00389a018

- Gray, D.A., Dugar, G., Gamba, P., Strahl, H., Jonker, M.J., Hamoen, L.W., 2019. Extreme slow growth as alternative strategy to survive deep starvation in bacteria. Nat Commun 10, 890. https://doi.org/10.1038/s41467-019-08719-8
- Grimbergen, A.J., Siebring, J., Solopova, A., Kuipers, O.P., 2015. Microbial bet-hedging: the power of being different. Curr Opin Microbiol 25, 67–72. https://doi.org/10.1016/j.mib.2015.04.008
- Guérin, F., Isnard, C., Sinel, C., Morand, P., Dhalluin, A., Cattoir, V., Giard, J.-C., 2016. Cluster-dependent colistin hetero-resistance in Enterobacter cloacae complex. J. Antimicrob. Chemother. 71, 3058–3061. https://doi.org/10.1093/jac/dkw260
- Hall, A.M., Gollan, B., Helaine, S., 2017. Toxin-antitoxin systems: reversible toxicity. Curr Opin Microbiol 36, 102–110. https://doi.org/10.1016/j.mib.2017.02.003
- Hall, B.G., 1998. Activation of the bgl operon by adaptive mutation. Mol Biol Evol 15, 1–5. https://doi.org/10.1093/oxfordjournals.molbev.a025842
- Händel, N., Schuurmans, J.M., Brul, S., ter Kuile, B.H., 2013. Compensation of the metabolic costs of antibiotic resistance by physiological adaptation in Escherichia coli. Antimicrob Agents Chemother 57, 3752–3762. https://doi.org/10.1128/AAC.02096-12
- Hansen, S., Vulić, M., Min, J., Yen, T.-J., Schumacher, M.A., Brennan, R.G., Lewis, K., 2012. Regulation of the Escherichia coli HipBA toxin-antitoxin system by proteolysis. PLoS One 7, e39185. https://doi.org/10.1371/journal.pone.0039185
- Harada, Y., Morinaga, Y., Kaku, N., Nakamura, S., Uno, N., Hasegawa, H., Izumikawa, K., Kohno, S., Yanagihara, K., 2014. In vitro and in vivo activities of piperacillin-tazobactam and meropenem at different inoculum sizes of ESBL-producing Klebsiella pneumoniae. Clin Microbiol Infect 20, O831-839. https://doi.org/10.1111/1469-0691.12677
- Harrison, F., Roberts, A.E.L., Gabrilska, R., Rumbaugh, K.P., Lee, C., Diggle, S.P., 2015. A 1,000-Year-Old Antimicrobial Remedy with Antistaphylococcal Activity. mBio 6, e01129-15. https://doi.org/10.1128/mBio.01129-15
- Hart, E.M., Mitchell, A.M., Konovalova, A., Grabowicz, M., Sheng, J., Han, X., Rodriguez-Rivera, F.P., Schwaid, A.G., Malinverni, J.C., Balibar, C.J., Bodea, S., Si, Q., Wang, H., Homsher, M.F., Painter, R.E., Ogawa, A.K., Sutterlin, H., Roemer, T., Black, T.A., Rothman, D.M., Walker, S.S., Silhavy, T.J., 2019. A small-molecule inhibitor of BamA impervious to efflux and the outer membrane permeability barrier. Proc Natl Acad Sci USA 116, 21748–21757. https://doi.org/10.1073/pnas.1912345116
- Held, K., Gasper, J., Morgan, S., Siehnel, R., Singh, P., Manoil, C., 2018. Determinants of Extreme β-Lactam Tolerance in the Burkholderia pseudomallei Complex. Antimicrob Agents Chemother 62. https://doi.org/10.1128/AAC.00068-18
- Helling, R.B., Kukora, J.S., 1971. Nalidixic acd-resistant mutants of Escherichia coli deficient in isocitrate dehydrogenase. J Bacteriol 105, 1224–1226. https://doi.org/10.1128/JB.105.3.1224-1226.1971
- Henderson, I.R., Owen, P., Nataro, J.P., 1999. Molecular switches--the ON and OFF of bacterial phase variation. Mol Microbiol 33, 919–932. https://doi.org/10.1046/j.1365-2958.1999.01555.x
- Hendrickx, A.P.A., Landman, F., de Haan, A., Borst, D., Witteveen, S., van Santen-Verheuvel, M.G., van der Heide, H.G.J., Schouls, L.M., Dutch CPE surveillance Study Group, 2020. Plasmid diversity among genetically related Klebsiella pneumoniae blaKPC-2 and blaKPC-3 isolates collected in the Dutch national surveillance. Sci Rep 10, 16778. https://doi.org/10.1038/s41598-020-73440-2

- Hikida, M., Kawashima, K., Yoshida, M., Mitsuhashi, S., 1992. Inactivation of new carbapenem antibiotics by dehydropeptidase-I from porcine and human renal cortex. J Antimicrob Chemother 30, 129–134. https://doi.org/10.1093/jac/30.2.129
- Hill, C.W., Gray, J.A., Brody, H., 1989. Use of the isocitrate dehydrogenase structural gene for attachment of e14 in Escherichia coli K-12. J Bacteriol 171, 4083–4084. https://doi.org/10.1128/jb.171.7.4083-4084.1989
- Hirakawa, H., Inazumi, Y., Masaki, T., Hirata, T., Yamaguchi, A., 2005. Indole induces the expression of multidrug exporter genes in Escherichia coli. Mol Microbiol 55, 1113–1126. https://doi.org/10.1111/j.1365-2958.2004.04449.x
- Hjort, K., Nicoloff, H., Andersson, D.I., 2016. Unstable tandem gene amplification generates heteroresistance (variation in resistance within a population) to colistin in Salmonella enterica. Mol Microbiol 102, 274–289. https://doi.org/10.1111/mmi.13459
- Ho, J.-Y., Lin, T.-L., Li, C.-Y., Lee, A., Cheng, A.-N., Chen, M.-C., Wu, S.-H., Wang, J.-T., Li, T.-L., Tsai, M.-D., 2011. Functions of some capsular polysaccharide biosynthetic genes in Klebsiella pneumoniae NTUH K-2044. PLoS One 6, e21664. https://doi.org/10.1371/journal.pone.0021664
- Hodgkin, D.C., 1949. The X-ray analysis of the structure of penicillin. Adv Sci 6, 85–89.
- Hoerr, V., Duggan, G.E., Zbytnuik, L., Poon, K.K.H., Große, C., Neugebauer, U., Methling, K., Löffler, B., Vogel, H.J., 2016. Characterization and prediction of the mechanism of action of antibiotics through NMR metabolomics. BMC Microbiol 16, 82. https://doi.org/10.1186/s12866-016-0696-5
- Holt, K.E., Wertheim, H., Zadoks, R.N., Baker, S., Whitehouse, C.A., Dance, D., Jenney, A., Connor, T.R., Hsu, L.Y., Severin, J., Brisse, S., Cao, H., Wilksch, J., Gorrie, C., Schultz, M.B., Edwards, D.J., Nguyen, K.V., Nguyen, T.V., Dao, T.T., Mensink, M., Minh, V.L., Nhu, N.T.K., Schultsz, C., Kuntaman, K., Newton, P.N., Moore, C.E., Strugnell, R.A., Thomson, N.R., 2015. Genomic analysis of diversity, population structure, virulence, and antimicrobial resistance in Klebsiella pneumoniae, an urgent threat to public health. Proc Natl Acad Sci U S A 112, E3574-3581. https://doi.org/10.1073/pnas.1501049112
- Honoré, N., Nicolas, M.H., Cole, S.T., 1986. Inducible cephalosporinase production in clinical isolates of Enterobacter cloacae is controlled by a regulatory gene that has been deleted from Escherichia coli. EMBO J 5, 3709–3714.
- Horna, G., López, M., Guerra, H., Saénz, Y., Ruiz, J., 2018. Interplay between MexAB-OprM and MexEF-OprN in clinical isolates of Pseudomonas aeruginosa. Scientific Reports 8, 16463. https://doi.org/10.1038/s41598-018-34694-z
- Hsu, C.-R., Lin, T.-L., Chen, Y.-C., Chou, H.-C., Wang, J.-T., 2011. The role of Klebsiella pneumoniae rmpA in capsular polysaccharide synthesis and virulence revisited. Microbiology 157, 3446–3457. https://doi.org/10.1099/mic.0.050336-0
- Hsu, J., 2020. How covid-19 is accelerating the threat of antimicrobial resistance. BMJ 369, m1983. https://doi.org/10.1136/bmj.m1983
- Hudson, M.J., Beyer, W., Böhm, R., Fasanella, A., Garofolo, G., Golinski, R., Goossens, P.L., Hahn, U., Hallis, B., King, A., Mock, M., Montecucco, C., Ozin, A., Tonello, F., Kaufmann, S.H.E., 2008. Bacillus anthracis: balancing innocent research with dual-use potential. Int J Med Microbiol 298, 345–364. https://doi.org/10.1016/j.ijmm.2007.09.007
- Hughes, D., Andersson, D.I., 2017. Evolutionary Trajectories to Antibiotic Resistance. Annu Rev Microbiol 71, 579–596. https://doi.org/10.1146/annurev-micro-090816-093813

- Imani, S., Buscher, H., Marriott, D., Gentili, S., Sandaradura, I., 2017. Too much of a good thing: a retrospective study of β-lactam concentration-toxicity relationships. J Antimicrob Chemother 72, 2891–2897. https://doi.org/10.1093/jac/dkx209
- Iskandar, K., Molinier, L., Hallit, S., Sartelli, M., Catena, F., Coccolini, F., Hardcastle, T.C., Roques, C., Salameh, P., 2020. Drivers of Antibiotic Resistance Transmissionin Low- and Middle-Income Countriesfrom a "One Health" Perspective-A Review. Antibiotics (Basel) 9. https://doi.org/10.3390/antibiotics9070372
- Jacoby, G.A., 2009. AmpC beta-lactamases. Clin Microbiol Rev 22, 161–182, Table of Contents. https://doi.org/10.1128/CMR.00036-08
- Jacoby, G.A., Mills, D.M., Chow, N., 2004. Role of beta-lactamases and porins in resistance to ertapenem and other beta-lactams in Klebsiella pneumoniae. Antimicrob Agents Chemother 48, 3203–3206. https://doi.org/10.1128/AAC.48.8.3203-3206.2004
- Jahn, L.J., Munck, C., Ellabaan, M.M.H., Sommer, M.O.A., 2017. Adaptive Laboratory Evolution of Antibiotic Resistance Using Different Selection Regimes Lead to Similar Phenotypes and Genotypes. Front Microbiol 8, 816. https://doi.org/10.3389/fmicb.2017.00816
- Jarzembowski, T., Wiśniewska, K., Jóźwik, A., Witkowski, J., 2009. Heterogeneity of methicillin-resistant Staphylococcus aureus strains (MRSA) characterized by flow cytometry. Curr Microbiol 59, 78–80. https://doi.org/10.1007/s00284-009-9395-x
- Jaurin, B., Grundström, T., Edlund, T., Normark, S., 1981. The E. coli beta-lactamase attenuator mediates growth rate-dependent regulation. Nature 290, 221–225. https://doi.org/10.1038/290221a0
- Jawetz, E., Gunnison, J.B., Coleman, V.R., 1950. The Combined Action of Penicillin with Streptomycin or Chloromycetin on Enterococci in Vitro. Science 111, 254–256. https://doi.org/10.1126/science.111.2880.254
- Jayol, A., Nordmann, P., Brink, A., Poirel, L., 2015. Heteroresistance to colistin in Klebsiella pneumoniae associated with alterations in the PhoPQ regulatory system. Antimicrob Agents Chemother 59, 2780–2784. https://doi.org/10.1128/AAC.05055-14
- Jeon, J., Lee, Jung, Lee, Jae, Park, K., Karim, A., Lee, C.-R., Jeong, B., Lee, S., 2015. Structural Basis for Carbapenem-Hydrolyzing Mechanisms of Carbapenemases Conferring Antibiotic Resistance. IJMS 16, 9654–9692. https://doi.org/10.3390/ijms16059654
- Jerome, J.P., Bell, J.A., Plovanich-Jones, A.E., Barrick, J.E., Brown, C.T., Mansfield, L.S., 2011. Standing genetic variation in contingency loci drives the rapid adaptation of Campylobacter jejuni to a novel host. PLoS One 6, e16399. https://doi.org/10.1371/journal.pone.0016399
- Johns, B.E., Purdy, K.J., Tucker, N.P., Maddocks, S.E., 2015. Phenotypic and Genotypic Characteristics of Small Colony Variants and Their Role in Chronic Infection. Microbiol Insights 8, 15–23. https://doi.org/10.4137/MBI.S25800
- Justice, S.S., Harrison, A., Becknell, B., Mason, K.M., 2014. Bacterial differentiation, development, and disease: mechanisms for survival. FEMS Microbiol Lett 360, 1–8. https://doi.org/10.1111/1574-6968.12602
- Kaldalu, N., Hauryliuk, V., Tenson, T., 2016. Persisters-as elusive as ever. Appl Microbiol Biotechnol 100, 6545–6553. https://doi.org/10.1007/s00253-016-7648-8
- Källman, O., Giske, C.G., Samuelsen, Ø., Wretlind, B., Kalin, M., Olsson-Liljequist, B., 2009. Interplay of efflux, impermeability, and AmpC activity contributes to cefuroxime resistance in clinical, non-ESBL-producing isolates of Escherichia coli. Microb Drug Resist 15, 91–95. https://doi.org/10.1089/mdr.2009.0883

- Källman, O., Motakefi, A., Wretlind, B., Kalin, M., Olsson-Liljequist, B., Giske, C.G., 2008. Cefuroxime non-susceptibility in multidrug-resistant Klebsiella pneumoniae overexpressing ramA and acrA and expressing ompK35 at reduced levels. J Antimicrob Chemother 62, 986–990. https://doi.org/10.1093/jac/dkn296
- Kang, S.-M., Jin, C., Kim, D.-H., Lee, Y., Lee, B.-J., 2020. Structural and Functional Study of the Klebsiella pneumoniae VapBC Toxin–Antitoxin System, Including the Development of an Inhibitor That Activates VapC. J. Med. Chem. 63, 13669–13679. https://doi.org/10.1021/acs.jmedchem.0c01118
- Kaspy, I., Rotem, E., Weiss, N., Ronin, I., Balaban, N.Q., Glaser, G., 2013. HipA-mediated antibiotic persistence via phosphorylation of the glutamyl-tRNA-synthetase. Nat Commun 4, 3001. https://doi.org/10.1038/ncomms4001
- Kawai, Y., Mercier, R., Mickiewicz, K., Serafini, A., Sório de Carvalho, L.P., Errington, J., 2019. Crucial role for central carbon metabolism in the bacterial L-form switch and killing by β-lactam antibiotics. Nat Microbiol 4, 1716–1726. https://doi.org/10.1038/s41564-019-0497-3
- Kayser, F.H., Benner, E.J., Hoeprich, P.D., 1970. Acquired and native resistance of Staphylococcus aureus to cephalexin and other beta-lactam antibiotics. Appl Microbiol 20, 1–5.
- Keating, G.M., Perry, C.M., 2005. Ertapenem: a review of its use in the treatment of bacterial infections. Drugs 65, 2151–2178. https://doi.org/10.2165/00003495-200565150-00013
- Keaton, M.A., Rosato, R.R., Plata, K.B., Singh, C.R., Rosato, A.E., 2013. Exposure of clinical MRSA heterogeneous strains to β-lactams redirects metabolism to optimize energy production through the TCA cycle. PLoS One 8, e71025. https://doi.org/10.1371/journal.pone.0071025
- Keren, I., Shah, D., Spoering, A., Kaldalu, N., Lewis, K., 2004. Specialized persister cells and the mechanism of multidrug tolerance in Escherichia coli. J Bacteriol 186, 8172–8180. https://doi.org/10.1128/JB.186.24.8172-8180.2004
- Keren, I., Wu, Y., Inocencio, J., Mulcahy, L.R., Lewis, K., 2013. Killing by bactericidal antibiotics does not depend on reactive oxygen species. Science 339, 1213–1216. https://doi.org/10.1126/science.1232688
- Khalid, A., Lubián, A.F., Ma, L., Lin, R.C.Y., Iredell, J.R., 2020. Characterizing the role of porin mutations in susceptibility of beta lactamase producing Klebsiella pneumoniae isolates to ceftaroline and ceftaroline-avibactam. Int J Infect Dis 93, 252–257. https://doi.org/10.1016/j.ijid.2020.02.005
- Khan, S.A., Sung, K., Layton, S., Nawaz, M.S., 2008. Heteroresistance to vancomycin and novel point mutations in Tn1546 of Enterococcus faecium ATCC 51559. Int J Antimicrob Agents 31, 27–36. https://doi.org/10.1016/j.ijantimicag.2007.08.007
- Khare, A., Tavazoie, S., 2020. Extreme Antibiotic Persistence via Heterogeneity-Generating Mutations Targeting Translation. mSystems 5. https://doi.org/10.1128/mSystems.00847-19
- Kidd, T.J., Mills, G., Sá-Pessoa, J., Dumigan, A., Frank, C.G., Insua, J.L., Ingram, R., Hobley, L., Bengoechea, J.A., 2017. A Klebsiella pneumoniae antibiotic resistance mechanism that subdues host defences and promotes virulence. EMBO Mol Med 9, 430–447. https://doi.org/10.15252/emmm.201607336
- Kim, K.S., Anthony, B.F., 1981. Importance of bacterial growth phase in determining minimal bactericidal concentrations of penicillin and methicillin. Antimicrob Agents Chemother 19, 1075–1077. https://doi.org/10.1128/aac.19.6.1075
- Kint, C.I., Verstraeten, N., Fauvart, M., Michiels, J., 2012. New-found fundamentals of bacterial persistence. Trends in Microbiology 20, 577–585. https://doi.org/10.1016/j.tim.2012.08.009

- Kitzis, M.D., Acar, J.F., Gutmann, L., 1989. Antibacterial activity of meropenem against gram-negative bacteria with a permeability defect and against staphylococci. J Antimicrob Chemother 24 Suppl A, 125–132. https://doi.org/10.1093/jac/24.suppl_a.125
- Klein, E.Y., Van Boeckel, T.P., Martinez, E.M., Pant, S., Gandra, S., Levin, S.A., Goossens, H., Laxminarayan, R., 2018. Global increase and geographic convergence in antibiotic consumption between 2000 and 2015. Proc Natl Acad Sci U S A 115, E3463–E3470. https://doi.org/10.1073/pnas.1717295115
- Klein, G., Raina, S., 2019. Regulated Assembly of LPS, Its Structural Alterations and Cellular Response to LPS Defects. Int J Mol Sci 20. https://doi.org/10.3390/ijms20020356
- Klemm, P., Schembri, M.A., 2000. Bacterial adhesins: function and structure. International Journal of Medical Microbiology 290, 27–35. https://doi.org/10.1016/S1438-4221(00)80102-2
- Knudsen, G.M., Fromberg, A., Ng, Y., Gram, L., 2016. Sublethal Concentrations of Antibiotics Cause Shift to Anaerobic Metabolism in Listeria monocytogenes and Induce Phenotypes Linked to Antibiotic Tolerance. Front Microbiol 7, 1091. https://doi.org/10.3389/fmicb.2016.01091
- Kohanski, M.A., Dwyer, D.J., Collins, J.J., 2010. How antibiotics kill bacteria: from targets to networks. Nat Rev Microbiol 8, 423–435. https://doi.org/10.1038/nrmicro2333
- Kohanski, M.A., Dwyer, D.J., Hayete, B., Lawrence, C.A., Collins, J.J., 2007. A common mechanism of cellular death induced by bactericidal antibiotics. Cell 130, 797–810. https://doi.org/10.1016/j.cell.2007.06.049
- Korch, S.B., Henderson, T.A., Hill, T.M., 2003. Characterization of the hipA7 allele of Escherichia coli and evidence that high persistence is governed by (p)ppGpp synthesis. Mol Microbiol 50, 1199–1213. https://doi.org/10.1046/j.1365-2958.2003.03779.x
- Kotková, H., Cabrnochová, M., Lichá, I., Tkadlec, J., Fila, L., Bartošová, J., Melter, O., 2019. Evaluation of TD test for analysis of persistence or tolerance in clinical isolates of Staphylococcus aureus. Journal of Microbiological Methods 167, 105705. https://doi.org/10.1016/j.mimet.2019.105705
- Kriengkauykiat, J., Porter, E., Lomovskaya, O., Wong-Beringer, A., 2005. Use of an efflux pump inhibitor to determine the prevalence of efflux pump-mediated fluoroquinolone resistance and multidrug resistance in Pseudomonas aeruginosa. Antimicrob Agents Chemother 49, 565–570. https://doi.org/10.1128/AAC.49.2.565-570.2005
- Laehnemann, D., Peña-Miller, R., Rosenstiel, P., Beardmore, R., Jansen, G., Schulenburg, H., 2014. Genomics of rapid adaptation to antibiotics: convergent evolution and scalable sequence amplification. Genome Biol Evol 6, 1287–1301. https://doi.org/10.1093/gbe/evu106
- Lallemand, E.A., Lacroix, M.Z., Toutain, P.-L., Boullier, S., Ferran, A.A., Bousquet-Melou, A., 2016. In vitro Degradation of Antimicrobials during Use of Broth Microdilution Method Can Increase the Measured Minimal Inhibitory and Minimal Bactericidal Concentrations. Front Microbiol 7, 2051. https://doi.org/10.3389/fmicb.2016.02051
- Lam, M.M.C., Wyres, K.L., Judd, L.M., Wick, R.R., Jenney, A., Brisse, S., Holt, K.E., 2018. Tracking key virulence loci encoding aerobactin and salmochelin siderophore synthesis in Klebsiella pneumoniae. Genome Medicine 10, 77. https://doi.org/10.1186/s13073-018-0587-5
- Landman, D., Salamera, J., Quale, J., 2013. Irreproducible and uninterpretable Polymyxin B MICs for Enterobacter cloacae and Enterobacter aerogenes. J Clin Microbiol 51, 4106–4111. https://doi.org/10.1128/JCM.02129-13

- Langstraat, J., Bohse, M., Clegg, S., 2001. Type 3 fimbrial shaft (MrkA) of Klebsiella pneumoniae, but not the fimbrial adhesin (MrkD), facilitates biofilm formation. Infect Immun 69, 5805–5812. https://doi.org/10.1128/iai.69.9.5805-5812.2001
- Lawrence, J.G., Ochman, H., 1997. Amelioration of bacterial genomes: rates of change and exchange. J Mol Evol 44, 383–397. https://doi.org/10.1007/pl00006158
- Lederberg, J., Zinder, N., 1948. Concentration of biochemical mutants of bacteria with penicillin. J Am Chem Soc 70, 4267. https://doi.org/10.1021/ja01192a521
- Lederman, E.R., Crum, N.F., 2005. Pyogenic liver abscess with a focus on Klebsiella pneumoniae as a primary pathogen: an emerging disease with unique clinical characteristics. Am J Gastroenterol 100, 322–331. https://doi.org/10.1111/j.1572-0241.2005.40310.x
- Lee, A.J., Wang, S., Meredith, H.R., Zhuang, B., Dai, Z., You, L., 2018. Robust, linear correlations between growth rates and β-lactam-mediated lysis rates. Proc Natl Acad Sci U S A 115, 4069–4074. https://doi.org/10.1073/pnas.1719504115
- Lee, H., Shin, J., Chung, Y.-J., Baek, J.Y., Chung, D.R., Peck, K.R., Song, J.-H., Ko, K.S., 2019. Evolution of Klebsiella pneumoniae with mucoid and non-mucoid type colonies within a single patient. International Journal of Medical Microbiology 309, 194–198. https://doi.org/10.1016/j.ijmm.2019.03.003
- Lee, J.S., Choi, J.-Y., Chung, E.S., Peck, K.R., Ko, K.S., 2019. Variation in the formation of persister cells against meropenem in Klebsiella pneumoniae bacteremia and analysis of its clinical features. Diagn Microbiol Infect Dis 95, 114853. https://doi.org/10.1016/j.diagmicrobio.2019.06.005
- Lee, T.D., Adie, K., McNabb, A., Purych, D., Mannan, K., Azana, R., Ng, C., Tang, P., Hoang, L.M.N., 2015. Rapid Detection of KPC, NDM, and OXA-48-Like Carbapenemases by Real-Time PCR from Rectal Swab Surveillance Samples. J. Clin. Microbiol. 53, 2731–2733. https://doi.org/10.1128/JCM.01237-15
- Lenhard, J.R., Bulman, Z.P., 2019. Inoculum effect of β-lactam antibiotics. J Antimicrob Chemother 74, 2825–2843. https://doi.org/10.1093/jac/dkz226
- Levin-Reisman, I., Balaban, N.Q., 2016. Quantitative Measurements of Type I and Type II Persisters Using ScanLag. Methods Mol Biol 1333, 75–81. https://doi.org/10.1007/978-1-4939-2854-5_7
- Levin-Reisman, I., Brauner, A., Ronin, I., Balaban, N.Q., 2019. Epistasis between antibiotic tolerance, persistence, and resistance mutations. Proc Natl Acad Sci U S A 116, 14734–14739. https://doi.org/10.1073/pnas.1906169116
- Levin-Reisman, I., Fridman, O., Balaban, N.Q., 2014. ScanLag: high-throughput quantification of colony growth and lag time. J Vis Exp. https://doi.org/10.3791/51456
- Levin-Reisman, I., Gefen, O., Fridman, O., Ronin, I., Shwa, D., Sheftel, H., Balaban, N.Q., 2010. Automated imaging with ScanLag reveals previously undetectable bacterial growth phenotypes. Nat Methods 7, 737–739. https://doi.org/10.1038/nmeth.1485
- Levin-Reisman, I., Ronin, I., Gefen, O., Braniss, I., Shoresh, N., Balaban, N.Q., 2017. Antibiotic tolerance facilitates the evolution of resistance. Science 355, 826–830. https://doi.org/10.1126/science.aaj2191
- Lewis, K., 2007. Persister cells, dormancy and infectious disease. Nat Rev Microbiol 5, 48–56. https://doi.org/10.1038/nrmicro1557
- Lewis, K., 2000. Translocases: a bacterial tunnel for drugs and proteins. Curr Biol 10, R678-681. https://doi.org/10.1016/s0960-9822(00)00682-5
- Li, H., Zhang, J., Liu, Y., Zheng, R., Chen, H., Wang, X., Wang, Z., Cao, B., Wang, H., 2014. Molecular characteristics of carbapenemase-producing Enterobacteriaceae in China from 2008 to

2011: Predominance of KPC-2 enzyme. Diagnostic Microbiology and Infectious Disease 78, 63–65. https://doi.org/10.1016/j.diagmicrobio.2013.10.002

- Li, J., Zhang, H., Ning, J., Sajid, A., Cheng, G., Yuan, Z., Hao, H., 2019. The nature and epidemiology of OqxAB, a multidrug efflux pump. Antimicrob Resist Infect Control 8, 44. https://doi.org/10.1186/s13756-019-0489-3
- Li, X.-Z., Plésiat, P., Nikaido, H., 2015. The challenge of efflux-mediated antibiotic resistance in Gram-negative bacteria. Clin Microbiol Rev 28, 337–418. https://doi.org/10.1128/CMR.00117-14
- Li, Y., Zhang, L., Zhou, Y., Zhang, Z., Zhang, X., 2018. Survival of bactericidal antibiotic treatment by tolerant persister cells of Klebsiella pneumoniae. J Med Microbiol 67, 273–281. https://doi.org/10.1099/jmm.0.000680
- Lim, S.P., Nikaido, H., 2010. Kinetic parameters of efflux of penicillins by the multidrug efflux transporter AcrAB-TolC of Escherichia coli. Antimicrob Agents Chemother 54, 1800–1806. https://doi.org/10.1128/AAC.01714-09
- Lin, C.-L., Chen, F.-H., Huang, L.-Y., Chang, J.-C., Chen, J.-H., Tsai, Y.-K., Chang, F.-Y., Lin, J.-C., Siu, L.K., 2017. Effect in virulence of switching conserved homologous capsular polysaccharide genes from Klebsiella pneumoniae serotype K1 into K20. Virulence 8, 487–493. https://doi.org/10.1080/21505594.2016.1228508
- Lin, X.-M., Yang, J.-N., Peng, X.-X., Li, H., 2010. A novel negative regulation mechanism of bacterial outer membrane proteins in response to antibiotic resistance. J Proteome Res 9, 5952–5959. https://doi.org/10.1021/pr100740w
- Liu, Y., Li, J., Du, J., Hu, M., Bai, H., Qi, J., Gao, C., Wei, T., Su, H., Jin, J., Gao, P., 2011. Accurate assessment of antibiotic susceptibility and screening resistant strains of a bacterial population by linear gradient plate. Sci China Life Sci 54, 953–960. https://doi.org/10.1007/s11427-011-4230-6
- Livermore, D.M., 2003. Properties and potential of ertapenem. Journal of Antimicrobial Chemotherapy 52, 331–344. https://doi.org/10.1093/jac/dkg375
- Livermore, D.M., 2002. Multiple mechanisms of antimicrobial resistance in Pseudomonas aeruginosa: our worst nightmare? Clin Infect Dis 34, 634–640. https://doi.org/10.1086/338782
- Livermore, D.M., Canton, R., Gniadkowski, M., Nordmann, P., Rossolini, G.M., Arlet, G., Ayala, J., Coque, T.M., Kern-Zdanowicz, I., Luzzaro, F., Poirel, L., Woodford, N., 2007. CTX-M: changing the face of ESBLs in Europe. J Antimicrob Chemother 59, 165–174. https://doi.org/10.1093/jac/dkl483
- Llobet, E., Tomás, J.M., Bengoechea, J.A., 2008. Capsule polysaccharide is a bacterial decoy for antimicrobial peptides. Microbiology (Reading) 154, 3877–3886. https://doi.org/10.1099/mic.0.2008/022301-0
- Lohans, C.T., Freeman, E.I., Groesen, E. van, Tooke, C.L., Hinchliffe, P., Spencer, J., Brem, J., Schofield, C.J., 2019. Mechanistic Insights into β-Lactamase-Catalysed Carbapenem Degradation Through Product Characterisation. Sci Rep 9, 13608. https://doi.org/10.1038/s41598-019-49264-0
- Lopatkin, A.J., Bening, S.C., Manson, A.L., Stokes, J.M., Kohanski, M.A., Badran, A.H., Earl, A.M., Cheney, N.J., Yang, J.H., Collins, J.J., 2021. Clinically relevant mutations in core metabolic genes confer antibiotic resistance. Science 371. https://doi.org/10.1126/science.aba0862
- López-Camacho, E., Paño-Pardo, J.R., Sotillo, A., Elías-López, C., Martínez-Martínez, L., Gómez-Gil, R., Mingorance, J., 2019. Meropenem heteroresistance in clinical isolates of OXA-48-producing Klebsiella pneumoniae. Diagn. Microbiol. Infect. Dis. 93, 162–166. https://doi.org/10.1016/j.diagmicrobio.2018.09.008

- Lowy, F.D., 2003. Antimicrobial resistance: the example of Staphylococcus aureus. J Clin Invest 111, 1265–1273. https://doi.org/10.1172/JCI18535
- Lu, M.-C., Chen, Y.-T., Chiang, M.-K., Wang, Y.-C., Hsiao, P.-Y., Huang, Y.-J., Lin, C.-T., Cheng, C.-C., Liang, C.-L., Lai, Y.-C., 2017. Colibactin Contributes to the Hypervirulence of pks+ K1 CC23 Klebsiella pneumoniae in Mouse Meningitis Infections. Front Cell Infect Microbiol 7, 103. https://doi.org/10.3389/fcimb.2017.00103
- Lukácová, M., Barák, I., Kazár, J., 2008. Role of structural variations of polysaccharide antigens in the pathogenicity of Gram-negative bacteria. Clin Microbiol Infect 14, 200–206. https://doi.org/10.1111/j.1469-0691.2007.01876.x
- Lyu, F., Pan, M., Patil, S., Wang, J.-H., Matin, A.C., Andrews, J.R., Tang, S.K.Y., 2018. Phenotyping antibiotic resistance with single-cell resolution for the detection of heteroresistance. Sensors and Actuators B: Chemical 270, 396–404. https://doi.org/10.1016/j.snb.2018.05.047
- MacFadden, D.R., McGough, S.F., Fisman, D., Santillana, M., Brownstein, J.S., 2018. Antibiotic Resistance Increases with Local Temperature. Nat Clim Chang 8, 510–514. https://doi.org/10.1038/s41558-018-0161-6
- Machado, D., Antunes, J., Simões, A., Perdigão, J., Couto, I., McCusker, M., Martins, M., Portugal, I., Pacheco, T., Batista, J., Toscano, C., Viveiros, M., 2018. Contribution of efflux to colistin heteroresistance in a multidrug resistant Acinetobacter baumannii clinical isolate. J Med Microbiol 67, 740–749. https://doi.org/10.1099/jmm.0.000741
- Macheboeuf, P., Contreras-Martel, C., Job, V., Dideberg, O., Dessen, A., 2006. Penicillin binding proteins: key players in bacterial cell cycle and drug resistance processes. FEMS Microbiol Rev 30, 673–691. https://doi.org/10.1111/j.1574-6976.2006.00024.x
- Macvanin, M., Johanson, U., Ehrenberg, M., Hughes, D., 2000. Fusidic acid-resistant EF-G perturbs the accumulation of ppGpp. Mol Microbiol 37, 98–107. https://doi.org/10.1046/j.1365-2958.2000.01967.x
- Magill, S.S., Edwards, J.R., Bamberg, W., Beldavs, Z.G., Dumyati, G., Kainer, M.A., Lynfield, R., Maloney, M., McAllister-Hollod, L., Nadle, J., Ray, S.M., Thompson, D.L., Wilson, L.E., Fridkin, S.K., Emerging Infections Program Healthcare-Associated Infections and Antimicrobial Use Prevalence Survey Team, 2014. Multistate point-prevalence survey of health care-associated infections. N Engl J Med 370, 1198–1208. https://doi.org/10.1056/NEJMoa1306801
- Magiorakos, A.-P., Srinivasan, A., Carey, R.B., Carmeli, Y., Falagas, M.E., Giske, C.G., Harbarth, S., Hindler, J.F., Kahlmeter, G., Olsson-Liljequist, B., Paterson, D.L., Rice, L.B., Stelling, J., Struelens, M.J., Vatopoulos, A., Weber, J.T., Monnet, D.L., 2012. Multidrug-resistant, extensively drug-resistant and pandrug-resistant bacteria: an international expert proposal for interim standard definitions for acquired resistance. Clin Microbiol Infect 18, 268–281. https://doi.org/10.1111/j.1469-0691.2011.03570.x
- Mah, T.F., O'Toole, G.A., 2001. Mechanisms of biofilm resistance to antimicrobial agents. Trends Microbiol 9, 34–39. https://doi.org/10.1016/s0966-842x(00)01913-2
- Maisnier-Patin, S., Andersson, D.I., 2004. Adaptation to the deleterious effects of antimicrobial drug resistance mutations by compensatory evolution. Res Microbiol 155, 360–369. https://doi.org/10.1016/j.resmic.2004.01.019
- Majcherczyk, P.A., Kunz, S., Hattenberger, M., Vaxelaire, J., Zak, O., O'Reilly, T., 1994. Isolation and in-vitro and in-vivo characterisation of a mutant of Pseudomonas aeruginosa PAO1 that exhibited a reduced postantibiotic effect in response to imipenem. J Antimicrob Chemother 34, 485–505. https://doi.org/10.1093/jac/34.4.485

- Makena, A., Brem, J., Pfeffer, I., Geffen, R.E.J., Wilkins, S.E., Tarhonskaya, H., Flashman, E., Phee, L.M., Wareham, D.W., Schofield, C.J., 2015a. Biochemical characterization of New Delhi metallo-β-lactamase variants reveals differences in protein stability. J Antimicrob Chemother 70, 463–469. https://doi.org/10.1093/jac/dku403
- Makena, A., Düzgün, A.Ö., Brem, J., McDonough, M.A., Rydzik, A.M., Abboud, M.I., Saral, A., Çiçek, A.Ç., Sandalli, C., Schofield, C.J., 2015b. Comparison of Verona Integron-Borne Metallo-β-Lactamase (VIM) Variants Reveals Differences in Stability and Inhibition Profiles. Antimicrob Agents Chemother 60, 1377–1384. https://doi.org/10.1128/AAC.01768-15
- March, C., Cano, V., Moranta, D., Llobet, E., Pérez-Gutiérrez, C., Tomás, J.M., Suárez, T., Garmendia, J., Bengoechea, J.A., 2013. Role of bacterial surface structures on the interaction of Klebsiella pneumoniae with phagocytes. PLoS One 8, e56847. https://doi.org/10.1371/journal.pone.0056847
- March, C., Moranta, D., Regueiro, V., Llobet, E., Tomás, A., Garmendia, J., Bengoechea, J.A., 2011. Klebsiella pneumoniae outer membrane protein A is required to prevent the activation of airway epithelial cells. J Biol Chem 286, 9956–9967. https://doi.org/10.1074/jbc.M110.181008
- Marshall, S., Hujer, A.M., Rojas, L.J., Papp-Wallace, K.M., Humphries, R.M., Spellberg, B., Hujer, K.M., Marshall, E.K., Rudin, S.D., Perez, F., Wilson, B.M., Wasserman, R.B., Chikowski, L., Paterson, D.L., Vila, A.J., van Duin, D., Kreiswirth, B.N., Chambers, H.F., Fowler, V.G., Jacobs, M.R., Pulse, M.E., Weiss, W.J., Bonomo, R.A., 2017. Can Ceftazidime-Avibactam and Aztreonam Overcome β-Lactam Resistance Conferred by Metallo-β-Lactamases in Enterobacteriaceae? Antimicrob Agents Chemother 61. https://doi.org/10.1128/AAC.02243-16
- Martínez-Martínez, L., 2008. Extended-spectrum beta-lactamases and the permeability barrier. Clin Microbiol Infect 14 Suppl 1, 82–89. https://doi.org/10.1111/j.1469-0691.2007.01860.x
- Mata, C., Miró, E., Alvarado, A., Garcillán-Barcia, M.P., Toleman, M., Walsh, T.R., de la Cruz, F., Navarro, F., 2012. Plasmid typing and genetic context of AmpC β-lactamases in Enterobacteriaceae lacking inducible chromosomal ampC genes: findings from a Spanish hospital 1999-2007. J Antimicrob Chemother 67, 115–122. https://doi.org/10.1093/jac/dkr412
- Mathers, A.J., Peirano, G., Pitout, J.D.D., 2015. The role of epidemic resistance plasmids and international high-risk clones in the spread of multidrug-resistant Enterobacteriaceae. Clin Microbiol Rev 28, 565–591. https://doi.org/10.1128/CMR.00116-14
- Matic, V., Bozdogan, B., Jacobs, M.R., Ubukata, K., Appelbaum, P.C., 2003. Contribution of beta-lactamase and PBP amino acid substitutions to amoxicillin/clavulanate resistance in beta-lactamase-positive, amoxicillin/clavulanate-resistant Haemophilus influenzae. J Antimicrob Chemother 52, 1018–1021. https://doi.org/10.1093/jac/dkg474
- Matthew, M., Hedges, R.W., Smith, J.T., 1979. Types of beta-lactamase determined by plasmids in gram-negative bacteria. J Bacteriol 138, 657–662. https://doi.org/10.1128/JB.138.3.657-662.1979
- Matuszewski, S., Hermisson, J., Kopp, M., 2015. Catch Me if You Can: Adaptation from Standing Genetic Variation to a Moving Phenotypic Optimum. Genetics 200, 1255–1274. https://doi.org/10.1534/genetics.115.178574
- Mazzariol, A., Cornaglia, G., Nikaido, H., 2000. Contributions of the AmpC beta-lactamase and the AcrAB multidrug efflux system in intrinsic resistance of Escherichia coli K-12 to beta-lactams. Antimicrob Agents Chemother 44, 1387–1390. https://doi.org/10.1128/aac.44.5.1387-1390.2000
- McGowan, S., 1998. Bacterial production of carbapenems and clavams: evolution of Î²-lactam antibiotic pathways. Trends in Microbiology 6, 203–208. https://doi.org/10.1016/S0966-842X(98)01251-7

- Mechler, L., Herbig, A., Paprotka, K., Fraunholz, M., Nieselt, K., Bertram, R., 2015. A novel point mutation promotes growth phase-dependent daptomycin tolerance in Staphylococcus aureus. Antimicrob Agents Chemother 59, 5366–5376. https://doi.org/10.1128/AAC.00643-15
- Melander, R.J., Zurawski, D.V., Melander, C., 2018. Narrow-Spectrum Antibacterial Agents. Medchemcomm 9, 12–21. https://doi.org/10.1039/C7MD00528H
- Meletis, G., Tzampaz, E., Sianou, E., Tzavaras, I., Sofianou, D., 2011. Colistin heteroresistance in carbapenemase-producing Klebsiella pneumoniae. J Antimicrob Chemother 66, 946–947. https://doi.org/10.1093/jac/dkr007
- Mengistu, Y., Edwards, C., Saunders, J.R., 1994. Continuous culture studies on the synthesis of capsular polysaccharide by Klebsiella pneumoniae K1. J Appl Bacteriol 76, 424–430. https://doi.org/10.1111/j.1365-2672.1994.tb01098.x
- Meredith, H.R., Andreani, V., Ma, H.R., Lopatkin, A.J., Lee, A.J., Anderson, D.J., Batt, G., You, L., 2018. Applying ecological resistance and resilience to dissect bacterial antibiotic responses. Sci Adv 4, eaau1873. https://doi.org/10.1126/sciadv.aau1873
- Meylan, S., Andrews, I.W., Collins, J.J., 2018. Targeting Antibiotic Tolerance, Pathogen by Pathogen. Cell 172, 1228–1238. https://doi.org/10.1016/j.cell.2018.01.037
- Michiels, J.E., Van den Bergh, B., Verstraeten, N., Fauvart, M., Michiels, J., 2016. In Vitro Emergence of High Persistence upon Periodic Aminoglycoside Challenge in the ESKAPE Pathogens. Antimicrob Agents Chemother 60, 4630–4637. https://doi.org/10.1128/AAC.00757-16
- Mike, L.A., Stark, A.J., Forsyth, V.S., Vornhagen, J., Smith, S.N., Bachman, M.A., Mobley, H.L.T., 2021. A systematic analysis of hypermucoviscosity and capsule reveals distinct and overlapping genes that impact Klebsiella pneumoniae fitness. PLoS Pathog 17, e1009376. https://doi.org/10.1371/journal.ppat.1009376
- Mitchell, P., 1949. Some observations on the mode of action of penicillin. Nature 164, 259–262. https://doi.org/10.1038/164259a0
- Molina-Quiroz, R.C., Silva-Valenzuela, C., Brewster, J., Castro-Nallar, E., Levy, S.B., Camilli, A., 2018. Cyclic AMP Regulates Bacterial Persistence through Repression of the Oxidative Stress Response and SOS-Dependent DNA Repair in Uropathogenic Escherichia coli. mBio 9. https://doi.org/10.1128/mBio.02144-17
- Moya, B., Dötsch, A., Juan, C., Blázquez, J., Zamorano, L., Haussler, S., Oliver, A., 2009. Beta-lactam resistance response triggered by inactivation of a nonessential penicillin-binding protein. PLoS Pathog 5, e1000353. https://doi.org/10.1371/journal.ppat.1000353
- Moyed, H.S., Bertrand, K.P., 1983. hipA, a newly recognized gene of Escherichia coli K-12 that affects frequency of persistence after inhibition of murein synthesis. J Bacteriol 155, 768–775. https://doi.org/10.1128/JB.155.2.768-775.1983
- Munoz-Price, L.S., Poirel, L., Bonomo, R.A., Schwaber, M.J., Daikos, G.L., Cormican, M., Cornaglia, G., Garau, J., Gniadkowski, M., Hayden, M.K., Kumarasamy, K., Livermore, D.M., Maya, J.J., Nordmann, P., Patel, J.B., Paterson, D.L., Pitout, J., Villegas, M.V., Wang, H., Woodford, N., Quinn, J.P., 2013. Clinical epidemiology of the global expansion of Klebsiella pneumoniae carbapenemases. The Lancet Infectious Diseases 13, 785–796. https://doi.org/10.1016/S1473-3099(13)70190-7
- Murray, A.K., 2020. The Novel Coronavirus COVID-19 Outbreak: Global Implications for Antimicrobial Resistance. Front Microbiol 11, 1020. https://doi.org/10.3389/fmicb.2020.01020
- Naas, T., Cuzon, G., Truong, H.-V., Nordmann, P., 2012. Role of IS Kpn7 and Deletions in bla $_{KPC}$ Gene Expression. Antimicrob. Agents Chemother. 56, 4753–4759. https://doi.org/10.1128/AAC.00334-12

- Naas, T., Cuzon, G., Villegas, M.-V., Lartigue, M.-F., Quinn, J.P., Nordmann, P., 2008. Genetic structures at the origin of acquisition of the beta-lactamase bla KPC gene. Antimicrob Agents Chemother 52, 1257–1263. https://doi.org/10.1128/AAC.01451-07
- Naas, T., Dortet, L., Iorga, B.I., 2016. Structural and Functional Aspects of Class A Carbapenemases. Curr Drug Targets 17, 1006–1028. https://doi.org/10.2174/1389450117666160310144501
- Naas, T., Nordmann, P., Vedel, G., Poyart, C., 2005. Plasmid-Mediated Carbapenem-Hydrolyzing β-Lactamase KPC in a Klebsiella pneumoniae Isolate from France. AAC 49, 4423–4424. https://doi.org/10.1128/AAC.49.10.4423-4424.2005
- Naas, T., Oueslati, S., Bonnin, R.A., Dabos, M.L., Zavala, A., Dortet, L., Retailleau, P., Iorga, B.I., 2017. Beta-lactamase database (BLDB) - structure and function. J Enzyme Inhib Med Chem 32, 917–919. https://doi.org/10.1080/14756366.2017.1344235
- Nagy, Z., Chandler, M., 2004. Regulation of transposition in bacteria. Res Microbiol 155, 387–398. https://doi.org/10.1016/j.resmic.2004.01.008
- Naparstek, L., Carmeli, Y., Chmelnitsky, I., Banin, E., Navon-Venezia, S., 2012. Reduced susceptibility to chlorhexidine among extremely-drug-resistant strains of Klebsiella pneumoniae. J. Hosp. Infect. 81, 15–19. https://doi.org/10.1016/j.jhin.2012.02.007
- Napier, B.A., Band, V., Burd, E.M., Weiss, D.S., 2014. Colistin heteroresistance in Enterobacter cloacae is associated with cross-resistance to the host antimicrobial lysozyme. Antimicrob Agents Chemother 58, 5594–5597. https://doi.org/10.1128/AAC.02432-14
- Navon-Venezia, S., Kondratyeva, K., Carattoli, A., 2017. Klebsiella pneumoniae: a major worldwide source and shuttle for antibiotic resistance. FEMS Microbiology Reviews 41, 252–275. https://doi.org/10.1093/femsre/fux013
- Nicholson, W.L., Fajardo-Cavazos, P., Rebeil, R., Slieman, T.A., Riesenman, P.J., Law, J.F., Xue, Y., 2002. Bacterial endospores and their significance in stress resistance. Antonie Van Leeuwenhoek 81, 27–32. https://doi.org/10.1023/a:1020561122764
- Nickolai, D.J., Lammel, C.J., Byford, B.A., Morris, J.H., Kaplan, E.B., Hadley, W.K., Brooks, G.F., 1985. Effects of storage temperature and pH on the stability of eleven beta-lactam antibiotics in MIC trays. J Clin Microbiol 21, 366–370. https://doi.org/10.1128/JCM.21.3.366-370.1985
- Nicoloff, H., Hjort, K., Levin, B.R., Andersson, D.I., 2019. The high prevalence of antibiotic heteroresistance in pathogenic bacteria is mainly caused by gene amplification. Nat Microbiol 4, 504–514. https://doi.org/10.1038/s41564-018-0342-0
- Nikaido, H., 2003. Molecular basis of bacterial outer membrane permeability revisited. Microbiol Mol Biol Rev 67, 593–656. https://doi.org/10.1128/mmbr.67.4.593-656.2003
- Nikaido, H., Rosenberg, E.Y., Foulds, J., 1983. Porin channels in Escherichia coli: studies with beta-lactams in intact cells. J Bacteriol 153, 232–240. https://doi.org/10.1128/JB.153.1.232-240.1983
- Nikaido, H., Zgurskaya, H.I., 2001. AcrAB and related multidrug efflux pumps of Escherichia coli. J Mol Microbiol Biotechnol 3, 215–218.
- Nodari, C.S., Ribeiro, V.B., Barth, A.L., 2015. Imipenem heteroresistance: high prevalence among Enterobacteriaceae Klebsiella pneumoniae carbapenemase producers. Journal of Medical Microbiology 64, 124–126. https://doi.org/10.1099/jmm.0.081869-0
- Nordmann, P., Cuzon, G., Naas, T., 2009. The real threat of Klebsiella pneumoniae carbapenemase-producing bacteria. The Lancet Infectious Diseases 9, 228–236. https://doi.org/10.1016/S1473-3099(09)70054-4
- Nordmann, P., Poirel, L., Walsh, T.R., Livermore, D.M., 2011. The emerging NDM carbapenemases. Trends Microbiol 19, 588–595. https://doi.org/10.1016/j.tim.2011.09.005

- Nugent, M.E., Hedges, R.W., 1979. The nature of the genetic determinant for the SHV-1 beta-lactamase. Mol Gen Genet 175, 239–243. https://doi.org/10.1007/BF00397222
- Ocampo, A.M., Chen, L., Cienfuegos, A.V., Roncancio, G., Chavda, K.D., Kreiswirth, B.N., Jiménez, J.N., 2016. A Two-Year Surveillance in Five Colombian Tertiary Care Hospitals Reveals High Frequency of Non-CG258 Clones of Carbapenem-Resistant Klebsiella pneumoniae with Distinct Clinical Characteristics. Antimicrob Agents Chemother 60, 332–342. https://doi.org/10.1128/AAC.01775-15
- Ochman, H., Lawrence, J.G., Groisman, E.A., 2000. Lateral gene transfer and the nature of bacterial innovation. Nature 405, 299–304. https://doi.org/10.1038/35012500
- Oethinger, M., Kern, W.V., Jellen-Ritter, A.S., McMurry, L.M., Levy, S.B., 2000. Ineffectiveness of topoisomerase mutations in mediating clinically significant fluoroquinolone resistance in Escherichia coli in the absence of the AcrAB efflux pump. Antimicrob Agents Chemother 44, 10–13. https://doi.org/10.1128/aac.44.1.10-13.2000
- Okusu, H., Ma, D., Nikaido, H., 1996. AcrAB efflux pump plays a major role in the antibiotic resistance phenotype of Escherichia coli multiple-antibiotic-resistance (Mar) mutants. J Bacteriol 178, 306–308. https://doi.org/10.1128/jb.178.1.306-308.1996
- Olaitan, A.O., Morand, S., Rolain, J.-M., 2014. Mechanisms of polymyxin resistance: acquired and intrinsic resistance in bacteria. Front Microbiol 5, 643. https://doi.org/10.3389/fmicb.2014.00643
- Olivares, J., Bernardini, A., Garcia-Leon, G., Corona, F., B Sanchez, M., Martinez, J.L., 2013. The intrinsic resistome of bacterial pathogens. Front Microbiol 4, 103. https://doi.org/10.3389/fmicb.2013.00103
- Om, C., McLaws, M.-L., 2016. Antibiotics: practice and opinions of Cambodian commercial farmers, animal feed retailers and veterinarians. Antimicrob Resist Infect Control 5, 42. https://doi.org/10.1186/s13756-016-0147-y
- O'Rourke, E.J., Lambert, K.G., Parsonnet, K.C., Macone, A.B., Goldmann, D.A., 1991. False resistance to imipenem with a microdilution susceptibility testing system. J Clin Microbiol 29, 827–829. https://doi.org/10.1128/JCM.29.4.827-829.1991
- Paczosa, M.K., Mecsas, J., 2016. Klebsiella pneumoniae: Going on the Offense with a Strong Defense. Microbiol Mol Biol Rev 80, 629–661. https://doi.org/10.1128/MMBR.00078-15
- Padilla, E., Llobet, E., Doménech-Sánchez, A., Martínez-Martínez, L., Bengoechea, J.A., Albertí, S., 2010. Klebsiella pneumoniae AcrAB efflux pump contributes to antimicrobial resistance and virulence. Antimicrob Agents Chemother 54, 177–183. https://doi.org/10.1128/AAC.00715-09
- Page, M.I., Badarau, A., 2008. The mechanisms of catalysis by metallo beta-lactamases. Bioinorg Chem Appl 576297. https://doi.org/10.1155/2008/576297
- Pages, J.-M., Lavigne, J.-P., Leflon-Guibout, V., Marcon, E., Bert, F., Noussair, L., Nicolas-Chanoine, M.-H., 2009. Efflux pump, the masked side of beta-lactam resistance in Klebsiella pneumoniae clinical isolates. PLoS One 4, e4817. https://doi.org/10.1371/journal.pone.0004817
- Pal, S., Verma, J., Mallick, S., Rastogi, S.K., Kumar, A., Ghosh, A.S., 2019. Absence of the glycosyltransferase WcaJ in Klebsiella pneumoniae ATCC13883 affects biofilm formation, increases polymyxin resistance and reduces murine macrophage activation. Microbiology 165, 891–904. https://doi.org/10.1099/mic.0.000827
- Pan, Y.-J., Lin, T.-L., Chen, C.-T., Chen, Y.-Y., Hsieh, P.-F., Hsu, C.-R., Wu, M.-C., Wang, J.-T., 2015. Genetic analysis of capsular polysaccharide synthesis gene clusters in 79 capsular types of Klebsiella spp. Scientific Reports 5, 15573. https://doi.org/10.1038/srep15573

- Pantel, A., Richaud-Morel, B., Cazaban, M., Bouziges, N., Sotto, A., Lavigne, J.-P., 2016. Environmental persistence of OXA-48-producing Klebsiella pneumoniae in a French intensive care unit. Am J Infect Control 44, 366–368. https://doi.org/10.1016/j.ajic.2015.09.021
- Papp-Wallace, K.M., Endimiani, A., Taracila, M.A., Bonomo, R.A., 2011. Carbapenems: past, present, and future. Antimicrob Agents Chemother 55, 4943–4960. https://doi.org/10.1128/AAC.00296-11
- Paredes-Sabja, D., Setlow, P., Sarker, M.R., 2011. Germination of spores of Bacillales and Clostridiales species: mechanisms and proteins involved. Trends Microbiol 19, 85–94. https://doi.org/10.1016/j.tim.2010.10.004
- Parkhill, J., Wren, B.W., Mungall, K., Ketley, J.M., Churcher, C., Basham, D., Chillingworth, T., Davies, R.M., Feltwell, T., Holroyd, S., Jagels, K., Karlyshev, A.V., Moule, S., Pallen, M.J., Penn, C.W., Quail, M.A., Rajandream, M.A., Rutherford, K.M., van Vliet, A.H., Whitehead, S., Barrell, B.G., 2000. The genome sequence of the food-borne pathogen Campylobacter jejuni reveals hypervariable sequences. Nature 403, 665–668. https://doi.org/10.1038/35001088
- Paterson, D.L., Bonomo, R.A., 2005. Extended-spectrum beta-lactamases: a clinical update. Clin Microbiol Rev 18, 657–686. https://doi.org/10.1128/CMR.18.4.657-686.2005
- Patiño-Navarrete, R., Rosinski-Chupin, I., Cabanel, N., Gauthier, L., Takissian, J., Madec, J.-Y., Hamze, M., Bonnin, R.A., Naas, T., Glaser, P., 2020. Stepwise evolution and convergent recombination underlie the global dissemination of carbapenemase-producing Escherichia coli. Genome Med 12, 10. https://doi.org/10.1186/s13073-019-0699-6
- Perrenoud, A., Sauer, U., 2005. Impact of global transcriptional regulation by ArcA, ArcB, Cra, Crp, Cya, Fnr, and Mlc on glucose catabolism in Escherichia coli. J Bacteriol 187, 3171–3179. https://doi.org/10.1128/JB.187.9.3171-3179.2005
- Pesesky, M.W., Tilley, R., Beck, D.A.C., 2019. Mosaic plasmids are abundant and unevenly distributed across prokaryotic taxa. Plasmid 102, 10–18. https://doi.org/10.1016/j.plasmid.2019.02.003
- Piddock, L.J.V., 2006. Multidrug-resistance efflux pumps - not just for resistance. Nat Rev Microbiol 4, 629–636. https://doi.org/10.1038/nrmicro1464
- Pinho, M.G., de Lencastre, H., Tomasz, A., 2001. An acquired and a native penicillin-binding protein cooperate in building the cell wall of drug-resistant staphylococci. Proc Natl Acad Sci U S A 98, 10886–10891. https://doi.org/10.1073/pnas.191260798
- Podschun, R., Acktun, H., Okpara, J., Linderkamp, O., Ullmann, U., Borneff-Lipp, M., 1998. Isolation of Klebsiella planticola from newborns in a neonatal ward. J Clin Microbiol 36, 2331–2332. https://doi.org/10.1128/JCM.36.8.2331-2332.1998
- Podschun, R., Ullmann, U., 1998. Klebsiella spp. as nosocomial pathogens: epidemiology, taxonomy, typing methods, and pathogenicity factors. Clin Microbiol Rev 11, 589–603.
- Poirel, L., Héritier, C., Tolün, V., Nordmann, P., 2004. Emergence of oxacillinase-mediated resistance to imipenem in Klebsiella pneumoniae. Antimicrob Agents Chemother 48, 15–22. https://doi.org/10.1128/aac.48.1.15-22.2004
- Poirel, L., Kämpfer, P., Nordmann, P., 2002. Chromosome-encoded Ambler class A beta-lactamase of Kluyvera georgiana, a probable progenitor of a subgroup of CTX-M extended-spectrum beta-lactamases. Antimicrob Agents Chemother 46, 4038–4040. https://doi.org/10.1128/aac.46.12.4038-4040.2002
- Poirel, L., Kieffer, N., Fernandez-Garayzabal, J.F., Vela, A.I., Larpin, Y., Nordmann, P., 2017. MCR-2-mediated plasmid-borne polymyxin resistance most likely originates from Moraxella pluranimalium. J Antimicrob Chemother 72, 2947–2949. https://doi.org/10.1093/jac/dkx225

- Poirel, L., Naas, T., Nordmann, P., 2010. Diversity, epidemiology, and genetics of class D beta-lactamases. Antimicrob Agents Chemother 54, 24–38. https://doi.org/10.1128/AAC.01512-08
- Poirel, L., Potron, A., Nordmann, P., 2012. OXA-48-like carbapenemases: the phantom menace. J Antimicrob Chemother 67, 1597–1606. https://doi.org/10.1093/jac/dks121
- Pollack, M., Charache, P., Nieman, R.E., Jett, M.P., Reimhardt, J.A., Hardy, P.H., 1972. Factors influencing colonisation and antibiotic-resistance patterns of gram-negative bacteria in hospital patients. Lancet 2, 668–671. https://doi.org/10.1016/s0140-6736(72)92084-3
- Pomakova, D.K., Hsiao, C.-B., Beanan, J.M., Olson, R., MacDonald, U., Keynan, Y., Russo, T.A., 2012. Clinical and phenotypic differences between classic and hypervirulent Klebsiella pneumonia: an emerging and under-recognized pathogenic variant. Eur J Clin Microbiol Infect Dis 31, 981–989. https://doi.org/10.1007/s10096-011-1396-6
- Pontes, M.H., Groisman, E.A., 2020. A Physiological Basis for Nonheritable Antibiotic Resistance. mBio 11. https://doi.org/10.1128/mBio.00817-20
- Pos, K.M., 2009. Drug transport mechanism of the AcrB efflux pump. Biochim Biophys Acta 1794, 782–793. https://doi.org/10.1016/j.bbapap.2008.12.015
- Poulou, A., Voulgari, E., Vrioni, G., Koumaki, V., Xidopoulos, G., Chatzipantazi, V., Markou, F., Tsakris, A., 2013. Outbreak caused by an ertapenem-resistant, CTX-M-15-producing Klebsiella pneumoniae sequence type 101 clone carrying an OmpK36 porin variant. J Clin Microbiol 51, 3176–3182. https://doi.org/10.1128/JCM.01244-13
- Pournaras, S., Kristo, I., Vrioni, G., Ikonomidis, A., Poulou, A., Petropoulou, D., Tsakris, A., 2010. Characteristics of meropenem heteroresistance in Klebsiella pneumoniae carbapenemase (KPC)-producing clinical isolates of K. pneumoniae. J. Clin. Microbiol. 48, 2601–2604. https://doi.org/10.1128/JCM.02134-09
- Pradel, N., Delmas, J., Wu, L.F., Santini, C.L., Bonnet, R., 2009. Sec- and Tat-dependent translocation of beta-lactamases across the Escherichia coli inner membrane. Antimicrob Agents Chemother 53, 242–248. https://doi.org/10.1128/AAC.00642-08
- Prim, N., Rivera, A., Coll, P., Mirelis, B., 2017. Intrinsic resistance versus intrinsic resistome: are we talking about the same concept? Reply to "Resistance to polymyxins in Gram-negative organisms." Int J Antimicrob Agents 50, 281. https://doi.org/10.1016/j.ijantimicag.2017.05.004
- Proctor, R., 2019. Respiration and Small Colony Variants of Staphylococcus aureus. Microbiol Spectr 7. https://doi.org/10.1128/microbiolspec.GPP3-0069-2019
- Proctor, R.A., von Humboldt, A., 1998. Bacterial energetics and antimicrobial resistance. Drug Resistance Updates 1, 227–235. https://doi.org/10.1016/S1368-7646(98)80003-4
- Puig-Asensio, M., Diekema, D.J., Boyken, L., Clore, G.S., Salinas, J.L., Perencevich, E.N., 2019. Contamination of health-care workers' hands with Escherichia coli and Klebsiella species after routine patient care: a prospective observational study. Clinical Microbiology and Infection S1198743X19306020. https://doi.org/10.1016/j.cmi.2019.11.005
- Queenan, A.M., Bush, K., 2007. Carbapenemases: the versatile beta-lactamases. Clin Microbiol Rev 20, 440–458, table of contents. https://doi.org/10.1128/CMR.00001-07
- Queenan, A.M., Shang, W., Flamm, R., Bush, K., 2010. Hydrolysis and Inhibition Profiles of -Lactamases from Molecular Classes A to D with Doripenem, Imipenem, and Meropenem. Antimicrobial Agents and Chemotherapy 54, 565–569. https://doi.org/10.1128/AAC.01004-09
- Ramirez, M.S., Iriarte, A., Reyes-Lamothe, R., Sherratt, D.J., Tolmasky, M.E., 2019. Small Klebsiella pneumoniae Plasmids: Neglected Contributors to Antibiotic Resistance. Front. Microbiol. 10, 2182. https://doi.org/10.3389/fmicb.2019.02182

- Rasheed, J.K., Kitchel, B., Zhu, W., Anderson, K.F., Clark, N.C., Ferraro, M.J., Savard, P., Humphries, R.M., Kallen, A.J., Limbago, B.M., 2013. New Delhi metallo-β-lactamase-producing Enterobacteriaceae, United States. Emerg Infect Dis 19, 870–878. https://doi.org/10.3201/eid1906.121515
- Raymond, K.N., Dertz, E.A., Kim, S.S., 2003. Enterobactin: An archetype for microbial iron transport. Proceedings of the National Academy of Sciences 100, 3584–3588. https://doi.org/10.1073/pnas.0630018100
- Reams, A.B., Roth, J.R., 2015. Mechanisms of gene duplication and amplification. Cold Spring Harb Perspect Biol 7, a016592. https://doi.org/10.1101/cshperspect.a016592
- Ren, H., He, X., Zou, X., Wang, G., Li, S., Wu, Y., 2015. Gradual increase in antibiotic concentration affects persistence of Klebsiella pneumoniae. J Antimicrob Chemother 70, 3267–3272. https://doi.org/10.1093/jac/dkv251
- Rendueles, O., Garcia-Garcerà, M., Néron, B., Touchon, M., Rocha, E.P.C., 2017. Abundance and co-occurrence of extracellular capsules increase environmental breadth: Implications for the emergence of pathogens. PLoS Pathog 13, e1006525. https://doi.org/10.1371/journal.ppat.1006525
- Rice, L.B., 2008. Federal funding for the study of antimicrobial resistance in nosocomial pathogens: no ESKAPE. J Infect Dis 197, 1079–1081. https://doi.org/10.1086/533452
- Rimbara, E., Mori, S., Kim, H., Suzuki, M., Shibayama, K., 2018. Mutations in Genes Encoding Penicillin-Binding Proteins and Efflux Pumps Play a Role in β-Lactam Resistance in Helicobacter cinaedi. Antimicrob Agents Chemother 62. https://doi.org/10.1128/AAC.02036-17
- Roberts, J.A., Kirkpatrick, C.M.J., Roberts, M.S., Robertson, T.A., Dalley, A.J., Lipman, J., 2009. Meropenem dosing in critically ill patients with sepsis and without renal dysfunction: intermittent bolus versus continuous administration? Monte Carlo dosing simulations and subcutaneous tissue distribution. J Antimicrob Chemother 64, 142–150. https://doi.org/10.1093/jac/dkp139
- Rocker, A., Lacey, J.A., Belousoff, M.J., Wilksch, J.J., Strugnell, R.A., Davies, M.R., Lithgow, T., 2020. Global Trends in Proteome Remodeling of the Outer Membrane Modulate Antimicrobial Permeability in Klebsiella pneumoniae. mBio 11. https://doi.org/10.1128/mBio.00603-20
- Ronde-Oustau, C., Lustig, S., Dupieux, C., Ferry, T., Lyon BJI Study group, 2017. Implant-associated ESBL-Klebsiella pneumonia producing small colony variant bone and joint infection in a healthy 40-year-old man. BMJ Case Rep 2017. https://doi.org/10.1136/bcr-2016-217542
- Ropp, P.A., Hu, M., Olesky, M., Nicholas, R.A., 2002. Mutations in ponA, the gene encoding penicillin-binding protein 1, and a novel locus, penC, are required for high-level chromosomally mediated penicillin resistance in Neisseria gonorrhoeae. Antimicrob Agents Chemother 46, 769–777. https://doi.org/10.1128/aac.46.3.769-777.2002
- Rosenberg, A., Ene, I.V., Bibi, M., Zakin, S., Segal, E.S., Ziv, N., Dahan, A.M., Colombo, A.L., Bennett, R.J., Berman, J., 2018. Antifungal tolerance is a subpopulation effect distinct from resistance and is associated with persistent candidemia. Nat Commun 9, 2470. https://doi.org/10.1038/s41467-018-04926-x
- Russo, T.A., Olson, R., MacDonald, U., Beanan, J., Davidson, B.A., 2015. Aerobactin, but not yersiniabactin, salmochelin, or enterobactin, enables the growth/survival of hypervirulent (hypermucoviscous) Klebsiella pneumoniae ex vivo and in vivo. Infect Immun 83, 3325–3333. https://doi.org/10.1128/IAI.00430-15
- Ryffel, C., Strässle, A., Kayser, F.H., Berger-Bächi, B., 1994. Mechanisms of heteroresistance in methicillin-resistant Staphylococcus aureus. Antimicrob Agents Chemother 38, 724–728. https://doi.org/10.1128/aac.38.4.724

- Sakoulas, G., Alder, J., Thauvin-Eliopoulos, C., Moellering, R.C., Eliopoulos, G.M., 2006. Induction of daptomycin heterogeneous susceptibility in Staphylococcus aureus by exposure to vancomycin. Antimicrob Agents Chemother 50, 1581–1585. https://doi.org/10.1128/AAC.50.4.1581-1585.2006
- Salvatore, P., Bucci, C., Pagliarulo, C., Tredici, M., Colicchio, R., Cantalupo, G., Bardaro, M., Del Giudice, L., Massardo, D.R., Lavitola, A., Bruni, C.B., Alifano, P., 2002. Phenotypes of a naturally defective recB allele in Neisseria meningitidis clinical isolates. Infect Immun 70, 4185–4195. https://doi.org/10.1128/iai.70.8.4185-4195.2002
- Sánchez-Romero, M.A., Casadesús, J., 2018. Contribution of SPI-1 bistability to Salmonella enterica cooperative virulence: insights from single cell analysis. Sci Rep 8, 14875. https://doi.org/10.1038/s41598-018-33137-z
- Sandegren, L., Andersson, D.I., 2009. Bacterial gene amplification: implications for the evolution of antibiotic resistance. Nat Rev Microbiol 7, 578–588. https://doi.org/10.1038/nrmicro2174
- Sanschagrin, F., Couture, F., Levesque, R.C., 1995. Primary structure of OXA-3 and phylogeny of oxacillin-hydrolyzing class D beta-lactamases. Antimicrob Agents Chemother 39, 887–893. https://doi.org/10.1128/aac.39.4.887
- Santajit, S., Indrawattana, N., 2016. Mechanisms of Antimicrobial Resistance in ESKAPE Pathogens. Biomed Res Int 2016, 2475067. https://doi.org/10.1155/2016/2475067
- Sauvage, E., Kerff, F., Terrak, M., Ayala, J.A., Charlier, P., 2008. The penicillin-binding proteins: structure and role in peptidoglycan biosynthesis. FEMS Microbiol Rev 32, 234–258. https://doi.org/10.1111/j.1574-6976.2008.00105.x
- Saw, H.T.H., Webber, M.A., Mushtaq, S., Woodford, N., Piddock, L.J.V., 2016. Inactivation or inhibition of AcrAB-TolC increases resistance of carbapenemase-producing Enterobacteriaceae to carbapenems. J Antimicrob Chemother 71, 1510–1519. https://doi.org/10.1093/jac/dkw028
- Scheler, O., Makuch, K., Debski, P.R., Horka, M., Ruszczak, A., Pacocha, N., Sozański, K., Smolander, O.-P., Postek, W., Garstecki, P., 2020. Droplet-based digital antibiotic susceptibility screen reveals single-cell clonal heteroresistance in an isogenic bacterial population. Sci Rep 10, 3282. https://doi.org/10.1038/s41598-020-60381-z
- Schembri, M.A., Blom, J., Krogfelt, K.A., Klemm, P., 2005. Capsule and fimbria interaction in Klebsiella pneumoniae. Infect Immun 73, 4626–4633. https://doi.org/10.1128/IAI.73.8.4626-4633.2005
- Schneiders, T., Amyes, S.G.B., Levy, S.B., 2003. Role of AcrR and ramA in fluoroquinolone resistance in clinical Klebsiella pneumoniae isolates from Singapore. Antimicrob Agents Chemother 47, 2831–2837. https://doi.org/10.1128/aac.47.9.2831-2837.2003
- Schukken, Y., Chuff, M., Moroni, P., Gurjar, A., Santisteban, C., Welcome, F., Zadoks, R., 2012. The "other" gram-negative bacteria in mastitis: Klebsiella, serratia, and more. Vet Clin North Am Food Anim Pract 28, 239–256. https://doi.org/10.1016/j.cvfa.2012.04.001
- Schwartz, K.L., Morris, S.K., 2018. Travel and the Spread of Drug-Resistant Bacteria. Curr Infect Dis Rep 20, 29. https://doi.org/10.1007/s11908-018-0634-9
- Sekowska, A., Wendel, S., Fischer, E.C., Nørholm, M.H.H., Danchin, A., 2016. Generation of mutation hotspots in ageing bacterial colonies. Sci Rep 6, 2. https://doi.org/10.1038/s41598-016-0005-4
- Seligman, S.J., 1966. Penicillinase-negative variants of methicillin-resistant Staphylococcus aureus. Nature 209, 994–996. https://doi.org/10.1038/209994a0

- Semanjski, M., Germain, E., Bratl, K., Kiessling, A., Gerdes, K., Macek, B., 2018. The kinases HipA and HipA7 phosphorylate different substrate pools in Escherichia coli to promote multidrug tolerance. Sci Signal 11. https://doi.org/10.1126/scisignal.aat5750
- Semin-Pelletier, B., Cazet, L., Bourigault, C., Juvin, M.E., Boutoille, D., Raffi, F., Hourmant, M., Blancho, G., Agard, C., Connault, J., Corvec, S., Caillon, J., Batard, E., Lepelletier, D., 2015. Challenges of controlling a large outbreak of OXA-48 carbapenemase-producing Klebsiella pneumoniae in a French university hospital. J Hosp Infect 89, 248–253. https://doi.org/10.1016/j.jhin.2014.11.018
- Shallcross, L.J., Davies, D.S.C., 2014. Antibiotic overuse: a key driver of antimicrobial resistance. Br J Gen Pract 64, 604–605. https://doi.org/10.3399/bjgp14X682561
- Shen, B., Yu, Y., Chen, H., Cao, X., Lao, X., Fang, Y., Shi, Y., Chen, J., Zheng, H., 2013. Inhibitor discovery of full-length New Delhi metallo-β-lactamase-1 (NDM-1). PLoS One 8, e62955. https://doi.org/10.1371/journal.pone.0062955
- Shin, J.-H., Choe, D., Ransegnola, B., Hong, H.-R., Onyekwere, I., Cross, T., Shi, Q., Cho, B.-K., Westblade, L.F., Brito, I.L., Dörr, T., 2021. A multifaceted cellular damage repair and prevention pathway promotes high-level tolerance to β-lactam antibiotics. EMBO Rep 22, e51790. https://doi.org/10.15252/embr.202051790
- Shore, A.C., Coleman, D.C., 2013. Staphylococcal cassette chromosome mec: recent advances and new insights. Int J Med Microbiol 303, 350–359. https://doi.org/10.1016/j.ijmm.2013.02.002
- Sieradzki, K., Roberts, R.B., Serur, D., Hargrave, J., Tomasz, A., 1999. Heterogeneously vancomycin-resistant Staphylococcus epidermidis strain causing recurrent peritonitis in a dialysis patient during vancomycin therapy. J Clin Microbiol 37, 39–44. https://doi.org/10.1128/JCM.37.1.39-44.1999
- Silva, A., Sousa, A.M., Alves, D., Lourenço, A., Pereira, M.O., 2016a. Heteroresistance to colistin in Klebsiella pneumoniae is triggered by small colony variants sub-populations within biofilms. Pathogens and Disease 74, ftw036. https://doi.org/10.1093/femspd/ftw036
- Singh, R., Ray, P., Das, A., Sharma, M., 2009. Role of persisters and small-colony variants in antibiotic resistance of planktonic and biofilm-associated Staphylococcus aureus: an in vitro study. J Med Microbiol 58, 1067–1073. https://doi.org/10.1099/jmm.0.009720-0
- Smith, K.P., Kirby, J.E., 2018. The Inoculum Effect in the Era of Multidrug Resistance: Minor Differences in Inoculum Have Dramatic Effect on MIC Determination. Antimicrob Agents Chemother 62. https://doi.org/10.1128/AAC.00433-18
- Smits, W.K., Kuipers, O.P., Veening, J.-W., 2006. Phenotypic variation in bacteria: the role of feedback regulation. Nat Rev Microbiol 4, 259–271. https://doi.org/10.1038/nrmicro1381
- Søgaard, P., 1985. Population analysis of susceptibility to cefotaxime in Enterobacteriaceae. Acta Pathol Microbiol Immunol Scand B 93, 365–369. https://doi.org/10.1111/j.1699-0463.1985.tb02902.x
- Song, W., Hong, S.G., Yong, D., Jeong, S.H., Kim, H.S., Kim, H.-S., Kim, J.-S., Bae, I.K., 2015. Combined Use of the Modified Hodge Test and Carbapenemase Inhibition Test for Detection of Carbapenemase-Producing Enterobacteriaceae and Metallo-β-Lactamase-Producing Pseudomonas spp. Ann Lab Med 35, 212. https://doi.org/10.3343/alm.2015.35.2.212
- Sorg, R.A., Lin, L., van Doorn, G.S., Sorg, M., Olson, J., Nizet, V., Veening, J.-W., 2016. Collective Resistance in Microbial Communities by Intracellular Antibiotic Deactivation. PLoS Biol 14, e2000631. https://doi.org/10.1371/journal.pbio.2000631
- Spratt, B.G., 1988. Hybrid penicillin-binding proteins in penicillin-resistant strains of Neisseria gonorrhoeae. Nature 332, 173–176. https://doi.org/10.1038/332173a0

- Spratt, B.G., 1975. Distinct penicillin binding proteins involved in the division, elongation, and shape of Escherichia coli K12. Proc Natl Acad Sci U S A 72, 2999–3003. https://doi.org/10.1073/pnas.72.8.2999
- Spudich, J.L., Koshland, D.E., 1976. Non-genetic individuality: chance in the single cell. Nature 262, 467–471. https://doi.org/10.1038/262467a0
- Steward, C.D., Mohammed, J.M., Swenson, J.M., Stocker, S.A., Williams, P.P., Gaynes, R.P., McGowan, J.E., Tenover, F.C., 2003. Antimicrobial Susceptibility Testing of Carbapenems: Multicenter Validity Testing and Accuracy Levels of Five Antimicrobial Test Methods for Detecting Resistance in Enterobacteriaceae and Pseudomonas aeruginosa Isolates. Journal of Clinical Microbiology 41, 351–358. https://doi.org/10.1128/JCM.41.1.351-358.2003
- Stewart, P.S., 2002. Mechanisms of antibiotic resistance in bacterial biofilms. Int J Med Microbiol 292, 107–113. https://doi.org/10.1078/1438-4221-00196
- Stokes, J.M., Lopatkin, A.J., Lobritz, M.A., Collins, J.J., 2019. Bacterial Metabolism and Antibiotic Efficacy. Cell Metab 30, 251–259. https://doi.org/10.1016/j.cmet.2019.06.009
- Struve, C., Bojer, M., Krogfelt, K.A., 2009. Identification of a conserved chromosomal region encoding Klebsiella pneumoniae type 1 and type 3 fimbriae and assessment of the role of fimbriae in pathogenicity. Infect Immun 77, 5016–5024. https://doi.org/10.1128/IAI.00585-09
- Struve, C., Bojer, M., Krogfelt, K.A., 2008. Characterization of Klebsiella pneumoniae type 1 fimbriae by detection of phase variation during colonization and infection and impact on virulence. Infect Immun 76, 4055–4065. https://doi.org/10.1128/IAI.00494-08
- Struve, C., Roe, C.C., Stegger, M., Stahlhut, S.G., Hansen, D.S., Engelthaler, D.M., Andersen, P.S., Driebe, E.M., Keim, P., Krogfelt, K.A., 2015. Mapping the Evolution of Hypervirulent Klebsiella pneumoniae. mBio 6, e00630. https://doi.org/10.1128/mBio.00630-15
- Sugawara, E., Kojima, S., Nikaido, H., 2016. Klebsiella pneumoniae Major Porins OmpK35 and OmpK36 Allow More Efficient Diffusion of β-Lactams than Their Escherichia coli Homologs OmpF and OmpC. J Bacteriol 198, 3200–3208. https://doi.org/10.1128/JB.00590-16
- Sulaiman, J.E., Lam, H., 2021. Evolution of Bacterial Tolerance Under Antibiotic Treatment and Its Implications on the Development of Resistance. Front Microbiol 12, 617412. https://doi.org/10.3389/fmicb.2021.617412
- Sulaiman, J.E., Lam, H., 2020. Proteomic Investigation of Tolerant Escherichia coli Populations from Cyclic Antibiotic Treatment. J Proteome Res 19, 900–913. https://doi.org/10.1021/acs.jproteome.9b00687
- Sumita, Y., Fukasawa, M., Okuda, T., 1990. Comparison of two carbapenems, SM-7338 and imipenem: affinities for penicillin-binding proteins and morphological changes. J Antibiot (Tokyo) 43, 314–320. https://doi.org/10.7164/antibiotics.43.314
- Sun, R., Zhang, H., Xu, Y., Zhu, H., Yu, X., Xu, J., 2021. Klebsiella pneumoniae-related invasive liver abscess syndrome complicated by purulent meningitis: a review of the literature and description of three cases. BMC Infect Dis 21, 15. https://doi.org/10.1186/s12879-020-05702-3
- Sutherland, R., Rolinson, G.N., 1964. CHARACTERISTICS OF METHICILLIN-RESISTANT STAPHYLOCOCCI. J Bacteriol 87, 887–899. https://doi.org/10.1128/JB.87.4.887-899.1964
- Tacconelli, E., Carrara, E., Savoldi, A., Harbarth, S., Mendelson, M., Monnet, D.L., Pulcini, C., Kahlmeter, G., Kluytmans, J., Carmeli, Y., Ouellette, M., Outterson, K., Patel, J., Cavaleri, M., Cox, E.M., Houchens, C.R., Grayson, M.L., Hansen, P., Singh, N., Theuretzbacher, U., Magrini, N., WHO Pathogens Priority List Working Group, 2018. Discovery, research, and development of new

antibiotics: the WHO priority list of antibiotic-resistant bacteria and tuberculosis. Lancet Infect Dis 18, 318–327. https://doi.org/10.1016/S1473-3099(17)30753-3

- Tada, T., Miyoshi-Akiyama, T., Shimada, K., Kirikae, T., 2014. Biochemical analysis of metallo-β-lactamase NDM-3 from a multidrug-resistant Escherichia coli strain isolated in Japan. Antimicrob Agents Chemother 58, 3538–3540. https://doi.org/10.1128/AAC.02793-13
- Tam, N.K.M., Uyen, N.Q., Hong, H.A., Duc, L.H., Hoa, T.T., Serra, C.R., Henriques, A.O., Cutting, S.M., 2006. The intestinal life cycle of Bacillus subtilis and close relatives. J Bacteriol 188, 2692–2700. https://doi.org/10.1128/JB.188.7.2692-2700.2006
- Tan, Y.H., Chen, Y., Chu, W.H.W., Sham, L., Gan, Y., 2020. Cell envelope defects of different capsule-null mutants in K1 hypervirulent Klebsiella pneumoniae can affect bacterial pathogenesis. Mol Microbiol 113, 889–905. https://doi.org/10.1111/mmi.14447
- Tato, M., Morosini, M., García, L., Albertí, S., Coque, M.T., Cantón, R., 2010. Carbapenem Heteroresistance in VIM-1-producing Klebsiella pneumoniae isolates belonging to the same clone: consequences for routine susceptibility testing. J Clin Microbiol 48, 4089–4093. https://doi.org/10.1128/JCM.01130-10
- Tavío, M.M., Vila, J., Perilli, M., Casañas, L.T., Maciá, L., Amicosante, G., Jiménez de Anta, M.T., 2004. Enhanced active efflux, repression of porin synthesis and development of Mar phenotype by diazepam in two enterobacteria strains. J Med Microbiol 53, 1119–1122. https://doi.org/10.1099/jmm.0.45613-0
- Taylor, P.C., Schoenknecht, F.D., Sherris, J.C., Linner, E.C., 1983. Determination of minimum bactericidal concentrations of oxacillin for Staphylococcus aureus: influence and significance of technical factors. Antimicrob Agents Chemother 23, 142–150. https://doi.org/10.1128/aac.23.1.142
- Tenover, F.C., Kalsi, R.K., Williams, P.P., Carey, R.B., Stocker, S., Lonsway, D., Rasheed, J.K., Biddle, J.W., McGowan, J.E., Hanna, B., 2006a. Carbapenem resistance in Klebsiella pneumoniae not detected by automated susceptibility testing. Emerg Infect Dis 12, 1209–1213. https://doi.org/10.3201/eid1208.060291
- the EuSCAPE Working Group, the ESGEM Study Group, David, S., Reuter, S., Harris, S.R., Glasner, C., Feltwell, T., Argimon, S., Abudahab, K., Goater, R., Giani, T., Errico, G., Aspbury, M., Sjunnebo, S., Feil, E.J., Rossolini, G.M., Aanensen, D.M., Grundmann, H., 2019. Epidemic of carbapenem-resistant Klebsiella pneumoniae in Europe is driven by nosocomial spread. Nat Microbiol 4, 1919–1929. https://doi.org/10.1038/s41564-019-0492-8
- Thulin, E., Andersson, D.I., 2019. Upregulation of PBP1B and LpoB in cysB Mutants Confers Mecillinam (Amdinocillin) Resistance in Escherichia coli. Antimicrob Agents Chemother 63. https://doi.org/10.1128/AAC.00612-19
- Tipper, D.J., Strominger, J.L., 1965. Mechanism of action of penicillins: a proposal based on their structural similarity to acyl-D-alanyl-D-alanine. Proc Natl Acad Sci U S A 54, 1133–1141. https://doi.org/10.1073/pnas.54.4.1133
- Tipton, K.A., Dimitrova, D., Rather, P.N., 2015. Phase-Variable Control of Multiple Phenotypes in Acinetobacter baumannii Strain AB5075. J Bacteriol 197, 2593–2599. https://doi.org/10.1128/JB.00188-15
- Tooke, C.L., Hinchliffe, P., Bragginton, E.C., Colenso, C.K., Hirvonen, V.H.A., Takebayashi, Y., Spencer, J., 2019. β-Lactamases and β-Lactamase Inhibitors in the 21st Century. J Mol Biol 431, 3472–3500. https://doi.org/10.1016/j.jmb.2019.04.002
- Toussaint, A., Chandler, M., 2012. Prokaryote genome fluidity: toward a system approach of the mobilome. Methods Mol Biol 804, 57–80. https://doi.org/10.1007/978-1-61779-361-5_4

- Tsai, Y.-K., Fung, C.-P., Lin, J.-C., Chen, J.-H., Chang, F.-Y., Chen, T.-L., Siu, L.K., 2011. Klebsiella pneumoniae outer membrane porins OmpK35 and OmpK36 play roles in both antimicrobial resistance and virulence. Antimicrob Agents Chemother 55, 1485–1493. https://doi.org/10.1128/AAC.01275-10
- Tseng, I.-L., Liu, Y.-M., Wang, S.-J., Yeh, H.-Y., Hsieh, C.-L., Lu, H.-L., Tseng, Y.-C., Mu, J.-J., 2015. Emergence of Carbapenemase Producing Klebsiella Pneumonia and Spread of KPC-2 and KPC-17 in Taiwan: A Nationwide Study from 2011 to 2013. PLoS ONE 10, e0138471. https://doi.org/10.1371/journal.pone.0138471
- Tuomanen, E., Cozens, R., Tosch, W., Zak, O., Tomasz, A., 1986. The rate of killing of Escherichia coli by beta-lactam antibiotics is strictly proportional to the rate of bacterial growth. J Gen Microbiol 132, 1297–1304. https://doi.org/10.1099/00221287-132-5-1297
- Turlin, E., Heuck, G., Simões Brandão, M.I., Szili, N., Mellin, J.R., Lange, N., Wandersman, C., 2014. Protoporphyrin (PPIX) efflux by the MacAB-TolC pump in Escherichia coli. Microbiologyopen 3, 849–859. https://doi.org/10.1002/mbo3.203
- Turton, Jane, Davies, F., Turton, Jack, Perry, C., Payne, Z., Pike, R., 2019. Hybrid Resistance and Virulence Plasmids in "High-Risk" Clones of Klebsiella pneumoniae, Including Those Carrying blaNDM-5. Microorganisms 7. https://doi.org/10.3390/microorganisms7090326
- van Asselt, G.J., Mouton, R.P., van Boven, C.P., 1996. A proposed standard for MIC-MBC laboratory techniques to detect penicillin tolerance in group A streptococci. Eur J Clin Microbiol Infect Dis 15, 182–183. https://doi.org/10.1007/BF01591499
- Van den Bergh, B., Michiels, J.E., Wenseleers, T., Windels, E.M., Boer, P.V., Kestemont, D., De Meester, L., Verstrepen, K.J., Verstraeten, N., Fauvart, M., Michiels, J., 2016. Frequency of antibiotic application drives rapid evolutionary adaptation of Escherichia coli persistence. Nat Microbiol 1, 16020. https://doi.org/10.1038/nmicrobiol.2016.20
- van der Bij, A.K., Pitout, J.D.D., 2012. The role of international travel in the worldwide spread of multiresistant Enterobacteriaceae. J Antimicrob Chemother 67, 2090–2100. https://doi.org/10.1093/jac/dks214
- van der Zwaluw, K., de Haan, A., Pluister, G.N., Bootsma, H.J., de Neeling, A.J., Schouls, L.M., 2015. The Carbapenem Inactivation Method (CIM), a Simple and Low-Cost Alternative for the Carba NP Test to Assess Phenotypic Carbapenemase Activity in Gram-Negative Rods. PLoS ONE 10, e0123690. https://doi.org/10.1371/journal.pone.0123690
- Veening, J.-W., Smits, W.K., Kuipers, O.P., 2008. Bistability, epigenetics, and bet-hedging in bacteria. Annu Rev Microbiol 62, 193–210. https://doi.org/10.1146/annurev.micro.62.081307.163002
- Villa, L., Feudi, C., Fortini, D., Brisse, S., Passet, V., Bonura, C., Endimiani, A., Mammina, C., Ocampo, A.M., Jimenez, J.N., Doumith, M., Woodford, N., Hopkins, K., Carattoli, A., 2017. Diversity, virulence, and antimicrobial resistance of the KPC-producing Klebsiella pneumoniae ST307 clone. Microb Genom 3, e000110. https://doi.org/10.1099/mgen.0.000110
- Villa, L., García-Fernández, A., Fortini, D., Carattoli, A., 2010. Replicon sequence typing of IncF plasmids carrying virulence and resistance determinants. J Antimicrob Chemother 65, 2518–2529. https://doi.org/10.1093/jac/dkq347
- Vincent, I.M., Ehmann, D.E., Mills, S.D., Perros, M., Barrett, M.P., 2016. Untargeted Metabolomics To Ascertain Antibiotic Modes of Action. Antimicrob Agents Chemother 60, 2281–2291. https://doi.org/10.1128/AAC.02109-15

- von Eiff, C., Heilmann, C., Proctor, R.A., Woltz, C., Peters, G., Götz, F., 1997. A site-directed Staphylococcus aureus hemB mutant is a small-colony variant which persists intracellularly. J Bacteriol 179, 4706–4712. https://doi.org/10.1128/jb.179.15.4706-4712.1997
- Waksman, S.A., Geiger, W.B., Reynolds, D.M., 1946. Strain Specificity and Production of Antibiotic Substances: VII. Production of Actinomycin by Different Actinomycetes. Proc Natl Acad Sci U S A 32, 117–120. https://doi.org/10.1073/pnas.32.5.117
- Wald-Dickler, N., Holtom, P., Spellberg, B., 2018. Busting the Myth of "Static vs Cidal": A Systemic Literature Review. Clin Infect Dis 66, 1470–1474. https://doi.org/10.1093/cid/cix1127
- Wallecha, A., Munster, V., Correnti, J., Chan, T., van der Woude, M., 2002. Dam- and OxyR-dependent phase variation of agn43: essential elements and evidence for a new role of DNA methylation. J Bacteriol 184, 3338–3347. https://doi.org/10.1128/jb.184.12.3338-3347.2002
- Walsh, T.R., Toleman, M.A., Poirel, L., Nordmann, P., 2005. Metallo-beta-lactamases: the quiet before the storm? Clin Microbiol Rev 18, 306–325. https://doi.org/10.1128/CMR.18.2.306-325.2005
- Walther-Rasmussen, J., Høiby, N., 2006. OXA-type carbapenemases. Journal of Antimicrobial Chemotherapy 57, 373–383. https://doi.org/10.1093/jac/dki482
- Wang, D., Chen, J., Yang, L., Mou, Y., Yang, Y., 2014. Phenotypic and enzymatic comparative analysis of the KPC variants, KPC-2 and its recently discovered variant KPC-15. PLoS One 9, e111491. https://doi.org/10.1371/journal.pone.0111491
- Wang, X., Kang, Y., Luo, C., Zhao, T., Liu, L., Jiang, X., Fu, R., An, S., Chen, J., Jiang, N., Ren, L., Wang, Q., Baillie, J.K., Gao, Z., Yu, J., 2014. Heteroresistance at the single-cell level: adapting to antibiotic stress through a population-based strategy and growth-controlled interphenotypic coordination. mBio 5, e00942-00913. https://doi.org/10.1128/mBio.00942-13
- Wang, X., Zhao, X., 2009. Contribution of oxidative damage to antimicrobial lethality. Antimicrob Agents Chemother 53, 1395–1402. https://doi.org/10.1128/AAC.01087-08
- Wannet, W., 2002. Spread of an MRSA clone with heteroresistance to oxacillin in the Netherlands. Euro Surveill 7, 73–74. https://doi.org/10.2807/esm.07.05.00367-en
- Wei, D., Yuminaga, Y., Shi, J., Hao, J., 2018. Non-capsulated mutants of a chemical-producing Klebsiella pneumoniae strain. Biotechnol Lett 40, 679–687. https://doi.org/10.1007/s10529-018-2524-5
- Weisenberg, S.A., Morgan, D.J., Espinal-Witter, R., Larone, D.H., 2009. Clinical outcomes of patients with Klebsiella pneumoniae carbapenemase-producing K. pneumoniae after treatment with imipenem or meropenem. Diagn Microbiol Infect Dis 64, 233–235. https://doi.org/10.1016/j.diagmicrobio.2009.02.004
- Westblade, L.F., Errington, J., Dörr, T., 2020. Antibiotic tolerance. PLoS Pathog 16, e1008892. https://doi.org/10.1371/journal.ppat.1008892
- White, R.L., Kays, M.B., Friedrich, L.V., Brown, E.W., Koonce, J.R., 1991. Pseudoresistance of Pseudomonas aeruginosa resulting from degradation of imipenem in an automated susceptibility testing system with predried panels. J Clin Microbiol 29, 398–400. https://doi.org/10.1128/JCM.29.2.398-400.1991
- Wilkins, B., Frost, L., 2002. Mechanisms of Gene Exchange Between Bacteria, in: Molecular Medical Microbiology. Elsevier, pp. 355–400. https://doi.org/10.1016/B978-012677530-3/50236-1
- Windels, E.M., Michiels, J.E., Fauvart, M., Wenseleers, T., Van den Bergh, B., Michiels, J., 2019. Bacterial persistence promotes the evolution of antibiotic resistance by increasing survival and mutation rates. ISME J 13, 1239–1251. https://doi.org/10.1038/s41396-019-0344-9

- Winther, K.S., Gerdes, K., 2012. Regulation of enteric vapBC transcription: induction by VapC toxin dimer-breaking. Nucleic Acids Res 40, 4347–4357. https://doi.org/10.1093/nar/gks029
- Wolfson, J.S., Hooper, D.C., McHugh, G.L., Bozza, M.A., Swartz, M.N., 1990. Mutants of Escherichia coli K-12 exhibiting reduced killing by both quinolone and beta-lactam antimicrobial agents. Antimicrob Agents Chemother 34, 1938–1943. https://doi.org/10.1128/aac.34.10.1938
- Woodford, N., Eastaway, A.T., Ford, M., Leanord, A., Keane, C., Quayle, R.M., Steer, J.A., Zhang, J., Livermore, D.M., 2010. Comparison of BD Phoenix, Vitek 2, and MicroScan Automated Systems for Detection and Inference of Mechanisms Responsible for Carbapenem Resistance in Enterobacteriaceae. Journal of Clinical Microbiology 48, 2999–3002. https://doi.org/10.1128/JCM.00341-10
- Woodford, N., Turton, J.F., Livermore, D.M., 2011. Multiresistant Gram-negative bacteria: the role of high-risk clones in the dissemination of antibiotic resistance. FEMS Microbiol Rev 35, 736–755. https://doi.org/10.1111/j.1574-6976.2011.00268.x
- Wootton, M., 2001. A modified population analysis profile (PAP) method to detect hetero-resistance to vancomycin in Staphylococcus aureus in a UK hospital. Journal of Antimicrobial Chemotherapy 47, 399–403. https://doi.org/10.1093/jac/47.4.399
- Wu, W., Feng, Y., Tang, G., Qiao, F., McNally, A., Zong, Z., 2019. NDM Metallo-β-Lactamases and Their Bacterial Producers in Health Care Settings. Clin Microbiol Rev 32. https://doi.org/10.1128/CMR.00115-18
- Wyres, K.L., Gorrie, C., Edwards, D.J., Wertheim, H.F.L., Hsu, L.Y., Van Kinh, N., Zadoks, R., Baker, S., Holt, K.E., 2015. Extensive Capsule Locus Variation and Large-Scale Genomic Recombination within the Klebsiella pneumoniae Clonal Group 258. Genome Biol Evol 7, 1267–1279. https://doi.org/10.1093/gbe/evv062
- Wyres, K.L., Holt, K.E., 2018. Klebsiella pneumoniae as a key trafficker of drug resistance genes from environmental to clinically important bacteria. Curr Opin Microbiol 45, 131–139. https://doi.org/10.1016/j.mib.2018.04.004
- Wyres, K.L., Lam, M.M.C., Holt, K.E., 2020. Population genomics of Klebsiella pneumoniae. Nat Rev Microbiol. https://doi.org/10.1038/s41579-019-0315-1
- Wyres, K.L., Wick, R.R., Gorrie, C., Jenney, A., Follador, R., Thomson, N.R., Holt, K.E., 2016. Identification of Klebsiella capsule synthesis loci from whole genome data. Microb Genom 2, e000102. https://doi.org/10.1099/mgen.0.000102
- Wyres, K.L., Wick, R.R., Judd, L.M., Froumine, R., Tokolyi, A., Gorrie, C.L., Lam, M.M.C., Duchêne, S., Jenney, A., Holt, K.E., 2019. Distinct evolutionary dynamics of horizontal gene transfer in drug resistant and virulent clones of Klebsiella pneumoniae. PLoS Genet 15, e1008114. https://doi.org/10.1371/journal.pgen.1008114
- Xia, H., Tang, Q., Song, J., Ye, J., Wu, H., Zhang, H., 2017. A yigP mutant strain is a small colony variant of E. coli and shows pleiotropic antibiotic resistance. Can J Microbiol 63, 961–969. https://doi.org/10.1139/cjm-2017-0347
- Xu, M., Fu, Y., Fang, Y., Xu, H., Kong, H., Liu, Y., Chen, Y., Li, L., 2019. High prevalence of KPC-2-producing hypervirulent Klebsiella pneumoniae causing meningitis in Eastern China. Infect Drug Resist 12, 641–653. https://doi.org/10.2147/IDR.S191892
- Xu, Y., Zheng, X., Zeng, W., Chen, T., Liao, W., Qian, J., Lin, J., Zhou, C., Tian, X., Cao, J., Zhou, T., 2020. Mechanisms of Heteroresistance and Resistance to Imipenem in Pseudomonas aeruginosa. IDR Volume 13, 1419–1428. https://doi.org/10.2147/IDR.S249475

- Yaikhan, T., Chuerboon, M., Tippayatham, N., Atimuttikul, N., Nuidate, T., Yingkajorn, M., Tun, A.W., Buncherd, H., Tansila, N., 2019. Indole and Derivatives Modulate Biofilm Formation and Antibiotic Tolerance of Klebsiella pneumoniae. Indian J Microbiol 59, 460–467. https://doi.org/10.1007/s12088-019-00830-0
- Yang, Y., Bhachech, N., Bush, K., 1995. Biochemical comparison of imipenem, meropenem and biapenem: permeability, binding to penicillin-binding proteins, and stability to hydrolysis by beta-lactamases. J Antimicrob Chemother 35, 75–84. https://doi.org/10.1093/jac/35.1.75
- Yigit, H., Queenan, A.M., Anderson, G.J., Domenech-Sanchez, A., Biddle, J.W., Steward, C.D., Alberti, S., Bush, K., Tenover, F.C., 2001. Novel carbapenem-hydrolyzing beta-lactamase, KPC-1, from a carbapenem-resistant strain of Klebsiella pneumoniae. Antimicrob Agents Chemother 45, 1151–1161. https://doi.org/10.1128/AAC.45.4.1151-1161.2001
- Yong, D., Toleman, M.A., Giske, C.G., Cho, H.S., Sundman, K., Lee, K., Walsh, T.R., 2009. Characterization of a new metallo-beta-lactamase gene, bla(NDM-1), and a novel erythromycin esterase gene carried on a unique genetic structure in Klebsiella pneumoniae sequence type 14 from India. Antimicrob Agents Chemother 53, 5046–5054. https://doi.org/10.1128/AAC.00774-09
- You, Y., Silbergeld, E.K., 2014. Learning from agriculture: understanding low-dose antimicrobials as drivers of resistome expansion. Front Microbiol 5, 284. https://doi.org/10.3389/fmicb.2014.00284
- Yu, V.L., Hansen, D.S., Ko, W.C., Sagnimeni, A., Klugman, K.P., von Gottberg, A., Goossens, H., Wagener, M.M., Benedi, V.J., International Klebseilla Study Group, 2007. Virulence characteristics of Klebsiella and clinical manifestations of K. pneumoniae bloodstream infections. Emerg Infect Dis 13, 986–993. https://doi.org/10.3201/eid1307.070187
- Yu, W.-L., Ko, W.-C., Cheng, K.-C., Lee, H.-C., Ke, D.-S., Lee, C.-C., Fung, C.-P., Chuang, Y.-C., 2006. Association between rmpA and magA Genes and Clinical Syndromes Caused by Klebsiella pneumoniae in Taiwan. Clinical Infectious Diseases 42, 1351–1358. https://doi.org/10.1086/503420
- Yurtsev, E.A., Chao, H.X., Datta, M.S., Artemova, T., Gore, J., 2013. Bacterial cheating drives the population dynamics of cooperative antibiotic resistance plasmids. Mol Syst Biol 9, 683. https://doi.org/10.1038/msb.2013.39
- Zahir, T., Camacho, R., Vitale, R., Ruckebusch, C., Hofkens, J., Fauvart, M., Michiels, J., 2019. High-throughput time-resolved morphology screening in bacteria reveals phenotypic responses to antibiotics. Commun Biol 2, 269. https://doi.org/10.1038/s42003-019-0480-9
- Zahir, T., Wilmaerts, D., Franke, S., Weytjens, B., Camacho, R., Marchal, K., Hofkens, J., Fauvart, M., Michiels, J., 2020. Image-Based Dynamic Phenotyping Reveals Genetic Determinants of Filamentation-Mediated β-Lactam Tolerance. Front. Microbiol. 11, 374. https://doi.org/10.3389/fmicb.2020.00374
- Zampieri, M., Enke, T., Chubukov, V., Ricci, V., Piddock, L., Sauer, U., 2017a. Metabolic constraints on the evolution of antibiotic resistance. Mol Syst Biol 13, 917. https://doi.org/10.15252/msb.20167028
- Zampieri, M., Zimmermann, M., Claassen, M., Sauer, U., 2017b. Nontargeted Metabolomics Reveals the Multilevel Response to Antibiotic Perturbations. Cell Rep 19, 1214–1228. https://doi.org/10.1016/j.celrep.2017.04.002
- Zavascki, A.P., Falci, D.R., da Silva, R.C.F., Dalarosa, M.G., Ribeiro, V.B., Rozales, F.P., Luz, D.I., Magagnin, C.M., Vieira, F.J., Sampaio, J.M., Barth, A.L., 2014. Heteroresistance to Carbapenems in New Delhi Metallo-β-Lactamase-1–Producing Isolates: A Challenge for Detection? Infect. Control Hosp. Epidemiol. 35, 751–752. https://doi.org/10.1086/676442

- Zeng, X., Lin, J., 2013. Beta-lactamase induction and cell wall metabolism in Gram-negative bacteria. Front Microbiol 4, 128. https://doi.org/10.3389/fmicb.2013.00128
- Zhanel, G.G., Craig, W.A., 1994. Pharmacokinetic contributions to postantibiotic effects. Focus on aminoglycosides. Clin Pharmacokinet 27, 377–392. https://doi.org/10.2165/00003088-199427050-00005
- Zhanel, G.G., Hoban, D.J., Harding, G.K., 1991. The postantibiotic effect: a review of in vitro and in vivo data. DICP 25, 153–163. https://doi.org/10.1177/106002809102500210
- Zhanel, G.G., Wiebe, R., Dilay, L., Thomson, K., Rubinstein, E., Hoban, D.J., Noreddin, A.M., Karlowsky, J.A., 2007. Comparative review of the carbapenems. Drugs 67, 1027–1052. https://doi.org/10.2165/00003495-200767070-00006
- Zhang, Y., Zborníková, E., Rejman, D., Gerdes, K., 2018. Novel (p)ppGpp Binding and Metabolizing Proteins of Escherichia coli. mBio 9. https://doi.org/10.1128/mBio.02188-17
- Zhao, W.-H., Hu, Z.-Q., 2011. IMP-type metallo-β-lactamases in Gram-negative bacilli: distribution, phylogeny, and association with integrons. Crit Rev Microbiol 37, 214–226. https://doi.org/10.3109/1040841X.2011.559944
- Zheng, J., Lin, Z., Sun, X., Lin, W., Chen, Z., Wu, Y., Qi, G., Deng, Q., Qu, D., Yu, Z., 2018. Overexpression of OqxAB and MacAB efflux pumps contributes to eravacycline resistance and heteroresistance in clinical isolates of Klebsiella pneumoniae. Emerging Microbes & Infections 7, 1–11. https://doi.org/10.1038/s41426-018-0141-y
- Zheng, J.-X., Lin, Z.-W., Sun, X., Lin, W.-H., Chen, Z., Wu, Y., Qi, G.-B., Deng, Q.-W., Qu, D., Yu, Z.-J., 2018. Overexpression of OqxAB and MacAB efflux pumps contributes to eravacycline resistance and heteroresistance in clinical isolates of Klebsiella pneumoniae. Emerg Microbes Infect 7, 139. https://doi.org/10.1038/s41426-018-0141-y
- Zhong, X., Xu, H., Chen, D., Zhou, H., Hu, X., Cheng, G., 2014. First emergence of acrAB and oqxAB mediated tigecycline resistance in clinical isolates of Klebsiella pneumoniae pre-dating the use of tigecycline in a Chinese hospital. PLoS One 9, e115185. https://doi.org/10.1371/journal.pone.0115185
- Zhou, H., Guo, W., Zhang, J., Li, Y., Zheng, P., Zhang, H., 2019. Draft genome sequence of a metallo-β-lactamase (blaAIM-1)-producing Klebsiella pneumoniae ST1916 isolated from a patient with chronic diarrhoea. J Glob Antimicrob Resist 16, 165–167. https://doi.org/10.1016/j.jgar.2019.01.010
- Zhu, M., Pan, Y., Dai, X., 2019. (p)ppGpp: the magic governor of bacterial growth economy. Curr Genet 65, 1121–1125. https://doi.org/10.1007/s00294-019-00973-z